UQAC
Université du Québec
à Chicoutimi

Approche hydrogéophysique d'évaluation du potentiel aquifère d'un milieu de dépôt quaternaire hétérogène et anisotrope : exemple de la moraine de Saint-Narcisse

Par

Yan Lévesque

Sous la direction de M. Julien Walter et M. Romain Chesnaux

Thèse présentée à l'Université du Québec à Chicoutimi dans le cadre d'un programme offert conjointement avec l'Université du Québec à Montréal en vue de l'obtention du grade de Philosophiae Doctor (Ph. D.) en Sciences de la Terre et de l'atmosphère

Jury :

Maxime Claprood, Professeur, Ph.D., UQAC, Président du Jury

Éric Rosa, Professeur, Ph.D., Université du Québec en Abitibi-Témiscamingue (UQAT), Membre externe

Marie Larocque, Professeur, Ph.D., Université du Québec à Montréal (UQAM), Membre interne

Julien Walter, Professeur, Ph.D., UQAC, Directeur

Romain Chesnaux, Professeur, Ph.D., UQAC, Co-Directeur

Renée-Luce, Professeur, Ph.D., UQAC, Directrice de l'unité des sciences de la Terre

Québec, Canada

RÉSUMÉ

Les dépôts quaternaires hétérogènes et anisotropes tel que les moraines présentent une importante variabilité spatiale de leur potentiel en eau souterraine. Bien qu'il existe des études géologiques et hydrogéologiques sur ces dépôts, peu de méthodes efficaces permettent une compréhension approfondie de leur potentiel en eau souterraine et de la circulation de l'eau au sein de ces formations du Quaternaire. En effet, les milieux sédimentaires hétérogènes de sous-surface sont composés d'une variété de sédiments tels que les tills, les argiles, les silts, les sables fins à grossiers et les graviers, ce qui complexifie davantage la compréhension de leurs propriétés hydrogéologiques et de leur potentiel en eau souterraine. La moraine de Saint-Narcisse constitue un exemple d'environnement de dépôt quaternaire fortement hétérogène et anisotrope, ce qui en fait un cadre idéal pour ce projet de doctorat. La compréhension de l'hydrogéologie (stratigraphie, piézométrie, propriétés hydrauliques, recharge) de tels dépôts quaternaires est limitée et nécessite des efforts supplémentaires pour expliquer la compartimentalisation spatiale du potentiel en eau souterraine au sein de certaines zones à l'intérieur d'un dépôt quaternaire tel qu'une moraine.

Pour répondre à cette exigence, le développement de nouvelles approches méthodologiques et d'outils d'investigation novateurs est essentiel pour estimer plus précisément le potentiel en eau souterraine des dépôts quaternaires. Les méthodologies utilisées pour générer chacun de ces outils d'investigation sont diverses, mais l'intégration de données géophysiques, telles que les relevés TEM, TRE et GPR, s'est avérée cruciale pour compléter les informations directes provenant des forages. Cette intégration des données géophysiques a facilité la corrélation entre les données stratigraphiques et piézométriques, ouvrant la voie à une modélisation numérique plus précise, ainsi qu'à une caractérisation et une évaluation plus juste du potentiel en eau souterraine des aquifères granulaires régionaux. Ces méthodes géophysiques, surtout lorsqu'elles sont combinées, ont démontré leur capacité à fournir un ensemble de données plus étendu et mieux réparti pour la modélisation à l'échelle régionale. Chaque méthode possède ses avantages et inconvénients, et leur combinaison contribue indéniablement à réduire les erreurs potentielles liées aux données indirectes.

Les résultats et les contributions importantes de cette étude sont (1) Une corrélation entre les données géophysiques, stratigraphiques et piézométriques, permettant ainsi la caractérisation des aquifères granulaires régionaux en termes de stratigraphie, de géométrie, d'épaisseur et d'étendue. (2) Une charte des valeurs de résistivité électrique englobant des gammes de résistivité applicables à quatorze catégories de sédiments, tant saturés que non saturés, dont sept n'ont pas fait l'objet d'études antérieures. Les résultats de cette investigation fournissent aux scientifiques et praticiens des données plus précises sur la résistivité électrique d'une gamme étendue de sédiments, qu'ils soient saturés ou non saturés. (3) L'utilisation de données géophysiques avec des méthodes combinées pour une évaluation plus juste des niveaux d'eau dans un aquifère non confiné en milieu granulaire. Grâce à une approche de modélisation discrète, cette étude démontre la comparabilité entre les niveaux d'eau souterrains estimés par les méthodes géophysiques et ceux obtenus par observation directe telles que les forages et les levés piézométriques. Les résultats soulignent la complémentarité des données géophysiques avec les observations directes, fournissant ainsi des informations hydrauliques supplémentaires pour les modélisateurs hydrologiques. (4) La calibration des modèles numériques d'écoulement en recourant à des données géophysiques. Cette méthode présente l'avantage d'optimiser les paramètres hydrauliques de manière économique, rapide et exhaustive. Suite à la calibration, le modélisateur est en mesure d'identifier de nouveaux paramètres hydrauliques, même dans les zones du modèle où il n'y en a pas. Cette approche contribue ainsi à améliorer la justesse et la fiabilité des modèles d'écoulement, tout en réduisant les coûts et les délais associés à la collecte de données.

L'expansion de ces outils d'investigations à d'autres régions et environnements climatiques permettra une compréhension plus holistique des réserves d'eau souterraine, soutenant ainsi le développement de stratégies de protection adaptées à chaque contexte géographique. Cette étude met en évidence le rôle croissant de la géophysique dans la caractérisation des aquifères et

l'évaluation de leur potentiel en eau souterraine, offrant une alternative peu coûteuse, non destructive, rapide, robuste et efficace par rapport aux méthodes d'observation directe. Bien que les approches et les outils d'investigation utilisés dans cette thèse ne soient pas originaux en eux-mêmes, leur combinaison spécifique pour l'étude du potentiel aquifère d'un dépôt quaternaire est novatrice, apportant une nouvelle perspective à la caractérisation spatiale d'un aquifère granulaire en nappe libre à l'échelle régionale.

TABLE DES MATIÈRES

LISTE DES TABLEAUX

LISTE DES FIGURES

DÉDICACE

L'électron sur quoi sont bâtis formes et mondes
a bondi dans l'être, particule de Dieu.
Étincelle de l'Énergie éternelle jaillie,
il est de l'Infini le minime séjour aveugle.

Dans ce menu char de flammes roule Shiva.
Le Un s'est avisé d'être innombrablement ;
Il cache Son unicité sous des formes imperceptibles,
infimes temples-du-Temps de l'Éternité.

Atome et molécule en leur plan invisible
étayent un édifice d'étranges unités,
Épanouissant son étincelle-d'âme en une épiphanie
de la vastitude sans-temps de l'Infinité.

Sri Aurobindo

REMERCIEMENTS

Tout d'abord, je tiens à exprimer ma gratitude envers mon directeur de recherche, Julien Walter, et à mon co-directeur de recherche, Romain Chesnaux, qui ont placé leur confiance en moi dès le début de ce projet de doctorat. Leur soutien et leurs compétences ont été précieux tout au long de cette aventure et ont grandement éclairé ma démarche. Julien, je tiens à te remercier pour ta compréhension, ta sensibilité, ton écoute et ton ouverture. Je te suis également reconnaissant de la liberté (tant géographique qu'académique) que tu m'as accordée tout au long de ce projet doctoral. Cette liberté est essentielle pour mon épanouissement personnel et mon appréciation d'un travail de longue haleine. Tu as su me cerner et me comprendre, et je t'en suis profondément reconnaissant.

Je souhaite également exprimer ma gratitude envers mon co-directeur de recherche, Romain Chesnaux, pour son précieux soutien. Ses suggestions novatrices et sa contribution aux différentes approches scientifiques ont enrichi mon projet de doctorat. Romain, je tiens à te remercier pour ton assistance, ta gentillesse, ton humanité et le respect dont tu as fait preuve à mon égard tout au long de cette aventure. Tu m'as toujours traité comme un collaborateur à part entière plutôt que comme un simple étudiant, et je t'en suis reconnaissant. Après quelques semaines laborieuses au début, nous avons finalement trouvé notre rythme, « la mayonnaise a fini par prendre » et je suis heureux de cette complicité. C'était vraiment une belle aventure académique et scientifique, et je tiens à vous remercier chaleureusement Julien et Romain.

Un remerciement particulier à l'équipe du PACES, à Mélanie Lambert, à David Noel et à Laura-Pier Desmeules, pour leur soutien tout au long de ce projet, ainsi que pour leur disponibilité lorsque j'avais des questions sur des points particulièrement complexes.

Jihed, mon cher ami, que dire de nos magnifiques soirées et de nos parties d'échecs épiques autour d'un bon café. L'amitié que nous avons développée durant ce doctorat est inestimable. Une amitié pour la vie !

Doudou, je ne saurais jamais assez te remercier pour ton amitié et ta grande générosité. Qui aurait cru que nous partagerions autant de bons moments depuis notre rencontre au baccalauréat ? Tu m'as toujours accueilli chez toi à bras ouverts, et je dois avouer que sans cette amitié et ce pied-à-terre à Chicoutimi, ma vie serait bien moins colorée et beaucoup moins simple ! Merci pour tout, mon ami, les discussions, les fous rires, les sorties en forêt et bien sûr... les potins !

Andrée, Pierrot, Seb, Eduardo, Fahed, André et Thomas, mes chers amis, je tiens à vous remercier du fond du cœur. Votre soutien inconditionnel, votre amitié sincère et les moments inoubliables que nous avons partagés ont illuminé mon parcours doctoral. Les belles soirées, les baignades, les promenades et les délicieux repas que nous avons partagés resteront gravés dans ma mémoire. Votre présence constante et votre capacité à me faire sourire ont été des sources d'inspiration et de motivation tout au long de cette expérience. Merci d'avoir rendu ce voyage académique non seulement fructueux, mais également joyeux et mémorable.

Enfin, je ne saurais oublier ma chère Omnain, qui m'a accompagné, aidé, soutenu et encouragé tout au long de cette aventure. Ta présence précieuse a fait toute la différence, et je te suis infiniment reconnaissant.

Merci du fond du cœur, Omi !

INTRODUCTION

En 2008, le Gouvernement du Québec a décidé de mettre en œuvre le Programme d'acquisition de connaissances sur les eaux souterraines (PACES). Ces projets PACES visaient à dresser un aperçu réaliste et concret des ressources en eaux souterraines des territoires municipalisés du Québec méridional dans le but de les protéger et d'en assurer la pérennité (Chesnaux et Elliott 2011, Cloutier et al. 2011, 2013, 2015, Ouellet et al. 2011, Rouleau et al. 2012, Carrier et al. 2013, Larocque et al. 2015, Montcoudiol et al. 2015, Nadeau et al. 2015, 2018, 2021, Laplante 2021, Walter et al. 2022, Delisle 2022, Gagné et al. 2022, Larocque 2023). Depuis 2009, le PACES a permis de subventionner dix-huit projets sur le territoire municipalisé du Québec, dont 13 ont été déjà complétés et 5 autres ont été terminés en 2022. À partir des données existantes et nouvellement acquises, le présent projet de doctorat s'insère en partie dans le programme de recherche du PACES. Celui-ci constitue un catalyseur pour la réalisation d'études plus approfondies afin d'affiner la compréhension des eaux souterraines et de développer des outils hydrogéologiques au Québec.

Dans l'est du Canada, la plupart des dépôts de surface sont hérités de la dernière phase de glaciation du Wisconsinien (entre ~ 24 et 14 ka BP). Durant cette glaciation, la calotte polaire Laurentidienne (Laurentidian Ice Sheet : LIS) recouvrait la majeure partie du Canada et pouvait même atteindre des épaisseurs de 5 kms à certains endroits (Dyke et Prest 1987, Dyke 2004, Evans 2005, Benn et Evans 2010, Margold et al. 2015, Stokes 2017, Lévesque et al. 2019, Brouard et al. 2021, McMartin et al. 2021, Godbout et al. 2023). Cet inlandsis était une masse de glace en mouvement qui broyait, arrachait et transportait la roche pour créer des dépôts glaciaires (c.-à-d. tills) constitués majoritairement de diamictons. Lors de ses avancées et ses reculs dus aux variations climatiques, la LIS a laissé sur place de nombreuses moraines frontales, sorte de longs cordons composés de sédiments quaternaires (p. ex., sédiments fluvioglaciaires, juxtaglaciaires (tills de fond, tills d'ablation et de fusion), glaciomarins et glaciolacustres) à l'avant du glacier et qui ont été laissées sur place lors du dernier cycle de déglaciation (Evans 2005, Benn et Evans 2010, Landry et al. 2012).

Parmi les nombreuses moraines retrouvées au Québec, la moraine de Saint-Narcisse constitue une des plus longues moraines frontales aujourd'hui documentées. Elle recoupe le territoire à l'étude (Mauricie-Est) dans le cadre du PACES 2018-2022. Celle-ci, dont l'âge se situe entre 12,7-12,4 cal. ka BP (Daigneault et Occhietti 2006) est une formation majeure qui s'étend de Saint-Siméon au Québec jusqu'aux Grands Lacs en Ontario. Elle est le résultat du retrait de l'inlandsis après une période de refroidissement daté du Dryas récent (Parent et Occhietti 1988, 1999, Simard et al. 2003, Daigneault et Occhietti 2006, Occhietti 2007) et son épaisseur peut atteindre jusqu'à 100 mètres, même si elle varie généralement entre 1 et 20 mètres localement (Occhietti 1977, 1980, 2007). Selon Occhietti (2007), la moraine de Saint-Narcisse est composée de dépôts quaternaires tels que des dépôts glaciomarins proximaux, des dépôts fluvioglaciaires et juxtaglaciaires, des tills et des argiles marines remaniées au niveau de la basse vallée du Saint-Maurice (Parent et Occhietti 1988, 1999, Occhietti et al. 2001, Simard et al. 2003). Ces imbrications et ces superpositions de couches sédimentaires d'origines variées peuvent devenir très morcelées en profondeur et générer ainsi une importante hétérogénéité dans la moraine, ce qui conditionne l'écoulement de son eau souterraine. À l'intérieur de la moraine, les sédiments se caractérisent généralement par des dépôts chaotiques glaciaires présentant localement un tri pauvre et donc, de faibles conductivités hydrauliques et transmissivités. Des zones de sables et graviers bien triés ont également été observées (Occhietti 1977, 2007, Girard 2001, Daigneault and Occhietti 2006) et elles constituent des aquifères potentiellement intéressants. Lorsqu'elles sont exposées à la surface de la moraine, ces unités perméables peuvent également constituer des zones de recharge (Fagnan 1998).

La moraine de Saint-Narcisse offre un cadre adéquat à ce projet doctoral. Ce site permet de développer une approche méthodologique et des outils d'investigation adaptés au besoin de l'hydrogéologie pour mieux évaluer le potentiel aquifère des milieux de dépôts quaternaires fortement hétérogènes et anisotropes. Le potentiel aquifère, également appelé potentiel en eau souterraine, réfère à la capacité d'un milieu à se recharger, à fournir de l'eau par unité de

volume (c.-à-d., le coefficient d'emmagasinement), et à se laisser traverser par un fluide (c.-à-d., la perméabilité intrinsèque du milieu).

1) PROBLÉMATIQUE

Dû à son potentiel aquifère, la moraine de Saint-Narcisse est localement exploitée à des fins d'alimentation en eau potable par plusieurs municipalités en Mauricie-Est (p. ex., Saint-Narcisse, Saint-Prosper, Saint-Maurice, Sainte-Geneviève-de-Batiscan). L'importante variabilité spatiale observée dans les dépôts quaternaires (Occhietti 1977, 2007, Sharpe et al. 2003, Bajc et al. 2014, Burt 2018) amène à se demander comment l'anisotropie et l'hétérogénéité de ces dépôts contrôlent le potentiel aquifère d'une moraine. Cette variabilité spatiale en profondeur augmente la difficulté de compréhension du potentiel aquifère, de même que l'absence de connaissances des paramètres hydrogéologiques qui contrôlent les volumes d'eau dans ce type de dépôts quaternaires. De plus, cette forte variabilité spatiale (hétérogénéité) des couches sédimentaires génère possiblement des effets d'échelle prononcés, comme cela a été documenté par de nombreux auteurs (Schulze-Makuch et al. 1999, Vogel et Roth 2003, Nastev et al. 2004, Chapuis et al. 2005, Chesnaux et Elliot 2011). Le gradient hydraulique et les tenseurs de perméabilité seront très influencés par l'hétérogénéité de l'aquifère à l'intérieur de la moraine. Cette hétérogénéité est présente localement en profondeur, mais latéralement, elle se manifeste également à l'échelle régionale en raison de la compartimentalisation des dépôts, entraînant ainsi une compartimentalisation hydraulique à l'échelle régionale. L'évaluation de la capacité aquifère de la formation est donc directement liée à l'évaluation des propriétés hydrogéologiques et à la compréhension du contexte géomorphologique local lors de la mise en place des dépôts quaternaires (Bajc et al. 2014, Richard et al. 2014, Arnaud et al. 2017).

Des approches fondamentalement différentes pour modéliser les relations hydro-géophysiques, telles que la représentation de la variabilité et de l'incertitude des paramètres hydrauliques dans des aquifères hétérogènes, impliquent l'application de techniques

géostatistiques. L'utilisation de ces méthodes est souvent essentielle pour optimiser les informations disponibles et évaluer la variabilité et l'incertitude dans la modélisation de tout type de réservoirs. Ces méthodes géostatistiques sont couramment appliquées aux champs de paramètres à grande échelle régionale dans les industries pétrolières et minières, et elles se prêtent naturellement à l'assimilation de données ayant différents degrés de résolution et de fiabilité.

Contrairement aux expressions théoriques ou empiriques, les techniques statistiques sont plus flexibles et nécessitent moins de connaissances géologiques préalables. Les méthodes statistiques proposées pour définir des relations hydro-géophysiques complexes incluent les modèles de régression linéaire normale (Chen et al. 2001), les réseaux de neurones artificiels (Saemi et al. 2007, Karimpouli et al. 2010), l'intégration de données hydrologiques et géophysiques à grande échelle, et les machines à vecteurs de support (Al-Anazi et Gates 2010, Helmy et al. 2010). L'approche stochastique est également bien adaptée pour modéliser les paramètres hydrologiques en intégrant différentes données géophysiques. Par exemple, les méthodes de clustering (Paasche et al. 2006, Gloaguen et al. 2007), la simulation bayésienne et les techniques de simulation conditionnelle (Tronicke et Holliger 2005, Ruggeri et al. 2013a, 2013b, Nussbaumer et al. 2020, Santos et al. 2024) présentent le grand avantage d'être flexibles car elles ne nécessitent aucune relation pétrophysique préalable et permettent l'intégration de toutes les données hydrogéologiques connues dans le modèle. Dans ce projet doctoral, nous n'avons pas recours aux techniques avancées de géostatistique, mais nous restons conformes aux méthodes standards couramment utilisées via une relation pétrophysique locale et empirique.

Le potentiel aquifère d’une moraine a été abordé à maintes reprises (Russell et al. 1998, Sharpe et al. 2003, Bajc et al. 2014, Burt 2018, Légaré-Couture et al. 2018). Cependant, rares sont les apports scientifiques qui ont permis la création d’outils d’investigations afin d’évaluer avec une plus grande précision le potentiel aquifère réel de ce type de dépôt quaternaire fortement hétérogène a l’échelle régionale. Des recherches récentes semblent s'engager dans

cette direction en proposant de nouvelles méthodes et outils d'investigation pour évaluer plus précisément le potentiel aquifère des dépôts quaternaires à l'échelle régionale (Sattel et Kgotlhang 2004, Knight et al. 2018, Nadeau et al. 2015, 2018, 2021). Cependant, des efforts supplémentaires sont nécessaires pour combler cette lacune.

En outre, les modèles conceptuels hydrogéologiques construits sur les moraines québécoises, ontariennes et ailleurs dans le monde, se concentrent essentiellement sur l'aspect stratigraphique (Russell et al. 1998, Sharpe et al. 2003, Bajc et al. 2014, Burt 2018, Légaré-Couture et al. 2018). Les paramètres hydrogéologiques qui contrôlent les volumes d'eaux, les directions d'écoulement et les mécanismes de recharge de ces dépôts quaternaires sont souvent évalués de façon sommaire et basée sur une caractérisation globale des grands aquifères et aquitards présents (Occhietti 1977, 2007, Ross et al. 2005, Bajc et al. 2014, Arnaud et al. 2017, Burt 2018, Légaré-Couture et al. 2018). Par exemple, la cartographie hydrogéologique régionale de nombreuses entités géologiques telles que les moraines semble souffrir d'un manque de précision dans l'attribution de leurs potentiels en eaux souterraines et des propriétés hydrogéologiques de leurs dépôts de surface et de sous-surface. En effet, l'utilisation du terme aquifère pour des dépôts granulaires est parfois erronée, car ces types de dépôts ne contiennent pas nécessairement une quantité d'eau exploitable, mais sont parfois asséchés et en réalité, leurs potentiels aquifères réels sont faibles, surtout si leurs recharges sont limitées. Bien que certains auteurs aient décrit de manière plus précise les dépôts de surface et de sous-surface d'une région, ainsi que le potentiel aquifère d'une région donnée (Nadeau et al. 2015, 2018), de nombreux auteurs considèrent les dépôts de sédiments granulaires comme des systèmes aquifères et décrivent l'ensemble d'une moraine comme un aquifère granulaire dans son ensemble, une généralisation souvent incorrecte (Barnett et al. 1998, Sharpe et al. 2003, Ross et al. 2005, Bajc et al. 2014, Arnaud et al. 2017, Burt 2018, Légaré-Couture et al. 2018). D'autres auteurs suggèrent que tout type de sédiments fins (c.-à-d. silts et argiles) et glaciaires (c.-à-d. tills) sont des aquitards ou des aquicludes, et que toute autre sorte de sédiments granulaires (c.-à-d. sables et graviers), de roches cristallines (c.-à-d. ignées et métamorphiques) et même tous types de sédiments indifférenciés sont

automatiquement classifiés comme étant des aquifères (Barnett et al. 1998, Ross et al. 2005, Bajc et al. 2014, Burt 2018). Par exemple, pour délimiter les entités hydrogéologiques, les chercheurs ont élaboré des protocoles impliquant la simplification, parfois excessive, de l'hétérogénéité naturelle des dépôts à une échelle sous-régionale, c'est-à-dire à l'échelle de l'entité hydrogéologique. Cette homogénéisation est particulièrement vraie pour les dépôts de surface, d'autant plus que la légende actuelle des cartes produites par le ministère des Ressources naturelles et de la Forêt correspond à une légende basée sur la genèse des dépôts (p. ex., glaciaire, fluvioglaciaire, glaciomarin) et n'est en aucun cas descriptive (c.-à-d., les caractéristiques physiques des dépôts tel que le silt, le sable, le gravier et l'argile).

Cette classification, qui ne précise pas le niveau de capacité aquifère réel génère de nombreuses contradictions. De plus, même si les moraines sont souvent composées en grande partie de tills, le terme de moraine ne se rapporte pas à une composition granulométrique, mais plutôt à la forme et à la genèse du dépôt (Evans 2005, Benn et Evans 2010, Landry et al. 2012). Ce type de classification cartographique est, encore aujourd'hui, de notoriété publique et couramment utilisé dans le domaine de l'hydrogéologie. Ces simplifications ne reflètent malheureusement pas le potentiel réel en eaux souterraines de la plupart, voire de la majorité des dépôts du Quaternaire.

Afin de déterminer la stratigraphie et d'évaluer le potentiel aquifère des dépôts morainiques, plusieurs études ont été réalisées dans le but de développer des modèles conceptuels. Cependant, ces modèles présentent généralement des limitations en termes de détails stratigraphiques et hydrogéologiques, ce qui rend difficile l'identification des limites des couches sédimentaires imbriquées en profondeur. Par conséquent, l'estimation du potentiel en eau souterraine manque souvent de justesse et ne permet pas de déterminer la géométrie, l'épaisseur et l'étendue de l'aquifère. Pour remédier à ces lacunes, de nouveaux outils hydrogéologiques ainsi que de nouvelles méthodologies doivent être développées. Ces méthodes doivent impérativement permettre de générer des modélisations numériques approfondies reposant sur un ensemble de données conséquent. Ces modélisations 3D

permettront d'améliorer la compréhension des caractéristiques stratigraphiques des dépôts morainiques, de préciser les limites des couches sédimentaires imbriquées en profondeur et d'obtenir une estimation plus précise du potentiel en eau souterraine. Ces nouvelles approches contribueront à combler les lacunes existantes et à favoriser une meilleure exploration et gestion des ressources aquifère (Nadeau et al. 2015, 2018, 2021, Knight et al. 2018).

La profondeur de la nappe (c-à-d., la piézométrie) est une autre donnée essentielle rarement considérée. Une différenciation entre les sédiments saturés et non saturés est pourtant essentielle afin de déterminer la profondeur de la nappe d'eau souterraine (et donc de l'aquifère) à l'échelle régionale (Daigneault et Occhietti 2006, Occhietti 2007, Bajc et al. 2014, Burt 2018, Légaré-Couture et al. 2018). Au Québec, la stratigraphie interne de la moraine de Saint-Narcisse a été étudiée principalement par Occhietti et al. (1977, 1980, 2001, 2007), Daigneault et Occhietti (2006), Girard (2001), Parent et Occhietti (1988, 1999) et Simard et al. (2003).

Bien qu'il existe une multitude de modèles conceptuels et de rapports géologiques et hydrogéologiques concernant les dépôts quaternaires, il existe peu d'outils d'investigation spécialisés afin de mieux déterminer et comprendre leur potentiel aquifère à l'échelle régionale, leurs caractéristiques hydrogéologiques internes, ainsi que le cheminement de l'eau à l'intérieur de ces dépôts fortement hétérogènes et anisotropes. La compréhension du système aquifère des dépôts quaternaires et des moraines est déficiente et nécessite un effort supplémentaire afin de déterminer pourquoi certaines zones à l'intérieur de ces dépôts sont de bons aquifères (en terme de recharge, coefficient d'emmagasinnement (rendement spécifique) et perméabilité intrinsèque) alors que d'autres ne le sont pas. Cette étude propose des méthodes de caractérisation hydrogéologique robustes conduisant à la modélisation numérique des écoulements à l'échelle régional à moindre coût, notamment en utilisant la géophysique.

2) OBJECTIFS

Ce travail de recherche vise à améliorer la compréhension de la capacité aquifère au sein d'un environnement de dépôt quaternaire hétérogène et à développer des outils d'investigation spécialisés et de nouvelles méthodes de caractérisation des eaux souterraines dans ces milieux. Afin d'y parvenir, les étapes et les objectifs suivants ont dû être atteints :

1) Définir la stratigraphie et le contexte géologique du système aquifère de la moraine de Saint-Narcisse.

2) Établir des relations entre les propriétés hydrogéologiques de la moraine et les caractéristiques physiques du sol en ayant recours à des techniques de mesures indirectes.

3) Acquérir une meilleure compréhension des unités hydrogéologiques, du potentiel en eau souterraine et des propriétés hydrauliques des systèmes aquifères dans des environnements de dépôts quaternaires hétérogènes et anisotropes en utilisant de nouveaux outils d'investigation.

4) Élaborer des approches innovantes de modélisation numérique qui intègrent les données géophysiques afin d'améliorer la caractérisation et l'évaluation du potentiel en eau souterraine d'un aquifère granulaire régional.

En atteignant ces objectifs, cette recherche permettra d'améliorer la compréhension des ressources en eau souterraine au sein des dépôts quaternaires hétérogènes, et fournira des informations précieuses pour une gestion durable et une utilisation optimale de ces systèmes aquifères.

L’objectif principal de cette thèse est donc de développer une approche méthodologique afin d’estimer le potentiel aquifère d'un milieu de dépôt quaternaire hétérogène et anisotrope. Afin d'y parvenir, plusieurs outils d'investigation pour déterminer le potentiel en eau souterraine ont été développés. Ces outils sont basés essentiellement sur une approche géophysique

couplée avec des données de forages et des données piézométriques. Des modèles numériques en trois dimensions ont également été développés et mis à contribution afin de développer ces nouveaux outils.

Ces outils d'investigation comprennent (1) une approche hydrogéophysique qui permet de corréler les informations stratigraphiques et piézométriques, et de caractériser les aquifères granulaires régionaux en termes de stratigraphie, de géométrie, d'épaisseur et d'étendue; (2) une charte des valeurs de résistivité électrique applicables à quatorze classes de sédiments saturés et non saturés dans l'est du Canada; (3) une approche de modélisation discrète qui met de l'avant l'utilisation de données géophysiques pour déterminer avec précision les niveaux d'eau dans un aquifère granulaire à nappe libre. Les résultats suggèrant que les niveaux d'eau souterraines estimés à l'aide des méthodes géophysiques sont comparables à ceux déterminés par observation directe dans des forages et lors des levés piézométriques. (4) une approche de calibration des modèles numériques d'écoulement avec des données géophysiques. Les approches 3 et 4 fournissent des informations hydrauliques supplémentaires aux modélisateurs hydrogéologiques et permettent d'optimiser des paramètres hydrauliques à moindre coût et avec une acquisition de données plus rapide et plus complète comparativement aux forages.

3) STRUCTURE DE LA THÈSE

Le contenu de cette thèse est organisé en cinq chapitres. Le chapitre 1 vise à présenter une vue d'ensemble générale du projet d'acquisition de connaissances sur les eaux souterraines (PACES) réalisé sur le territoire de l'est de la Mauricie. Il donne un aperçu général de la région d'étude, ainsi que des outils d'investigation et des méthodologies qui sont proposés dans les quatre autres articles produits dans le cadre de ce doctorat. Ce chapitre fournit donc des informations substantielles sur la caractérisation des aquifères et de leurs

environnements géologiques, afin de mieux gérer et protéger les ressources en eaux souterraines.

Le chapitre 2 constitue le premier outil d'investigation développé dans cette approche méthodologique visant à améliorer l'évaluation du potentiel aquifère dans des milieux de dépôts quaternaires hétérogènes et anisotropes. Étant donné que les contextes géologiques qui ont des lacunes en termes d'informations stratigraphiques et piézométriques sont initialement difficiles à cartographier sur le plan hydrogéologique, ce chapitre propose une approche permettant de caractériser un aquifère régional en utilisant des données géophysiques (Transient ElectroMagnetic surveys - levés électromagnétiques transitoires (TEM)). Cette approche permet de corréler les informations stratigraphiques et piézométriques et de caractériser les aquifères granulaires régionaux en termes de stratigraphie, de géométrie, d'épaisseur et d'étendue.

Le chapitre 3 constitue le deuxième outil d'investigation développé dans cette approche méthodologique. Il propose une charte des valeurs de résistivité électrique comprenant des plages de résistivité applicables à quatorze catégories de sédiments saturés et non saturés au Québec, dont sept, à notre connaissance, n'ont pas été incluses dans des études antérieures. Parmi ces classes de sédiments nouvellement considérées, nous trouvons les argiles limoneuses, les argiles avec du sable/gravier/cailloux, les silts argileux non saturés avec du sable, les sables limoneux saturés et non saturés, ainsi que les sables argileux saturés et non saturés avec du gravier. Les résultats de cette étude fournissent aux scientifiques et aux praticiens des caractéristiques précises de la résistivité électrique d'une vaste gamme de sédiments saturés et non saturés. Ces informations permettent une évaluation plus précise des ressources en eau souterraine, offrant ainsi des avantages importants pour les études hydrogéologiques et la gestion des ressources en eau.

Le chapitre 4 de cette thèse constitue le troisième outil d'investigation et met en avant l'utilisation de données géophysiques pour une détermination précise des niveaux d'eau dans un aquifère granulaire à nappe libre. Grâce à une approche de modélisation discrète, cette étude suggère que les niveaux d'eau souterraines estimés à l'aide des méthodes

géophysiques sont comparables à ceux obtenus par observation directe. Les résultats mettent en évidence comment les données géophysiques peuvent compléter les observations directes, telles que les forages et les levés piézométriques, afin de fournir des informations hydrauliques supplémentaires aux modélisateurs hydrologiques.

Le chapitre 5 constitue le quatrième outil d'investigation, proposant une approche novatrice pour la calibration des modèles numériques d'écoulement en utilisant des données géophysiques. Cette approche offre l'avantage d'optimiser les paramètres hydrauliques à moindre coût et avec une acquisition de données plus rapide et plus exhaustive. Après la calibration, le modélisateur est également en mesure d'identifier plus aisément de nouveaux paramètres hydrauliques dans les zones du modèle qui en avait aucun. Cette méthode permet ainsi d'améliorer la précision et la fiabilité des modèles d'écoulement tout en réduisant les coûts et les délais associés à la collecte de données.

Les chapitres quatre et cinq apportent des contributions précieuses à la communauté des modélisateurs en hydrogéologie en proposant de nouveaux outils pour améliorer les modèles numériques d'écoulement à l'échelle régionale. Ces outils sont cruciaux pour une gestion appropriée des ressources en eau souterraine, tant au Québec et au Canada qu'à l'échelle mondiale. Ainsi, les méthodes géophysiques se présentent comme une alternative peu coûteuse, non destructive, rapide, robuste et efficace par rapport aux méthodes d'observation directes. Elles permettent de caractériser avec précision les niveaux d'eau, les dimensions internes et la variabilité stratigraphique des aquifères non confinés dans des régions où les données sont limitées. En conséquence, les méthodes géophysiques offrent une évaluation plus précise des ressources en eau souterraine, tout en étant rapides et plus économiques par rapport aux méthodes traditionnelles. Ces avancées contribuent ainsi à une meilleure gestion des ressources en eau souterraine, en particulier dans les régions où les données sont rares ou limitées.

Les chapitres 1, 2, 3, 4 et 5 font l'objet de publications scientifiques et sont présentés dans cette thèse sous forme d'articles scientifiques évalués par les pairs. L'article 1 (chapitre 1) a été publié dans la Revue canadienne des ressources hydriques (Canadian Water

Resources Journal – IF : 2) le 26 juillet 2023. L'article 2 (chapitre 2) a été publié dans la revue Geosciences (IF : 3,03) en octobre 2021. L'article 3 (chapitre 3) a été publié dans la revue Environmental Earth Sciences (IF : 3,15) le 1er juin 2023. L'article quatre (chapitre 4) a été publié dans la revue Hydrogeology Journal (IF : 3,18) en janvier 2023. Finalement, l'article cinq (chapitres 5) sera soumis prochainement dans la revue Environmental Earth Sciences (IF : 3,15).

LISTE DE RÉFÉRENCES

Al-Anazi, A., and Gates, I.D. 2010. A support vector machine algorithm to classify lithofacies and model permeability in heterogeneous reservoirs. Engineering Geology, 114: 267–277. Elsevier.

Arnaud, E., McGill, M., Trapp, A., and Smith, J.E. 2017. Subsurface heterogeneity in the geological and hydraulic properties of the hummocky Paris Moraine, Guelph, Ontario. Canadian Journal of Earth Sciences, 55: 768–785. NRC Research Press.

Bajc, A.F., Russell, H.A.J., and Sharpe, D.R. 2014. A three-dimensional hydrostratigraphic model of the Waterloo Moraine area, southern Ontario, Canada. Canadian Water Resources Journal/Revue canadienne des ressources hydriques, 39: 95–119. Taylor & Francis.

Barnett, P.J., Sharpe, D.R., Russell, H.A.J., Brennand, T.A., Gorrell, G., Kenny, F., and Pugin, A. 1998. On the origin of the Oak Ridges Moraine. Canadian Journal of Earth Sciences, 35: 1152–1167. NRC Research Press.

Benn, D., and Evans, D.J.A. 2010. Glaciers and glaciation. In 1ST edition. Routledge, London and New York. doi:10.4324/9780203785010.

Brouard, E., Roy, M., Godbout, P.-M., and Veillette, J.J. 2021. A framework for the timing of the final meltwater outbursts from glacial Lake Agassiz-Ojibway. Quaternary Science Reviews, 274: 107269. Elsevier.

Burt, A. 2018. Three-dimensional hydrostratigraphy of the Orangeville Moraine area, southwestern Ontario, Canada. Canadian Journal of Earth Sciences, 55: 802–828. GeoScienceWorld. doi:10.1139/cjes-2017-0077.

Carrier, M.-A., Lefebvre, R., Rivard, C., Parent, M., Ballard, J.-M., Benoît, N., Vigneault, H., Beaudry, C., Malet, X., and Laurencelle, M. 2013. Portrait des ressources en eau souterraine en Montérégie Est, Québec, Canada. Rapport de recherche (R1433). INRS, Centre Eau Terre Environnement, Québec (Qc), 319 p.

Chapuis, R.P., Dallaire, V., Marcotte, D., Chouteau, M., Acevedo, N., and Gagnon, F. 2005. Evaluating the hydraulic conductivity at three different scales within an unconfined sand aquifer at Lachenaie, Quebec. Canadian geotechnical journal, 42: 1212–1220. doi:10.1139/t05-045.

Chen, J., Hubbard, S., and Rubin, Y. 2001. Estimating the hydraulic conductivity at the South Oyster Site from geophysical tomographic data using Bayesian techniques based on the normal linear regression model. Water Resources Research, 37: 1603–1613. Wiley Online Library.

Chesnaux, R., and Elliott, A.-P. 2011. Demonstrating evidence of hydraulic connections between granular aquifers and fractured rock aquifers. In Proceedings of GeoHydro 2011, Joint Meeting of the Canadian Quaternary Association and the Canadian Chapter of the International Association of Hydrogeologists. pp. 28–31.

Cloutier, V., Aubert, T., Audet-Gagnon, F., Blanchette, D., Castelli, S., Cheng, L.Z., Dallaire, P.-L., Fallara, F., Godbout, G., and Nadeau, S. 2011. Projet d'acquisition de connaissances sur les eaux souterraines de l'Abitibi-Témiscamingue, Québec. Proceedings, Geohydro,.

Cloutier, V., Blanchette, D., Dallaire, P.-L., Nadeau, S., Roy, M., and Rosa, E. 2013. Projet d'acquisition de connaissances sur les eaux souterraines de l'Abitibi-Témiscamingue (partie 1). Rapport final déposé au MDDEFP 135 p., 26 annexes, 25 cartes thématiques.

Cloutier, V., Rosa, E., Nadeau, S., Dallaire, P.-L., Blanchette, D., & Roy, M. 2015. Projet d'acquisition de connaissances sur les eaux souterraines de l'Abitibi-Témiscamingue (partie 2). Rapport de recherche P002.R3. Groupe de recherche sur l'eau souterraine,

Institut de recherche en mines et en environnement, Université du Québec en Abitibi-Témiscamingue, 313 p., 15 annexes, 24 cartes thématiques (1:100 000).

Daigneault, R.-A., and Occhietti, S. 2006. Les moraines du massif Algonquin, Ontario, au début du Dryas récent, et corrélation avec la Moraine de Saint-Narcisse. Géographie physique et Quaternaire, 60: 103–118. doi:10.7202/016823ar.

Delisle, R. 2022. Développement d'une démarche collaborative pour l'élaboration d'un plan d'action sur l'eau souterraine en Estrie. Université Laval.

Denis, R. 1974. Late Quaternary geology and geomorphology in the Lake Maskinongé area, Québec. Uppsala, Sweden.

Dietrich, P., Ghienne, J., Schuster, M., Lajeunesse, P., Nutz, A., Deschamps, R., Roquin, C., and Duringer, P. 2017. From outwash to coastal systems in the Portneuf–Forestville deltaic complex (Quebec North Shore): Anatomy of a forced regressive deglacial sequence. Sedimentology, 64: 1044–1078. Wiley Online Library.

Dyke, A.S. 2004. An outline of the deglaciation of North America with emphasis on central and northern Canada. Quaternary Glaciations-Extent and Chronology, Part II: North America, 2b: 373-424. doi:10.1016/S1571-0866(04)80209-4.

Dyke, A.S., and Prest, V.K. 1987. Late Wisconsinan and Holocene history of the Laurentide Ice Sheet. Geographie Physique et Quaternaire, 41: 237–263. doi:10.7202/032681ar.

Evans, D. 2005. Glacial landsystems. In 1ST edition. Edited ByRoutledge. Routledge, London (UK) and New York (USA). doi:10.4324/9780203784976.

Fagnan, N. 1998. Cartographie hydrogéologique régionale et vulnérabilité des aquifères de la MRC de Portneuf. Université du Québec, Institut national de la recherche scientifique.

Gagné, S., Larocque, M., Morard, A., and Roux, M. 2022. Projet d'acquisition de connaissances sur les eaux souterraines dans la région des Laurentides et de la MRC les Moulins. Rapport synthèse. Rapport déposé au ministère de l'Environnement et de la Lutte contre les changements climatiques. Université du Québec à Montréal.

Girard, F. 2001. Architecture et hydrostratigraphie d'un complexe morainique et deltaïque dans

la région de Saint-Raymond de Portneuf, Québec. PhD Thesis, Université du Québec, Institut national de la recherche scientifique, Quebec (Qc), 177 p.

Gloaguen, E., Giroux, B., Marcotte, D., and Dimitrakopoulos, R. 2007. Pseudo-full-waveform inversion of borehole GPR data using stochastic tomography. Geophysics, 72: J43–J51. Society of Exploration Geophysicists.

Godbout, P.-M., Brouard, E., and Roy, M. 2023. 1-km resolution rebound surfaces and paleotopography of glaciated North America since the Last Glacial Maximum. Scientific Data, 10: 735. Nature Publishing Group UK London.

Helmy, T., Fatai, A., and Faisal, K. 2010. Hybrid computational models for the characterization of oil and gas reservoirs. Expert Systems with Applications, 37: 5353–5363. Elsevier.

Karimpouli, S., Fathianpour, N., and Roohi, J. 2010. A new approach to improve neural networks' algorithm in permeability prediction of petroleum reservoirs using supervised committee machine neural network (SCMNN). Journal of Petroleum Science and Engineering, 73: 227–232. Elsevier.

Knight, R., Smith, R., Asch, T., Abraham, J., Cannia, J., Viezzoli, A., and Fogg, G. 2018. Mapping aquifer systems with airborne electromagnetics in the Central Valley of California. Groundwater, 56: 893–908. Wiley Online Library.

Landry, B., Beaulieu, J., Gauthier, M., Lucotte, M., Moingt, S., Occhietti, S., Pinti, D.L., and Quirion, M. 2012. Notions de géologie. In Modulo, Montréal, 4nd ed. Modulo, Montréal (Qc).

Laplante, R. 2021. Évaluation d'approches complémentaires pour déterminer la connectivité entre les milieux humides et l'eau souterraine et de surface.

Larocque, M. 2023. Eaux souterraines Un premier inventaire des connaissances scientifiques. Vecteur Environnement, 56: 22–24. Réseau Environnement.

Larocque, M., Meyzonnat, G., Ouellet, M.-A., Graveline, M.-H., Gagné, S., Barnetche, D., and Dorner, S. 2015. Projet de connaissance des eaux souterraines de la zone Vaudreuil-Soulanges: rapport final déposé au ministère du Développement durable, de l'Environnement et de la Lutte contre les changements climatiques. Université du Québec à Montréal, Montréal, Québec, 202 p.

Légaré-Couture, G., Leblanc, Y., Parent, M., Lacasse, K., and Campeau, S. 2018. Three-dimensional hydrostratigraphical modelling of the regional aquifer system of the St. Maurice Delta Complex (St. Lawrence Lowlands, Canada). Canadian Water Resources Journal/Revue canadienne des ressources hydriques, 43: 92–112. doi:10.1080/07011784.2017.1316215.

Lévesque, Y., St-Onge, G., Lajeunesse, P., Desiage, P., and Brouard, E. 2019. Defining the maximum extent of the Laurentide Ice Sheet in Home Bay (eastern Arctic Canada) during the Last Glacial episode. Boreas, 49: 52–70. doi:10.1111/bor.12415.

Margold, M., Stokes, C.R., and Clark, C.D. 2015. Ice streams in the Laurentide Ice Sheet: Identification, characteristics and comparison to modern ice sheets. Earth-Science Reviews, 143: 117–146. doi:10.1016/j.earscirev.2015.01.011.

McMartin, I., Godbout, P., Campbell, J.E., Tremblay, T., and Behnia, P. 2021. A new map of glacigenic features and glacial landsystems in central mainland Nunavut, Canada. Boreas, 50: 51–75. Wiley Online Library.

Montcoudiol, N., Molson, J., Lemieux, J.-M., and Cloutier, V. 2015. A conceptual model for groundwater flow and geochemical evolution in the southern Outaouais Region, Québec, Canada. Applied Geochemistry, 58: 62–77. Elsevier.

Nadeau, S., Rosa, E., Cloutier, V., Daigneault, R.-A., and Veillette, J. 2015. A GIS-based approach for supporting groundwater protection in eskers: Application to sand and gravel extraction activities in Abitibi-Témiscamingue, Quebec, Canada. Journal of Hydrology: Regional Studies, 4: 535–549. Elsevier.

Nadeau, S., Rosa, E., and Cloutier, V. 2018. Stratigraphic sequence map for groundwater assessment and protection of unconsolidated aquifers: A case example in the Abitibi-Témiscamingue region, Québec, Canada. Canadian Water Resources Journal/Revue canadienne des ressources hydriques, 43: 113–135. Taylor & Francis.

Nadeau, S., Rosa, E., Cloutier, V., Mayappo, D., Paran, F., and Graillot, D. 2021. Spatial analysis approaches for the evaluation and protection of groundwater resources in large watersheds of the Canadian Shield. Hydrogeology Journal, 29: 2053–2075. Springer Nature BV.

Nastev, M., Savard, M.M., Lapcevic, P., Lefebvre, R., and Martel, R. 2004. Hydraulic properties

and scale effects investigation in regional rock aquifers, south-western Quebec, Canada. Hydrogeology Journal, 12: 257–269.

Nussbaumer, R., Mariethoz, G., Gloaguen, E., and Holliger, K. 2020. Hydrogeophysical data integration through Bayesian Sequential Simulation with log-linear pooling. Geophysical Journal International, 221: 2184–2200. Oxford University Press.

Occhietti. 1977. Stratigraphie du Wisconsinien de la région de Trois-Rivières-Shawinigan, Québec. Géographie physique et Quaternaire, 31: 307–322. doi:10.7202/1000280ar.

Occhietti. 1980. Le quaternaire de la région de Trois Rivières-Shawinigan, Québec. Contribution à la paléogéographie de la vallée moyenne du Saint-Laurent et corrélations stratigraphiques. Paleo-Quebec Trois-Rivières.

Occhietti, S., David, P., Gadd, N.R., and Lebuis, J. 1982. Fiches des principales unités lithostratigraphiques quaternaires du québec méridional. Géographie physique et Quaternaire, 36, n: 15-49.

Occhietti. 2007. The Saint-Narcisse morainic complex and early Younger Dryas events on the southeastern margin of the Laurentide Ice Sheet. Géographie physique et Quaternaire, 61: 89–117. doi:10.7202/038987ar.

Occhietti, Chartier H, M., Hillaire-Marcel, C., Cournoyer, M., Cumbaa, S., and Harington, R. 2001. Paléoenvironnements de la Mer de Champlain dans la région de Québec, entre 11 300 et 9750 BP: le site de Saint-Nicolas. Géographie physique et Quaternaire, 55: 23–46. doi:10.7202/005660ar.

Ouellet, M., Lamontagne, C., and Labbé, J.-Y. 2011. Le programme d'acquisition de connaissances sur les eaux souterraines du Québec et ses retombées. Geohydro2011,: 28–31.

Paasche, H., Tronicke, J., Holliger, K., Green, A.G., and Maurer, H. 2006. Integration of diverse physical-property models: Subsurface zonation and petrophysical parameter estimation based on fuzzy c-means cluster analyses. Geophysics, 71: H33–H44. Society of Exploration Geophysicists.

Parent, M., and Occhietti, S. 1988. Late Wisconsinan deglaciation and Champlain sea invasion in the St. Lawrence valley, Québec. Géographie physique et Quaternaire, 42: 215–246.

Les Presses de l'Université de Montréal. doi:10.7202/032734ar.

Parent, M., and Occhietti, S. 1999. Late Wisconsinan deglaciation and glacial lake development in the Appalachians of southeastern Québec. Géographie physique et Quaternaire, 53: 117–135. doi:10.7202/004859ar.

Richard, S.K., Chesnaux, R., Rouleau, A., Morin, R., Walter, J., and Rafini, S. 2014. Field evidence of hydraulic connections between bedrock aquifers and overlying granular aquifers: examples from the Grenville Province of the Canadian Shield. Hydrogeology journal, 22: 1889–1904. Springer.

Ross, M., Parent, M., and Lefebvre, R. 2005. 3D geologic framework models for regional hydrogeology and land-use management: a case study from a Quaternary basin of southwestern Quebec, Canada. Hydrogeology Journal, 13: 690–707. Springer. doi:10.1007/s10040-004-0365-x.

Rouleau, A., Larocque, M., Walter, J., Gagné, S., Tremblay, L., and Germaneau, D. 2012. Le programme d'acquisition de connaissances sur les eaux souterraines. In Vecteur Environnement. Réseau Environnement, Montréal, Québec, Canada.

Ruggeri, P., Irving, J., Gloaguen, E., and Holliger, K. 2013a. Regional–scale integration of multiresolution hydrological and geophysical data using a two-step Bayesian sequential simulation approach. Geophysical Journal International, 194: 289–303. Oxford University Press.

Ruggeri, P., Irving, J., Holliger, K., Gloaguen, E., and Lefebvre, R. 2013b. Hydrogeophysical data integration at larger scales: Application of Bayesian sequential simulation for the characterization of heterogeneous alluvial aquifers. The Leading Edge, 32: 766–774. GeoScienceWorld.

Russell, H.A.J., Brennand, T.A., Logan, C., and Sharpe, D.R. 1998. Standardization and assessment of geological descriptions from water well records: Greater Toronto and Oak Ridges Moraine areas, southern Ontario. Current Research,: 89–102.

Saemi, M., Ahmadi, M., and Varjani, A.Y. 2007. Design of neural networks using genetic algorithm for the permeability estimation of the reservoir. Journal of Petroleum Science and Engineering, 59: 97–105. Elsevier.

Santos, V.S. dos, Gloaguen, E., and Tirdad, S. 2024. Enhancing Lithological Mapping with Spatially Constrained Bayesian Network (SCB-Net): An Approach for Field Data-Constrained Predictions with Uncertainty Evaluation. arXiv preprint arXiv:2403.20195,.

Sattel, D., and Kgotlhang, L. 2004. Groundwater exploration with AEM in the Boteti area, Botswana. Exploration Geophysics, 35: 147–156. Taylor & Francis.

Schulze-Makuch, D., Carlson, D.A., Cherkauer, D.S., and Malik, P. 1999. Scale dependency of hydraulic conductivity in heterogeneous media. Groundwater, 37: 904–919. Wiley Online Library.

Sharpe, D.R., Pugin, A., Pullan, S.E., and Gorrell, G. 2003. Application of seismic stratigraphy and sedimentology to regional hydrogeological investigations: an example from Oak Ridges Moraine, southern Ontario, Canada. Canadian Geotechnical Journal, 40: 711–730. NRC Research Press.

Simard, J., Occhietti, S., and Robert, F. 2003. Retrait de l'inlandsis sur les Laurentides au début de l'Holocène: transect de 600 km entre le Saint-Maurice et le Témiscamingue (Québec). Géographie physique et Quaternaire, 57: 189–204. Les Presses de l'Université de Montréal.

Stokes, C.R. 2017. Deglaciation of the Laurentide Ice Sheet from the Last Glacial Maximum. Cuadernos de investigación geográfica., 43: 377–428. doi:10.18172/cig.3237.

Tronicke, J., and Holliger, K. 2005. Quantitative integration of hydrogeophysical data: Conditional geostatistical simulation for characterizing heterogeneous alluvial aquifers. Geophysics, 70: H1–H10. Society of Exploration Geophysicists.

Vogel, H.-J., and Roth, K. 2003. Moving through scales of flow and transport in soil. Journal of Hydrology, 272: 95–106.

Walter, J., Chesnaux, R., Rouleau, A., Ferroud, A., and Lambert, M. 2022. Résultats du projet d'acquisition de connaissances sur les eaux souterraines du territoire municipalisé de Lanaudière, de l'est de la Mauricie et de la Moyenne-Côte-Nord, PACES-LAMEMCN–section Lanaudière, 210 p.

CHAPITRE 1

MULTITECHNIQUE APPROACH FOR CHARACTERIZING THE HYDROGEOLOGY OF AQUIFER SYSTEMS: APPLICATION TO THE MAURICIE REGION OF QUÉBEC, CANADA

Le chapitre 1 de cette thèse est présenté sous forme d'article scientifique et vise à dresser un portrait général du projet d'acquisition de connaissances sur les eaux souterraines (PACES) réalisé sur le territoire de l'est de la Mauricie. Le PACES a permis de développer des méthodes de caractérisation des eaux souterraines pour fournir un aperçu global de la ressource en eau dans l'est de la Mauricie. Il a notamment contribué de manière significative à l'accroissement des connaissances sur les eaux souterraines de la province de Québec en développant de nouveaux outils et de nouvelles méthodes d'investigation. Celles-ci fournissent des informations sur les unités hydrogéologiques, permettant ainsi d'établir un profil des principaux paramètres hydrauliques caractérisant les aquifères présents sur le territoire.

Ce chapitre donne donc un aperçu général de la région d'étude, ainsi que des outils et des méthodologies qui sont proposés dans les quatre autres articles produits dans le cadre de ce doctorat. Ce chapitre fournit donc des informations substantielles sur la caractérisation des aquifères et de leurs environnements géologiques, afin de mieux gérer et protéger les ressources en eaux souterraines au Québec et au Canada.

Le présent article a été soumis dans la Revue canadienne des ressources hydriques (Canadian Water Resources Journal – IF : 2) le 24 novembre 2022 et publié le 26 juillet 2023. https://doi.org/10.1080/07011784.2023.2234864

Yan Lévesque [1, 2]*, Julien Walter [1, 2], Lamine Boumaiza [3], Mélanie Lambert [1, 2], Anouck Ferroud [1, 2], Romain Chesnaux [1, 2]

[1]Université du Québec à Chicoutimi, Department of Applied Sciences, Saguenay, QC, G7H 2B1 Canada;

[2]Centre d'études sur les ressources minérales (CERM), Groupe de recherche risque ressource eau (R2EAU), Université du Québec à Chicoutimi, Saguenay, QC, Canada G7H 2B1, Canada

[3]University of Waterloo, Department of Earth and Environmental Sciences, Waterloo, ON, N2T 0A4, Canada

Email: julien_walter@uqac.ca;lamine.boumaiza@uwaterloo.ca;romain_chesnaux@uqac.ca; melanie_lambert@uqac.ca; anouck.ferroud1@uqac.ca

*corresponding author: yan.levesque1@uqac.ca

Orcid ID: YL: 0000-0002-6198-6315; RC: 0000-0002-1722-9499; JW: 0000-0003-2514-6180; LB: 0000-0001-9953-451X

1.1 ABSTRACT

The Groundwater Knowledge Acquisition Project (Programme d'acquisition de connaissances sur les eaux souterraines, PACES) in eastern Mauricie, Québec, aimed to develop multiple groundwater characterization methods and provided a more comprehensive portrait of this resource across the region. The proper management and protection of regional groundwater require an accurate characterization and detailed description of regional aquifers. Here, a comprehensive summary is presented, showcasing the amalgamation of specialized

investigation tools and diverse groundwater characterization methods developed throughout the Eastern Mauricie PACES project. This holistic approach unveils valuable insights into hydrogeological units while identifying the crucial parameters that define the regional aquifers. Information related to groundwater surface or subsurface distribution is presented through comprehensive thematic maps, stratigraphic sections, 3D fence diagrams, novel geophysical techniques, conceptual models, and numerical modeling. Integrating a comprehensive spatially referenced database, targeted subregional studies, and peer-reviewed research has significantly enhanced our understanding of regional groundwater. This paper offers substantial information on regional aquifers and their surrounding geology. The approach developed during the eastern Maurice PACES project will serve to better manage and protect groundwater resources in Québec and elsewhere.

Le projet d'acquisition de connaissances sur les eaux souterraines (PACES) réalisé sur le territoire de l'est de la Mauricie a permis de développer des méthodes de caractérisation des eaux souterraines pour fournir un portrait global de cette ressource. Afin de mieux gérer et protéger les eaux souterraines du territoire de l’est de la Mauricie, une caractérisation et une évaluation des aquifères régionaux s'imposaient. Le PACES réalisé sur le territoire de l’est de la Mauricie a contribué de manière significative à l'accroissement des connaissances sur les eaux souterraines de la province de Québec en développant de nouveaux outils et de nouvelles méthodes d'investigation qui fournissent des informations adéquates sur les unités hydrogéologiques, permettant ainsi d'établir un profil des principaux paramètres caractérisant les aquifères présents sur le territoire. Les principaux résultats du PACES fournissent des informations adéquates sur la distribution des eaux souterraines en surface et en sous-surface, tels que des cartes thématiques, des sections stratigraphiques, des diagrammes barrières, des nouvelles techniques de géophysique, des modèles conceptuels et des modélisations numériques. Grâce à une base de données géospatiale et des recherches collatérales, ce document fournit des informations substantielles sur la caractérisation des aquifères et leurs environnements géologiques pour mieux gérer et protéger les ressources en eaux souterraines

au Québec et au Canada. Cet article résume également les principaux résultats du projet et les particularités des principaux aquifères de la région de l'est de la Mauricie.

Keywords: eastern Mauricie, geospatial database, groundwater resources, investigation tools and methods, thematic maps

1.2 INTRODUCTION

In southern Québec, groundwater supplies 90% of the municipal territory, where over two million people rely on groundwater for their drinking water supply (Larocque et al. 2018). As this resource is vulnerable to contamination, a wide-scale integrated portrait of existing groundwater resources is essential to ensure effective and sustainable groundwater management. Nonetheless, information related to groundwater system functioning and the quantity and quality of groundwater within aquifers has remained fragmentary over a large part of the province of Québec, Canada. To address this critical information gap in southern Québec, the Québec Ministry of the Environment (*Ministère de l'Environnement et de la Lutte contre les Changements Climatiques,* MELCC) implemented the Groundwater Knowledge Acquisition Program (*Programme d'acquisition de connaissances sur les eaux souterraines,* PACES) in 2008. Québec universities undertook the multifaceted PACES program to develop multiple approaches to investigate groundwater and aquifers and provide an integrated portrait of groundwater resources for 13 inhabited territories in Québec (Chesnaux et al. 2011, Cloutier et al. 2011, 2013, Rouleau et al. 2012, Gogorza et al. 2012, Larocque et al. 2015, Montcoudiol et al. 2015, Nadeau et al. 2015, 2018, 2021, Turgeon et al. 2018, Walter et al. 2018, 2022, Ferroud 2018, Ferroud et al. 2019, Boumaiza et al. 2020, 2022, Labrecque et al. 2020, Laplante 2021, Delisle 2022, Gagné et al. 2022, Larocque 2023). The hydrogeology research group of the Centre d'études sur les ressources minérales (CERM) at the Université du Québec à Chicoutimi (UQAC) was mandated by the MELCC to acquire and consolidate knowledge relating to the groundwater resources of the municipal territories of Lanaudière, the eastern Mauricie, and central North Shore (CERM-PACES 2022b; 2022a; Lambert et al. 2022). This project was undertaken between 2018 and 2022. These studied

territories, when combined with territories under the mandate of other hydrogeology research groups, completed the portrait of groundwater resource knowledge for the municipal territories of Québec. In this paper, the key findings and outcomes of the eastern Mauricie portion of this PACES project are presented; the full results for this and the two other regions (Lanaudière and central North Shore) are described in the CERM-PACES final report (Lambert et al. 2022). The characteristics and distribution in eastern Mauricie were partially known through previous hydrogeological studies. Various public and private organizations had stored hydrogeological data (e.g., well logs, borehole data as mainly logs and stratigraphic descriptions), hydrogeological studies, and geophysical data) acquired from private consulting firms, municipalities, and government agencies. These data had already been exploited; however, they remained largely underused, and their difficult access for hydrogeologists and land-use managers prevented the comprehensive knowledge of regional hydrogeological units and their subsurface distribution in eastern Mauricie. Consequently, several hydrogeological studies had limited application at a regional scale because they were local in scope and scale (Denis 1974, Occhietti 1977, 2007, Occhietti et al. 1982, McCormack 1983). These past studies often noted the good aquifer potential of the surficial and near-surface sediments in the eastern Mauricie region, but they sometimes lacked a solid database or specialized tools to characterize and locate these regional aquifers with greater accuracy (Denis 1974, McCormack 1983, Légaré Couture et al. 2018). Despite these preliminary attempts to map and characterize regional aquifers, there remained a lack of data, tools, and comprehensive knowledge to better assess the groundwater resources in eastern Mauricie. To effectively manage and protect groundwater resources in the region, it was determined that a more thorough characterization and assessment of regional aquifers were needed. The primary objectives of the eastern Mauricie PACES project were to (1) develop and optimize a comprehensive geospatial groundwater database; and (2) produce a combination of specialized investigation tools and multiple groundwater characterization methods to provide adequate information for better assessing hydrogeological units and their surface or subsurface distribution. These

approaches included comprehensive thematic maps, geophysical methods, stratigraphic sections, 3D fence diagram, conceptual models, and numerical modelling.

In this paper, the developed regional geospatial database is described. Implemented within a geographic information system (GIS), this database holds thematic maps containing geographical, geological, and hydrogeological information in a homogeneous and continuous format for the entire eastern Mauricie region. This database integrates existing data from public and private organizations. It set up a profile of the main parameters characterizing groundwater (e.g., hydraulic conductivity, transmissivity, recharge, porosity, piezometry, geochemistry, geological environment) and provides fundamental information for a variety of subregional projects and collateral research related to aquifer characterization (e.g., the protection, potential, and quality of groundwater resources) in eastern Mauricie (Tremblay et al. 2021; Abi et al. 2022; Boumaiza et al. 2022; Lévesque, Walter, and Chesnaux 2021; Lévesque, Chesnaux, and Walter 2023a; Lévesque et al. 2023b). This paper also presents the specialized investigation tools and diverse groundwater characterization methods developed throughout the eastern Mauricie PACES project for improving the identification and characterization of hydrogeological units to manage groundwater resources more effectively. Finally, the project's main results and the singular aspects of the hydrogeological features of eastern Mauricie are discussed. Hydrogeological data corresponding to all the technical information characterizing groundwater in terms of quantity and quality (e.g., hydrogeochemistry, geophysics, piezometry) are also highlighted.

1.3 STUDY AREA

1.3.1 LOCATION AND HYDROGRAPHY OVERVIEW

The municipal territory of eastern Mauricie covers a region of approximately 6,000 km^2, extending 37 km from northeast to southwest and approximately 158 km north to south (Figure 1). The regional population is 37,179 inhabitants. Regional topography may be divided

into three zones differing in altitude and landforms: the Laurentian Highlands (180–617 m asl), the Piedmont (80–180 m asl), and the Saint Lawrence Lowlands (<80 m asl). A dense network of lakes and water bodies characterizes the region's hydrography. The main rivers follow an N–S axis and are tributaries along the northern shore of the Saint Lawrence River (i.e., Batiscan, Saint-Maurice, and Loup rivers). Wetlands are common in eastern Mauricie areas and cover 4% of the region. Eastern Mauricie is mostly rural, containing small towns and villages, rather than major urban centers. The pumping tests, groundwater samples, and piezometric surveys conducted within the context of the PACES program originate primarily from individual private wells. Among the industrial activities, several quarries and sand pits are exploited throughout the region.

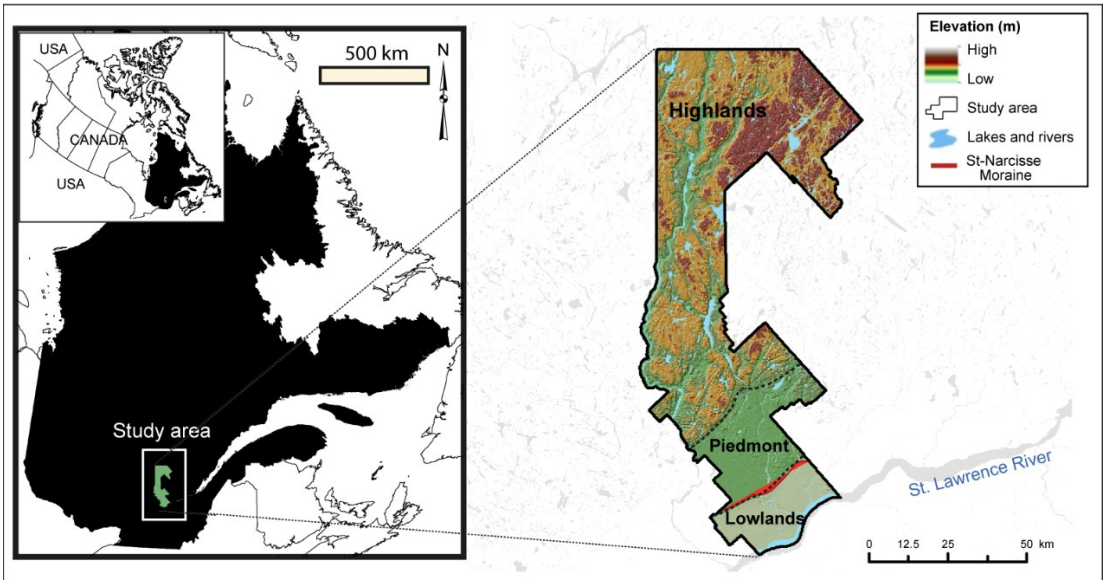

FIGURE 1: Location of the eastern Mauricie region, Québec, and its principal physiographic features. The delineation of the study area is adapted from CERM-PACES (2022) (Lambert et al., 2022; pages 44 and 98).

1.3.2 GEOLOGICAL OVERVIEW AND BASEMENT GEOLOGY

The geology of the eastern Mauricie is characterized by rock outcrops and a variety of Quaternary surface deposits (Gadd and Karrow 1960; Gadd and Goldthwait 1971; Occhietti 2007; Occhietti et al. 1982; Lasalle and Chagnon 1968). The main lithological units

of the region are (1) the crystalline rocks of the Grenville Province of the Canadian Shield (i.e., high-grade igneous and intrusive metamorphic rocks: metasedimentary, metavolcanic, felsic intrusive ; Rivers, Gool, and Connelly 1993), mainly found in the highlands and underneath Piedmont, and (2) the stratified Paleozoic sedimentary rocks of the Saint Lawrence Platform, dominating the lowlands. Most of the platform is buried under the surface sediments and marine clay related to the incursion of the Champlain Sea during the last deglaciation. The rocks of the Saint Lawrence Platform are composed mainly of Ordovician carbonate (Trenton Group) but also include shale, mudstone (Utica and Lorraine groups), and Ordovician sandstone (Black River Group) deposited in a marine environment (Légaré-Couture et al. 2018; Globensky 1987; Occhietti 1977; Douglas et al. 1970; Occhietti 1980; Simard, Occhietti, and Robert 2003). Mudstone and shale are sedimentary rocks of very fine grain size and therefore have low permeability. Moreover, the water that passes into the shale is of poor drinking quality because these rocks often contain natural gas and oil (Légaré-Couture et al. 2018; Globensky 1987).

The Saint Lawrence Platform overlays the crystalline rock formations of the Canadian Shield and is bounded to the southeast by the Appalachians and to the northwest by the Precambrian Canadian Shield (Figure 1). The sedimentary rocks of the Saint Lawrence Platform lie in angular unconformity or in normal fault contact on the Precambrian basement and generally have good permeability, adding to the permeability of the fracture network. During the Paleozoic, the continental rift's opening set up a half-graben near the Saint Lawrence River. This rifting produced a set of NE-SW-oriented normal faults, such as the Saint-Maurice and the Saint-Prosper faults that cross the study area (Figure 2). The Saint-Prosper fault marks the contact between the Precambrian and the Ordovician rocks in the Saint Lawrence Lowlands (Figure 2). Brittle structures, such as faults and joints, increase the aquifer potential of the bedrock (Abi et al. 2022; Walter et al. 2018; Richard et al. 2014; Roy et al. 2011). Finally, the limestones vary in their permeability depending on the fracturing or karstification of the rock.

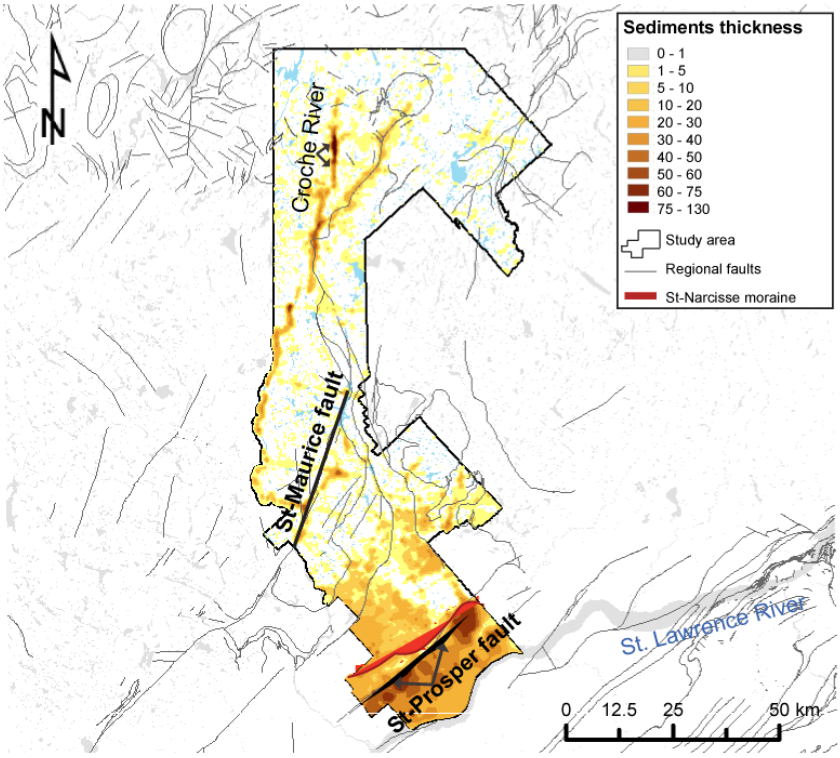

Figure 2: The thickness of unconsolidated deposits in eastern Mauricie, Québec, the main regional faults, and the location of the S**aint**-Narcisse Moraine (in red). Adapted from CERM-PACES 2022 (Lambert et al., 2022; page 68; CERM-PACESa; page 16).

The Piedmont region is characterized by a combination of features from the Highlands (i.e., Precambrian rocks of the Canadian Shield) and the Saint Lawrence Lowlands (i.e., Paleozoic sedimentary rocks). It exhibits uplifts of the bedrock, resulting in the exposure of crystalline basement rocks. The northern boundary of the Piedmont is located at the base of the high-relief features of the Highlands. This significant slope break represents the expression of the Saint. Lawrence half-graben. In the southern part of Piedmont, there is a noticeable topographic threshold consisting of numerous rock outcrops and the accumulation of till, particularly near the municipalities of Saint-Tite and Saint-Adelphe. Southern Piedmont is predominantly composed of the Saint-Narcisse moraine. However, in the eastern and central parts of Piedmont in Mauricie, it occasionally borders the Saint-Prosper fault, juxtaposing the crystalline rocks of the Grenville Province and the sedimentary rocks of the Saint Lawrence

Platform. This contrast in contact between these two significant geological provinces partly explains the variations in topography along the southern boundary of Piedmont.

1.3.3 QUATERNARY SEDIMENTARY DEPOSITS

During the last glacial maximum (LGM), the Laurentide Ice Sheet (LIS) covered most of Canada (Dyke and Prest 1987; Lévesque et al. 2019; Brouard et al. 2021, McMartin et al. 2021, Godbout et al. 2023) and produced extensive glacial deposits such as diamicton (i.e., till) and glaciofluvial, glaciolacustrine, and glaciomarine sediments. The Saint Lawrence Platform is generally covered by a thick layer of these Quaternary sediments (i.e., clay, sand, gravel, and till) of varying nature, that overlie the crystalline and sedimentary bedrock. The main Quaternary sedimentary units found in eastern Mauricie are glacial sediments (till, moraine), glaciofluvial sediments, glaciolacustrine and lacustrine sediments (fine to medium deposits associated with former or current lakes), glaciomarine sediments (littoral or deltaic deposits and seabed), and alluvial sediments associated with present-day rivers. During deglaciation, the marine transgression and incursion of the Champlain Sea flooded the valleys in the lowlands and led to deposits that reflect both shallow and deep marine environments (i.e., proximal and distal glaciomarine deposits). Isostatic rebound during the Holocene triggered a marine regression, and the Champlain Sea deposited regressive sand during its retreat (Parent and Occhietti 1999; 1988). This glaciation and the ensuing marine transgression and regression deposited an accumulation of varied unconsolidated sediments onto the bedrock, deposits that vary in their permeability. In the lowlands, sediment thickness can reach 130 m, and these thicker deposits are located mainly along the Saint-Narcisse Moraine, surrounding it (Lévesque, Walter, and Chesnaux 2021). In the highlands, the valleys contain much thinner deposits, generally between 10 and 40 m thick, although deposits can sometimes locally reach over 100 m thick in deeply buried valleys, particularly along the Croche River sector (Figure 2).

1.3.4 THE SAINT-NARCISSE MORAINE

The discontinuous Saint-Narcisse frontal Moraine is remarkably well preserved and is one of Canada's longest-documented frontal moraines (Daigneault and Occhietti 2006). Like many moraines in eastern Canada, the Saint-Narcisse Moraine was left behind during the last deglaciation and reflected the climate-related phases of LIS advance and retreat (Benn and Evans 2010; Evans 2005; Landry et al. 2012). The Saint-Narcisse Moraine in eastern Mauricie is at the interface between Piedmont and the Saint Lawrence Lowlands (Figure 1) and extends over 35 km across the study area. The moraine varies between 1 and 40 m thick locally, with some regions reaching a thickness of 130m (Figure 2; Occhietti 1977; Tricart 1983; Lévesque et al. 2021). The uplift of the bedrock at the border of Piedmont and the Saint Lawrence Lowlands facilitated the deposition of the Saint-Narcisse Moraine in this region by the Laurentide ice sheet during the Younger Dryas period. This moraine rests atop a higher elevation of bedrock relative to that in the southern region (Figure 3). This topographical difference favored a greater depth of material and, thus, the significant accumulation of sediment in some of the areas to the south of the moraine. During deglaciation, the Champlain Sea deposited significant amounts of sediment, including regressive sands and clays, in these southern areas of the moraine (Figure 3). The formation of marine terraces and the significant variation in relief between the Precambrian–Paleozoic bedrock are fault–controlled in this region (Castonguay et al. 2006; Clark and Globensky 1975; Globensky 1987; Clark and Globensky 1976; Nadeau and Brouillette 1995).

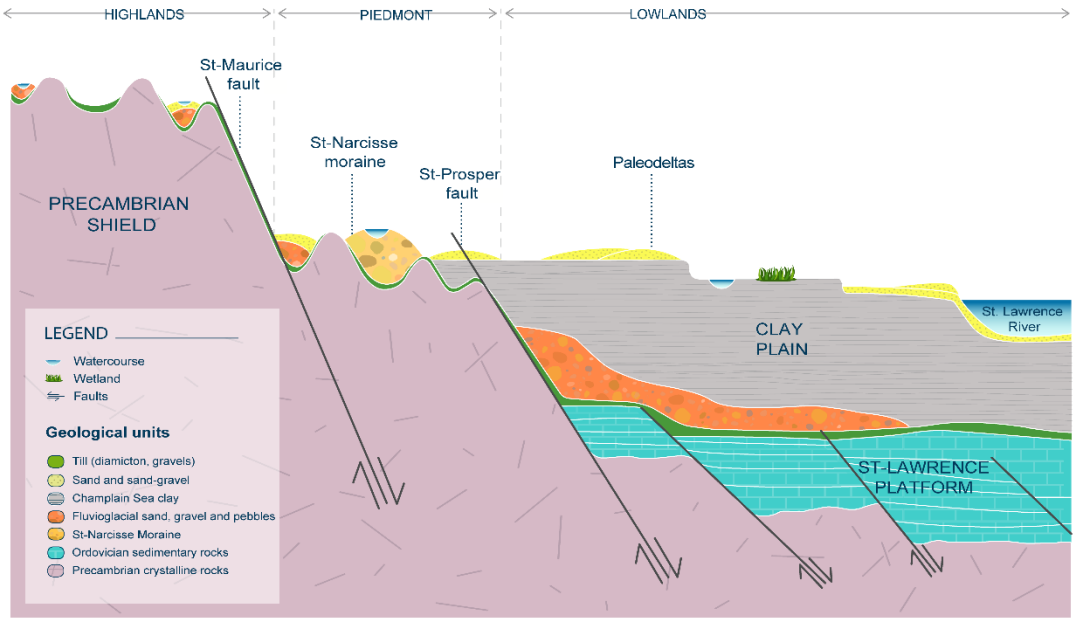

Figure 3: Conceptual section of the major geomorphological and geological units of eastern Mauricie, Québec (adapted from CERM-PACES 2022; Lambert et al., 2022; page 102).

According to Occhietti (1977, 2007), the stratigraphic sections of the moraine comprise a variety of sedimentary facies, including till wedges, subglacial till from the last glaciation, proximal and distal glaciomarine deposits, as well as glaciofluvial and ice-marginal outwash deposits. In low-lying areas around the moraine, the Champlain Sea deposited a thick layer of clay covered by regressive sands during its retreat. Consequently, this imposing glacial sediment complex is partially confined on its sides by clay, thus retaining water inside the moraine. At higher elevations, such as along the sides and on top of the moraine, the Champlain Sea left behind proximal glaciomarine sediments and reworked the glacial tills deposited during the Younger Dryas readvance (Daigneault and Occhietti 2006; Occhietti 2007; Parent and Occhietti 1988, 1999). As a result of wave and current reworking, visible terraces formed on the seaward side of the moraine, mainly composed of coastal and sublittoral sands deposited in the shallow areas of the Champlain Sea and glaciofluvial sediments from small and large deltas in the valleys at the mouths of rivers flowing into the Champlain Sea (Parent and Occhietti 1988; Occhietti 2007; Occhietti et al. 2001). Locally, numerous well-

sorted sand and gravel areas have been observed in the moraine; these deposits constitute potential aquifers (Lévesque, Walter, and Chesnaux 2021). When exposed at the surface, these permeable units can also serve as recharge areas for the moraine and the underlying rocky aquifers. The importance of the local aquifer capacity is evidenced by the surrounding municipalities (e.g., Saint-Narcisse, Saint-Prosper-de-Champlain, Saint-Maurice, Sainte-Geneviève-de-Batiscan) that exploit the moraine locally to supply drinking water.

1.4 MATERIALS AND METHODS

The PACES project in eastern Mauricie included specific research phases: (1) collection of existing data and their integration into a geospatial database; (2) fieldwork and data acquisition and (3) data integration and interpretation (including a regional synthesis).

Initial phase: collecting existing information

The initial phase focused on the inventory, collection, evaluation, digitization, and archiving of existing data into a GIS-based comprehensive database; this existing information included 414 stratigraphic descriptions, 250 chemical analysis results, 117 hydraulic property estimates, 25 piezometric maps, and 5 stratigraphic descriptions of outcrops (i.e., lithological logs) stratigraphic cross-sections(CERM-PACES 2022b). This phase concluded with drafting a summary report of the existing information, identifying missing data, and planning the work required to fill these information gaps. This geospatial database was implemented within a GIS framework coupled to a relational database management system (RDBMS; Chesnaux et al. 2011); it contained information related to 7,112 points corresponding to data from existing databases, hydrogeological reports owned and hosted by municipalities in eastern Mauricie, and data acquired as part of the eastern Mauricie PACES. These data, originating from a wide range of sources and methods, varied in their format and quality levels and required much time and effort to gather and integrate into a common database. Building this database also required a rigorous method for digitizing and archiving data and applying quality control to screen the data to ensure accuracy and quality.

The transmissivity (T), hydraulic conductivity (K), and storage coefficient (S) values applied to estimate the hydraulic properties of aquifers in eastern Mauricie were derived from interpreting pumping tests available in hydrogeological consultant reports. A total of 198 reports were collected, digitized, and archived in the georeferenced database. These reports are now easily accessible and contain data covering the fields of (1) hydrogeology (e.g., water research, drinking water supply, wells construction, water quality, chemical analysis, water production, and water level monitoring in wells), (2) geotechnics (e.g., bank stability, construction of various infrastructure), and (3) environment (e.g., studies of contaminated land, dry material deposits, waste snow dumps). All data was processed to standardize the units. All transmissivity values were converted to m^2/s, hydraulic conductivity values were standardized to m/s, whereas storage remained dimensionless. A total of 117 hydraulic property data points were extracted from the consultants' reports: 10 hydraulic conductivity values in granular deposits, 95 transmissivity values (57 estimates in granular deposits and 38 in fractured rock), and 12 storage values (9 estimates in granular deposits and 3 in fractured rock). Hydraulic properties were grouped into two categories according to geology: granular aquifers (Quaternary sediment deposits) and fractured rock aquifers (crystalline and sedimentary rocks).

Second phase: fieldwork to acquire additional information

The second phase involved the fieldwork collection of additional or missing information and integrating these new data into the developed database (CERM-PACES 2022b). These new data included 106 hydrogeochemical samples, 114 lithological logs derived from stratigraphic descriptions of outcrops obtained through field campaigns (mainly from sand/gravel pits), 1 rotosonic drilled borehole, and 258 geophysical surveys using multiple geophysical techniques, including transient electromagnetic (TEM), electrical resistivity (ERT), and ground-penetrating radar (GPR) methods, and 147 groundwater outcrops (i.e., springs). In addition, one permanent piezometer was installed near the village of Saint-Maurice at a depth of 12 m.

The geochemical characteristics of groundwater were investigated by analyzing 106 samples collected between 2019 and 2021. A total of 91 domestic wells and 13 springs were sampled. Twenty-eight of these wells are in the Laurentian Highlands (77 % of the territory), and the remaining 63 wells are randomly distributed between Piedmont (14 % of the territory) with 40 wells and the Saint Lawrence Lowlands (9 % of the territory) with 23 wells. The collection and analysis of groundwater samples aimed to quantitatively assess the inorganic chemistry of the water, particularly the parameters defining its potability according to the regulations respecting drinking water quality in Québec (RQEP) and Health Canada's guidelines for drinking water quality.

Geophysical surveys used by PACES in eastern Mauricie included non-invasive methods based on electromagnetic waves (i.e., GPR and TEM) and the intrinsic resistance of electric current flow (i.e., ERT). Geophysical approaches provided an excellent complement to direct observations (e.g., borehole logs, lithological logs (stratigraphic descriptions of outcrops), piezometric surveys in wells), and they provided an effective alternative to boreholes for characterizing the internal structures of deposits, the water table, and flow directions. For this study, 134 TEM induction surveys, 27 ERT surveys (~6 km), and 97 GPR surveys (~22 km) were collected in southeastern Mauricie. The surveys were conducted within or in proximity to the Saint-Narcisse Moraine. Two methods confirmed the validity of our geophysical results (see Lévesque et al. (2021, 2023a): 1) comparison with lithological logs (n=114) acquired during field campaigns, boreholes (n=94), and piezometric surveys (n=170) near the surveys to "ground truth" the geophysical interpretation; and 2) when no data was available near the surveys, multiple geophysical methods were conducted to validate our observation. Combining multiple geophysical approaches significantly diminished uncertainty because each method possesses its unique strengths and limitations, and by combining methods, the weaknesses of one method can be compensated by the strengths of another (Lévesque, Chesnaux, and Walter 2023a).

The main objective of this geophysical campaign was to determine the stratigraphy and architecture of the Saint-Narcisse Moraine sediments, correlate the stratigraphic and piezometric information, and characterize the granular aquifers of the moraine in terms of stratigraphy, geometry, thickness, and extent (Lévesque, Walter, and Chesnaux 2021; Lévesque, Chesnaux, and Walter 2023a; Lévesque et al. 2023b). The geophysical data acquired during PACES aimed to develop a methodological approach and a hydrogeophysical tool to better assess the aquifer potential of a heterogeneous glacial deposit environment. The geospatial database led to producing two field reports and six technical reports (https://cerm.uqac.ca/paces/).

Third phase: data integration, analysis, and interpretation

The final phase involved integrating and analyzing all existing and newly collected data to produce hydrogeological maps, an atlas, and a final report. This phase synthesized information as 30 thematic maps of natural and human environments distinguished by geological context (i.e., bedrock and unconsolidated deposits). A total of 44 regional stratigraphic sections were created using geomatic tools to map bedrock topography, the sedimentary deposit thickness, the main aquifers' limits, and the study area's hydrogeological contexts.

1.4.1 STRATIGRAPHIC SECTIONS

The production of 44 stratigraphic sections (CERM-PACES 2022b) was derived from 533 stratigraphic descriptions (414 boreholes and 119 outcrops obtained through the project's initial and second phases. The process for producing these sections involved six steps: 1) data simplification; 2) source data identification; 3) mapping of selected stations in a cross-sectional view; 4) interpretation of geological units in the sections; 5) completion of the stratigraphic sections; and 6) generation of fence diagrams. Because the objectives of the stratigraphic sections were to delimit the regional aquifers and determine the thickness of the deposits across the territory, the source data from cartography and boreholes were simplified. For the eastern Mauricie region, the basement geology was simplified into two major units: the

crystalline rocks of the Canadian Shield and the Ordovician sedimentary rocks of the Saint Lawrence Platform. Unconsolidated deposits were also simplified according to their grain size. Six distinct units are found in the eastern Mauricie region: 1) till; 2) glaciofluvial gravel and sand; 3) glaciomarine, marine, and lacustrine clay and silt deposited in deep water; 4) glaciolacustrine, glaciomarine, and marine sand and undifferentiated gravel sediments; 5) locally deposited silty sand; and 6) organic sediments in thin layers at the surface. These simplifications allowed identifying the primary regional stratigraphic contexts.

The selection of control points – boreholes and lithological logs – for the stratigraphic sections was performed manually in the ArcMap interface of ArcGIS software. The stations were selected according to various criteria, such as their proximity to the stratigraphic section, depth, bedrock presence, and consistency with the nearby stations. The selected points (stratigraphic descriptions) were then projected into a cross-sectional view using the functionalities of the Subsurface Analyst Module of the Arc Hydro Groundwater software. A GIS-based template was established using ArcGIS software to enhance the interpretability of the geological units in the section view. This template incorporated a digital elevation model, a Quaternary geology map, a geological bedrock map including the main regional faults, and a sectional view that displayed the topographic surface, rock outcrops, stratigraphic descriptions with their simplified stratigraphy, preliminary rock topography, main hydrography, and points of intersection with other stratigraphic sections. Once all stratigraphic sections had been digitized, they were projected into a 3D environment using the Subsurface Analyst Module of Arc Hydro Groundwater software to create regional-scale fence diagrams.

1.4.2 THEMATIC MAPS

The third phase also saw the production of maps that presented an initial version of regional piezometry, the preferential zones of recharge, and the vulnerability of the regional aquifers. Some of these maps provided a first glimpse of groundwater use and quality. A

conceptual model was also created to improve the environmental context of the eastern Mauricie region (Figure 3). The insight provided by this conceptual model regarding the geological and environmental context made it easier to produce a series of results, such as stratigraphic sections and fence diagrams, and validate the relevance of several thematic maps. Regional piezometry was estimated from elevations recorded in the hydrographic network. The elevation measurements were extracted from a digital elevation model (DEM) from the Québec topographic database (BDTQ) and were converted to point data using ArcMap (ArcGIS). Moreover, new piezometric data was acquired through groundwater pumping tests carried out during field work in existing wells. Regional piezometry was derived by interpolating the elevation of hydraulic head values, also known as the potentiometric surface, using the "topo to raster" method in ArcMap (ArcGIS). By using the surface topography and piezometry values, the relative depth of the water table was determined by subtracting the land surface elevation from the piezometry. In the following section, we highlight the key findings of the PACES and some singular aspects of the hydrogeological features in eastern Mauricie.

1.5 RESULTS

1.5.1 SPATIAL REFERENCE DATABASE

The geospatial database's architecture used GIS (Esri format) technology (CERM-PACES 2022b). It was first developed and implemented during the previous PACES projects (i.e., PACES-CHCN (Charlevoix and Haute-Côte-Nord) and PACES-SLSJ (Saguenay-Lac-Saint-Jean)) which ran from 2009 to 2013 (Chesnaux et al. 2011; Walter et al. 2018). This architecture was repeated to store the PACES-LAMEMCN project data (Lanaudière and eastern Mauricie region); it has since been highly upgraded and modified from the previous database to fulfill the project's new and particular needs. Overall, the centralized architecture of a data repository, characterized by a central table having several linked tables, enhances data exploitation through a client interface such as a geographic information system (GIS). The need for an optimized data repository architecture is to facilitate data exploitation via a GIS

capable of efficiently managing and preserving a large volume of groundwater information. In the optimized structure, the data were implemented into an Esri geodatabase file, which offers several advantages over the traditional shapefile format (as done in previous projects):

1. The storage of all layers in a single structure, which simplifies data management;

2. The geodatabase, consisting of only one file per layer, as opposed to the shapefile, which comprises four to six files, thereby reducing the risk of data loss if one file is damaged;

3. The reduction in data storage space, with the data stored in a geodatabase occupying approximately one-third of the space occupied by data stored in a shapefile;

4. The improvement in query performance and speed, even for extensive data sets, because of its data structure with spatial and attribute indexes;

5. The capability of referencing raster data in a geodatabase (mosaic dataset) – not supported by the shapefile – which only supports vector data;

6. The availability of attribute domains allows defining a range of potential values for a field in the attribute table; this ensures data integrity by preventing the entry of values that do not conform with the attribute rules.

These features ensure the accuracy and security of the groundwater information, allowing for quick and reliable responses to various data requests within a GIS environment. Knowledge of the region's aquifer systems resides in numerous local studies (e.g., consultant reports, analyses by eastern Mauricie municipality's, private well analyses) that were once difficult to access. This comprehensive groundwater database has gathered all these relevant sources of groundwater-related information.

The PACES geospatial database contains the source data (the data used for the analysis and creation of the maps) and all analysis and cartographic results. The PACES geospatial database gathered data from 13,870 stations distributed throughout the region: 6,758 bedrock outcrops and 6,718 previously documented stations, mainly from the Hydrogeological Information System (HIS), the Ministry of Transport du Québec (MTQ), the Geomining Information System (SIGEOM), neighbouring PACES projects, and consultant reports obtained from municipalities, e.g., boreholes, pumping tests, geophysical surveys, piezometric surveys, geochemical data, hydraulic properties, and lithological logs derived from stratigraphic descriptions of outcrops. Another 625 stations were acquired through diverse fieldworks, as discussed in description of the project's second phase.

These 13,870 stations are derived from a wide range of data and are evenly distributed across the regions of Highlands, Piedmont, and Saint Lawrence Lowlands within the Mauricie territory. For instance, several of these stations have been localized in thematic maps of the groundwater knowledge acquisition project's summary report in Mauricie's eastern municipalized territory (Lambert et al., 2022). These include among others: (1) 104 stations sampled for hydrogeochemical parameters within different types of aquifers (i.e., fractured rock or granular deposits; page 24); (2) 104 stations indicating the type of water catchment (i.e., springs, tubular and surface wells, gelignite; page 25); (3) 37 pumping test stations conducted during the field campaign in the summer of 2019 (page 27); (4) 56 field surveys (i.e., water table, outcrops, bedrock outcrops, chemical analysis results) carried out as part of the PACES to address research project objectives (page 28); (5) 28 quarry and mine location (page 65); (6) 2,657 stations indicating rock depth (page 82); (7) 6,758 stations indicating rock outcrops (page 83); (8) 121 stations providing hydraulic property data (i.e., hydraulic conductivity, transmissivity, storativity) extracted from consultant reports (page 114); (9) 121 stations indicating groundwater samples for isotopic analysis from private wells (page 177); (10) 3 rainfall measurement stations (page 178).

1.5.2 STRATIGRAPHIC SECTIONS

Another significant output of the eastern Maurice PACES campaign was the production of 44 stratigraphic sections (Figures 4 and 5) derived from 533 stratigraphic descriptions. The objective of having stratigraphic sections distributed regularly over the region is to delineate bedrock topography and the thickness of overlying layers of surficial deposits to characterize regional aquifers across the region (Walter et al. 2018). The elements found in the stratigraphic sections were (1) the projected boreholes with their simplified stratigraphy; (2) the interpreted geological units; (3) the interpreted major faults; (4) land surface topography with only the extent of organic deposits; (5) the main hydrography and name of the watercourses; and (6) the intersection points of intersection with the other stratigraphic sections. It is important to note that stratigraphic sections do not replace key lithological information (i.e., in situ data and studies) because the accuracy and the precision of the information contained in these stratigraphic sections depend on the quality and quantity of information available at the regional scale.

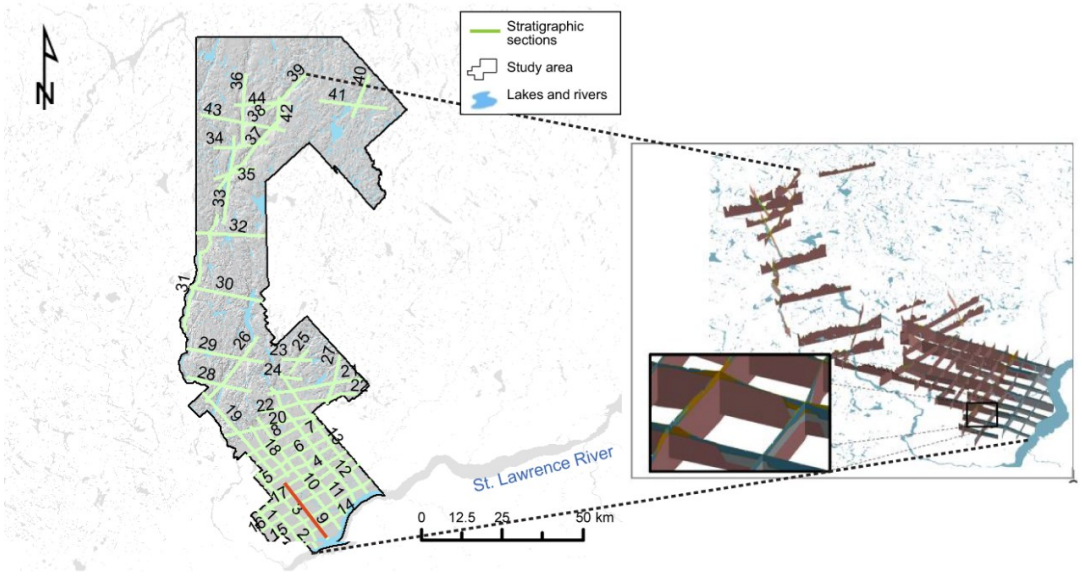

Figure 4: **(left)** Location of the 44 stratigraphic sections interpreted over the entire study area in the eastern Mauricie region, Québec and **(right)** their representation in the form of fence diagrams. The stratigraphic Section #9 (see Figure 5) is represented by the red line. (adapted from CERM-PACES 2022; Lambert et al., 2022; pages 74 and 81).

1.5.3 FENCE DIAGRAMS

The 3D fence diagrams illustrate the lateral continuity of unconsolidated units observed in the 2D stratigraphic sections and provide more information related to the main regional stratigraphic context (Figure 4). The stacking and sequence of the stratigraphic units of unconsolidated deposits were then translated into hydrogeological contexts.

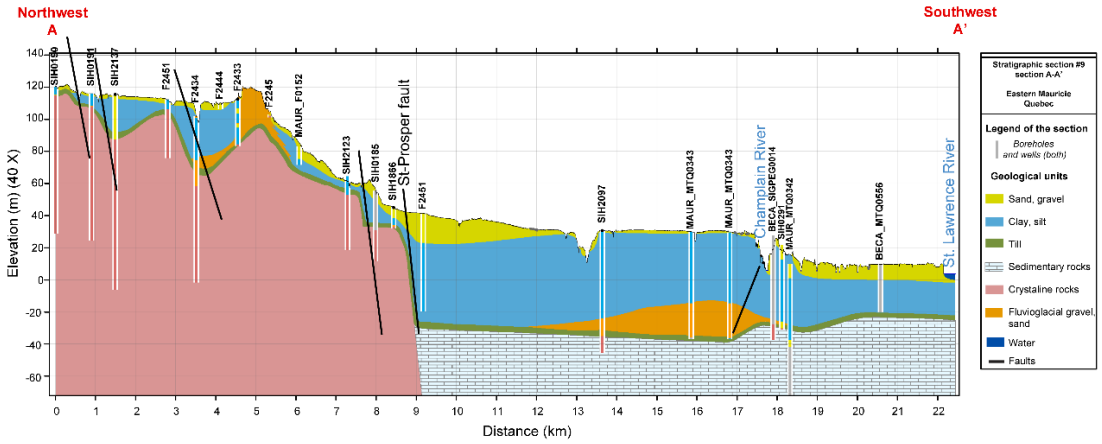

Figure 5: Stratigraphy of Section #9 (adapted from CERM-PACES 2022; Lambert et al., 2022; pages 80 and 100).

1.5.4 EASTERN MAURICIE HYDROGEOLOGICAL FRAMEWORK

The limits of aquifer systems and their hydrogeological contexts in eastern Mauricie were established through fieldwork described in the project's second phase. They are indicators of groundwater and can define future investigation targets, such as drilling, stratigraphic interpretations, piezometric surveys, and pumping tests. However, delineation of the territorial aquifers occurred at a regional scale, and even if thematic maps provide good insight into the hydrogeological context, they cannot replace local studies. Further investigation must obtain information on the parameters that characterize each aquifer within the region. The major aquifer systems (confined and unconfined) in the Mauricie region are composed of geological units dating from the Proterozoic to the Quaternary. These units include (1) the Precambrian crystalline basement of the Grenville Province, covering 61% of the region, mainly in the

highlands; (2) a silty layer deposited in a lacustrine environment, covering 5% of the region; (3) a layer of Champlain Sea marine clay deposited during the sea's incursion at the end of the last glaciation (i.e., between 13 and 11.2 cal. ka BP), covers 18% of the region; (4) Holocene glacial and proglacial deposits, mainly permeable granular deposits of glaciofluvial (e.g., Saint-Narcisse Moraine, deltaic, and glaciolacustrine origin), covering 7% of the region; (5) the Ordovician sedimentary basement located in the lowlands, covering 2% of the region, and (6) glaciomarine proximal, littoral, and deltaic sediments related to the Champlain Sea, covering 7% of the region.

The major hydrogeological context, stratigraphic sections, and regional-scale fence diagrams across the region led to a conceptual section that illustrates the depositional sequence of the various geological units and the region's hydrogeological contexts (Figure 3).

1.5.5 REGIONAL PIEZOMETRY AND RECHARGING ZONES

The piezometric map developed for the PACES revealed a shallow groundwater depth (Figure 6A), particularly in the lowlands (0–20 m from the surface). The mainstream flow direction is from north to south toward the Saint Maurice River and, ultimately, the Saint Lawrence River (Figure 6B).

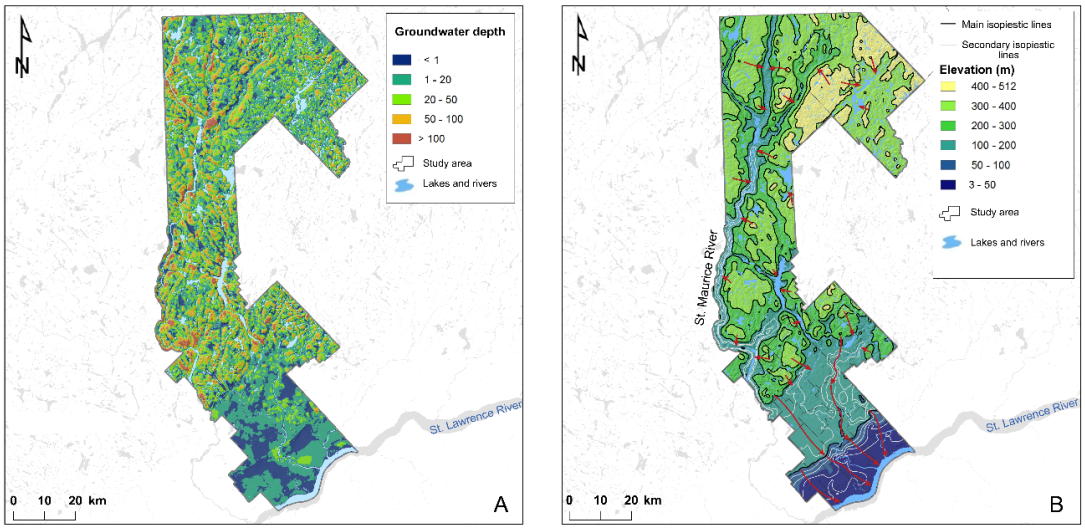

Figure 6: **A)** Groundwater depth (to the first aquifer encountered from the surface); **B)** main directions of regional groundwater flow (red arrows) in the eastern Mauricie region, Québec (CERM-PACES 2022; Lambert et al., 2022; pages 123-124).

Boumaiza et al. (2020) calculated the recharge in similar hydrogeological context for the SLSJ region using a water budget approach (Steenhuis and Van der Molen 1986), which considers that the difference between the input and output fluxes of water in the aquifer system is equal to the change in water storage (Boumaiza et al. 2022; Boumaiza et al. 2020). Applying Boumaiza et al.'s (2020) approach, the groundwater recharge rates for eastern Mauricie were estimated for mapping recharge at regional scale (Figure 7). Estimated vertical inflow from rainfall and snowmelt, surface runoff (RuS), and actual evapotranspiration (AET) were the parameters to calculate the regional recharge. These parameters are well constrained in the study area because of the expertise acquired in previous PACES-related work in other regions (i.e., Saguenay-Lac-Saint-Jean, Charlevoix, Côte-Nord; Chesnaux et al. 2011a; Chesnaux and Elliott 2011; Walter et al. 2018).

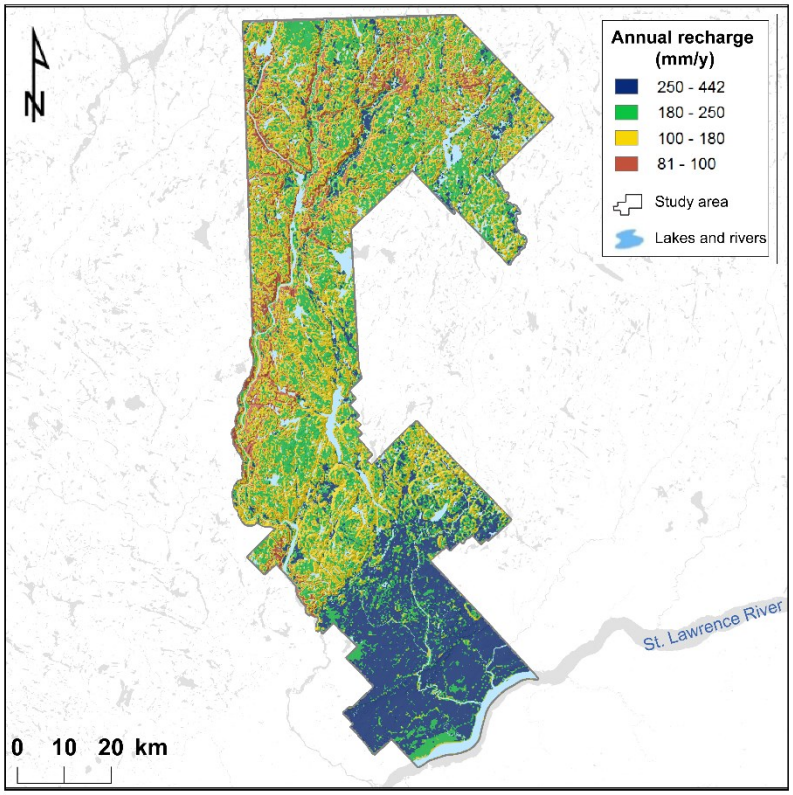

Figure 7: Recharge rates within the eastern Mauricie territory of Québec (CERM-PACES 2022; Lambert et al., 2022; page 133). Recharge was calculated using a water budget approach. This method considers that the difference between the input and output fluxes of water in the aquifer system is equal to the change in water storage. The estimated vertical inflow from rainfall and snowmelt, surface runoff (RuS), and actual evapotranspiration (AET) were used as key parameters to determine the recharge.

1.5.6 BEDROCK AQUIFERS

The brittle and ductile faults and the lineaments were interpreted across the region (Figure 2). The fracturing of crystalline bedrock can be very heterogeneous and variable, and in eastern Mauricie, aquifers in fractured environments can be highly permeable in some places and almost impermeable in others. They are exploited by a few municipalities such as Saint-Stanislas and Saint-Geneviève-de-Batiscan. Significant variations in the rock topography in eastern Mauricie are also suitable for marked accumulations of granular sediments (i.e., deeply buried valleys).

Even if the average annual precipitation is 752 mm/year, the PACES project in eastern Mauricie found that groundwater recharge in the crystalline bedrock aquifer and sedimentary rocks were very low (~81 mm/y), although recharge values varied locally (Figure 7). The transmissivity (T) and the storage coefficient (S) of fractured bedrock aquifers (i.e., sedimentary and crystalline rocks) in eastern Mauricie are summarized in Table 1.

TABLE 1: Summary of the regional statistics for hydraulic properties. These values were generated using data collected from consultant reports.

	Aquifers	Minimum	Maximum	Mean	Median	Number of samples
Transmissivity T (m^2/s)	Granular	2.2×10^{-4}	9.1×10^{-2}	2.3×10^{-3}	2.4×10^{-3}	35
	Fractured bedrock	4.0×10^{-5}	3.1×10^{-3}	2.1×10^{-4}	1.7×10^{-4}	15
Hydraulic conductivity K (m/s)	Granular	6.1×10^{-5}	4.8×10^{-3}	4.2×10^{-4}	6.6×10^{-4}	8
	Fractured bedrock	N/A	N/A	N/A	N/A	N/A
Storage coefficient S	Granular	2.2×10^{-6}	1.1×10^{-1}	2.5×10^{-3}	6.6×10^{-3}	7
	Fractured bedrock	2.2×10^{-5}	1.6×10^{-2}	6.1×10^{-4}	1.1×10^{-3}	3

1.5.7 GRANULAR AQUIFERS

The Quaternary surface deposits in the eastern Mauricie (mapped during the PACES project of eastern Mauricie (Figure 8)) are mainly related to the last glaciation (i.e., Wisconsinan glaciation) and Holocene deglaciation. These deposits frequently exceed 100 m in thickness in eastern Mauricie. The map's representation distinguishes outcropping bedrock units (in red) from overlying units (Figure 8).

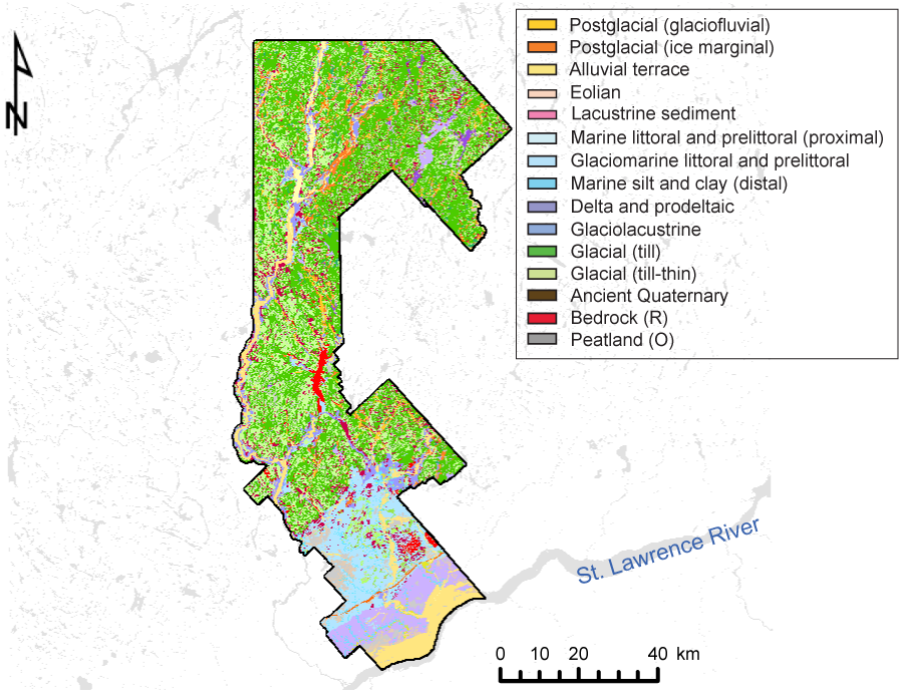

Figure 8: Quaternary surficial deposits overlying the eastern Mauricie region, Québec. This map was produced by combining the 1:50,000-scale maps created as part of the mapping work of UQAC and Université Laval (Brouard et al., 2021). A literature review of the regional stratigraphy of Quaternary deposits was carried out by LaSalle (1985). Adapted from CERM-PACES 2022; CERM-PACESa; page 12.

Over most of the lowlands, the region is generally covered by a thick layer of Quaternary sediments (i.e., clay, sand, gravel, and till) of various origins, overlying the bedrock. These units (1–4) are: 1) eolian, alluvial, lacustrine, and coastal sediments on the surface. These sediments are grouped as surficial undifferentiated granular sediments and are mainly composed of sand and gravelly sand. These granular formations are permeable and constitute excellent unconfined aquifers; 2) fine sediments related to the Champlain Sea below the surface sediments. These sediments comprise mainly clay and silt and are much less permeable than the granular units. Therefore, they constitute a confinement layer. This impermeable unit also acts as a chronostratigraphic marker, distinguishing between the upper aquifers (e.g., unconfined aquifer, and the lower aquifers; Figure 3). Beneath the clays are glaciofluvial and glaciolacustrine sediments deposited during the last glacial advance or retreat. These sediments of glacial origin can outcrop at the surface or be covered by clays and/or

surface sand. Glaciofluvial sediments include proglacial and juxtaglacial (i.e., ice marginal) sediments, such as the Saint-Narcisse frontal Moraine (Figure 9). These very permeable sediments comprise mainly gravel, sand, and boulders in varying proportions with a high recharge potential and can be excellent aquifers when they have a sufficient deposit thickness over extensive areas. Lévesque et al. (2021) revealed large unconfined granular aquifers overlying the bedrock and the compartmentalization of an extensive aquifer system in the eastern Mauricie (Figure 9). These Saint-Narcisse Moraine aquifers sometimes extend laterally for over 12 km, with granular deposits reaching a thickness greater than 94 m (Lévesque, Walter, and Chesnaux 2021). However, despite the marked sediment heterogeneity, the distinctive character of this frontal moraine lies in the presence of a large amount of well-sorted sand and gravel. The compartmentalization of the aquifers is caused primarily by finer sediments deposited by the Champlain Sea at lower elevations (Occhietti 1980, 1977, 2007; Parent and Occhietti 1988; Daigneault and Occhietti 2006; Figure 9). These impermeable sediments function as a natural barrier, separating the aquifers from each other and enhancing the discontinuous nature of the Saint-Narcisse frontal Moraine. The presence of a continuous coarse-grained aquifer in the Saint-Narcisse Moraine, consisting mainly of sand and sand-gravel, is described through the use of boreholes combined with transient electromagnetic (TEM) surveys, a sediment resistivity calibration chart (as presented in Lévesque, Walter, and Chesnaux 2021), and a 3D geological model and a 3D flow model (as detailed in Lévesque, Chesnaux, and Walter 2023a). Several municipalities in eastern Mauricie extract groundwater from the sand and gravel of glaciofluvial formations (e.g., Saint-Prosper-de-Champlain, Sainte-Geneviève-de-Batiscan, Saint-Narcisse, Saint-Adelphe; Figure 9). The LIS also left glacial deposits on top of the bedrock, including diamicton (i.e., till). According to the PACES regional interpretation, a thin layer of continuous till is presumed over almost all of the region (Figure 8). This layer is mainly composed of diamicton and is considered low permeability; therefore, flow can occur between two aquifers through this layer. However, this layer does not have aquifer potential.

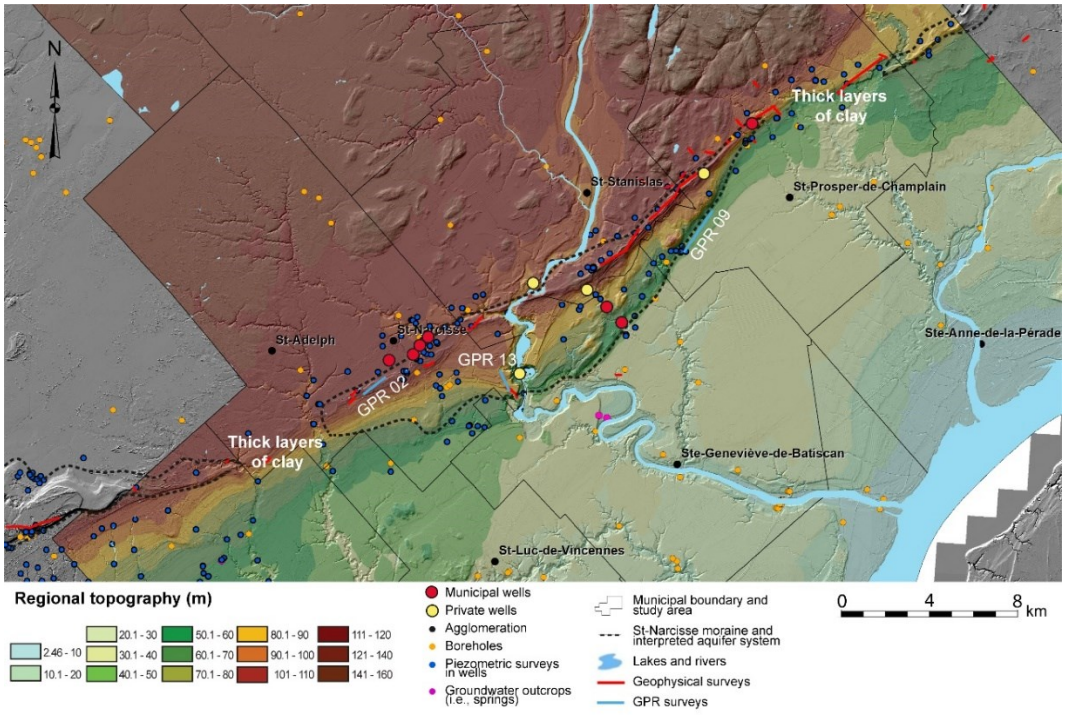

Figure 9: Boreholes, springs, municipal and private wells, geophysical surveys, and piezometric surveys located along the Saint-Narcisse Moraine, Québec. The red lines represent geophysical surveys, while the pale blue-pink line represents geophysical data collected using ground-penetrating radar (GPR), as depicted in figures 10 and 11. The delimitation of the aquifer system is based on Lévesque et al. (2021, 2023a)

The region's relief strongly influenced the glacial retreat, and the topography is marked by lineaments composed of ridges and depressions oriented mainly N–S, NNE–SSW, and NE–SW. For example, glaciofluvial deposits were deposited in valleys, thalwegs, and slopes (Prichonnet, Doiron, and Cloutier 1982). In the highlands, these deposits are outcropping and fill the valleys; however in Piedmont and the Saint Lawrence Lowlands, they are covered by clayey Champlain Sea sediments, which can be overlain by deltaic, lacustrine, alluvial, and eolian sediments locally.

The hydraulic conductivity, the transmissivity and the storage coefficient of the granular aquifers in eastern Mauricie are summarized in Table 1. These hydraulic conductivity and transmissivity values correspond well to the range of medium sand to fine gravel and are sufficiently high enough to form suitable aquifers.

1.5.8 RESEARCH CONTRIBUTIONS

Geophysics

The primary objective of geophysical surveys during the PACES project in eastern Mauricie was to determine the stratigraphy and architecture of the moraine sediments and characterize the granular aquifers of the moraine in terms of stratigraphy, geometry, thickness, and extent. The performed geophysical surveys consisted mainly of acquiring a fine-scale knowledge of the Saint-Narcisse Moraine stratigraphy and understanding its role in the regional groundwater flow system. GPR uses radiowave reflections to detect the water table (Reynolds 2011; Neal 2004) and provides quite accurate results (approximately to the metre). The water table surface is evident on radargrams as a continuous, horizontal reflector with a large amplitude (Figure 10). The radargrams also sometimes revealed paleoriver channels (Figure 10) or oblique reflectors associated with interfaces between sandy layers of different grain sizes or clayey and sandy sediments (Figure 11). These oblique reflections indicate the apparent flow directions at the origin of these structures (Cojan and Renard 2013). Figures 10 and 11 suggest that the current trend is established from north to south. The collected TEM and ERT data also identified a clear groundwater table elevation and bedrock depth when the survey penetrated sufficiently deep into the unconsolidated sediments.

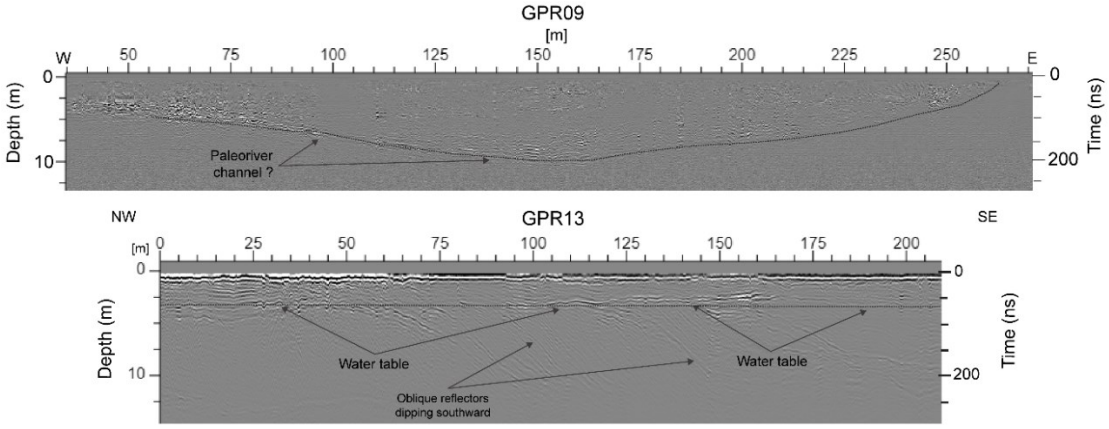

Figure 10: Example of geophysical data collected using ground-penetrating radar (GPR) in eastern Mauricie, Québec. These radargrams (GPR09-13) were acquired along the Saint-Narcisse Moraine with a MALÅ GX (Ground Explorer) system. The black dashed lines show a paleoriver channel on GPR09 and the water table surface, clearly evident on GPR13 as a continuous, horizontal reflector with a large amplitude. See Figure 9 for the transect locations.

Lévesque et al. (2021) proposed an approach for characterizing regional aquifers in remote territories through transient electromagnetic (TEM) surveys. TEM data combined with piezometric mapping and the sedimentary records from boreholes and lithological logs revealed the presence of two large unconfined granular aquifers overlying the bedrock within the Saint-Narcisse Moraine. These compartmentalized aquifers extended over 12 km east to west across southeastern Mauricie and varied between 25 and >94 m thick.

Finally, coupling the collected ERT, TEM, and GPR data produced accurate estimates of groundwater levels. Lévesque et al. (2023a, b) demonstrated the usefulness of geophysical data, i.e., indirect measurements, to bring additional hydraulic information and complement direct observations (i.e., boreholes, piezometric surveys) for accurately assessing water levels and validating numerical regional groundwater flow models, especially in areas with limited direct piezometric information. Given that, groundwater flow models are now standard items for visualizing flow scenarios through the subsurface to adequately manage groundwater resources and improve the protection of aquifers (Hudon-Gagnon et al. 2015;

Calvache et al. 2009; Preisig, Cornaton, and Perrochet 2014; Cui et al. 2021), this contribution provides the groundwater modeling community an interesting additional tool.

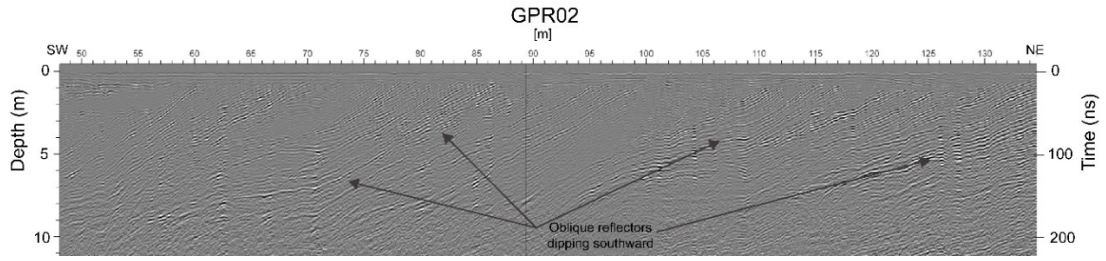

Figure 11: Example of geophysical data collected using ground-penetrating radar (GPR) in eastern Mauricie, Québec. This radargram (GPR02) was acquired along the Saint-Narcisse Moraine with a MALÅ GX (Ground Explorer) system. The multiple oblique southward-dipping reflectors are evident in the radargram. See Figure 9 for the transect locations.

Groundwater geochemistry

In the Saint Lawrence Lowlands, 30% of samples exceeded the new drinking standards (https://www.legisquebec.gouv.qc.ca), and excessive fluoride concentrations were ubiquitous in these samples. Among 94 samples, 129 aesthetic objectives (EO) exceedances were identified, including aluminum (3 exceedances), chloride (5), copper (1), estimated hardness (2), iron (11), estimated total dissolved solids (TDS; 8), manganese (40), sodium (4), pH (50), and sulphide (5). The concentrations of some of these elements fell beyond federal (i.e., the maximum acceptable concentrations (MAC) of Health Canada) or provincial (i.e., maximum concentration (CM) for the RQEP) guidelines/recommendations for drinking water quality (see Table 2 for examples of these exceedances). Table 2 shows parameters whose concentrations are higher than the standards, such as fluoride (>1.5 mg/L), manganese (>0.12 mg/L), but also less commonly copper (>2 mg/L) and lead (>0.005 mg/L). Tremblay et al. (2021) showed that manganese exceedances were generally located 40 to 700 m from a swamp, marsh, or wetland. The presence of organic matter decreases the oxygen levels in groundwater, creating a reductive environment that accelerates the solubilization of manganese (Tremblay et al. 2021). The high fluoride concentrations are usually found in deep wells and

are likely related to local bedrock. Indeed, the Grenville Province has a high fluoride concentration because of its high tonalitic and trondhjemitic gneiss composition (Nadeau and Brouillette 1995; Bédard 1971; Béland and Bergeron 1959).

Table 2: Descriptive statistics for groundwater chemistry; fluoride (>1.5 mg/L), manganese (>0.12 mg/L), copper (>2 mg/L), and lead (>0.005 mg/L) of samples collected from eastern Mauricie, Québec.

Parameter	Number of analysis[1]	Number of detection	Detection limit	Minimum[2]	Q1-25%	Median	Q3-75%	Maximum	Maximum Acceptable Concentrations (MAC)	Number of samples exceeding drinking standards
Cu (mg/l)	94	74	0.0005	0.00025	0.0007	0.0026	0.01	5.1	2	1
F (mg/l)	94	94	0.01	0.016	0.058	0.13	0.728	7.3	1.5	11
Mn (mg/l)	94	85	0.0004	0.0002	0.0016	0.012	0.072	0.41	0.12	15
Pb (mg/l)	94	62	0.0001	0.00005	0.00005	0.0002	0.0005	0.27	0.005	1

[1] A total of 104 wells or resurgences were sampled, but only 94 samples respecting electroneutrality (EN) were evaluated.
[2] A concentration equal to half the detection limit was considered for the undetected elements.

1.6 DISCUSSION

The UQAC-led PACES project in eastern Mauricie characterized the hydrogeological systems across this 6 000 km2 territory's municipalized portion. The synthesis of all existing and newly collected hydrogeological information resulted in the production of thematic maps of aquifer boundaries and hydrogeological contexts of groundwater in this region. The produced cartographic data and the integration of the third dimension from 2D results are some of the original elements of this PACES campaign. The third dimension was incorporated by creating various fence diagrams, a simplified conceptual model, and geological and numerical flow models of the Saint-Narcisse Moraine unconfined aquifer, between the Batiscan and Croche rivers (Lévesque, Chesnaux, and Walter 2023a; CERM-PACES 2022b; 2022a). These novel approaches provide new perspectives for applied hydrogeology at local and regional scales. Moreover, conceptual models can provide important insight into the regional stratigraphic and hydrogeological contexts and often allow obtaining a better overview of the regional environment. The stratigraphic context, such as bedrock elevation, the presence of thick clay

layers at depth or regressive sands at the surface, and the presence of thick till layers overlying the bedrock, often enables validating thematic maps, including the thickness of Quaternary sediments in certain areas, the piezometric map of eastern Mauricie, and the regional distribution of confined and unconfined aquifers. This section focuses on recommendations resulting from the analyses of the hydrogeological information collected during this PACES project to improve the sustainable management of groundwater resources and enhance regional hydrogeological knowledge among the scientific community, governmental agencies, municipal policymakers, and consultants from watershed agencies and private firms.

1.6.1 QUATERNARY SURFACE DEPOSITS AND THEIR GROUNDWATER POTENTIAL

The eastern Mauricie municipal territory is characterized by several substantial surface accumulations (e.g., sand, gravel, and sandy gravel) of glacial or postglacial origin, exhibiting a high groundwater potential. Many of these deposits exceed a thickness of 100 m. Morainic complexes such as the Saint-Narcisse Moraine have spatial arrangements and hydraulic characteristics (i.e., particle size, porosity, and permeability) that favour groundwater storage (Parriaux and Nicoud 1993; Burt 2018). Previous studies in the Mauricie region had suggested the presence of large regional granular aquifers within the Saint-Narcisse Moraine based on the large quantity of granular sediments at its surface (Grenier and Denis 1974; McCormack 1983; Légaré-Couture et al. 2018; Légaré-Couture 2013; Leblanc et al. 2013). Lévesque et al. (2021) confirmed this potential by providing precise information on regional stratigraphy and the moraine aquifers' geometry, thickness, and extension. Combining sedimentary records from boreholes, piezometric mapping, and geophysical data revealed a multikilometer, compartmentalized morainic aquifer system overlying the bedrock. Lévesque et al. (2021) identified the need for more detailed studies in glacial deposits to better assess their underestimated groundwater resources.

Compared with the Saint-Narcisse Moraine, Ontario's large moraines, including the Waterloo, Orangeville, Dorchester, Paris, and Oak Ridges moraines, also hold significant

importance as drinking water sources for several municipalities. These moraines are widely recognized as some of Canada's largest drinking water aquifers. In order to better understand and manage these valuable resources have been characterized by the creation of conceptual models relying on a robust data set (Barnett et al. 1998, Sharpe et al. 2003, Bajc et al. 2014, Burt 2018). In Northern Québec, the Harricana-Lake McConnell interlobate glaciofluvial complex and the Sakami frontal moraine represent also two of the largest moraines found in Canada. These moraines exhibit substantial accumulations of granular sediment, primarily composed of sand with a large amount of gravel (Veillette 1983; Hardy 1982; Hillaire-Marcel, Occhietti, and Vincent 1981). The Harricana-Lake McConnell morainic complex is a relatively continuous and linear accumulation of stratified sand and gravel (Brennand and Shaw 1996). The Sakami moraine consists predominantly of fluvioglacial and proglacial materials with thicknesses reaching up to 40 meters. It is mainly composed of well-sorted sands and gravels deposited by glacial meltwater. Unlike the moraines in Ontario, these extensive northern moraines supply water to few municipalities due to their location in sparsely populated areas. However, they exhibit similar groundwater potential due to the significant amount of granular materials.

While moraines generally do not serve as significant aquifers in various northern regions worldwide, including Canada, Russia, and Scandinavia, there are exceptions to this rule, particularly with large frontal and interlobate moraines such as Saint-Narcisse, Waterloo, Oak Ridges, Orangeville, Sakami, and the Harricana-Lake McConnell morainic complex. These moraines display characteristics that enable them to store and transmit substantial amounts of groundwater. Ontario's and Québec’s extensive interlobate and frontal moraines, characterized by granular sediments at the surface and subsurface, exhibit comparable sedimentary and hydraulic properties to the Saint-Narcisse frontal Moraine (Burt 2018; Bajc, Russell, and Sharpe 2014; Parriaux and Nicoud 1993; Barnett et al. 1998; Lévesque, Chesnaux, and Walter 2023; Lévesque, Walter, and Chesnaux 2021; Légaré-Couture et al. 2018; Hardy 1982; Brennand and Shaw 1996; Hillaire-Marcel, Occhietti, and Vincent 1981; Veillette 1983). In these contexts, the hydraulic characteristics are mainly attributed to the significant abundance

of coarse-grained sediments, encompassing a range of sand and gravel sizes (from fine to coarse), which exhibit high hydraulic conductivity and transmissivity values. These granular sediments contribute to forming suitable aquifers for groundwater storage and flow. The flow of groundwater, as well as its recharge and storage within these formations, is controlled by various factors such as morphology, grain size, porosity, water-holding capacity, internal sedimentary structures, and permeability (Parriaux and Nicoud 1993). However, these characteristics can vary among moraines due to differences in their formation processes (i.e., genesis), local glacial history, and the specific sediments they contain (Landry et al. 2012; Benn and Evans 2010; Evans 2005).

Managing water resources in these settings poses particular challenges. While interlobate and frontal moraines share similar characteristics, the sedimentary architecture, aquifer distribution, and potential can vary locally. The approach employed in this study for characterization can be applied in such complex settings to make evidence-based water management decisions tailored to the unique glacial context of each location. The Saint-Narcisse, Waterloo, Orangeville, Dorchester, Oak Ridges, Sakami, and Harricana-Lake McConnell moraines are examples of extensive deposits of granular sediment with favorable spatial arrangements and hydraulic characteristics that facilitate groundwater storage. These moraines are typically composed of sand and gravel, with stones and occasional boulders, favoring high effective porosity and significant storage capacities (Burt 2018; Bajc, Russell, and Sharpe 2014; Parriaux and Nicoud 1993; Barnett et al. 1998; Lévesque, Walter, and Chesnaux 2021; Lévesque, Chesnaux, and Walter 2023a). The permeability of these moraines is generally high, although it can be reduced by the presence of interbedded sedimentary layers or impermeable sections that compartmentalize the aquifers vertically (i.e., aquitard) and sometimes horizontally (Lévesque, Walter, and Chesnaux 2021).

1.6.2 Protecting and monitoring groundwater quality: ensuring the safety and sustainability of aquifers

The samples with the highest proportion of EO exceedances were in the lowlands; for example, 43% exceeded the aesthetic criteria for manganese (0,02 mg/L), and 16% exceeded the value of 0.12 mg/L recommended by Health Canada. Twenty-seven of these samples are in the Saint Lawrence Lowlands, and the remaining 67 are in the Piedmont and the Laurentian Highlands. The parameters characterizing water quality within the framework of the PACES on eastern Mauricie are essentially physical and chemical. However, even if overall the parameters analyzed reveal suitable quality groundwater (as nearly 73% of the samples acquired in the region do not exceed drinking water standard thresholds), they are incomplete to qualify the potability of the water. Indeed, among the chemical parameters, cyanide and mercury were not analyzed, and no microbiological parameters were analyzed. Furthermore, local studies are required to clarify the risks of anthropogenic or natural contamination because of the vulnerability of groundwater in specific sectors. These contaminations are generally associated with significant accumulations of surface sand. For example, the Saint-Maurice valley has been identified as a fjord-like valley related to the Champlain Sea lying north of the study area (Parent and Occhietti 1988); consequently, some salinity is anticipated in the granular aquifers at the bottom of the Saint-Maurice valley. Increasing our knowledge of groundwater quality to protect public health in eastern Mauricie requires establishing an extensive groundwater sampling of private wells to better access and monitor the groundwater chemical conditions across this region. This campaign could identify more problematic wells and regions in eastern Mauricie with regular sampling of the wells. Autonomous septic systems near private wells also pose major health risk challenges in the province of Québec. Viruses in sewage are the pathogenic organisms that pose the most significant risk of gastroenteric infection to citizens of isolated residences.

The vulnerability of groundwater to surface contamination for the region of eastern Mauricie can be defined according to the DRASTIC method (US EPA; Aller 1985), which

provides an overview of the vulnerability of groundwater to contamination. The most vulnerable sectors to groundwater contamination in the study area correspond to deposits of glaciofluvial, glaciolacustrine, and glaciomarine origin (Figures 8 and 12) because these granular deposits are exposed at the surface. Moreover, large portions of these unconfined granular aquifers are not contained within the capture zones of existing pumping wells. Therefore, they are not protected because groundwater exploitation for public drinking water supply indirectly protects against contamination. This lack of protection may jeopardize precious aquifers in eastern Mauricie.

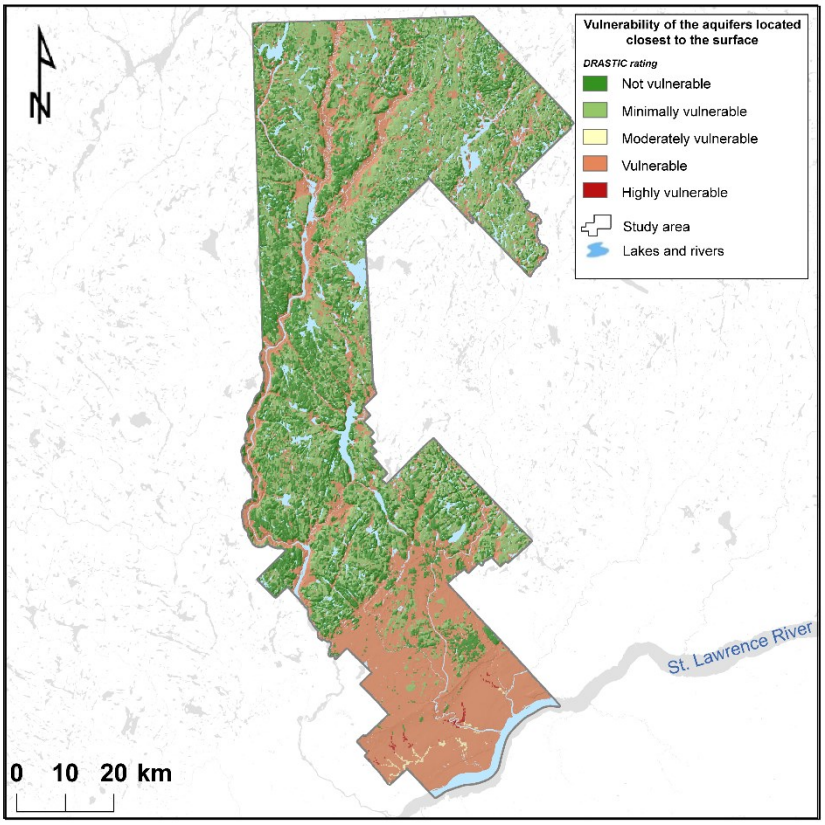

Figure 12: DRASTIC rating of aquifer vulnerability in eastern Mauricie, Québec, for aquifers closest to the surface. The most vulnerable sectors correspond to deposits of fluvioglacial, glaciolacustrine, and glaciomarine origin, mainly located in the lowlands (adapted from CERM-PACES 2022; Lambert et al., 2022; pages 142-143).

The results obtained by the PACES project provide a baseline knowledge of water quality at the regional scale. A sampling and monitoring program would permit tracking the possible evolution (degradation?) of regional drinking water quality. The data acquired, listed, and mapped during this project provide a good starting point for defining the regional aquifers that most require protection and establishing a management plan to protect drinking water resources in eastern Mauricie. This is particularly important for identifying sectors where water supply is not currently exploited and/or is of lower quality relative to standards and recommendations set by Québec and Health Canada.

1.6.4 THE NEED FOR FURTHER GROUNDWATER KNOWLEDGE ACQUISITION AND DATABASE MANAGEMENT

Before PACES, little information on groundwater was available across the province of Québec. After more than a decade of research on groundwater and related fields (e.g., geotechnics, geological basement, geophysics), high-quality hydrogeological information is available and accessible for a vast territory across southern Québec. The PACES project in eastern Mauricie has significantly increased knowledge of regional groundwater resources and established a comprehensive spatially referenced groundwater database detailing regional aquifer systems and groundwater within the region. The high density of data observation points in the database is suited to answer groundwater management needs for local or regional applications. Several applications can be made from the contained data to address geotechnical or groundwater-related problems, such as work on seismic risks (Salsabili et al. 2021b; Richer et al. 2023), landslide risk zoning from the Québec Ministry of Transport (MTQ), water research (Lévesque, Walter, and Chesnaux 2021), groundwater quality (Tremblay et al. 2021), and specific methodologies to develop regional 3D modelling (Salsabili et al. 2021a; Lévesque, Chesnaux, and Walter 2023a; Boumaiza et al. 2022; Boumaiza et al. 2021; Boumaiza et al. 2022; Boumaiza et al. 2021a; Boumaiza, Walter, et al. 2021).

However, the significant volume of current and future groundwater-related information in Québec poses challenges for decision-makers and policymakers, such as data access and

management, as well as understanding the diverse groundwater data. Moreover, regional water practitioners do not always have the expertise to understand the advanced concepts associated with groundwater. The data, as currently produced within the framework of the various PACES, are not sufficiently adapted to the needs of regional water practitioners, and they must be interpreted and combined to create valuable knowledge that can be used for (1) land-use planning; (2) ensuring the sustainability of the groundwater resource; (3) developing the groundwater resource; and (4) addressing conflicts of use between different economic and municipal activities. Technical tools alone are insufficient for fully utilizing this knowledge, and it is necessary to complement these tools with personalized guidance from a groundwater expert. The databases produced by the participating universities and provided to the Québec MELCC contain immense volumes of information. The challenge is to take advantage of this new knowledge by integrating it into territorial planning at different scales. According to Lavoie (2013) and Mayrand (2021), the challenges could initially be grouped into seven themes: raising awareness of local and regional practitioners, training of basic knowledge in hydrogeology, ensuring the effective and appropriate dissemination of results, popularizing new knowledge, clarifying groundwater protection mechanisms, and identifying the roles and responsibilities of the various regional practitioners. Finally, there must be the manifestation of a strong political will for the sustainable management of water resources (Lavoie, Joerin, and Rodriguez 2014; Mayrand 2021).

Across Québec, it is essential to continue gaining knowledge related to groundwater, including updating the existing groundwater databases. Government agencies, municipalities, and consulting firms continually produce new, relevant, and accurate data (e.g., well drilling, piezometric surveys, pumping tests, geophysical surveys, and groundwater quality tests). These data must be integrated into the established databases as they are produced to ensure they remain current and relevant for future projects involving the management and protection of water resources. Several organizations can be responsible for updating these data and providing the governance of these databases. These organizations include government agencies, consultants, regional county municipalities (RCM), one or a consortium of

universities, and watershed organizations (organismes de bassins versants du Québec, OBV). However, without a clear and strong political will, the protection and sustainable management of groundwater are not assured. This should manifest itself through specific mandates, the availability of the necessary resources, and the creation of specific tools to ensure the sustainability of this essential resource.

Canada and other countries provide diverse solutions and methods to enhance accessibility and autonomy in accessing databases and facilitate information exchange among regional decision-makers and policymakers in water resources management. For instance, notable examples include the databases of TRCA in the Greater Toronto Region, Ontario, Canada (https://trca.ca/conservation); AGS, Alberta, Canada (https://ags.aer.ca/); InfoTerre-BRGM, France (https://infoterre.brgm.fr); Bundesanstalt fur Gewasserkunde, Germany (https://www.bafg.de/de/home/homepage); US Geological Survey, USA (https://www.usgs.gov/); IGME, Spain (https://igme.maps.arcgis.com/home/gallery); eHYD, Czech Republic (https://ehyd.gv.at/#); and OFEV, Switzerland (https://s.geo.admin.ch/9b181a62f6).

These databases are often attached to energy, mines, or sustainable development ministries, with little or no involvement from the academic sector. All these databases have the same objective: meet users' expectations when they seek to acquire geoscientific data (i.e., researchers, professionals, the general population, and government agencies) and protect groundwater resources. The private sector sometimes agrees to share its information with the public sector to create global databases, but this collaboration often makes the database inaccessible to the general public. However, access to data is essential, which is why many countries have established strict regulations to implement systems capable of collecting groundwater information and establishing global databases with guarantees of easy access (for some examples, see the databases references above).

1.7 CONCLUSION

The eastern Mauricie PACES project has contributed significantly to increasing knowledge of regional groundwater resources by (1) integrating existing data from regional partners and recently collected data within a geospatial groundwater database; (2) establishing a profile of the main parameters characterizing groundwater resources; (3) developing a combination of specialized investigation tools and multiple groundwater characterization methods to provide detailed information about hydrogeological units and their surface and subsurface distribution; and (4) mapping aquifer environments and the main parameters that characterize these aquifers and their geological environments. The PACES geodatabase for the eastern Mauricie region also provides substantial information for diverse related research and subregional projects related to aquifer characterization, such as the protection and the quality of groundwater in eastern Mauricie.

Although the results of the PACES for the eastern Mauricie region are significant, knowledge acquisition is an evolving process, and it remains that a project of this sort offers only an initial portrait of the regional groundwater resources and does not provide more precise information, such as the available and exploitable groundwater volumes. However, at a more local scale, these estimates should be more manageable by accessing the data now collected and easily accessible in a database.

The main singular features of aquifer systems in eastern Mauricie are:

- Several large-scale accumulations of unconsolidated surface deposits, such as sand, gravel, and clay, sometimes reach thicknesses exceeding 100 m;

- Granular deposits of glacial or postglacial origin are the main aquifer type exploited for drinking water supply by municipalities;

- Several sectors in the region are likely to have significant aquifer reservoirs that have not yet been exploited, in particular, the Saint-Narcisse Moraine and the Piedmont regions;

- Surface sands of deltaic origin have heterogeneous granulometric and hydraulic characteristics favorable to groundwater and are also exploited to supply drinking water to municipalities;

- The piezometric map developed in this project indicates the shallow groundwater depth in the St Lawrence Lowlands (i.e., 0–20 m from the surface);

- The bedrock has a highly spatially variable topography. Therefore, the deep valleys in eastern Mauricie can contain substantial granular accumulations (i.e., deeply buried valleys), and the interpretation of the stratigraphic sections presented in this study could help to locate these valleys;

- Groundwater in eastern Mauricie is of good quality; 73% of the collected samples taken in the region had no exceedance of drinking water standards. However, 43% of the samples exceeded the aesthetic criteria, and 16% exceeded the new potability recommendations of Health Canada for manganese. Fluoride exceedance is also ubiquitous in the lowlands sector of the study area.

Following PACES, it is essential to continue acquiring groundwater-related information and monitoring groundwater quality, including updating the spatially referenced groundwater database that could be improved in a targeted way, starting with exploited groundwater or the aquifers identified as more vulnerable. More information is required regarding the parameters characterizing each aquifer in the region, such as hydraulic properties, hydrogeochemistry, piezometry, and recharge, to ensure the proper protection of vulnerable aquifers. Land-use and water managers (i.e., governmental agencies, watershed agencies, municipal policymakers, and consultants) must apply the information compiled in this database to ensure the sustainability and protection of this water resource.

Gathering groundwater information, mapping groundwater reservoirs, and establishing a spatially referenced groundwater database can be implemented for areas around the globe,

irrespective of geographical location, climatic conditions, or hydrological characteristics. These areas may include regions characterized by cold weather, such as polar and temperate climates, as well as warmer tropical and arid regions. Protecting and preserving the world's groundwater resources is a critical and even essential objective, which can be favored by characterizing aquifers. This characterization involves assessing the hydraulic properties, hydrogeochemistry, piezometry, and recharge to ensure the proper protection of vulnerable aquifers.

LISTE DES REFERENCES

Abi, A., Walter, J., Saeidi, A., and Chesnaux, R. 2022. A cluster-based multiparametric similarity test for the compartmentalization of crystalline rocks into structural domains. Quarterly Journal of Engineering Geology and Hydrogeology, 55. Geological Society of London.

Aller, L. 1987. DRASTIC: a standardized system for evaluating groundwater pollution potential using hydrogeologic settings. Robert S. Kerr Environmental Research Laboratory, Office of Research and Development. US Environmental Protection Agency., Oklahoma.

Bajc, A.F., Russell, H.A.J., and Sharpe, D.R. 2014. A three-dimensional hydrostratigraphic model of the Waterloo Moraine area, southern Ontario, Canada. Canadian Water Resources Journal/Revue canadienne des ressources hydriques, 39: 95–119. Taylor & Francis.

Barnett, P.J., Sharpe, D.R., Russell, H.A.J., Brennand, T.A., Gorrell, G., Kenny, F., and Pugin, A. 1998. On the origin of the Oak Ridges Moraine. Canadian Journal of Earth Sciences, 35: 1152–1167. NRC Research Press.

Bédard, J. 1971. Carte Géologique de la Région de Cartier-Tracy, Comtés de Montcalm, Joliette et Berthier. Ministère des Richesses Naturelles: Quebec, QC, Canada.

Béland, J., and Bergeron, R. 1959. Esquisse géologique du Québec méridional. Cah. Geogr. Que, 3: 131–138.

Benn, D., and Evans, D.J.A. 2010. Glaciers and glaciation. In 1ST edition. Routledge, London and New York. doi:10.4324/9780203785010.

Boumaiza, L., Chesnaux, R., Walter, J., and Meghnefi, F. 2021a. Assessing response times of an alluvial aquifer experiencing seasonally variable meteorological inputs. Groundwater for Sustainable Development, 14: 100647. Elsevier.

Boumaiza, L., Chesnaux, R., Walter, J., and Stumpp, C. 2020. Assessing groundwater recharge and transpiration in a humid northern region dominated by snowmelt using vadose-zone depth profiles. Hydrogeology Journal, 28: 2315–2329. Springer. doi:10.1111/gwat.13056.

Boumaiza, L., Chesnaux, R., Walter, J., and Stumpp, C. 2021b. Numerical assessment of water transit-time through a thick heterogeneous aquifer vadose-zone. In Geotechnical Conference and the 14th Joint CGS/IAH-CNC Groundwater Conference. Edited by Proceedings of the 74th Canadian Geotechnical Conference and the 14th Joint CGS/IAH-CNC Groundwater Conference (GeoNiagara-2021). Niagara Falls, Ontario, Canada. p. 6.

Boumaiza, L., Chesnaux, R., Walter, J., and Stumpp, C. 2021c. Constraining a flow model with field measurements to assess water transit time through a vadose zone. Groundwater, 59: 417–427. Wiley Online Library. doi:10.1111/gwat.13056.

Boumaiza, L., Rouleau, A., and Cousineau, P. 2015. Estimation of hydraulic conductivity and porosity of the identified lithofacies in the granular deposits of Valin river paleodelta in Saguenay region of Quebec. Edited by Proceedings of the 68th Canadian Geotechnical Conference (GeoQuebec-2015). Quebec City, Quebec, Canada. p. 9.

Boumaiza, L., Rouleau, A., and Cousineau, P. 2017. Determining hydrofacies in granular deposits of the Valin River paleodelta in the Saguenay region of Quebec. In Proceedings of the 70th Canadian Geotechnical Conference and the 12th Joint CGS/IAH-CNC Groundwater Conference, Ottawa, Ontario, Canada.

Boumaiza, L., Rouleau, A., and Cousineau, P. 2019. Combining shallow hydrogeological characterization with borehole data for determining hydrofacies in the Valin River paleodelta. In Proceedings of the 72nd Canadian Geotechnical Conference, St-John's, Newfoundland, Canada. p.

Boumaiza, L., Walter, J., Chesnaux, R., Brindha, K., Elango, L., Rouleau, A., Wachniew, P., and Stumpp, C. 2021d. An operational methodology for determining relevant DRASTIC factors and their relative weights in the assessment of aquifer vulnerability to contamination. Environmental Earth Sciences, 80: 1–19. Springer.

Boumaiza, L., Walter, J., Chesnaux, R., Lambert, M., Jha, M.K., Wanke, H., Brookfield, A., Batelaan, O., Galvão, P., and Laftouhi, N. 2022a. Groundwater recharge over the past 100 years: regional spatiotemporal assessment and climate change impact over the Saguenay-Lac-Saint-Jean region, Canada. Hydrological Processes,: e14526. Wiley Online Library. doi:10.1002/hyp.14526.

Boumaiza, L., Walter, J., Chesnaux, R., Stotler, R.L., Wen, T., Johannesson, K.H., Brindha, K., and Huneau, F. 2022b. Chloride-salinity as indicator of the chemical composition of groundwater: empirical predictive model based on aquifers in Southern Quebec, Canada. Environmental Science and Pollution Research, 29: 59414–59432. Springer. doi:10. 1007/ s11356- 022- 19854-z.

Brennand, T.A., and Shaw, J. 1996. The Harricana glaciofluvial complex, Abitibi region, Quebec: its genesis and implications for meltwater regime and ice-sheet dynamics. Sedimentary Geology, 102: 221–262. Elsevier. doi:10.1016/0037-0738(95)00069-0.

Brouard, E., Roy, M., Godbout, P.-M., and Veillette, J.J. 2021. A framework for the timing of the final meltwater outbursts from glacial Lake Agassiz-Ojibway. Quaternary Science Reviews, 274: 107269. Elsevier.

Burt, A. 2018. Three-dimensional hydrostratigraphy of the Orangeville Moraine area, southwestern Ontario, Canada. Canadian Journal of Earth Sciences, 55: 802–828. GeoScienceWorld. doi:10.1139/cjes-2017-0077.

Burt, A.K. 2012. Conceptual Geologic model for the Orangeville Moraine threedimensional project. In Summary of Field work and other Activities.

Calvache, M.L., Ibáñez, S., Duque, C., Martín-Rosales, W., López-Chicano, M., Rubio, J.C., González, A., and Viseras, C. 2009. Numerical modelling of the potential effects of a dam on a coastal aquifer in S. Spain. Hydrological Processes: An International Journal, 23: 1268–1281. Wiley Online Library. doi:10.1002/hyp.7234.

Castonguay, S., Dietrich, J., Shinduke, R., and Laliberté, J.Y. 2006. Nouveau regard sur l'architecture de la plate-forme du Saint-Laurent et des Appalaches du sud du Québec par le retraitement des profils de sismique réflexion M-2001, M-2002 et M-2003. Geological Survey of Canada, Open File, 5328: 19.

CERM-PACES. 2022a. Bases de Donnees Numeriques Publiques, (Donnees Quebec); Retrieved in january 2023 from https://cerm.uqac.ca/paces/lanaudiere-mauricie-est-moyenne-cote-nord/.

CERM-PACES. 2022b. Atlas_Rapport synthèse: retrived in november 2022 from https://constellation.uqac.ca/id/eprint/8531/2/ME_Atlas_RapportSynth%C3%A8se_VF5.pdf.

Chesnaux, R., Baudement, C., and Hay, M. 2011a. Assessing and comparing the hydraulic properties of granular aquifers on three different scales. Proceedings of Geohydro,: 28–31.

Chesnaux, R., and Elliott, A.-P. 2011. Demonstrating evidence of hydraulic connections between granular aquifers and fractured rock aquifers. In Proceedings of GeoHydro 2011, Joint Meeting of the Canadian Quaternary Association and the Canadian Chapter of the International Association of Hydrogeologists. pp. 28–31.

Chesnaux, R., Lambert, M., Walter, J., Fillastre, U., Hay, M., Rouleau, A., Daigneault, R., Moisan, A., and Germaneau, D. 2011b. Building a geodatabase for mapping hydrogeological features and 3D modeling of groundwater systems: Application to the Saguenay–Lac-St.-Jean region, Canada. Computers & Geosciences, 37: 1870–1882. Elsevier. doi:10.1016/j.cageo.2011.04.013.

Chesnaux, R., and Stumpp, C. 2018. Advantages and challenges of using soil water isotopes to assess groundwater recharge dominated by snowmelt at a field study located in Canada. Hydrological Sciences Journal, 63: 679–695. Taylor & Francis.

Clark, T., and Globensky, Y. 1975. Rapport géologique de la région des Grondines. Ministères des Richesses naturelles, Direction générale des mines.

Clark, T., and Globensky, Y. 1976. Carte géologique de la région de Sorel et la partie sud-est de Saint-Gabriel-de-Brandon, districts électoraux de Berthier, Joliette, Richelieu et Maskinongé. Edited ByD. générales des mines. Ministère des richesses naturelles.

Cloutier, V., Aubert, T., Audet-Gagnon, F., Blanchette, D., Castelli, S., Cheng, L.Z., Dallaire, P.-L., Fallara, F., Godbout, G., and Nadeau, S. 2011. Projet d'acquisition de connaissances sur les eaux souterraines de l'Abitibi-Témiscamingue, Québec. Proceedings, Geohydro,.

Cloutier, V., Blanchette, D., Dallaire, P.-L., Nadeau, S., Roy, M., and Rosa, E. 2013. Projet d'acquisition de connaissances sur les eaux souterraines de l'Abitibi-Témiscamingue (partie 1). Rapport final déposé au MDDEFP 135 p., 26 annexes, 25 cartes thématiques.

Cloutier, V., Rosa, E., Nadeau, S., Dallaire, P.-L., Blanchette, D., & Roy, M. 2015. Projet d'acquisition de connaissances sur les eaux souterraines de l'Abitibi-Témiscamingue (partie 2). Rapport de recherche P002.R3. Groupe de recherche sur l'eau souterraine, Institut de recherche en mines et en environnement, Université du Québec en Abitibi-Témiscamingue, 313 p., 15 annexes, 24 cartes thématiques (1:100 000).

Cojan, I., and Renard, M. 2013. Sédimentologie-3e édition. Dunod, Paris, France.

Cui, T., Sreekanth, J., Pickett, T., Rassam, D., Gilfedder, M., and Barrett, D. 2021. Impact of model parameterization on predictive uncertainty of regional groundwater models in the context of environmental impact assessment. Environmental Impact Assessment Review, 90: 106620. Elsevier. doi:10.1016/j.eiar.2021.106620.

Daigneault, R.-A., and Occhietti, S. 2006. Les moraines du massif Algonquin, Ontario, au début du Dryas récent, et corrélation avec la Moraine de Saint-Narcisse. Géographie physique et Quaternaire, 60: 103–118. Les Presses de l'Université de Montréal. doi:10.7202/016823ar.

Delisle, R. 2022. Développement d'une démarche collaborative pour l'élaboration d'un plan d'action sur l'eau souterraine en Estrie. Université Laval.

Denis, R. 1974. Late Quaternary geology and geomorphology in the Lake Maskinongé area, Québec. Uppsala, Sweden.

Douglas, R.J.W., Poole, W.H., Sanford, B. V, Williams, H., and Kelly, D.G. 1970. Geology and Economic minerals of Canada. In Geology and economic minerals of canada. Geological Survey of Canada Ottawa, Ontario. pp. 649–662.

Dyke, A.S., and Prest, V.K. 1987. Late Wisconsinan and Holocene history of the Laurentide Ice Sheet. Geographie Physique et Quaternaire, 41: 237–263. doi:10.7202/032681ar.

Evans, D. 2005. Glacial landsystems. In 1ST edition. Edited ByRoutledge. Routledge, London (UK) and New York (USA). doi:10.4324/9780203784976.

Ferroud, A. 2018. Analyse des dimensions d'écoulement et caractérisation hydrodynamique des aquifères complexes: du pompage à l'interprétation diagnostique. Université du Québec à Chicoutimi.

Ferroud, A., Rafini, S., and Chesnaux, R. 2019. Using flow dimension sequences to interpret non-uniform aquifers with constant-rate pumping-tests: A review. Journal of Hydrology X, 2: 100003. Elsevier.

Gadd, N., and Goldthwait, J.W. 1971. Pleistocene geology of the central St. Lawrence lowland with selected passage from an unpublished manuscript - The St. Lawrence Lowland, by J.W. Goldthwait.

Gadd, N., and Karrow, P.F. 1960. Surficial Geology, Trois-Rivières, St-Maurice, Champlain, Maskinonge and Nicolet Counties, Quebec. Geological Survey of Canada, Trois-Rivières, St-Maurice, Québec. doi:doi.org/10.4095/108651.

Gagné, S., Larocque, M., Morard, A., and Roux, M. 2022. Projet d'acquisition de connaissances sur les eaux souterraines dans la région des Laurentides et de la MRC les Moulins. Rapport synthèse. Rapport déposé au ministère de l'Environnement et de la Lutte contre les changements climatiques. Université du Québec à Montréal.

Globensky, Y. 1987. Géologie des Basses-Terres du Saint-Laurent. Ministère de l'énergie et des ressources, direction générale de l'exploration géologique et minérale, Québec (Qc).

Godbout, P.-M., Brouard, E., and Roy, M. 2023. 1-km resolution rebound surfaces and paleotopography of glaciated North America since the Last Glacial Maximum. Scientific Data, 10: 735. Nature Publishing Group UK London.

Grenier, C., and Denis, R. 1974. Etude hydrogeomorphologique dans la region du Lac Maskinongé, Québec. Canadian Journal of Earth Sciences, 11: 733–754. NRC Research Press Ottawa, Canada.

Hardy, L. 1982. La moraine frontale de Sakami, Québec subarctique The Sakami Moraine. Subarctic Québec. Géographie physique et quaternaire, 41: 18–32. doi:10.7202/032469ar.

Hillaire-Marcel, C., Occhietti, S., and Vincent, J.S. 1981. Sakami moraine, Quebec: A 500-km-long moraine without climatic control. Geology, 9: 210–214. doi:10.1130/0091-7613(1981)9<210:SMQAKM>2.0.CO;2.

https://ags.aer.ca/research-initiatives/water-resources. (n.d.). Alberta Geological Survey (Accessed january 2023).

Https://ehyd.gv.at/#. (n.d.). ehyd Republic Tcheck (Accessed October 2022).

https://igme.maps.arcgis.com/home/gallery. (n.d.). IGME Spain (Accessed October 2022).

https://infoterre.brgm.fr. (n.d.). Infoterre France (Accessed October 2022).

https://s.geo.admin.ch/9b181a62f6. (n.d.). Geo admin Switzerland (Accessed October 2022).

https://trca.ca/conservation/. (n.d.). Ontario Geological Survey (Accessed january 2023).

https://www.bafg.de/de/home/homepage. (n.d.). BAFG Germany (Accessed October 2022).

https://www.legisquebec.gouv.qc.ca/fr/document/rc/Q-2, 20r.%2040%20/. (n.d.). Legislation Quebec gouvernement (Accessed january 2023).

https://www.usgs.gov/. (n.d.). USGS governement United State (Accessed October 2022).

Hudon-Gagnon, E., Chesnaux, R., Cousineau, P.A., and Rouleau, A. 2015. A hydrostratigraphic simplification approach to build 3D groundwater flow numerical models: example of a Quaternary deltaic deposit aquifer. Environmental earth sciences, 74: 4671–4683. Springer. doi:10.1007/s12665-015-4439-y.

Labrecque, G., Chesnaux, R., and Boucher, M.-A. 2020. Water-table fluctuation method for assessing aquifer recharge: application to Canadian aquifers and comparison with other methods. Hydrogeology Journal, 28: 521–533. Springer.

Lambert, M., Ferroud, A., Desmeules, L.-P., and Walter, J. 2022. CERM-PACES LAMEMCN public report, (Donnees Quebec); https://constellation.uqac.ca/id/eprint/8531/1/ME_Rapport_Scientifique_VF5.pdf.

Landry, B., Beaulieu, J., Gauthier, M., Lucotte, M., Moingt, S., Occhietti, S., Pinti, D.L., and Quirion, M. 2012. Notions de géologie. In Modulo, Montréal, 4nd ed. Modulo, Montréal (Qc).

Laplante, R. 2021. Évaluation d'approches complémentaires pour déterminer la connectivité entre les milieux humides et l'eau souterraine et de surface.

Larocque, M., Cloutier, V., Levison, J., and Rosa, E. 2018. Results from the Quebec groundwater knowledge acquisition program. Taylor & Francis.

Larocque, M., Meyzonnat, G., Ouellet, M.-A., Graveline, M.-H., Gagné, S., Barnetche, D., and Dorner, S. 2015. Projet de connaissance des eaux souterraines de la zone Vaudreuil-Soulanges: rapport final déposé au ministère du Développement durable, de l'Environnement et de la Lutte contre les changements climatiques. Université du Québec à Montréal, Montréal, Québec, Montréal, Québec, Canada.

Larocque, M. 2023. Eaux souterraines Un premier inventaire des connaissances scientifiques. Vecteur Environnement, 56: 22–24. Réseau Environnement.

Lasalle, P., and Chagnon, J.-Y. 1968. An ancient landslide along the Saguenay River, Quebec. Canadian Journal of Earth Sciences, 5: 548–549. doi:10.1139/e68-049.

Lavoie, R., Joerin, F., and Rodriguez, M.J. 2014. Incorporating groundwater issues into regional planning in the Province of Quebec. Journal of Environmental Planning and Management, 57: 516–537. Taylor & Francis.

Leblanc, Y., Légaré, G., Lacasse, K., Parent, M., and Campeau, S. 2013. Caractérisation hydrogéologique du sud-ouest de la Mauricie. Rapport déposé au ministère du Développement durable, de l'Environnement, de la Faune et des Parcs dans le cadre du Programme d'acquisition de connaissances sur les eaux souterraines du Québec: Département des sciences de l'environnement, Université du Québec a Trois-Rivière.

Légaré-Couture, G. 2013. Hydrostratigraphie et modélisation géologique 3D du sud-ouest de la Mauricie. Université du Québec à Trois-Rivières.

Légaré-Couture, G., Leblanc, Y., Parent, M., Lacasse, K., and Campeau, S. 2018. Three-dimensional hydrostratigraphical modelling of the regional aquifer system of the St. Maurice Delta Complex (St. Lawrence Lowlands, Canada). Canadian Water Resources Journal/Revue canadienne des ressources hydriques, 43: 92–112. Taylor & Francis. doi:10.1080/07011784.2017.1316215.

Lévesque, Y., Chesnaux, R., and Walter, J. 2023a. Using geophysical data to assess groundwater levels and the accuracy of a regional numerical flow model. Hydrogeology Journal,. doi:10.1007/s10040-023-02591-z.

Lévesque, Y., St-Onge, G., Lajeunesse, P., Desiage, P., and Brouard, E. 2019. Defining the maximum extent of the Laurentide Ice Sheet in Home Bay (eastern Arctic Canada)

during the Last Glacial episode. Boreas, 49: 52–70. Wiley Online Library. doi:10.1111/bor.12415.

Lévesque, Y., Walter, J., and Chesnaux, R. 2021. Transient Electromagnetic (TEM) Surveys as a First Approach for Characterizing a Regional Aquifer: The Case of the Saint-Narcisse Moraine, Quebec, Canada. Geosciences, 11: 415–442. Multidisciplinary Digital Publishing Institute. doi:10.3390/ geosciences11100415.

Lévesque, Y., Walter, J., Chesnaux, R., Dugas, S., and David, N. 2023b. Electrical resistivity of saturated and unsaturated sediments in northeastern Canada. Environmental earth sciences,. doi:10.1007/s12665-023-10998-w.

Mayrand, J. 2021. Appropriation des connaissances sur l'eau souterraine vers une intégration dans le schéma d'aménagement et développement. Unpub. Ms.C. dissertation, Laval University, Quebec city, Quebec, Canada.

McCormack, R. 1983. Etude hydrogéologique de la rive nord du Saint-Laurent. Énergie et ressource naturelle (Service des eaux souterraines), Québec (Qc). p. 188.

McMartin, I., Godbout, P., Campbell, J.E., Tremblay, T., and Behnia, P. 2021. A new map of glacigenic features and glacial landsystems in central mainland Nunavut, Canada. Boreas, 50: 51–75. Wiley Online Library.

Montcoudiol, N., Molson, J., Lemieux, J.-M., and Cloutier, V. 2015. A conceptual model for groundwater flow and geochemical evolution in the southern Outaouais Region, Québec, Canada. Applied Geochemistry, 58: 62–77. Elsevier.

Nadeau, L., and Brouillette, P. 1995. Structural Map of Trois-Rivières_Grenville Province; Map 1:250,000. Geological Survey of Canada: Ottawa, ON, Canada. doi:10.4095/205047.

Nadeau, S., Rosa, E., and Cloutier, V. 2018. Stratigraphic sequence map for groundwater assessment and protection of unconsolidated aquifers: A case example in the Abitibi-Témiscamingue region, Québec, Canada. Canadian Water Resources Journal/Revue canadienne des ressources hydriques, 43: 113–135. Taylor & Francis.

Nadeau, S., Rosa, E., Cloutier, V., Daigneault, R.-A., and Veillette, J. 2015. A GIS-based approach for supporting groundwater protection in eskers: Application to sand and gravel extraction activities in Abitibi-Témiscamingue, Quebec, Canada. Journal of Hydrology: Regional Studies, 4: 535–549. Elsevier.

Nadeau, S., Rosa, E., Cloutier, V., Mayappo, D., Paran, F., and Graillot, D. 2021. Spatial analysis approaches for the evaluation and protection of groundwater resources in large watersheds of the Canadian Shield. Hydrogeology Journal, 29: 2053–2075. Springer Nature BV.

Neal, A. 2004. Ground-penetrating radar and its use in sedimentology: principles, problems and progress. Earth-science reviews, 66: 261–330. Elsevier. doi:10.1016/j.earscirev.2004.01.004.

Occhietti. 1977. Stratigraphie du Wisconsinien de la région de Trois-Rivières-Shawinigan, Québec. Géographie physique et Quaternaire, 31: 307–322. Les Presses de l'Université de Montréal. doi:10.7202/1000280ar.

Occhietti. 1980. Le quaternaire de la région de Trois Rivières-Shawinigan, Québec. Contribution à la paléogéographie de la vallée moyenne du Saint-Laurent et corrélations stratigraphiques. Paleo-Quebec Trois-Rivières,.

Occhietti. 2007. The Saint-Narcisse morainic complex and early Younger Dryas events on the southeastern margin of the Laurentide Ice Sheet. Géographie physique et Quaternaire, 61: 89–117. Les Presses de l'Université de Montréal. doi:10.7202/038987ar.

Occhietti, ChartierH, M., Hillaire-Marcel, C., Cournoyer, M., Cumbaa, S., and Harington, R. 2001. Paléoenvironnements de la Mer de Champlain dans la région de Québec, entre 11 300 et 9750 BP: le site de Saint-Nicolas. Géographie physique et Quaternaire, 55: 23–46. Les Presses de l'Université de Montréal. doi:10.7202/005660ar.

Occhietti, S., David, P., Gadd, N.R., and Lebuis, J. 1982. Fiches des principales unités lithostratigraphiques quaternaires du québec méridional. Géographie physique et Quaternaire, 36, n: 15-49.

Parent, M., and Occhietti, S. 1988. Late Wisconsinan deglaciation and Champlain sea invasion in the St. Lawrence valley, Québec. Géographie physique et Quaternaire, 42: 215–246. Les Presses de l'Université de Montréal. doi:10.7202/032734ar.

Parent, M., and Occhietti, S. 1999. Late Wisconsinan deglaciation and glacial lake development in the Appalachians of southeastern Québec. Géographie physique et Quaternaire, 53: 117–135. Les Presses de l'Université de Montréal. doi:10.7202/004859ar.

Parriaux, A., and Nicoud, G. 1993. De la montagne à la mer, les formations glaciaires et l'eau souterraine. Exemple du contexte Nord-alpin occidental. Quaternaire, 4: 61–67. Association française pour l'étude du quaternaire. doi:10.3406/quate.1993.1993.

Preisig, G., Cornaton, F.J., and Perrochet, P. 2014. Regional flow and deformation analysis of basin-fill aquifer systems using stress-dependent parameters. Groundwater, 52: 125–135. Wiley Online Library. doi:10.1111/gwat.12034.

Prichonnet, G., Doiron, A., and Cloutier, M. 1982. Le mode de retrait glaciaire tardiwisconsinien sur la bordure appalachienne au sud du Québec. Géographie physique et Quaternaire, 36: 125–137. Les Presses de l'Université de Montréal.

Reynolds, J.M. 2011. An introduction to applied and environmental geophysics. In 2nd edition. John Wiley & Sons, West Sussex, UK.

Richard, S.K., Chesnaux, R., Rouleau, A., Morin, R., Walter, J., and Rafini, S. 2014. Field evidence of hydraulic connections between bedrock aquifers and overlying granular aquifers: examples from the Grenville Province of the Canadian Shield. Hydrogeology journal, 22: 1889–1904. Springer.

Rivers, T., Gool, J.A.M. van, and Connelly, J.N. 1993. Contrasting tectonic styles in the northern Grenville province: Implications for the dynamics of orogenic fronts. Geology, 21: 1127–1130. Geological Society of America. doi:10.1130/0091-7613(1993)021<1127:CTSITN>2.3.CO;2.

Rouleau, A., Larocque, M., Walter, J., Gagné, S., Tremblay, L., and Germaneau, D. 2012. Le programme d'acquisition de connaissances sur les eaux souterraines. In Vecteur Environnement. Réseau Environnement, Montréal, Québec, Canada.

Roy, J., Morin, R., Chesnaux, R., Richard, S., Pino, D.S., Rouleau, A., Roy, D.W., Walter, J., and Noël, D. 2011. Hydrogeological insight from geophysical water-well logging in hard rocks in the Saguenay region, Québec. GeoHydro, Quebec, Canada. Proceedings Papers, DOC-2288,.

Russell, H.A.J., Brennand, T.A., Logan, C., and Sharpe, D.R. 1998. Standardization and assessment of geological descriptions from water well records: Greater Toronto and Oak Ridges Moraine areas, southern Ontario. Current Research,: 89–102.

Salsabili, M., Saeidi, A., Rouleau, A., and Nastev, M. 2021a. Seismic microzonation of a region with complex surficial geology based on different site classification approaches. Geoenvironmental Disasters, 8: 1–13. SpringerOpen.

Salsabili, M., Saeidi, A., Rouleau, A., and Nastev, M. 2021b. 3D Probabilistic Modelling and Uncertainty Analysis of Glacial and Post-Glacial Deposits of the City of Saguenay, Canada. Geosciences, 11: 204. MDPI.

Sharpe, D.R., Pugin, A., Pullan, S.E., and Gorrell, G. 2003. Application of seismic stratigraphy and sedimentology to regional hydrogeological investigations: an example from Oak Ridges Moraine, southern Ontario, Canada. Canadian Geotechnical Journal, 40: 711–730. NRC Research Press.

Simard, J., Occhietti, S., and Robert, F. 2003. Retrait de l'inlandsis sur les Laurentides au début de l'Holocène: transect de 600 km entre le Saint-Maurice et le Témiscamingue (Québec). Géographie physique et Quaternaire, 57: 189–204. Les Presses de l'Université de Montréal.

Steenhuis, T.S., and Van der Molen, W.H. 1986. The Thornthwaite-Mather procedure as a simple engineering method to predict recharge. Journal of Hydrology, 84: 221–229. Elsevier. doi:10.1016/0022-1694(86)90124-1.

Tremblay, R., Walter, J., Chesnaux, R., and Boumaiza, L. 2021. Investigating the Potential Role of Geological Context on Groundwater Quality: A Case Study of the Grenville and St. Lawrence Platform Geological Provinces in Quebec, Canada. Geosciences, 11: 503. MDPI.

Tricart, J. 1983. S. Occhietti, Le Quaternaire de la région de Trois-Rivières-Shawinigan, Québec. Contribution à la paléogéographie de la vallée moyenne du St-Laurent et corrélations stratigraphiques. In Annales de géographie. Edited by Armand Colin. Persée-Portail des revues scientifiques en SHS, Paris, France. pp. 242–245.

Turgeon, F., Larocque, M., Meyzonnat, G., Dorner, S., and Bourgault, M.-A. 2018. Examining the challenges of simulating surface water–groundwater interactions in a post-glacial environment. Canadian Water Resources Journal/Revue canadienne des ressources hydriques, 43: 262–280. Taylor & Francis.

Veillette, J. 1983. Déglaciation de la vallée supérieure de l'Outaouais, le lac Barlow et le sud du lac Ojibway, Québec. Géographie physique et Quaternaire, 37: 67–84. Érudit. doi:10.7202/032499ar.

Walter, J., Rouleau, A., Chesnaux, R., Lambert, M., and Daigneault, R. 2018. Characterization of general and singular features of major aquifer systems in the Saguenay-Lac-Saint-Jean region. Canadian Water Resources Journal/Revue canadienne des ressources hydriques, 43: 75–91. Taylor & Francis. doi:10.1080/07011784.2018.1433069.Abu-Abi, Attoumane, Julien Walter, Ali Saeidi, and Romain Chesnaux. 2022. "A Cluster-Based Multiparametric Similarity Test for the Compartmentalization of Crystalline Rocks into Structural Domains." *Quarterly Journal of Engineering Geology and Hydrogeology* 55 (3).

CHAPITRE 2

TRANSIENT ELECTROMAGNETIC (TEM) SURVEYS AS A FIRST APPROACH FOR CHARACTERIZING A REGIONAL AQUIFER: THE CASE OF THE SAINT-NARCISSE MORAINE, QUEBEC, CANADA

Le chapitre 2 de cette thèse est présenté sous la forme d'un article scientifique. Il s'agit du premier outil d'investigation développé dans notre approche méthodologique pour mieux évaluer le potentiel aquifère d'un milieu de dépôt quaternaire hétérogène et anisotrope. Étant donné que les contextes géologiques qui manquent d'informations stratigraphiques et piézométriques sont difficiles à cartographier initialement en termes d'hydrogéologie, ce chapitre propose une approche pour caractériser un aquifère régional en utilisant des données géophysiques (Transient ElectroMagnetic surveys - levés électromagnétiques transitoires (TEM)) en support aux autres données conventionnelles d'acquisition de données en hydrogéologie. Cette approche permet de corréler les informations stratigraphiques et piézométriques, et de caractériser les aquifères granulaires régionaux en termes de stratigraphie, de géométrie, d'épaisseur et d'étendue.

Dans cette étude, les données TEM, combinées à la cartographie piézométrique et aux enregistrements sédimentaires des forages et des coupes stratigraphiques, ont révélé la compartimentation d'un système morainique de plusieurs kilomètres et ont indiqué la présence de deux grands aquifères granulaires à nappe libre recouvrant le substratum rocheux. Ces aquifères s'étendent sur plus de 12 km d'est en ouest à travers la zone d'étude et ont une épaisseur comprise entre 25 et >94 m. La méthode TEM fournit des informations critiques sur les eaux souterraines à une échelle régionale en acquérant des données à partir de plusieurs stations dans un court laps de temps à un degré non possible avec d'autres méthodologies existantes.

Le présent article a été soumis dans la revue Geosciences (IF : 3,03) le 17 août 2021 et publié le 6 octobre 2021. https://doi.org/10.3390/ geosciences11100415

Yan Lévesque [1, 2]*, Julien Walter [1, 2], Romain Chesnaux [1, 2]

[1]Université du Québec à Chicoutimi, Department of Applied Sciences, Saguenay, QC, G7H 2B1 Canada;

[2]Centre d'études sur les ressources minérales (CERM), Groupe de recherche risque ressource eau (R2EAU), Université du Québec à Chicoutimi, Saguenay, QC, Canada G7H 2B1, Canada

Email: julien_walter@uqac.ca; romain_chesnaux@uqac.ca

*corresponding author: yan.levesque1@uqac.ca

Orcid ID: YL: 0000-0002-6198-6315; RC: 0000-0002-1722-9499; JW: 0000-0003-2514-6180

2.1 ABSTRACT

Geological contexts that lack minimal stratigraphic and piezometric information can be challenging to produce an initial hydrogeological map in remote territories. This study proposes an approach to characterize a regional aquifer using transient electromagnetic (TEM) surveys. Given the presence of randomly dispersed boreholes, the Saint-Narcisse moraine in the Mauricie region of Quebec (Canada) is an appropriate site for collecting the required geophysical data, correlating the stratigraphic and piezometric information, and characterizing regional granular aquifers in terms of stratigraphy, geometry, thickness, and extent. In order to use all TEM results (i.e., 47 stations) acquired in the moraine area, we also correlated 13 TEM stations, 7 boreholes, and 6 stratigraphic cross-sections to derive an empirical and local petrophysical relationship and to establish a calibration chart of the sediments. Our TEM data, combined with piezometric mapping and the sedimentary records from boreholes and stratigraphic cross-sections, revealed the compartmentalization of a multi-kilometer morainic system and indicated the presence of two large unconfined granular aquifers overlying the bedrock. These aquifers extend more than 12 km east to west across the study area and are between 25 and >94 m thick. The TEM method provides critical information on groundwater

at a regional scale by acquiring information from multiple stations within a short time span to a degree not possible with other existing methodologies.

Keywords: Transient electromagnetic surveys (TEM); Saint-Narcisse moraine; stratigraphy; sediments; aquifer; regional piezometry; groundwater potential

2.2 INTRODUCTION

Morainic complexes have a spatial arrangement and hydraulic characteristics (i.e., permeability, porosity, and particle size) that are favorable for groundwater storage (Parriaux and Nicoud 1993, Burt 2018). Often located in northern environments and far from urban areas, moraines are sometimes difficult to access, and collecting data using conventional hydrogeological methods, such as boreholes and piezometers, can be challenging in these environments. Geophysical surveys can quickly investigate an accumulation of glacial sediments (e.g., a moraine) to efficaciously assess the internal dimensions and stratigraphic variability of any contained aquifers. The transient electromagnetic (TEM) method applied to groundwater exploration provides a non-invasive, inexpensive, and effective means of characterizing the internal structure of moraine deposits and delineating the geometrical features of various hydrogeological targets (Schrott et al. 2003, Sass 2006, McClymont et al. 2010).

In the province of Quebec, Canada, the deglacial period saw the formation of complex granular aquifers, such as those associated with the Saint-Narcisse morainic complex. This deposit is a major Quaternary formation that stretches along the southern margin of the Canadian Shield and extends from the town of Saint-Siméon in Quebec to the Great Lakes in Ontario (Daigneault and Occhietti 2006, Occhietti 2007). This vestige of the Younger Dryas cooling period (12.7–12.4 cal. ka BP; (Occhietti et al. 2001, Occhietti 2007)) was deposited during a readvance of the Laurentide ice sheet (LIS). Thick layers of well-sorted sands and gravels have been observed at the surface of this morainic complex (Occhietti 1977, 2007, Girard 2001, Daigneault and Occhietti 2006); these deposits represent potential aquifers. The overall extent of the Saint-Narcisse morainic complex is not continuous and is frequently interrupted by multiple sections composed of finer

sediments deposited by the Champlain Sea (Daigneault and Occhietti 2006) during its incursion into the isostatically depressed region following the retreat of the LIS. These less permeable sediments (i.e., clay and silt) act as natural impermeable barriers that limit connections between granular aquifers, create a discontinuity of the stratigraphic units within the moraine, and compartmentalize any contained aquifers.

In the Mauricie region of Quebec, Canada (Figure 13), municipalities have collected hydrogeological data (e.g., borehole logs, pumping tests, and piezometric surveys) from around the moraine. Nonetheless, the distribution of these aquifers remains poorly constrained and documented, and no study has yet to investigate their spatial extent, thickness, and location. Furthermore, the existing groundwater-related data have never been integrated into a regional-scale portrait of these morainic aquifers. The Saint-Narcisse morainic complex is mainly located in rural areas, and several sectors of the moraine are difficult to access and are thus characterized by a lack of data. Here, we aim to improve the existing stratigraphic data by establishing: (1) the simplified architecture of the deposits; (2) the groundwater elevation; and (3) the depth of the bedrock.

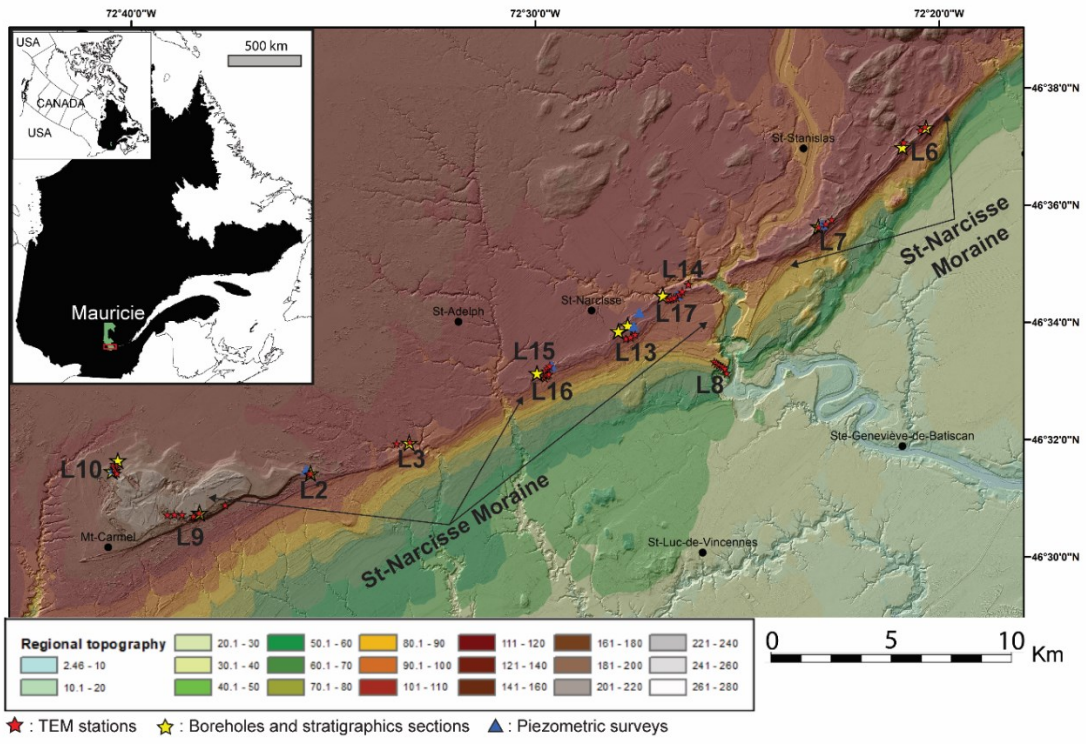

Figure 13: Regional topography of the study area and location of TEM 2D sections, boreholes, stratigraphic cross-sections, and piezometric surveys acquired from the Saint-Narcisse moraine. (Top left) General map spanning over the region of the Mauricie in the Province of Québec in Canada. The red rectangle represents the study area.

The electrical resistivity values of the Saint-Narcisse moraine deposits are unknown, and establishing a correlation between the stratigraphy and the geophysical response is not straightforward (Légaré-Couture et al. 2018). Several authors (Palacky 1987, 1993, Sorensen et al. 2000, Danielsen et al. 2003, Reynolds 2011, Goldman and Kafri 2020) have shown that different subsurface sedimentary layers can share a similar resistivity; therefore, there can be a possible overlap between different stratigraphic units and electrical resistivity values. To circumvent this overlap problem and efficaciously use the TEM approach, we develop, in an initial step, a calibration chart of electrical resistivity values associated with each sediment class typically found within the Saint-Narcisse moraine in the Mauricie region. This chart allows for the interpretation of the obtained electrical resistivity values for both unsaturated and saturated sediments. The chart also extends the interpretation of TEM results collected during the field campaign to locations where no boreholes or piezometric observations are available (i.e., 27 stations). To characterize the Saint-Narcisse morainic

aquifers at a regional scale, we then use TEM to collect geophysical data in support of hydrogeological mapping to (1) improve the understanding of the sediment architecture within the moraine and (2) delineate the spatial extent of the Saint-Narcisse moraine aquifers in the Mauricie region. This study was conducted in 2019–2020 as part of the Groundwater Knowledge Acquisition Program (PACES; (Chesnaux et al. 2011, Larocque et al. 2015, Walter et al. 2018)), sponsored by the Quebec Ministry of the Environment (MDDELCC). The various PACES projects aim to produce a realistic portrait of existing groundwater resources of the municipalized territories of southern Quebec to protect these aquifers and ensure their longterm sustainability.

2.3 STUDY AREA AND GEOLOGICAL OVERVIEW

2.3.1 BASEMENT GEOLOGY

The study area is in the southeastern portion of the Mauricie region, situated between Montreal and Quebec City (Figure 13). This area, lying between the St. Lawrence Lowlands and the Grenville Province, consists mainly of a relatively flat topography where agriculture is the main economic activity. The St. Lawrence Platform (i.e., St. Lawrence Lowlands) lies to the south of the moraine and is composed of Paleozoic sedimentary rocks, which are covered by a thick layer of Quaternary sediments. These sedimentary rocks are composed mainly of Ordovician sandstone (Black River group), carbonate (Trenton group), and shales (Utica and Lorraine groups) deposited in a marine environment (Douglas et al. 1970, Occhietti 1977, Globensky 1987, Légaré-Couture et al. 2018). This geological province is bounded to the northwest by the Precambrian Canadian Shield and to the southeast by the Appalachians. The Grenville Province, the youngest province of this Precambrian shield, lies to the north of the study area and consists mainly of high-grade igneous and metamorphic intrusive rocks (Rivers et al. 1993). The lithologic composition of the Grenville Province varies depending on the area; anorthosite, mangerite, charnockite, orthogneiss, paragneiss, migmatite, and marble are the main rocks found near the study area (Nadeau and Brouillette n.d., Globensky 1987, Légaré-Couture et al. 2018).

2.3.2 QUATERNARY SEDIMENT DEPOSITS

Quaternary surface deposits in the Mauricie region (Figure 14) were mapped recently under the 2018–2021 PACES project directed by the University of Quebec at Chicoutimi (UQAC). Most Quaternary deposits associated with the Saint-Narcisse moraine relate to the last glaciation (i.e., Wisconsinan glaciation) and were deposited during deglaciation. The isostatic depression caused by the LIS, combined with a rapid global rise in sea level, led to a marine transgression and the incursion of the Champlain Sea into the region. The sea flooded the valleys of the lowlands and led to deposits reflecting both deep and shallow marine environments (i.e., distal and proximal glacio-marine deposits) in the study area. This marine transgression lasted about 2000 years (13–11.2 cal. ka BP) and reached an elevation of about 200 m asl (i.e., above present-day sea level; (Parent and Occhietti 1988, 1999)). Isostatic rebound during the Holocene provoked a marine regression, and the Champlain Sea deposited regressive sands during its retreat.

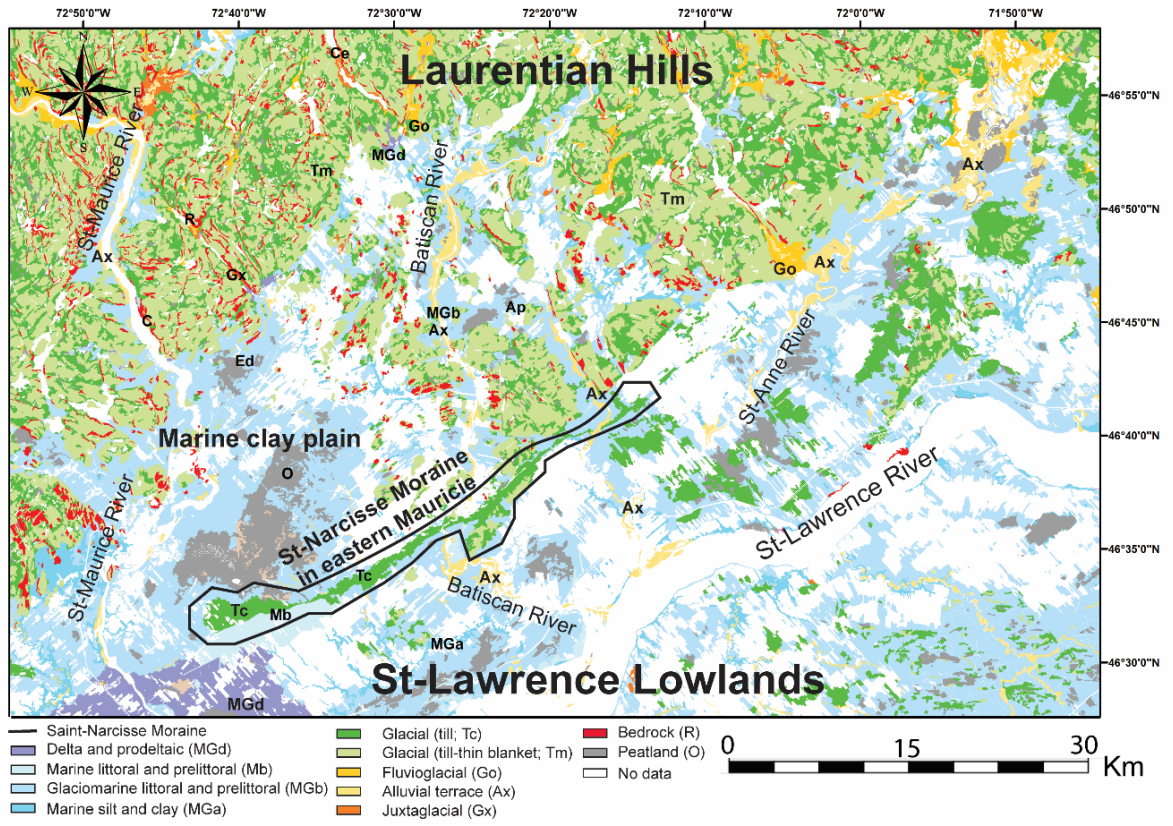

Figure 14: Surface deposit map of Quaternary sediments from the southeastern Mauricie region. The four main hydrogeological contexts are identified: Laurentian Mountains, marine clay, Saint-Narcisse moraine, and St. Lawrence Lowlands.

2.3.2 SAINT-NARCISSE MORAINE

During the last glacial period, the LIS covered most of Canada and attained a thickness of 5 km in places (Dyke and Prest 1987, Evans 2005, Benn and Evans 2010, Dietrich et al. 2010, Margold et al. 2015, Stokes 2017, Lévesque et al. 2019). This ice sheet crushed, removed, and transported rocks and sediments and produced glacial deposits composed mainly of diamicton (i.e., tills). Climate-related phases of LIS advance and retreat left behind numerous frontal moraines represented by long ridges composed of glacial sediments (Evans 2005, Benn and Evans 2010, Landry et al. 2012). The Saint-Narcisse morainic complex is discontinuous but extends over more than 1,400 km and is one of the longest documented frontal moraines in Canada (Daigneault and Occhietti 2006). The moraine can reach up to 100 m thick, although it generally varies locally between 1 and 20 m (Occhietti 1977,

Tricart 1983). A variety of sedimentary facies make up the stratigraphic sections of this moraine: till wedges, subglacial or melt-out till deposited during the last glaciation, proximal and distal glaciomarine deposits, as well as juxtaglacial and fluvioglacial deposits (i.e., ice-marginal outwash (Occhietti 1977, 2007)).

In low-lying areas, the Champlain Sea event deposited a thick layer of clay covered by regressive sands deposited during the marine regression. At higher elevations (e.g., the sides and top of the moraine), the Champlain Sea deposited proximal glaciomarine sediments and reworked the glacial tills put in place during deglaciation or the Younger Dryas readvance (YG; (Parent and Occhietti 1988, 1999, Daigneault and Occhietti 2006, Occhietti 2007)). The till deposits were reworked by waves and currents to form visible terraces on the seaward side of the moraine (Figures 13 and 14). Therefore, these terraces are essentially composed of coastal and sublittoral sands deposited in the shallowest areas of the Champlain Sea and by fluvioglacial sediments of small and large deltas that formed in the valleys at the mouths of rivers entering the Champlain Sea (Parent and Occhietti 1988, Occhietti et al. 2001, Occhietti 2007, Légaré-Couture et al. 2018).

Groundwater found in these areas is the main source of drinking water and is exploited locally to supply several municipalities (e.g., Saint-Narcisse, Saint-Prosper, and Saint-Maurice), which attests to the local aquifer capacity of the moraine. It is therefore possible to deduce that there is likely a high groundwater potential in this area of the Saint-Narcisse morainic complex. Our goal is to validate this potential and delimit the aquifer's boundaries.

2.4 MATERIALS AND METHODS

2.4.1 TEM FIELD SETUP

TEM measurements are performed using loops of electrical wire deployed on the ground. A time-varying current is injected into a transmitter loop (Tx), which induces a primary electromagnetic field into the subsoil. This initial electromagnetic field interacts with the subsurface geological materials to produce an electric current that induces a secondary electromagnetic field; this secondary field contains information regarding the underground electrical properties and is detected by a receiving loop (Rx) on the surface connected to a receptor that measures the rate of decay of

the electromagnetic field. The rate of decrease is then reversed in electrical resistivity (Nabighian and Macnae 1991, Fitterman and Labson 2005). This method does not involve direct electrical contact with the ground (i.e., electrodes) and produces results for a range of depths, from a few to several hundred meters. The advantages of this method are numerous. It is inexpensive, non-destructive, fast, robust, and ensures efficient operations within various environmental conditions (e.g., swamps, coastal areas, forests, and mountains; (Fitterman and Stewart 1986, Kafri et al. 1997, Parsekian et al. 2015, Kalisperi et al. 2018)). On the other hand, it has the disadvantage of being sensitive to proximity interference (buried or not), such as the presence of metal pipes, cables, fences, and power lines (Sorensen et al. 2000, Danielsen et al. 2003).

For this study, TEM data were collected over three months (summer 2020) and involved 47 TEM surveys acquired at 12 locations across the Saint-Narcisse moraine in the Mauricie region. The TEM instrument used for this study consisted of an NT-32 transmitter and a 32II multifunction GDP-receiver (MacInnes and Raymond 2001) and included a portable battery-operated transmitter-receiver (TX-RX) console. For this series of soundings, we used a square-sized loop configuration of 20 × 20 m for the TEM transmitter. The pulse current in the generating loop was set at 3A, and the frequency of the filter was set at 32 Hz with a 50% duty cycle. The turn-off time was 1.5 μs with the damping resistor set at 250 Ω. The induced voltage was measured using a 5 × 5 m receiver loop (in-loop configuration). The NanoTEM equipment consisted of a high-speed sampling card with a fixed gain stage of Å~10. Data were stacked in 8 blocks of 4096 cycles each, giving a total of 32,768 stacks. This resulted in a noise level of approximately 10 μV/A.

2.4.2 TEM DATA INVERSION

Once the resistivity data were acquired, our main goal was to deduce the subsurface resistivity distribution by inverting the data. Converting the TEM signals into an electrical resistivity model of the ground involves three processing steps relying on different software packages. First, raw data are averaged using TEMAVG Zonge software (MacInnes and Raymond 2001, 2005). This step also filters inconsistent data points (i.e., outliers), which must be deleted before the inversion (Figure 15). Because the magnetic field intensity decreases with depth, the amplitude of the

measured data decreases over time, with time playing the role of pseudo-depth. Here, the results are represented by a variation of the apparent resistivity. When the noise level (distortion) increases and the decay rate of the signal becomes discontinuous, the variations of the induced voltage (i.e., dB/dt) increase greatly, and the obtained results are no longer reliable. It is therefore necessary to remove these inconsistent data points (i.e., outliers; red crosses on Figure 15) manually when processing data with TEMAVG to retain only high-quality data. Figure 15 provides an overview of the acquired data and shows measured raw data (as crosses), the residual number, the inversion best fit (black line), and the corresponding resistivity model.

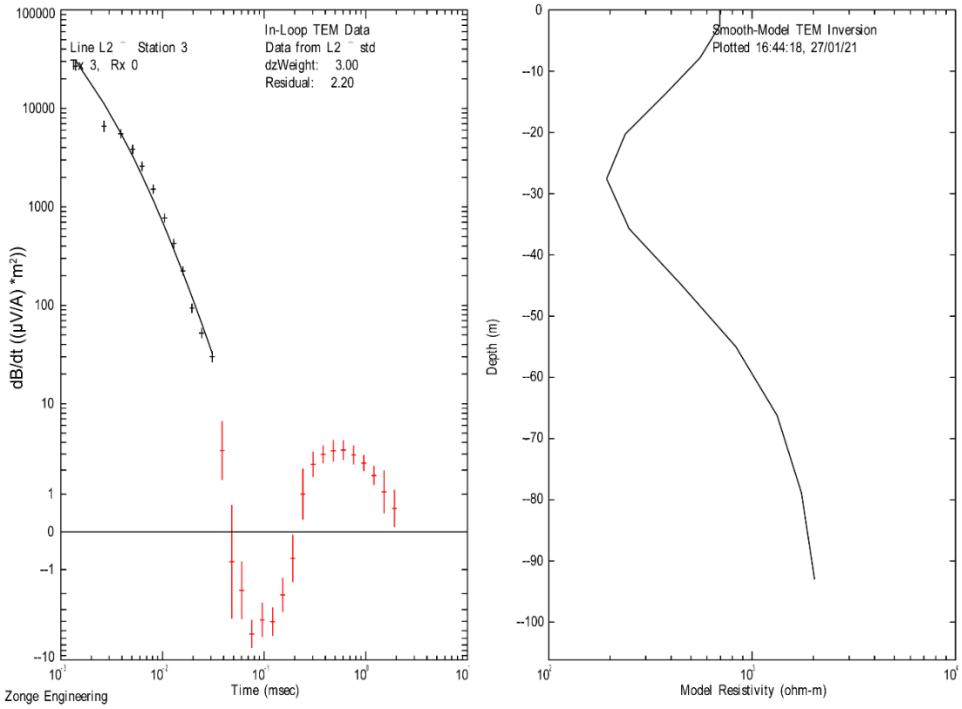

Figure 15: **(Left)** Typical induced voltage decay from Line 2 (L2), Station 3. Measured data are shown as crosses and inversion fitting as a black line. The noise level is approximately 25 μV/A. The inversion residual is 2.2. **(Right)** The obtained smooth-model TEM inversion.

STEMINV software (MacInnes and Raymond 2001) is used for inversion in order to develop a 1D inversion model of the transient EM sounding curves. After importing the data file containing the measured sounding curve from TEMAVG, we used the software to generates a consistent 1D smoothed inversion model of electrical resistivity versus depth on the basis of the iterative Occam

inversion scheme (Constable and Parker 1987). Calculations of maximum depth are given in the Zonge manual (MacInnes and Raymond 2001). We used MODSECT software (MacInnes and Raymond 2001) for the final phase of data processing to build a 2D model by using the 1D resistivity model acquired with STEMINV (MacInnes and Raymond 2005). MODSECT interpolates vertical columns with Catmul–Rom splines and then interpolates across the model with splines to provide a 2D view from 1D data in order to visualize the geometry of the geoelectrical structure of each line (Figure 16).

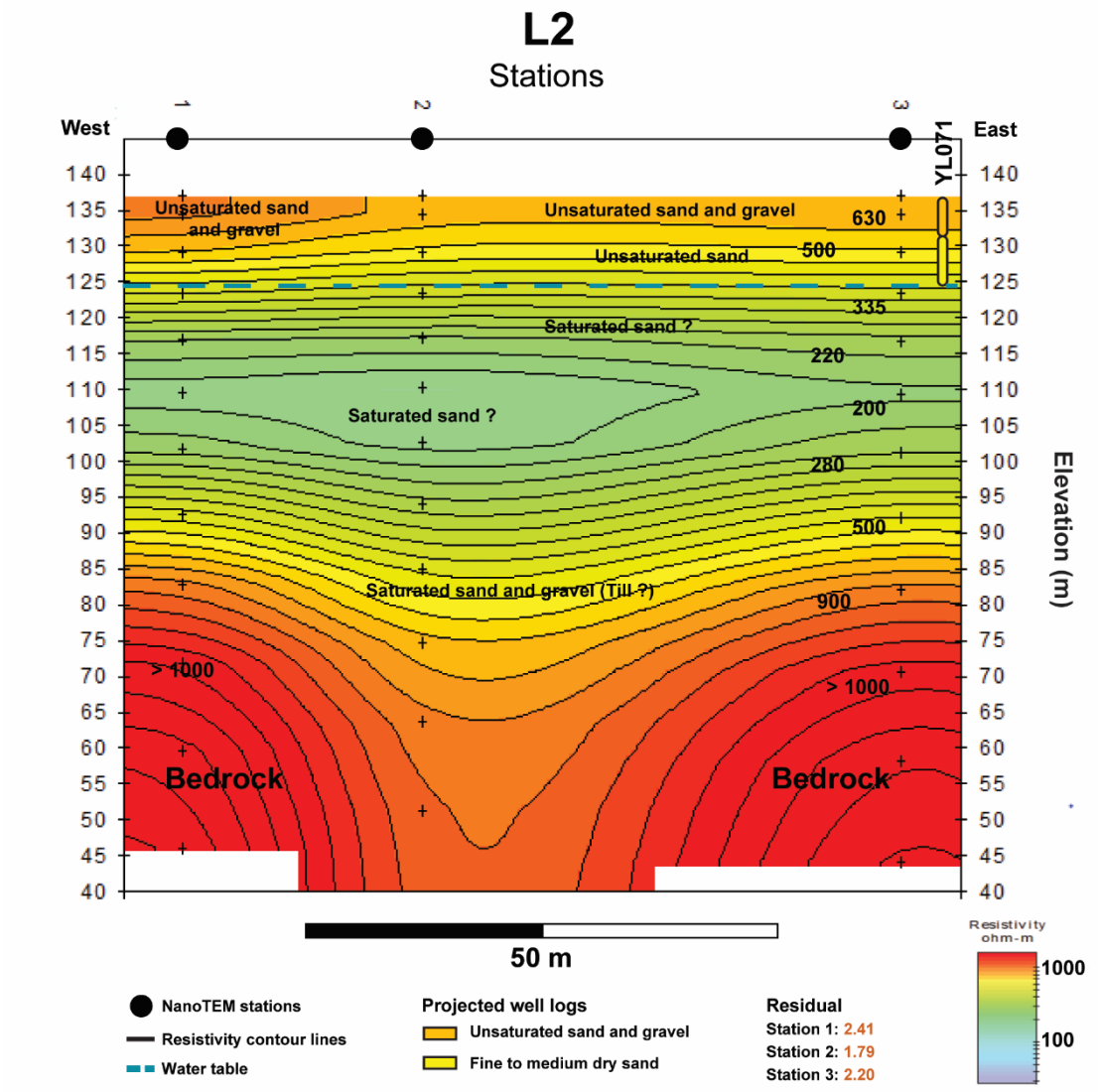

Figure 16: The interpreted 2D Section L2 and stratigraphic cross-section YL071 taken near Notre-Dame-du-Mont-Carmel, Quebec. The surface deposit elevation is obtained from lidar data. The blue dashed line represents the projected water table from direct observations in the field. The legend indicates only those sediments observed directly in the area (YL071). If no boreholes (or stratigraphic cross-sections) were acquired, the subsurface information is deduced from the calibration chart.

2.4.3 TEM CALIBRATION

Indirect geophysical methods are a necessary complement to direct observations obtained through borehole logs, stratigraphic cross-sections, and piezometric surveys. These direct measurements are used to calibrate the geophysical results, thereby allowing the extrapolation of all

TEM results (i.e., 40 stations) over a larger study area, even for areas lacking nearby sites where data were acquired directly. This calibration involves comparing the stratigraphic and piezometric information with the TEM results to obtain an equivalence of the electrical resistivity values for the unsaturated and saturated sediments of the study area. We selected TEM stations (1D resistivity models) near sites where boreholes, stratigraphic cross-sections, and piezometric surveys had been obtained previously.

2.4.4 STRATIGRAPHIC CALIBRATION

For the calibration, 13 TEM stations, 7 boreholes, and 6 stratigraphic cross-sections acquired from various locations across the moraine were correlated to derive an empirical and local petrophysical relationship to establish a resistivity chart of the sediments for the Saint-Narcisse moraine. First, the boreholes (and/or stratigraphic cross-sections) must be projected and compared to the nearest TEM station (i.e., co-located data) in areas considered to be representative of the moraine sediments. The selected boreholes and stratigraphic cross-sections were mainly located within a radius of 100 m from, at a minimum, one station (Figure 13). The contribution of the stratigraphic cross-sections is substantial because they were detailed from sand pits, and their associated TEM stations were set near the same position at a higher elevation. The electrical resistivity values can thus be directly associated with the various sediment facies of these stratigraphic cross-sections. In order to derive this calibration chart, we associated each class of sediment derived from borehole logs and stratigraphic cross-sections to an electrical resistivity value of a nearby TEM station. In addition, to create this chart, the calibration was based on unsaturated or saturated sediments using static groundwater levels (water table position) to distinguish between an absence or presence of water. However, the determination of the water table using the TEM method relies on identifying significant electrical resistivity contrasts between saturated and unsaturated sediments. Consequently, determining the elevation of the water table from the resistivity contrasts obtained in TEM and ERT surveys introduces a degree of uncertainty regarding its precise location. This uncertainty can range from decimeters to, in some instances, even meters. These variations are inherent to the nature of the geophysical methods employed, which, although powerful for estimating

piezometric levels, exhibit resolution limits that must be carefully considered in the interpretation of the data.

2.4.5 GROUNDWATER PIEZOMETRIC MAP AND THE SATURATED / UNSATURATED SEDIMENT RESISTIVITY CHART

To associate electrical resistivity values with water-saturated sediments, we had to estimate the piezometric level of groundwater. A piezometric map was therefore created to determine whether the sediments used to create the resistivity chart were water-saturated or unsaturated. According to a previous study that estimated the depth of the top of the saturated zone (Dewar and Knight 2020), above and below the groundwater table, the resistivity values were associated, respectively, with unsaturated and saturated sediments. To build an interpolated groundwater-depth map (i.e., piezometric map) for the Saint-Narcisse moraine in the Mauricie region, we gathered and compiled all existing pertinent data; such a database contains borehole logs and piezometric survey information. We performed the interpolation using the ArcGIS software hosting the PACES groundwater geodatabase of the Mauricie region. Regional piezometry was defined using a total of 465 piezometric surveys initially available from on and around the Saint-Narcisse moraine. The static groundwater levels (water table position) were obtained from 170 wells located in the unconfined granular aquifers of the moraine area. In addition, 295 surface surveys were taken using the water levels of several streams and rivers flowing across the moraine. These streams and rivers constrain the water table height because the unconfined aquifers are in direct hydraulic contact with surface waters. Although groundwater levels fluctuate over time, we assume that these fluctuations are negligible at a regional scale. To test the accuracy of the initial data set and the piezometric map, we calculated a root mean square error (RMS; Equation 1). The RMS acts as an indicator of modeling quality in terms of the spatial distribution and density of the observed data, as well as model precision and accuracy (McCormack 1983, Zimmerman et al. 1999, Wise 2000, Jones et al. 2003, Dewar and Knight 2020).

$$RMS = \left(\frac{1}{n} \sum_{i=1}^{n} (model_i - observed_i)^2 \right)^{1/2} \quad (1)$$

The RMS parameter (Equation (1)) corresponds to the mean of the differences between the observed (i.e., water table elevation) and interpolated values, in this case, the isopiestic lines. The RMS value indicates the reliability of the model in representing reality. A reliable model, in terms of accuracy and precision, will generate a lower RMS value. Thus, the lower the difference between the modeled and observed water table values, the more accurate the model output in representing reality. To assess the accuracy of the results, we used 25 observation points (i.e., water table elevation) as a verification data set to perform cross-validation and to calculate the RMS. These points, distributed regularly over the entire study area, were randomly extracted from the data set. They were equivalent to 15% of the total well data set (170 wells).

In addition to the piezometric map constructed from the interpolation of data available in the regional database, we undertook direct surveys of the groundwater table where possible. These direct records of the groundwater table correspond to observations of springs or the emergence of free water at the surface of areas exploited for aggregates (sand/gravel pits).

2.5 RESULTS

2.5.1 GROUNDWATER PIEZOMETRIC MAP

The interpolated map of groundwater depth (i.e., piezometric map) of the Saint-Narcisse moraine in the Mauricie region illustrates the sizable number of evenly distributed piezometric surveys. This distribution ensures a proper interpolation of static groundwater levels (Figure 17). Depending on the topographic elevation, the water table varies between 0 and 20 m below the ground surface. For the piezometric map, the calculated RMS value is 2.96 m, a relatively low value indicating a high-quality model. Above the groundwater table, resistivity values are high and associated with unsaturated sediments, whereas below the water table, the sediments are saturated, and the associated resistivity values are much lower. The transition between the vadose zone and the saturated zone via the capillary fringe generates variable saturation gradients but on a very thin layer

(i.e., 1–2 m). As we cannot expect a resolution better than a few meters from TDEM data, the capillary fringe is not considered at a regional scale.

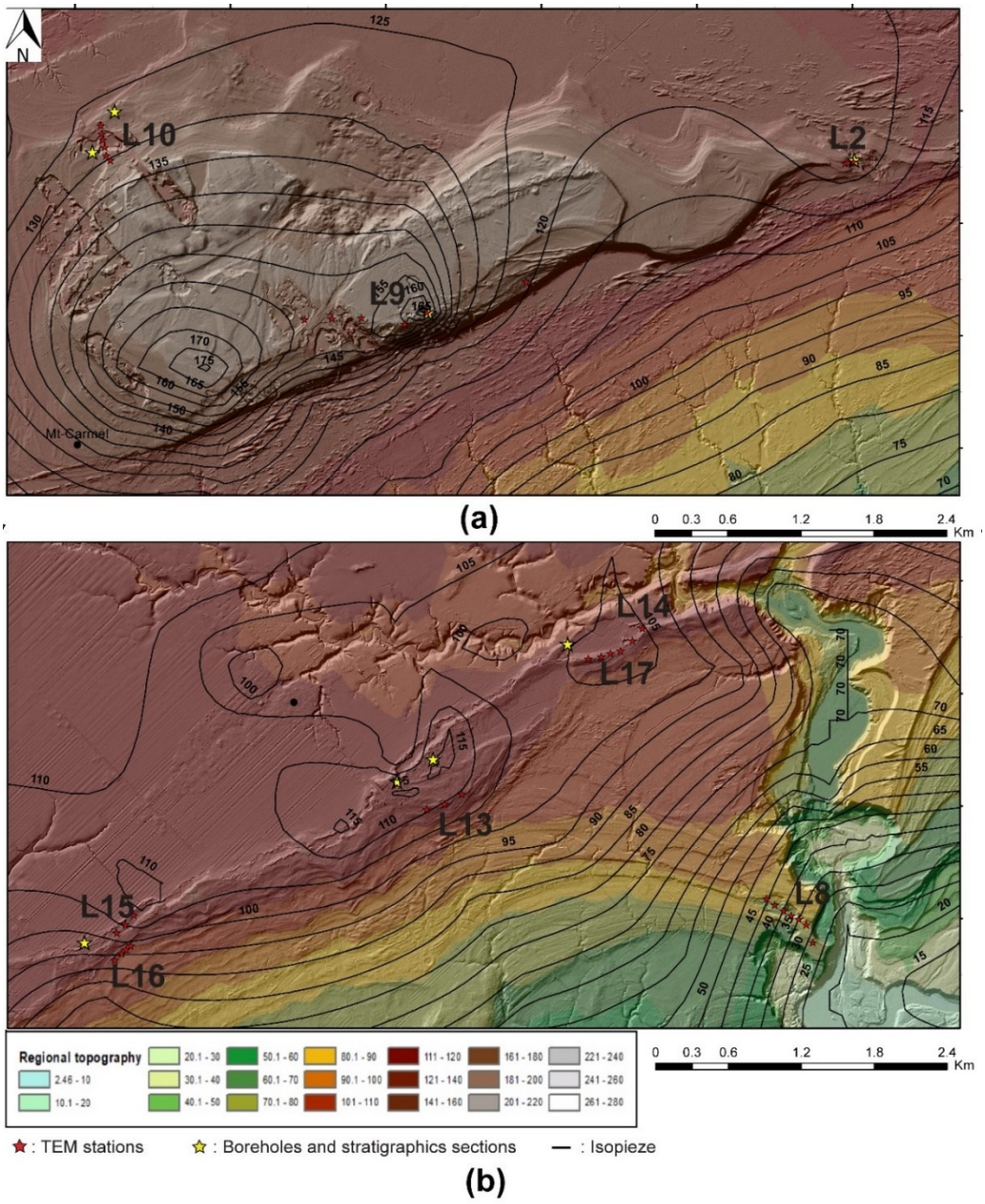

Figure 17: **(a)** Interpolated water table elevation and regional piezometry of the eastern Saint-Narcisse moraine near Notre-Dame-du-Mont-Carmel in Mauricie, Quebec; **(b)** interpolated water table elevation and regional piezometry of the central Saint-Narcisse moraine near Ste-Geneviève-de-Batiscan and Saint-Narcisse in Mauricie, Quebec. The water table elevations are expressed in meters above sea level for both figures.

2.5.2 TEM CALIBRATION

Figure 15 presents the induced voltage decay of Line 2, Station 3 (near YL071) and also represents the induced (and similar) voltage decay curves of Line 2, stations 1 and 2. Figure 16 (Section L2) illustrates the local surface deposit, the location of a stratigraphic cross-section (YL071) taken on the side of a sandpit, and the 2D section obtained on the basis of three TEM stations. The manually acquired piezometric surveys and piezometric map identify the water table at about 11 m depth. The electrical resistivity values associated with stratigraphic cross-section YL071 are 650-695 Ωm for unsaturated sand and gravel, 465–625 Ωm, and for unsaturated fine to medium sand (Table 3).

Table 3: TEM stations, with all nearby boreholes and stratigraphic sections, and their associated electrical resistivity values. Depths are identified by parentheses. The blue color in the electrical resistivity column represents the approximate depths at which which the water table has been reached. The water table has been determined by 1) in situ observations and 2) use of the piezometric map

TEM stations	Boreholes	Stratigraphic sections	Electrical resistivity (Ohm.m)	Elevation (m)	Water table (m)
L2_ST3	—	**YL071** (0-5) sand and gravel (5-11) fine to medium sand	(0-5) 625-695 (5-11) 465-625	ST3: 137 YL071: 137	11
L3_ST1	**F1-PACES** (0-6) medium to coarse sand (6-12) fine to medium sand with silt and clay (12-46) clay		(0-6) 350-405 (6-12) 110-350 (12-46) 15-110	ST1: 114 F1-PACES: 114	No water
L6_ST5	—	**YL057** (0-3): sand and gravel	(0-3) 610-620	ST5: 120 YL057: 120	No water
L6_ST7	—	**YL019** (0-9): sand and gravel with boulders	(0-3) no data (3-9) 430-745	ST7: 120 YL019: 123	No water
L7_ST1	—	**COMP016-18** (0-11): sand and gravel with pebbles and boulders (11-16): medium to coarse sand (16-18): fine to medium sand	(0-11) 460-720 (11-16) 345-460 (16-18) 170-330	ST1: 139 COMP016-18: 139	18
L9_ST5	**ME1843** (0-13): fine to coarse sand and gravel (13-27): sand (27-30); gravel and clay (till)	—	(0-13) 540-910 (13-27) 215-540 (27-30) 200-215	ST5: 180 ME1843: 180	Not availabl e in situ
L10_ST1-2	**MAUR0345** (0-19): sand and gravel	—	(0-14) 400-835 (14-19) 250-400	ST1-2: 140 MAUR0345: 140	14

L10_ST5	—	**YL080** (0-12): fine to coarse sand	(0-12) 380-550	ST5: 146 YL080: 146	14
L13_ST1	**ME0704** (0-8): sand and gravel (8-19): sand and gravel with clay (19-27): clay	—	(0-8) 150-230 (8-19) 60-150 (19-27) 40-60	ST1: 118 ME0954: 118	1-2
L13_ST3	**P12** (0-9): sand	—	(0-9): 110-150	ST3: 118 P12: 118	1-2
L15_ST1	**ME1615** (0-13): sand and gravel (13-38): sand and gravel with clay (38-50): sand and gravel		(0-3): 360-390 (3-13): 165-360 (13-38): 80-165 (38-50): 150-285	ST1: 115 ME1615: 114	2-3
L17_ST1	**ME0954** (0-8): sand and gravel (8-13): sand and gravel (13-17): sand (17-27): sand with clay	—	(0-2): no data (2-8): 300-415 (8-13): 180-300 (13-17): 110-180 (17-27): 60-110	ST1: 116 ME0954: 118	8

Figure 18 (Section L3) shows a 2D section and a borehole stratigraphy (F1-PACES) recovered from an unsaturated subsoil. This TEM line comprises two stations. The induced voltage decay of Station 1, located near the borehole, shows a similar pattern as the induced voltage decay of Station 2 (Figure 19). Here, the water table is not attained by the borehole, and a thick layer of clay is found at 12 to 46 m depth. The resistivity values for the stratigraphic units of the F1-PACES borehole are 350–405 Ωm for medium to coarse sand, 110–350 Ωm for fine to medium sand with silt and clay and 15–110 Ωm for clay in these unsaturated conditions (Table 3). The presence of a small amount of silt and clay in fine to medium sand at 6 to 12 m depth decreases the electrical resistivity values considerably.

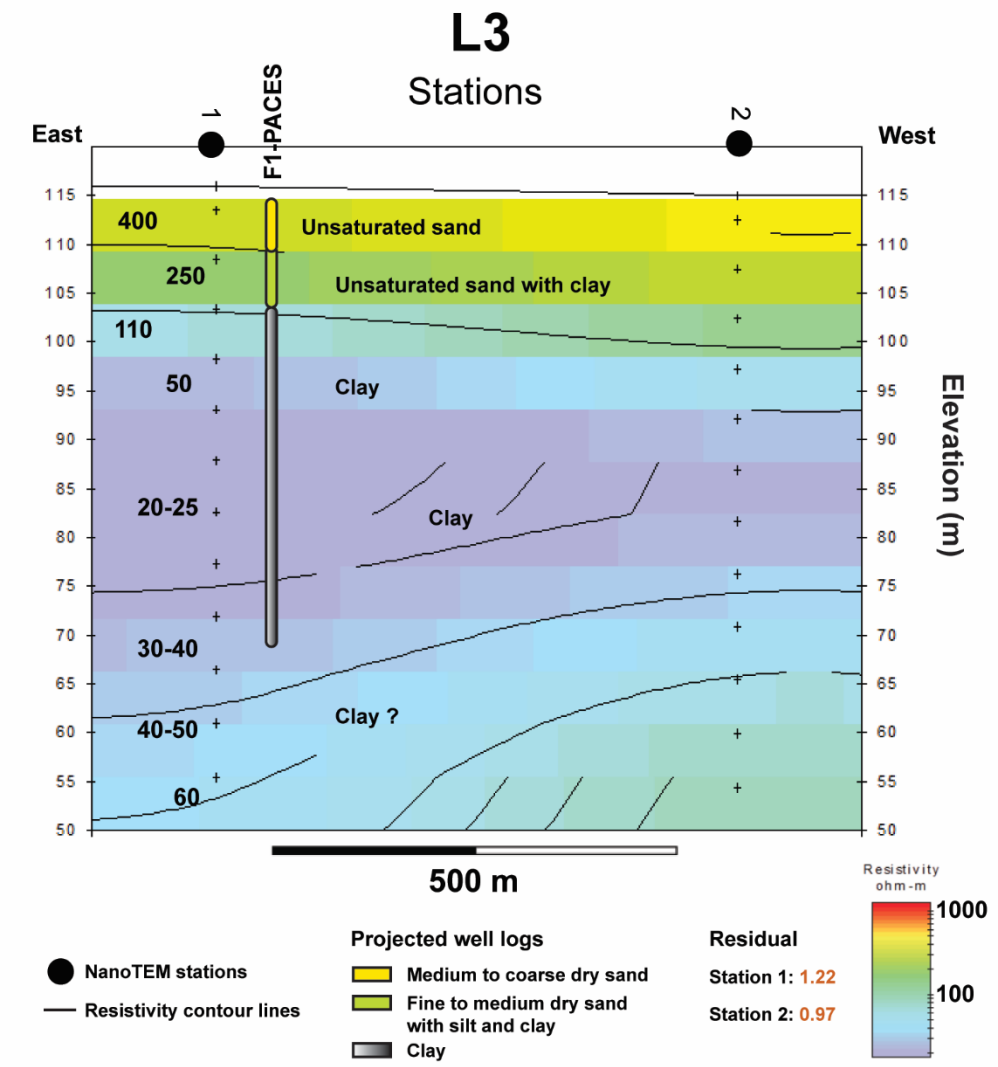

Figure 18: Interpreted 2D Section L3 and borehole F1-PACES collected near Saint-Maurice, Quebec. The surface deposit elevation is obtained from lidar data. At the site, no groundwater was observed, and the basement was completely dry and mainly composed of clay.

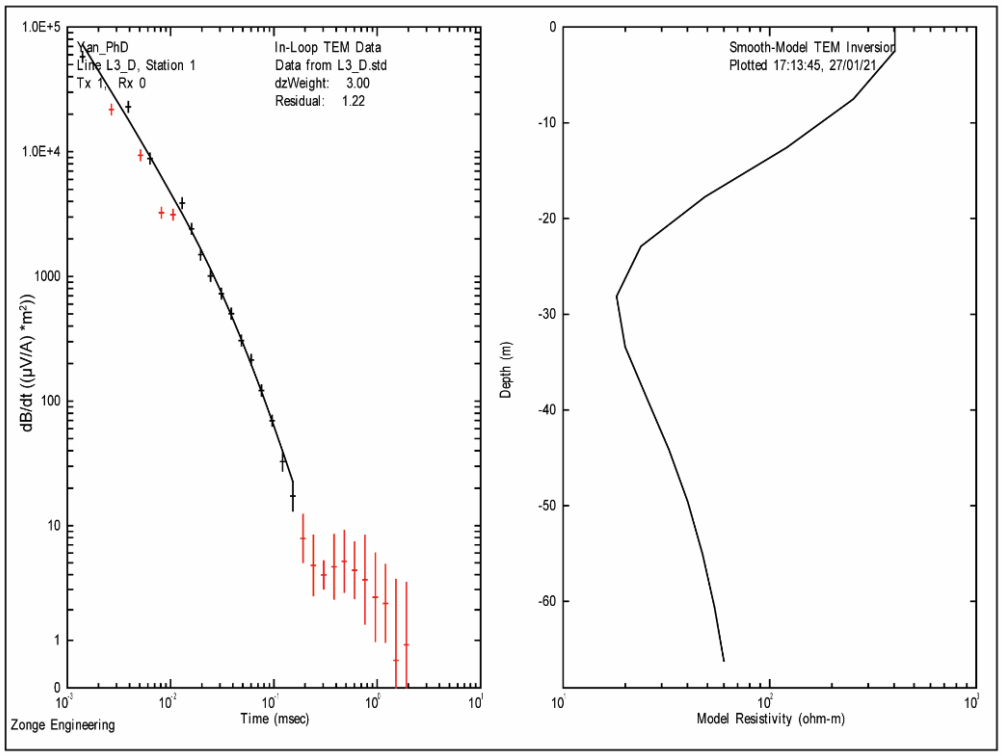

Figure 19: **(Left side)** Typical induced voltage decay from Line 3 (L3), Station 1. Measured data are shown as crosses and inversion fitting as a black line. Noise level is approximately 10 μV/A. The inversion residual is 1.22. **(Right side)** The obtained smooth model TEM inversion.

Figure 20 (Section L7) presents a 2D section, and two stratigraphic sections (YL016 and YL018) collected on the side of a sandpit. These two sections are located at different elevations (129 and 134 m, respectively) and can be superimposed to create a composite (COMP016-18). This section was acquired on top of a sandpit with three TEM stations. The induced voltage decay of Station 1 (located near YL071) is similar to other stations on this 2D section (Figure 21). The manually acquired piezometric surveys and the interpolated piezometric map (Figure 17) identify a water table at about 14 m depth. The electrical resistivity values for the stratigraphic units that make up the COMP016-18 section are 460–720 Ωm for coarse unsaturated sand and gravel with boulders, 345-460 Ωm for medium to coarse unsaturated sand, and 170–330 Ωm for fine to medium saturated sand (Table 3).

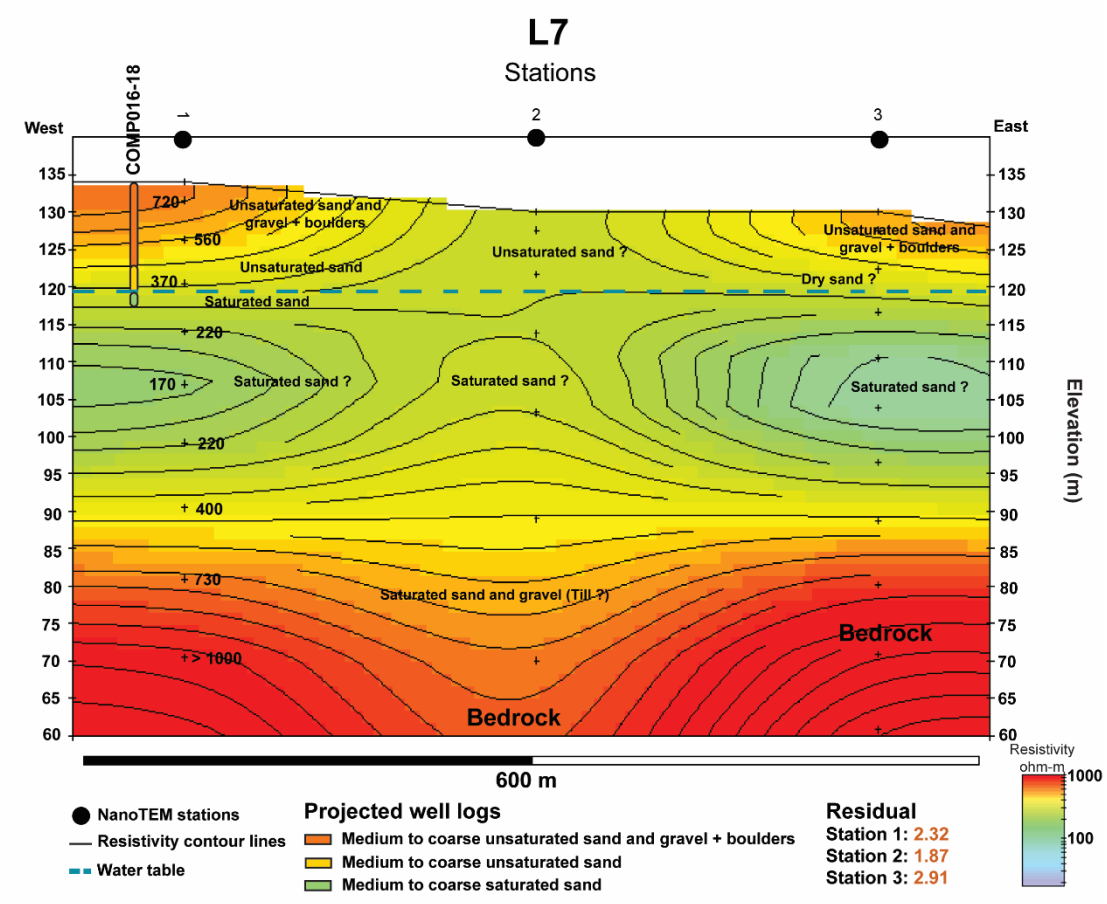

Figure 20: Interpreted 2D Section L7 near Saint-Stanislas, Quebec. Stratigraphic cross-sections YL016 and YL018 have been Scheme 016. The surface deposit elevation is obtained from lidar data. The blue dashed line represents the projected water table from direct observations in the field. The legend indicates only the sediments observed in situ. The deeper sedimentary facies are deduced from the empirical and petrophysical relationship (i.e., the calibration chart).

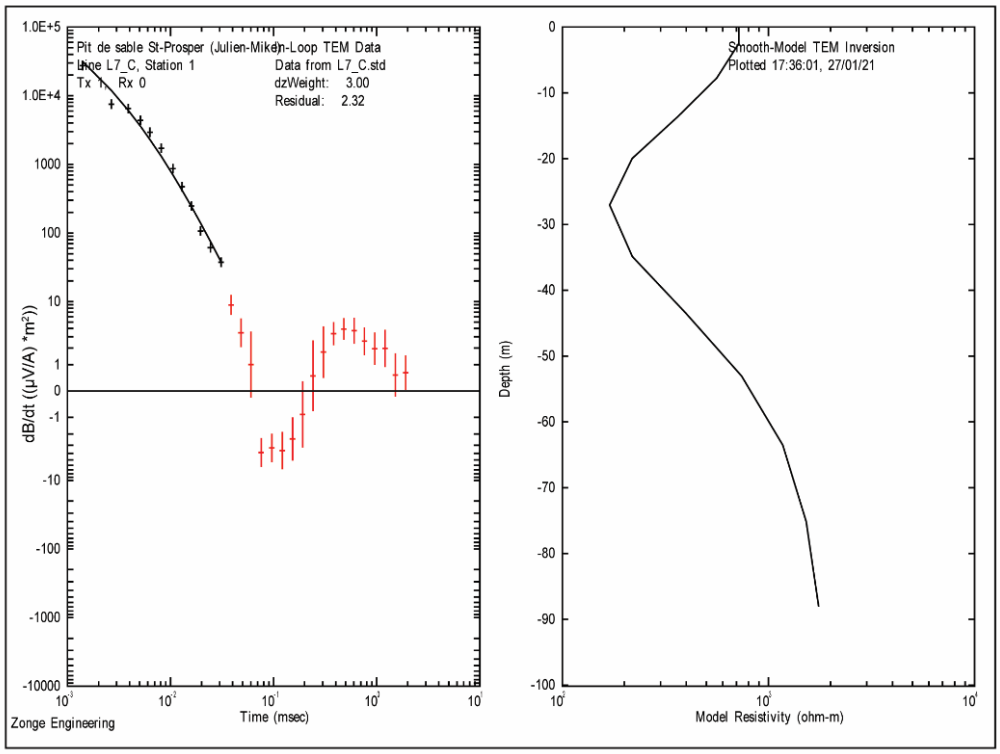

Figure 21: **(Left side)** Typical induced voltage decay from Line 7 (L7), Station 1. Measured data are shown as crosses and inversion fitting as a black line. Noise level is approximately 10 µV/A. The inversion residual is 2.32. **(Right side)** The obtained smooth model TEM inversion.

Figure 22 (Section L10) reveals the local surface deposits of a 2D section with a borehole (MAUR0345) to the northwest and a stratigraphic cross-section (YL080) taken from the side of a sandpit to the southeast. This 2D section was obtained using six TEM stations.

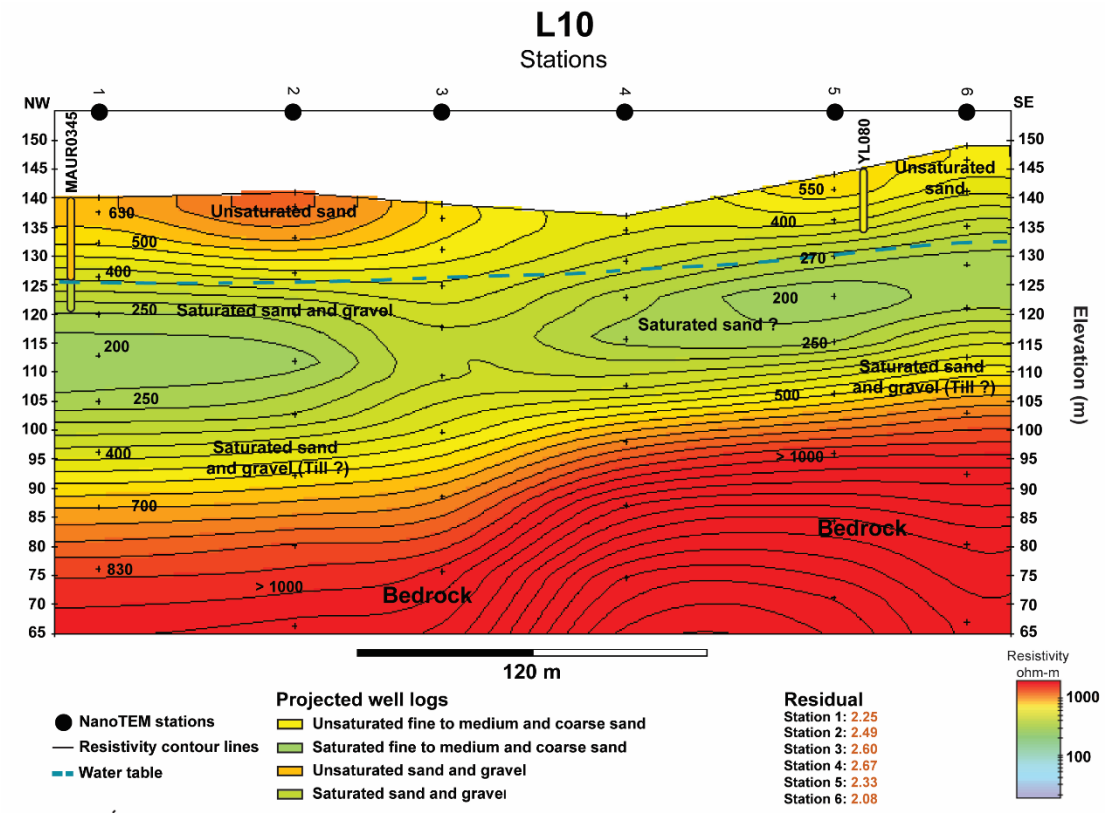

Figure 22: Interpreted 2D Section L10, stratigraphic cross-section YL080, and borehole MAUR0345 acquired near Notre-Dame-du-Mont-Carmel, Quebec. The surface deposit elevation is obtained from lidar data. The 6 m variation of the water table height is probably due to a marked topographical variability of the bedrock surface as well as the regional topographic gradient, which increases rapidly toward the southeast.

Figure 23 presents a typical induced voltage decay profile from the sector. For this 2D section, which is more than 350 m in length, the water table is located at a depth of 14 m (Figure 17) to the northwest and increases slightly, by a few meters, to the southeast. The electrical resistivity values for the stratigraphic units that make up the YL080 cross-section (fine and medium to coarse unsaturated sand) are 380–550 Ωm in unsaturated conditions (Table 3). The electrical resistivity values recorded for borehole MAUR0345 are 400–835 Ωm and 250–400 Ωm in unsaturated and saturated sand and gravel, respectively (Table 3).

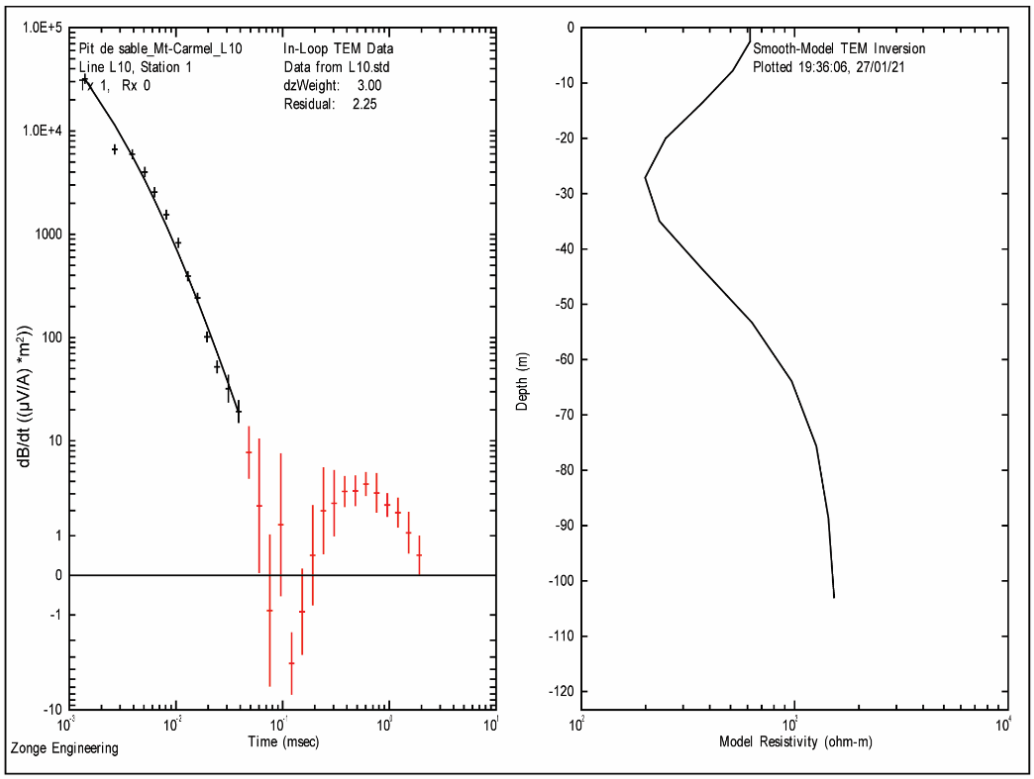

Figure 23: **(Left side)** Typical induced voltage decay from Line 10 (L10), Station 1. Measured data are shown as crosses and inversion fitting as a black line. Noise level is approximately 10 μV/A. The inversion residual is 2.35. **(Right side)** The obtained smooth model TEM inversion.

Figure 24 (Section L13) presents a 2D section obtained for a saturated subsoil. The 2D section is derived from three TEM stations and two boreholes (ME0704; P12) recovered near the village of Saint-Narcisse. The manually acquired piezometric surveys and the interpolated piezometric map place the water table near the surface at less than 2 m depth.

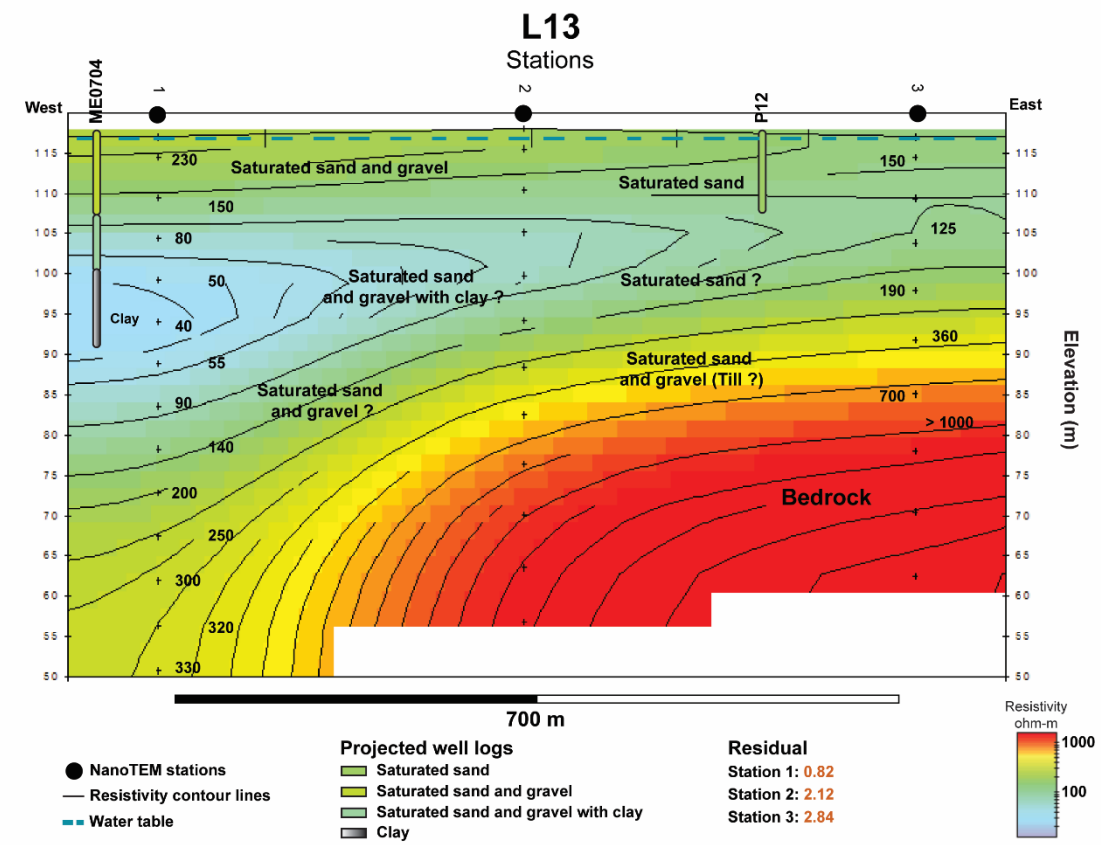

Figure 24: Interpreted 2D Section L13 and borehole ME0704 acquired near Saint-Narcisse, Quebec. The surface deposit elevation is obtained from lidar data.

Figure 25 exhibits a typical induced voltage decay profile obtained for this sector. The resistivity values for the stratigraphic units that make up the ME0704 borehole are 150–230 Ωm for sand and gravel, 60–150 Ωm for sand and gravel with clay, and 40–60 Ωm for clay, all units in saturated conditions (Table 3). For the P12 drill site, the electrical resistivity values are 110–150 Ωm for saturated sand. West of the 2D Section L13, a 10 m thick clay lens (at least) lies at a depth of about 20 m and reduces the electrical resistivity values considerably.

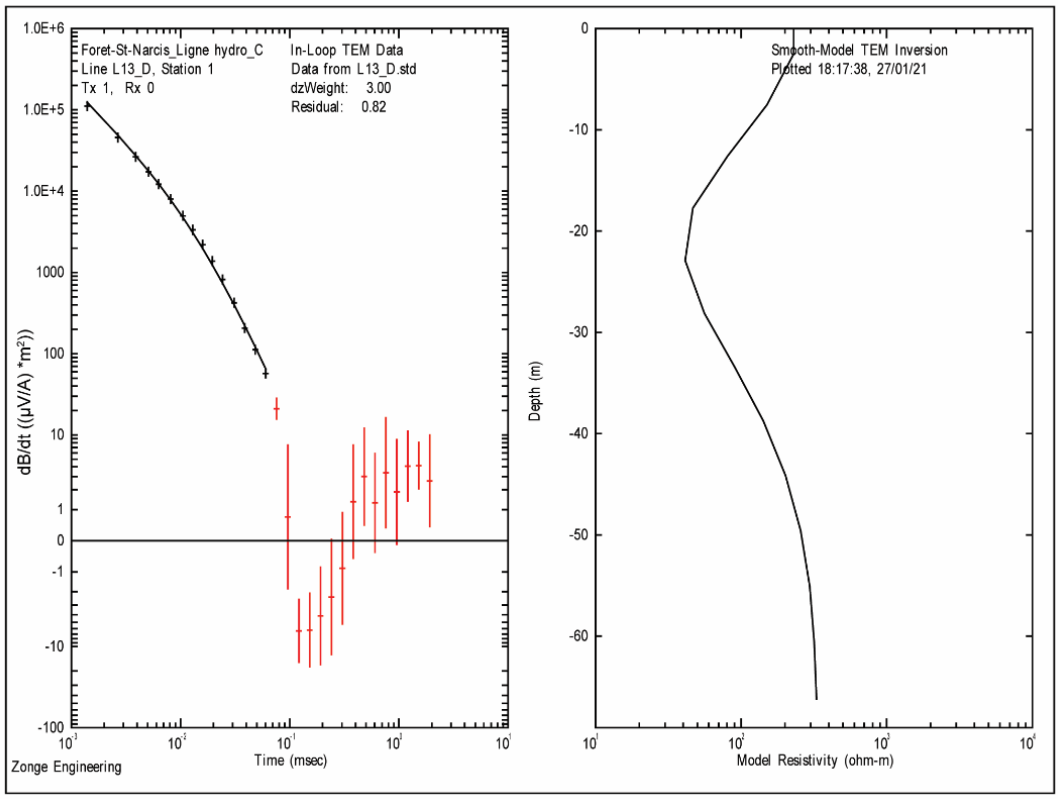

Figure 25: **(Left side)** Typical induced voltage decay from Line 13 (L13), Station 1. Measured data are shown as crosses and inversion fitting as a black line. Noise level is approximately 25 μV/A. The inversion residual is 0.82. **(Right side)** The obtained smooth model TEM inversion.

Finally, Figure 26 (Section L17) reveals the local surface deposit of a 2D section acquired from three TEM stations and the available borehole (ME0954), located on the northern side of the moraine near the village of Saint-Narcisse. The induced voltage decay of Station 1, which is located near the borehole, is similar to that of stations 2 and 3. The water table is located at 8 m depth to the west and gradually approaches the surface, reaching a depth of less than 1 m on the eastern side of the section. The electrical resistivity values for the stratigraphic units that make up the ME0954 borehole are 300–415 Ωm in unsaturated sand and gravel, 180–300 Ωm in saturated sand and gravel, 110–180 Ωm in saturated sand, and 60–110 Ωm in saturated sand with clay (Table 3). Table 3 also details other nearby TEM stations (L6_ST5; L6_ST7; L15_ST1) having stratigraphic cross-sections that were used to create the resistivity chart.

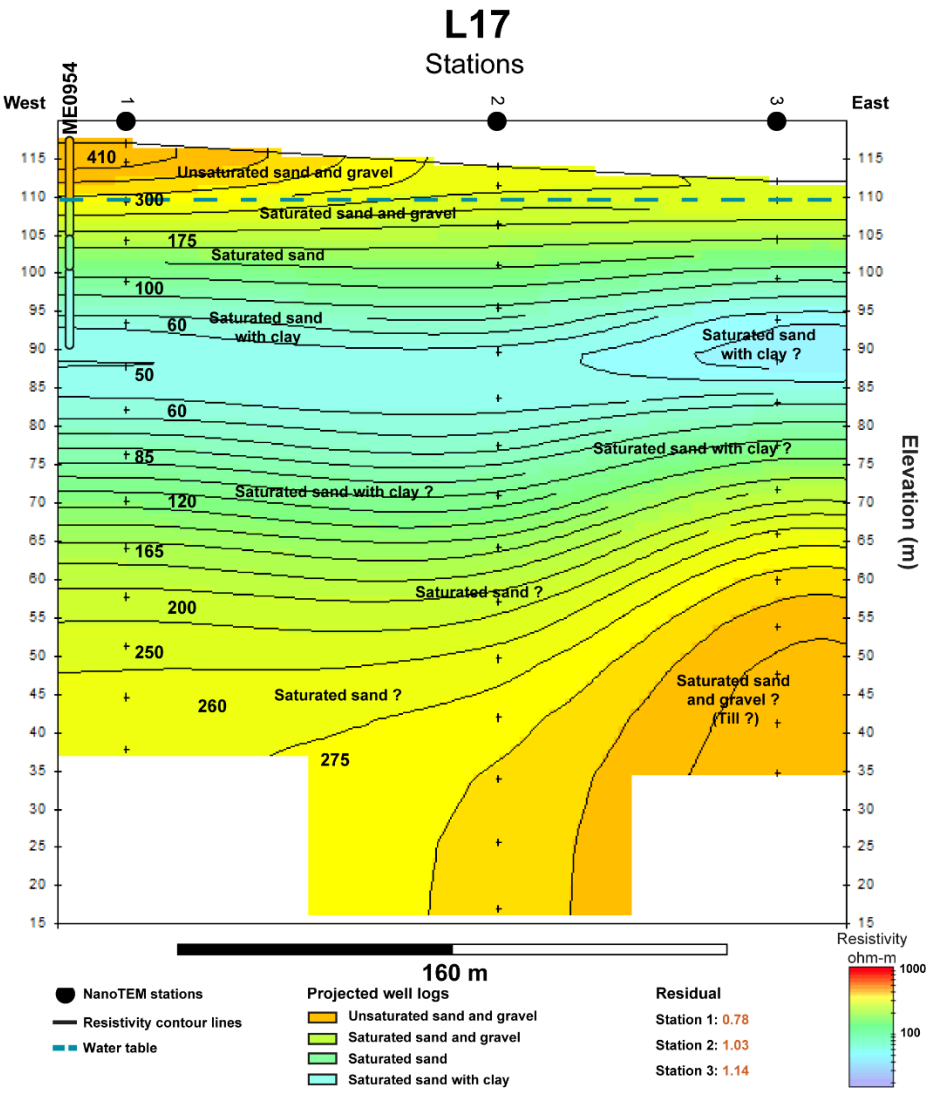

Figure 26: : Interpreted 2D Section L17 and borehole ME0954 acquired near Saint-Narcisse, Quebec. The surface deposit elevation is obtained from lidar data.

Since TEM profiles are interpolations between 1D soundings, the limitations of this approach bear uncertainty related to the interpolation and the smoothing. In fact, it is challenging to determine precisely which types of sediment are found at depth (and between the stations) only with indirect measurement (i.e., geophysics). However, within a distance of 22 km (east–west) in the Saint-Narcisse moraine in Mauricie, 13 TEM stations out of the 40 stations available in this zone can be compared to boreholes or stratigraphic cross-sections nearby. In addition, the piezometric map also provides additional information and allows us to validate the presence of saturated sediments,

regardless of the shortcomings inherent to the inversion process (smoothing) and interpolation. Consequently, this significant amount of field data (boreholes, stratigraphic cross-sections, and 365 piezometric surveys) helps to decrease the uncertainty related to smoothing and interpolation between TEM stations and greatly strengthen the stratigraphic interpretation.

Here are the guidelines and some thresholds used to globally delimit the units: At depth (at the base of Figures 16, 20, 24, 27, 28 and 30), when the resistivity values are greater than 900 Ωm, we estimate that the bedrock is reached. Between 500 and 900 Ωm, mainly tills (sand and gravel with pebbles/boulders) are overlying the bedrock, which is according to the literature (Occhietti 1977, 2007, Occhietti et al. 2001). On the surface, the resistivity values range between 400 and 850 Ωm, suggesting that there is a presence of unsaturated sand and gravel with pebbles/boulders or unsaturated sand. When the water table is reached, the resistivity decreases sharply along the entire length of the TEM sections, indicating saturated sediments. If the values range between 100 and 400 Ωm, it suggests saturated sand and gravel or saturated sand. In order to determine the sediment classes with the greatest possible accuracy, we also based our observations on the continuity of the surface layers that we observed during the fieldwork, but mainly on stratigraphic cross-sections and boreholes available near the TEM sections. We hypothesized that if the resistivity values are relatively constant with depth, the type of sediment will stay similar. For example, if unsaturated sand is observed at the surface, and the resistivity values are relatively stable below the water table, the unsaturated sand is probably perpetuated at depth. When changes in resistivity are less gradual and more abrupt, there appears to be a change in sediment class that can be linked to a variation of porosity (and then a variation of water content) and so probably to heterogeneity. Alternatively, the low resistivity values can also be linked to a higher clay content within granular sediment. If the resistivity values are lower than 110 Ωm, we mainly find clay or mixed clay.

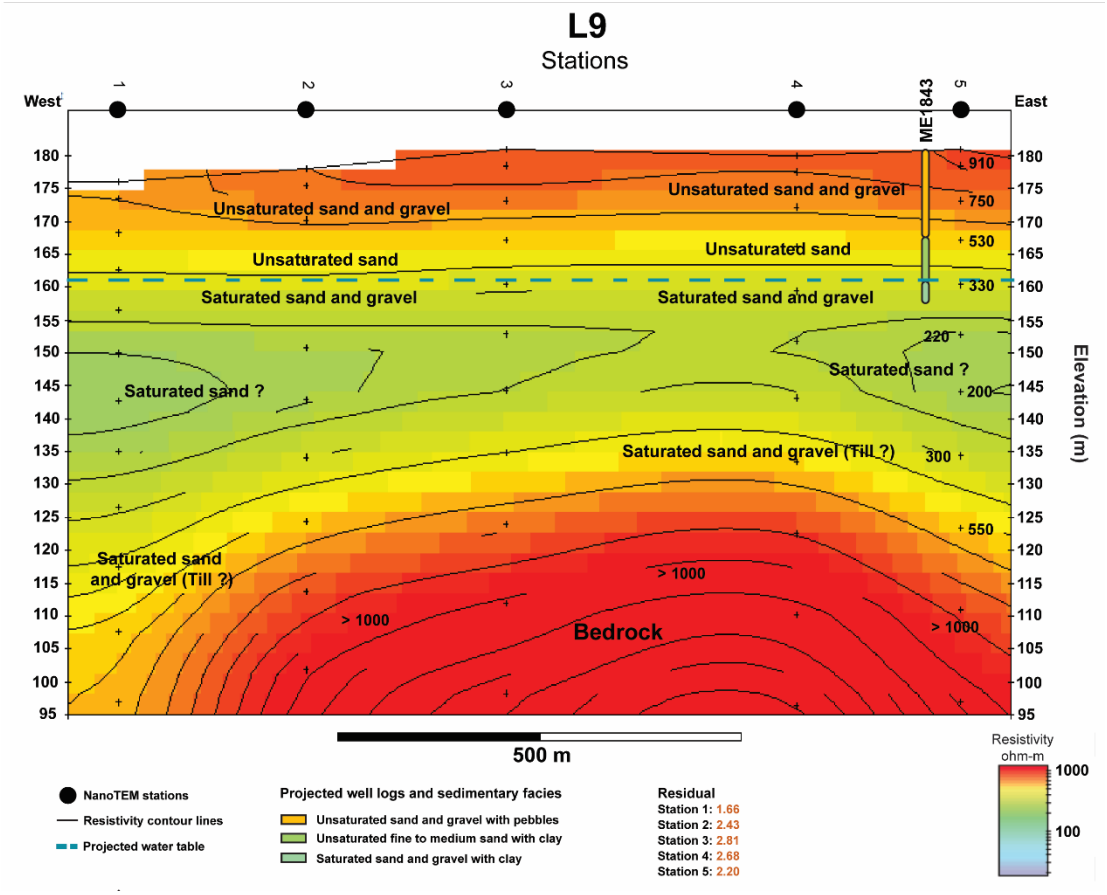

Figure 27: Interpreted 2D Section L9 and borehole ME1843 near Notre-Dame-du-Mont-Carmel, Quebec. The surface deposit elevation is obtained from lidar data. The blue dashed line represents the projected water table, and all direct observations have been acquired in the field.

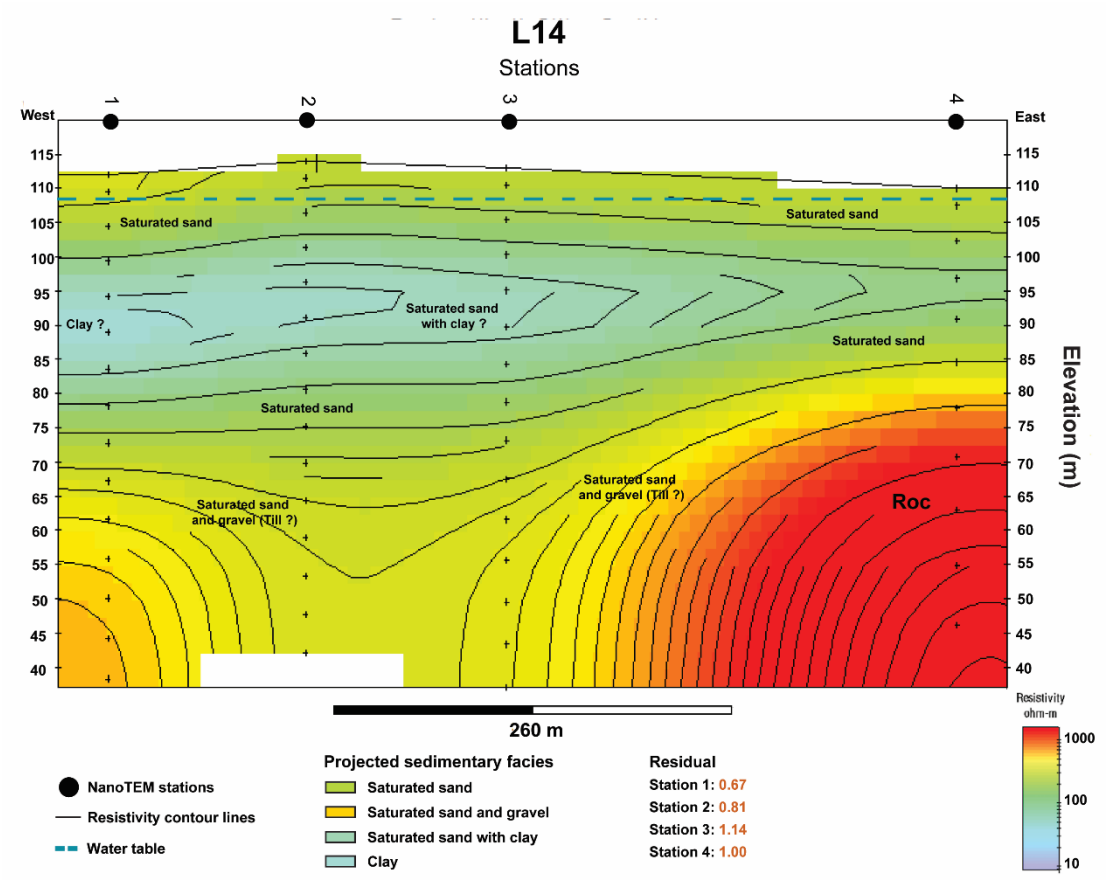

Figure 28: Interpreted 2D Section L14 near Saint-Narcisse, Quebec. The surface deposit elevation is obtained from lidar data.

2.5.3 COMPILATION AND CALIBRATION CHART

Table 4 and Figure 29 lists the electrical resistivity values obtained for each type of unsaturated and saturated Quaternary sediment found in the Saint-Narcisse moraine. Seven sediment classes are represented in the calibration chart: (1) unsaturated sand, (2) saturated sand, (3) unsaturated sand and gravel with pebbles/boulders, (4) saturated sand and gravel, (5) unsaturated sand, sand, and gravel (all with clay), (6) saturated sand, sand and gravel (all with clay), and (7) clay. When the sediments are saturated with water or contain clay, resistivity values are low and generally less than 400 Ωm; clay sediments produce the overall lowest values and reach a maximum resistivity

of 110 Ωm. Resistivity values for clay usually vary between 15 and 110 Ωm (Table 3; Figure 29). As the proportion of sand and gravel to clay increases, so does resistivity. For the unsaturated sand with clay, the resistivity varies with a correspondingly low resistivity, ranging between 110 and 350 Ωm (unsaturated) and 60 and 360 Ωm (saturated). In comparison, unsaturated and saturated sands have a resistivity range of 345–650 Ωm and 110–330 Ωm, respectively (Figure 29). The potential increase in resistivity from saturated to unsaturated sand can reach up to 88% at maximum values (345-650 Ωm). Unsaturated and saturated sand and gravel with pebbles/boulders produce respective resistivity ranges of 370–835 Ωm and 150–400 Ωm (Figure 29). The potential increase from saturated to unsaturated sand and gravel can reach up to 109% (400–835 Ωm).

Table 4: Measured electrical resistivity of Quaternary sediments in the Saint-Narcisse moraine, eastern Mauricie, Quebec, Canada.

Sediment class (unsaturated and saturated)	**Electrical resistivity (ohm.m)**
Unsaturated sand	345 - 650
Saturated sand	110 - 330
Unsaturated sand and gravel with pebbles/boulders	370 - 835
Saturated sand and gravel	150 - 400
Unsaturated sand with clay	110 - 350
Saturated sand; Sand and gravel; (with clay)	60 - 165
Clay	< 110
Bedrock	> 1000

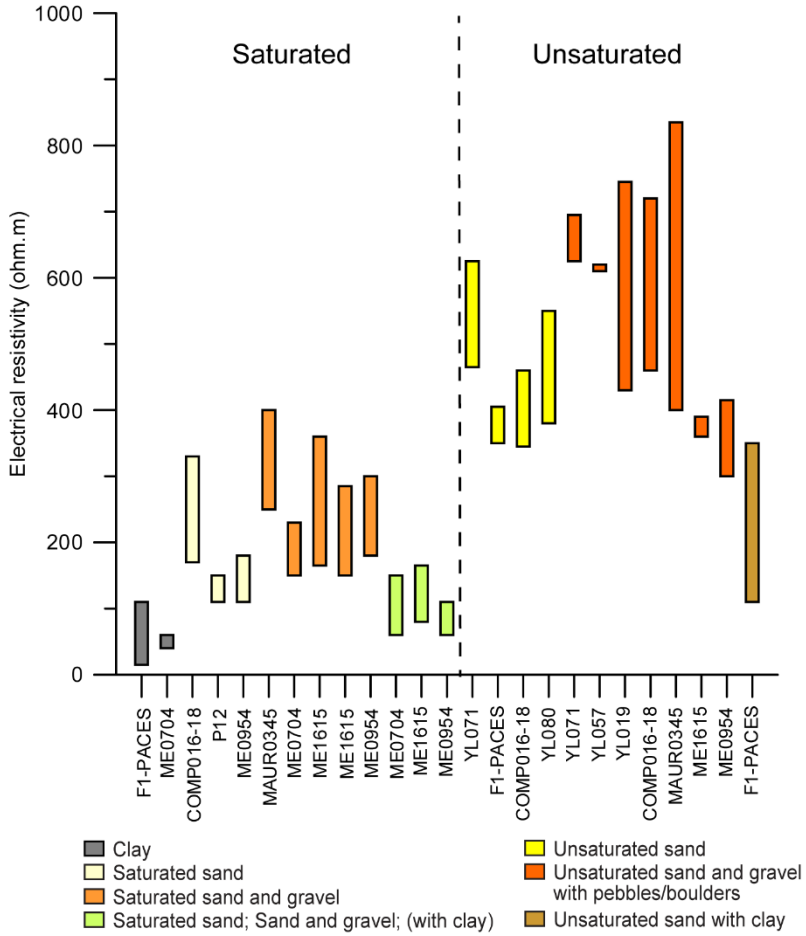

Figure 29: Respective resistivity for the seven sediment classes proposed in the calibration chart. They are deduced from borehole logs to display the minimum and maximum values for each saturated and unsaturated sediment. The horizontal axis represents each of the boreholes and stratigraphic cross-sections and their associated facies. The bedrock is not considered in this figure.

2.5.4 TEM RESULTS

Western Sector (Notre-Dame-du-Mont-Carmel)

Figure 13 shows the location of three 2D TEM sections in the western portion of the study area (Figures 16, 22 and 27). From the produced calibration chart, Figure 22 (2D Section L10) shows saturated sand and saturated sand and gravel at a depth of 10 to 15 m. The thickness of this water-saturated zone varies between 25 and 35 m and extends over a length of approximately 350 m. A layer of saturated sand and gravel overlies the bedrock in this area. Further southeast, about 2.5 km from Section L10, the 2D Section L9 (Figure 27) also shows the presence of saturated sand at about

15 m depth. This layer of saturated sand varies between 30 and 50 m thick and extends more than 1 km from east to west. The observations from borehole ME1843 and the calibration chart show that the sediments found in L9 are, from top to bottom, sand and gravel interspersed with fine to medium sandy facies and then sand and gravel, pebbles, and boulders overlying the bedrock. From the stratigraphic section YL071 and the calibration chart (Figure 16), Section L2, situated 3 km northeast of Section L9, also shows the presence of saturated sand (as observed for sections L9 and L10) at about 10 to 15 m depth, which juxtaposes a layer of saturated sand and gravel overlying the bedrock. In Section L2, the thickness of the saturated granular sediments varies between 35 and 45 m and extends (east–west) over a distance of 75 m.

Central Sector (Saint-Narcisse)

Six 2D TEM sections (Figures 24, 26, 30 and 37; sections L13, L17, L8, L14, L15, and L16) lie within the central zone of the moraine, situated southeast of the village of Saint-Narcisse and west of the Batiscan River (Figures 13 and 14). The four stations of the 2D Section L16 (Figure 37) attain a depth of about 76 m without reaching bedrock. The produced calibration chart (Table 4) indicates the presence of saturated granular sediment from the top to the bottom of Section L16, containing (1) fine to coarse saturated sand (western side) and saturated sand and gravel (eastern side); (2) saturated sand with clay; and (3) saturated sand or saturated sand and gravel. The saturated sediment in L16 has a lateral east–west extension of 200 m (length of Section L16) and a thickness varying between 66 and 76 m. The subsurface layers exposed in Section L16 appear very similar to those of the 2D Section L15 (Figure 37), located approximately 300 m to the north (Figure 13). Section L15 comprises three stations, and the calibration chart indicates the presence of >87 m thick, saturated sand over a distance of at least 200 m (east–west). The main difference relative to Section L16 is that the resistivity values in Section L15 increase at about 35 m depth. This increase suggests the presence of saturated sand and gravel between 35 and 80 m depth. At 2.5 km northeast of sections L15 and L16 lies the 2D Section L13 (Figure 24), which comprises three stations. Similar to sections L15 and L16, Section L13 also shows the presence of saturated sediment. Boreholes ME0704 and P12 and the calibration chart indicate that the Section L13 sediments are, from top to bottom, saturated sand

(east) and saturated sand and gravel (west) at the surface. On the western side of Section L13, between 15 and 35 m depth, a clay lens drags down the resistivity values to 40 Ωm. Around the clay lens on the eastern side of Section L13, the resistivity is higher, and the borehole ME0704 shows the presence of sand and gravel mixed with clay. The higher resistivity values at the base of Section L13 (Figure 24) are associated with saturated sand and gravel, pebbles, and boulders. Here, the saturated granular sediment (i.e., sand, sand, and gravel) varies in thickness from 25 to 70 m with an extension (east–west) over nearly 1 km. The variations in bedrock topography for Section L13 generate a larger range in the aquifer thickness. The 2D cross-sections of sections L17 and L14 (Figures 26 and 28) are located about 1.5 km northeast of Section L13 in the north-central part of the moraine. Sections L17 and L14 comprise four and three stations, respectively, with respective lengths of 500 m and 200 m. Borehole ME0954 and the calibration chart indicate that these two sections are composed of sand and gravel with variable amounts of clay and sandy facies at depth, 50 to 80 m depth for Section L17 and 42 to 75 m depth for Section L14. These two sections contain saturated granular sediments (from top to bottom: sand and gravel with clay, sand with clay, sand, sand, and gravel) with a thickness varying between 31 and 94 m. The thickness of the sediments depends mainly on the topographic undulations of the bedrock. The two combined lines indicate saturated sediment extending over nearly 700 m along an east–west axis. Finally, the 2D Section L8 (Figure 30) is located 2.5 km south of sections L14 and L17. Section L8 comprises seven stations, totaling 600 m in a north–south axis. According to the calibration chart, this section shows the bedrock overlain by sand and gravel and sandy facies (saturated and unsaturated). The saturated sediment varies in thickness from 25 to 35 m and extends over 600 m (i.e., the full length of Section L8). In the central sector of the moraine, these six 2D sections (L8, L13, L14, L15, L16, and L17) have a total length of 2.5 km and cover an area of approximately 21 km^2 (Figures 13 and 30). Typical induced voltage decay profiles (1D smooth inversion model) obtained for each section are shown in figures 25, 31, 32, 33, 34, 35 and 36.

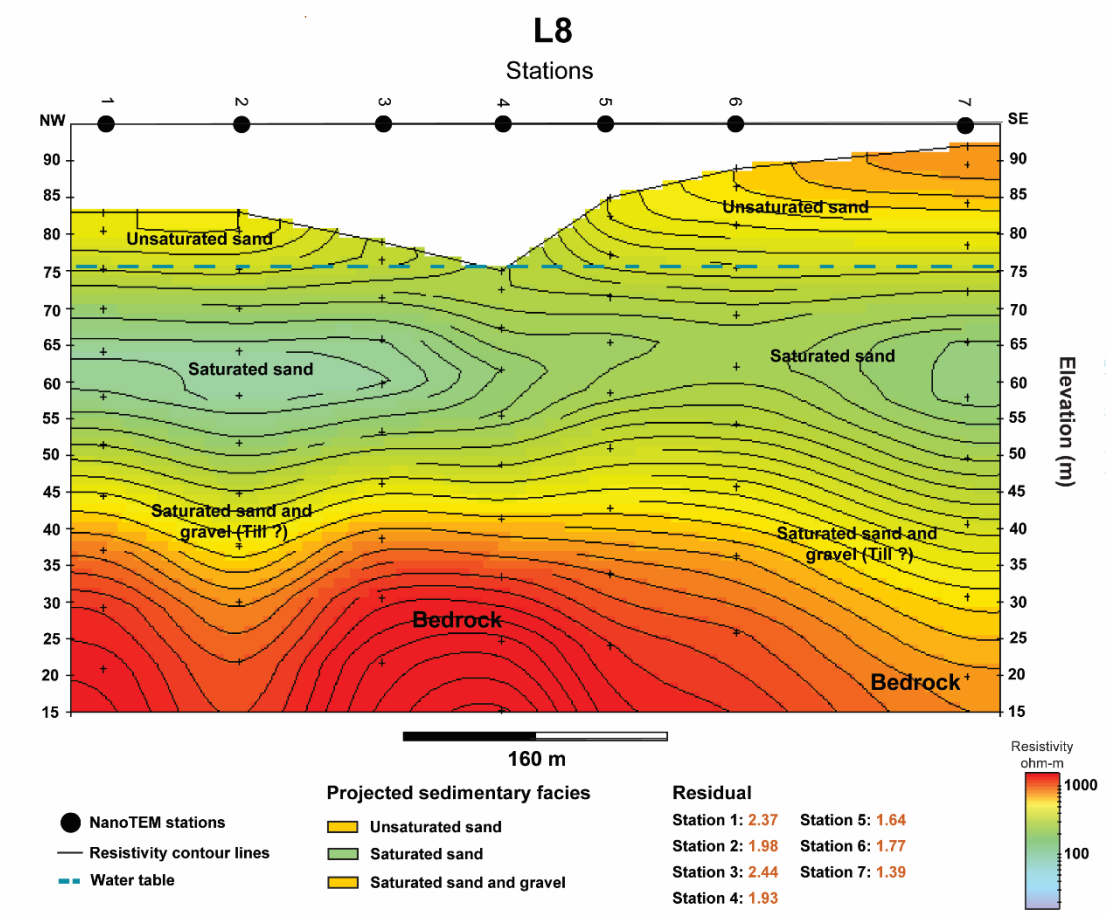

Figure 30: Interpreted 2D Section L8 near Saint-Narcisse and Saint-Geneviève-de-Batiscan, Quebec. The surface deposit elevation is obtained from lidar data.

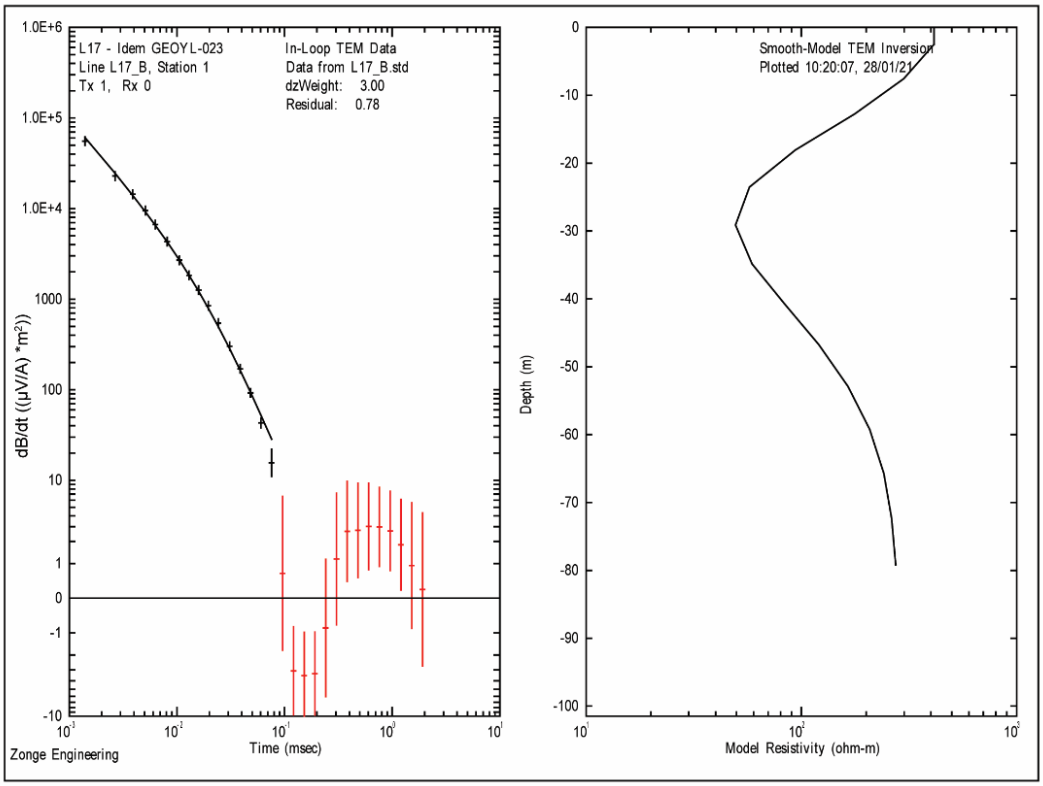

Figure 31: **(Left side)** Typical induced voltage decay from Line 17 (L17), Station 1. Measured data are shown as crosses and inversion fitting as a black line. Noise level is approximately 8 μV/A. The inversion residual is 0.78. **(Right side)** The obtained smooth model TEM inversion.

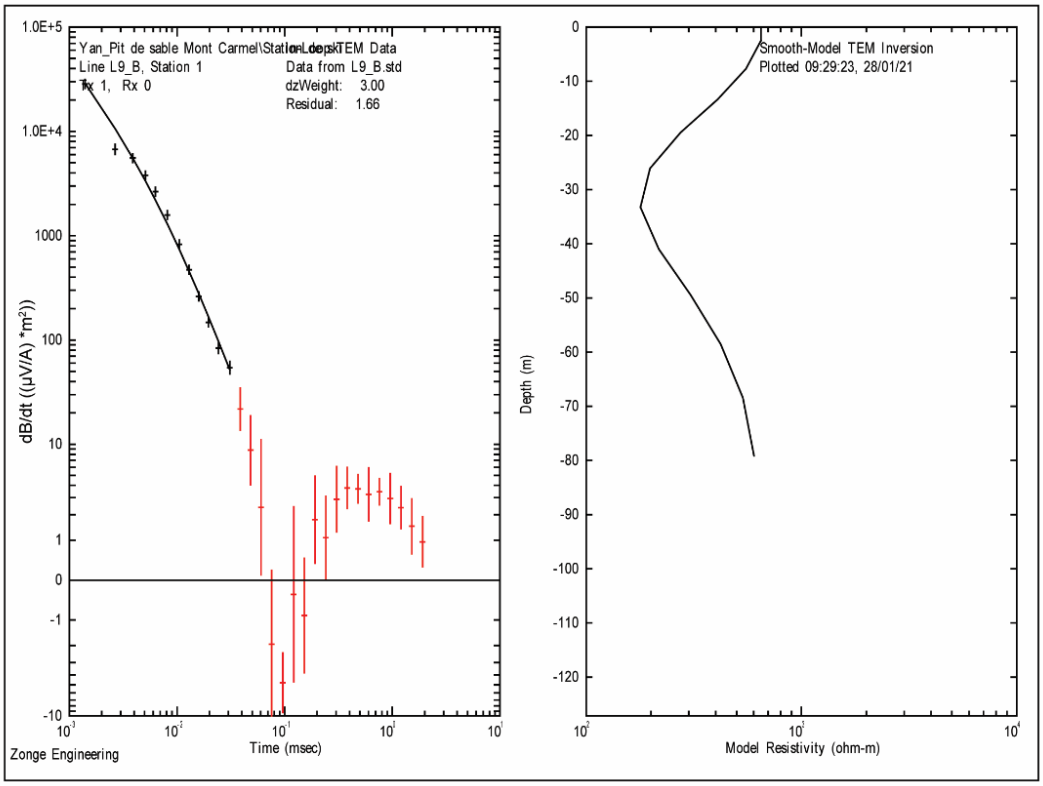

Figure 32: **(Left side)** Typical induced voltage decay from Line 9 (L9), Station 1. Measured data are shown as crosses and inversion fitting as a black line. Noise level is approximately 30 µV/A. The inversion residual is 1.66. **(Right side)** The obtained smooth model TEM inversion.

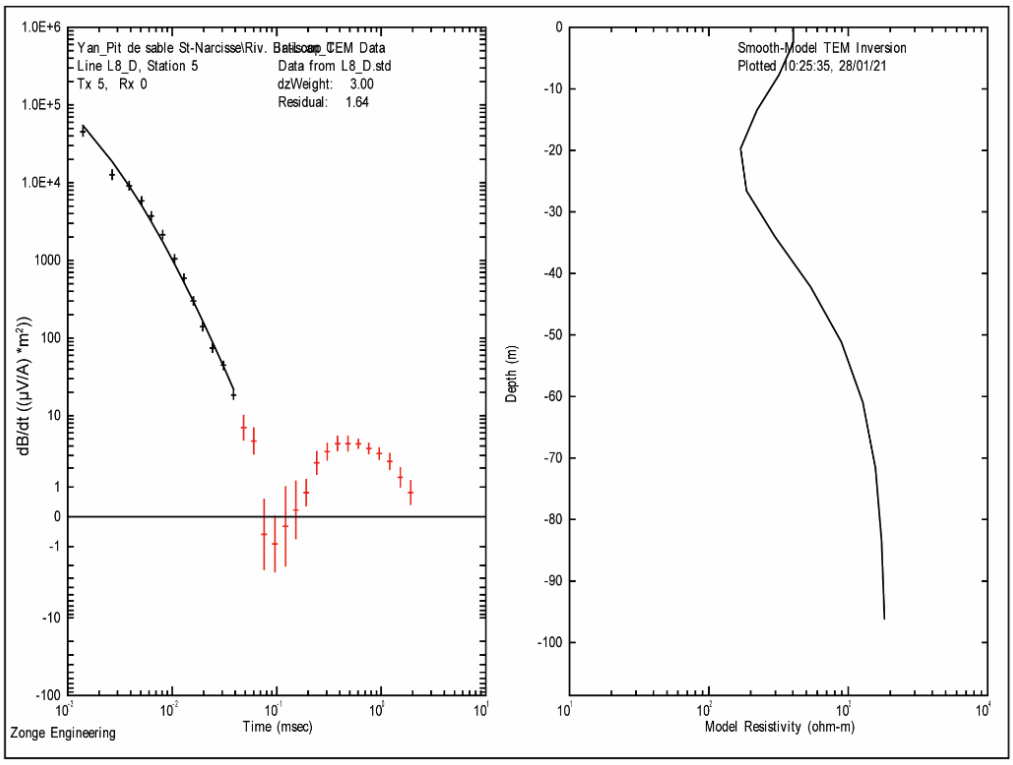

Figure 33: **(Left side)** Typical induced voltage decay from Line 8 (L8), Station 5. Measured data are shown as crosses and inversion fitting as a black line. Noise level is approximately 9 µV/A. The inversion residual is 1.64. **(Right side)** The obtained smooth model TEM inversion.

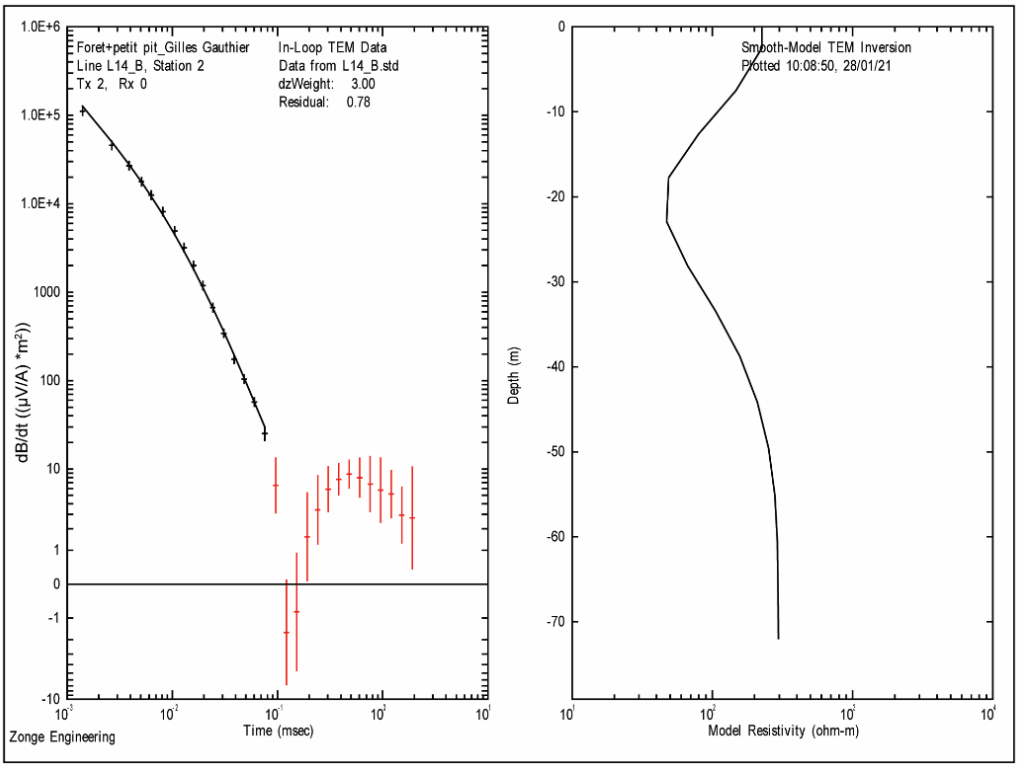

Figure 34: **(Left side)** Typical induced voltage decay from Line 14 (L14), Station 2. Measured data are shown as crosses and inversion fitting as a black line. Noise level is approximately 10 µV/A. The inversion residual is 0.78. **(Right side)** The obtained smooth model TEM inversion.

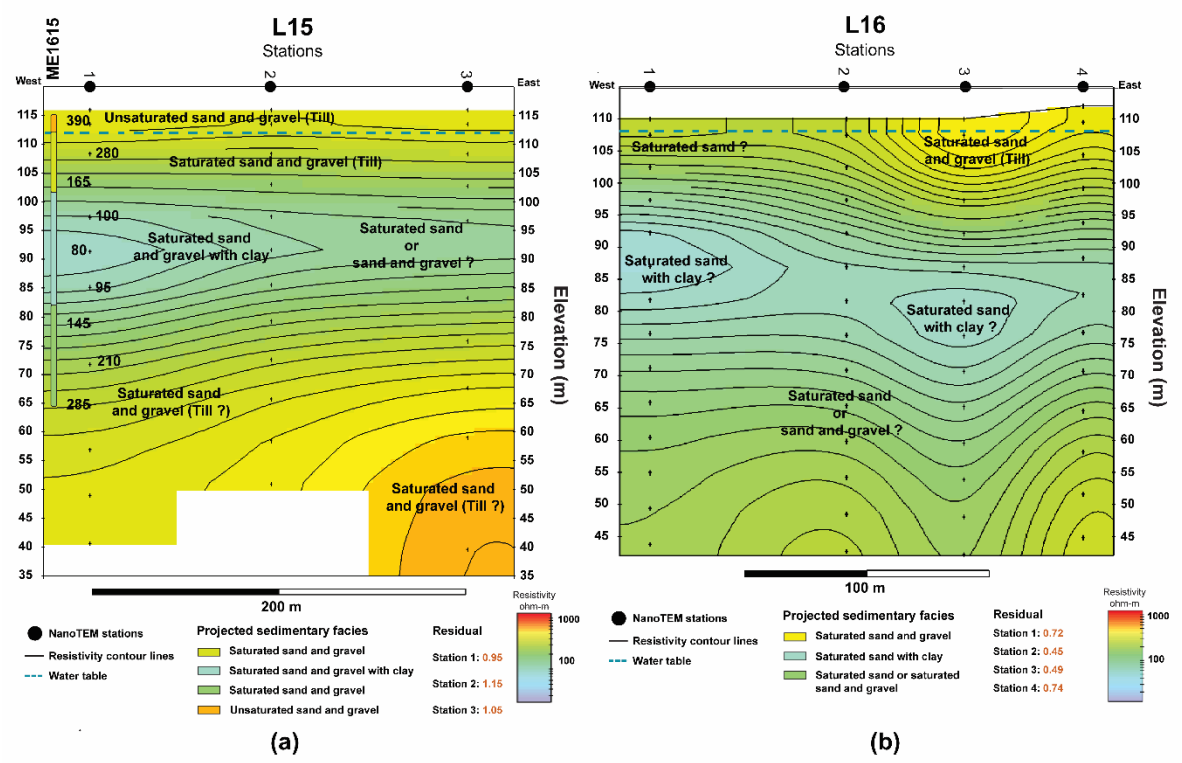

Figure 35: **A.** Interpreted 2D Section L15 near Saint-Narcisse, Quebec. **B.** Interpreted 2D Section L16 near Saint-Narcisse, located approximately 300 m further south of L15. The surface deposit elevation of both sections was obtained from lidar data.

2.6 DISCUSSION

2.6.1 SEDIMENTARY FACIES RESISTIVITY

Variation in electrical resistivity relates to the electrical resistivity of water being much lower than that of soils (Abu-Hassanein et al. 1996, Shukla and Yin 2006, Pandey et al. 2015), and resistivity is much lower for sediments having a high water content (McCarter 1984, Reynolds 2011). The circulation of the electric current in the basement, however, takes place mainly by volume conduction (or electrolytic conduction) through the pore water of these formations (McCarter 1984, Abu-Hassanein et al. 1996). Thus, the conduction of an electric current occurs primarily through the water contained in the pores or at the interface between the minerals and the pore water (surface electrical conductivity).

The calibrated chart highlights that electrical resistivity values for unsaturated sand and sand and gravel with pebbles/boulders are much higher, potentially up to 97% higher than for these same sediments when saturated. Clay has a low resistance to the passage of an electric current, and the resistivity values are low to very low. If clay horizons are found within sand or sand and gravel facies, the resistivity can decrease to 60 Ωm (Table 4). Low resistivity is a function of surface conduction from the higher clay mineral concentrations (Reynolds 2011). In contrast, sand/gravel/pebbles are much less conductive and provide greater resistance to the passage of an electric current. Grain size and even grain shape can also alter the bulk electrical and dielectric behaviors, thus affecting resistivity values (Kemna et al. 2004, Reynolds 2011).

The greater resistivity associated with increased grain size is visible, for example, at the base of several 2D sections of the Saint-Narcisse moraine (sections L2, L7, L8, L9, L10, L13, L14, and L17). During deglaciation, juxtaglacial and fluvioglacial deposits (e.g., ice-marginal outwash) generated by the melting ice were superimposed onto the glacial till sequence left by the passage of the LIS (Occhietti 1977, 2007). Fine-grained sediments (e.g., clay and silt) have high conductivity and low resistance to the passage of electric currents; resistivity increases as sediment grain size coarsens. The calibration chart reflects these particle size changes; therefore, the chart links the sedimentary facies (i.e., clay, sand, sand, and gravel), the associated electrical resistivity, and water content. Although overlap exists in the distributions between sediment classes and making the interpretation quite difficult, some of the resistivity ranges are well separated (Figure 29). In particular, saturated and unsaturated sediment shows very little overlap for the same category of sediment (i.e., saturated and unsaturated sand; saturated and unsaturated sand and gravel; Figure 29), which means that TEM is able to accurately identify the presence of water, except when there is a significant amount of clay mixed with the granular sediment, which drags down the resistivity. It is also challenging to discriminate between sand and gravel and the sand due to their close range of resistivity. Although these two categories show substantial overlap (Figure 29) and illustrate an inherent lack of the chart, the main objective of this study is to determine the presence of water (saturated sediment) with the greatest possible precision in order to identify potential aquifers. Consequently, even if these two sediment classes share similar resistivity values, they have a common characteristic, which is to be

lithological units of high permeability that can be crossed by water and possibly act as a reservoir. In fact, the presence of saturated and unsaturated granular sediments (i.e., below and above the water table), regardless of their granulometric size, can be validated with relative precision by the piezometric contour map (Figure 17), the boreholes, and the stratigraphic cross-sections. Indeed, even if there is an overlap between these categories of sediments and the TEM profiles are interpolations between 1D soundings and bears uncertainty related to these interpolations, the direct data (i.e., piezometric map built with 465 piezometric surveys, the boreholes, and the stratigraphic cross-sections) strengthen the stratigraphic interpretation and thus reduce the erroneous hypotheses linked to smoothing, interpolations and overlaps. Moreover, the ultimate goal of this study is essential to identify the presence of groundwater and its spatial continuity.

2.6.2 RELATIONSHIP BETWEEN THE CALIBRATION CHART AND THE TEM SECTIONS

Geophysical data provide an effective alternative to borehole surveys for characterizing the internal structures of deposits. The extrapolation of geophysical results over the entire study area requires creating a calibration chart to relate obtained electrical resistivity values to various unsaturated and saturated sediments. Once the calibration is achieved, however, multiple TEM profiles can be obtained in a short time span, and the stratigraphy of a large area can be evaluated. An equivalent characterization using boreholes is often impractical given the time-consuming and expensive nature of borehole drilling campaigns. Furthermore, cores are generally limited in number with considerable spacing between sites, making correlations between boreholes difficult.

The developed electrical resistivity chart (Table 4) allows us to use all collected 2D TEM sections west of the Batiscan River. Several 2D sections (Figures 27, 30, 35 and 36; sections L8, L9, L15, and L16) cannot be associated with any stratigraphic cross-sections, boreholes, or piezometric surveys, but nonetheless, provide valuable information regarding the geometry and extension of groundwater tables at the regional scale. These TEM sections, which can be linked to the other TEM sections used to build the calibration chart (Figures 16, 22, 26 and 28; sections L2, L10, L13, L17, and L14), therefore provide additional stratigraphic information and permit the assessment of a much

larger zone of the Saint-Narcisse moraine. The linking of sedimentology and geophysical data provides much insight in regard to the scale, arrangement, and granulometry of the sediment facies and their associated hydrogeological properties. The geophysical results of our study can support hydrogeological inferences of aquifer thickness, variation, and continuity.

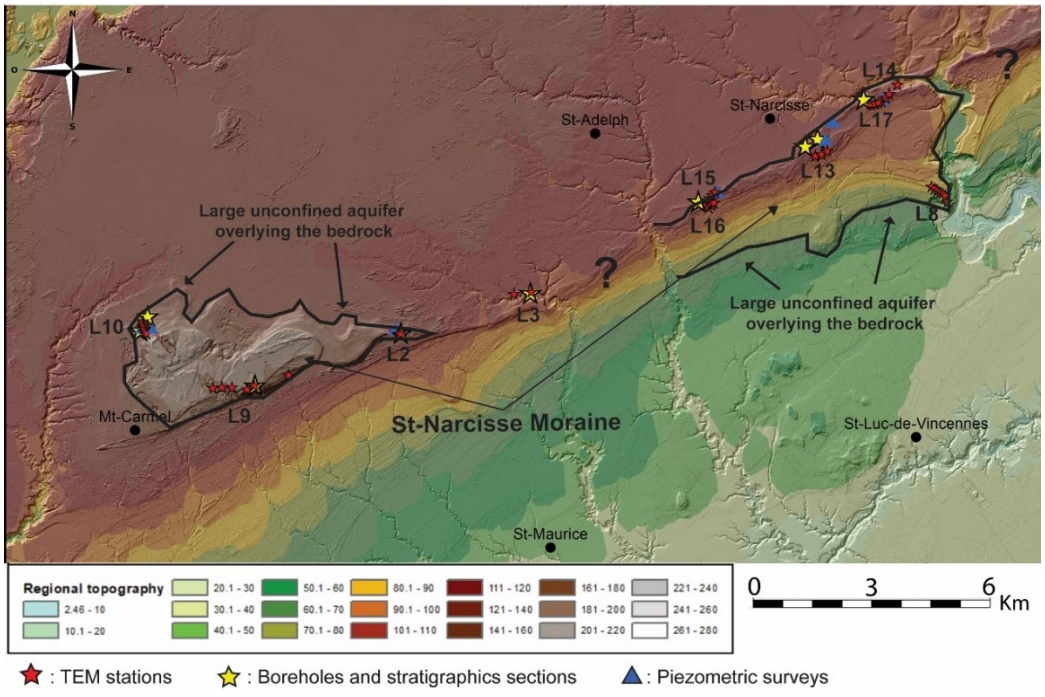

Figure 36: Regional topography of the study area and location of TEM stations, boreholes, stratigraphic cross-sections, and piezometric surveys acquired on the Saint-Narcisse moraine, Quebec. The black lines delimit two large unconfined regional aquifers west of Notre-Dame-du-Mont-Carmel and southeast of Saint-Narcisse.

2.6.3 HYDROGEOLOGICAL EXPLORATION TARGETS

Western Sector (Notre-Dame-du-Mont-Carmel)

Three 2D TEM sections (sections L2, L9, and L10) have a total length of 1.4 km and are spread over an area of approximately 11 km^2 east of Notre-Dame du Mont Carmel (Figure 36). These TEM sections share a similar sediment architecture and several other geological similarities; thus, we can assume a stratigraphic continuity and a hydraulic connection between these sections. For these three

sections, we observed that (1) the bedrock is located between 45 and 65 m for each of the 14 TEM stations; (2) a few meters of glacial till (i.e., sand and gravel) overlie the bedrock; (3) 5 to 15 m of unsaturated granular sediments, mainly sand/sand and gravel, are deposited over the surface of the moraine; (4) small amounts of clay are intermixed with the granular sediment. Greater amounts of clay would provide a natural impermeable barrier and increase the heterogeneity of the environment, thereby reducing the hydraulic connections at local and regional scales; and (5) the thickness of the water-saturated granular sediment varies between 30 and 60 m, the changes in sediment thickness being related to variations in local bedrock topography.

Previous studies have demonstrated that the sector of the moraine near Notre-Dame-du-Mont-Carmel (Figure 13) is composed primarily of granular sediments overlying bedrock, a continuity of the stratigraphic units, and the presence of extensive unconfined regional aquifers (Tricart 1983, Ferland and Occhietti 1990, Occhietti 2007, Légaré-Couture et al. 2018). These Quaternary sequences consist of subglacial or melt-out till (i.e., mainly sand and gravel) deposited during the last glaciation and the Saint-Narcisse readvance, proximal and distal glaciomarine deposits (mainly fine, medium, and coarse sands lay down by the Champlain Sea), as well as juxtaglacial and fluvioglacial deposits (Occhietti 1977, 2007). The saturated sediment and the water table elevation (Figure 17) also suggest a continuity of stratigraphic units and a hydraulic connection in this sector of the moraine. When comparing the piezometric contour depicted in Figure 17 with the reduction in resistivity values linked to saturated sediments for each TEM section, there is generally a correlation in depth within 1 to 3 meters. The drop in resistivity values is caused by the transition from unsaturated to saturated sediment at the top of the groundwater table. This strong correlation combined with a low RMS (i.e., 2.96 m), associated with a high-quality model, suggests that the piezometric map is representative of reality and that a hydraulic connection does exist between the TEM lines (i.e., sections L2, L9, and L10) in the sector of Notre-Dame-du-Mont-Carmel. In this case, the piezometric contours reflect the continuity of the water table elevation as well as the saturated sediments between the TEM sections. By correlating sections L2, L9, and L10 and assuming that the areas where no geophysical data have been collected have such continuity for their stratigraphic units, we can deduce, as Légaré-Couture et al. (2018) hypothesized previously, that an unconfined aquifer covers the entire area northeast of

Notre-Dame-du-Mont-Carmel (Figure 36). This large aquifer has a lateral extension of more than 6 km, a thickness varying from 30 to 60 m, and a depth between 5 and 15 m from the surface.

Central Sector (Saint-Narcisse)

These six 2D TEM sections of this part of the morainic complex (i.e., sections L8, L13, L14, L15, L16, and L17) have a total length of 2.7 km and are spread over an area of approximately 19.5 km^2 southeast of the village of Saint-Narcisse (Figure 36). Except for Section L8, few unsaturated sediments are recorded within these TEM sections, and the water table is near the surface, generally varying between 1 and 5 m depth. The bedrock is much deeper here than around the Notre-Dame-du-Mont-Carmel area, sometimes even up to 94 m (sections L15, L16, and L17) below the surface. This observation also agrees with previous studies, which sometimes locate the bedrock under the moraine as much as 100 m below present sea level (Légaré-Couture et al. 2018). This regional configuration (a deep bedrock and a shallow water level) and the substantial thicknesses of granular sediment deposits (i.e., sand, sand and gravel, sand and gravel with clay) into a series of bedrock depressions observed along the Saint-Narcisse moraine are suitable for creating unconfined aquifers. Moreover, according to previous studies, the thickest deposits can reach 150 m in south Mauricie (Légaré-Couture et al. 2018). The wa-ter-saturated sediments in the central section of the moraine are therefore quite thick, varying from 30 to over 94 m in thickness. The low amount of clay intermixed with the granular sediment observed in the TEM sections of this area of the moraine also suggests a suitable hydraulic connection owing to the absence of impermeable barriers at the local and regional scales. The Quaternary sequences and the type of sediment deposited within the central section of Saint-Narcisse moraine are similar to those within the Notre-Dame-du-Mont-Carmel area (i.e., subglacial or melt-out till, proximal and distal glaciomarine deposits, juxtaglacial and fluvioglacial deposits). In addition, the piezometric contour of Figure 17 is also well correlated with the decreased resistivity associated with saturated sediments for each of the TEM sections. This drop in resistivity is caused by the transition from unsaturated to saturated sediment at the top of the groundwater table. In the sector of Notre-Dame-du-Mont-Carmel, the robust correlation observed between the piezometric contour and the TEM sections, along with a

low RMS value, indicates that the resulting piezometric map accurately reflects the genuine regional stratigraphy and sediment characteristics. Consequently, a hydraulic connection owing to the continuity of the stratigraphic units does exist between the TEM sections in this area of the moraine located southeast of the village of Saint-Narcisse. Here, the piezometric contour reflects the continuity of the water table elevation and the saturated sediments between the TEM sections. Finally, by correlating these six TEM sections (i.e., sections L8, L13, L14, L15, L16, and L17) and assuming that the areas characterized by an absence of collected geophysical data show a continuity of their stratigraphic units, it is possible to identify a vast unconfined aquifer in the central sector of the moraine (Figure 36). From these assumptions, this aquifer covers an area of more than 6.5 × 3.0 km (>19.5 km2), varies between 25 and more than 94 m thick (depending on the sector), and is usually found within 1 to 2 m of the surface of the moraine.

Compartmentalization of the Aquifers

The Saint-Narcisse moraine in the Mauricie region contains thick layers of well-sorted sand and gravel deposits and holds two large unconfined aquifers overlying the bedrock. According to Légaré et al. (2018), although the hydrostratigraphy of the moraine is complex, it nonetheless contains a large regional unconfined aquifer within the surface sands. The Saint-Narcisse moraine has hydrogeological conditions favorable for groundwater extraction, and most municipalities located along the moraine and on the adjacent marine clay plain (e.g., Saint-Narcisse, Saint-Prosper, Saint-Maurice, Notre-Dame-du-Mont-Carmel, and Sainte-Geneviève-de-Batiscan) already draw their drinking water from this aquifer (Légaré-Couture et al. 2018), which attests to the aquifer capacity of these sectors. Previous studies have hypothesized the presence of these large regional aquifers on the basis of the large quantity of granular sediments at the moraine's surface (Grenier and Denis 1974, McCormack 1983, Légaré-Couture et al. 2018).

Our study validates the presence of these aquifers (Figure 36) and goes further by providing precise information related to regional stratigraphy and the aquifers' geometry, thickness, and extension. This study also suggests compartmentalization of the aquifers and a discontinuity of the stratigraphic units within the Saint-Narcisse moraine in the area. This compartmentalization separates

the aquifers from each other and is mainly produced by the presence of less permeable sediments, as the discontinuous nature of the moraine is frequently interrupted by multiple sections composed of finer sediments deposited by the Champlain Sea (Daigneault and Occhietti 2006). Both granular aquifers (Figure 36), from the surface, do not appear to be connected hydraulically because of the presence of these low-permeability barriers (e.g., mud units; Figure 18) that limit groundwater flow between this pair of highly conductive bodies (Grenier and Denis 1974, Tricart 1983, Ferland and Occhietti 1990, Occhietti 2007, Légaré-Couture et al. 2018).

2.7 CONCLUSION

The TEM method used in this study of the Saint-Narcisse moraine in the Mauricie region of Quebec revealed the compartmentalization of a multi-kilometer morainic system. Mud units deposited by the Champlain Sea during the deglacial marine incursion act as impermeable barriers to create a discontinuity of the stratigraphic granular units within the moraine and the compartmentalization of its contained aquifers. TEM demonstrated its utility for investigating the stratigraphic nature and the production of initial hydrogeological maps of other remote territories and geological contexts that lack minimal stratigraphic and piezometric information. To use all TEM results acquired for this study, we built an electrical resistivity calibration chart for saturated and unsaturated Quaternary sediments applying specifically to the Saint-Narcisse moraine in eastern Mauricie. The procedure can also be used in various environments if there are enough data. This chart links granulometric facies (i.e., clay, sand, sand, and gravel) and their respective electrical resistivity and water content. Once calibrated and applied to several TEM profiles along the Saint-Narcisse moraine, the chart helped identify two large unconfined granular aquifers overlying the bedrock west of the Batiscan River. Within the study area, these aquifers extend for a minimum distance of 12 km (east–west) and vary in thickness between 25 and more than 94 m. The TEM approach offers a relatively fast, simple, inexpensive, non-destructive, and effective means of acquiring valuable groundwater-related information to help municipalities and local entrepreneurs manage regional groundwater and ensure its preservation. Our findings highlight the need for more detailed studies of the Saint-Narcisse morainic complex to

better assess its groundwater resources. Greater details regarding this pair of identified aquifers can be obtained using direct approaches, including pumping tests, boreholes, and a more detailed hydrogeological mapping of targeted areas.

2.8 CONCLUSION DU CHAPITRE 2

Le caractère innovant de cette étude est la méthodologie qui réside dans le développement d'une approche permettant une meilleure caractérisation spatiale des aquifères régionaux à l'aide de méthodes géophysiques. Cette caractérisation spatiale vise à identifier plus précisément la stratigraphie, la géométrie, l'extension et l'épaisseur des aquifères régionaux dans les sédiments quaternaires. La calibration effectuée, représentée par la charte de résistivité locale proposée, permet essentiellement l'utilisation intégrale de toutes les données TEM collectées dans cette région, tandis que la carte piézométrique valide la robustesse des données TEM en termes d'élévation du toit de la nappe.

Dans cette procédure de calibration stratigraphique, les plages de résistivité sont établies simplement en corrélant les classes de sédiments rencontrées dans les forages avec leurs résistivités électriques respectives. Tel que décrit dans la méthodologie, cette calibration joue un rôle essentiel en fournissant une balise afin d'utiliser toutes les données TEM collectées sur le terrain. Malgré les chevauchements inévitables observés dans toutes les chartes existantes, l'objectif est de fournir des repères, tant au niveau régional que local, pour obtenir une vue d'ensemble des couches de subsurface et de la stratigraphie régionale dans la région de la moraine de Saint-Narcisse.

L'accent est particulièrement mis sur l'identification de l'élévation du toit de la nappe et des sédiments granulaires, qu'il s'agisse de sable, de gravier ou d'un mélange des deux, constituant l'aquifère. La taille granulométrique des sédiments est une considération secondaire dans ce contexte, l'objectif principal étant d'évaluer la capacité de stockage en eau d’un aquifère granulaire en nappe libre. Si le contexte géologique est similaire (par exemple, les moraines de Sakami et d'Harricana ou tout autre environnement quaternaire similaire), ces plages de résistivité pourraient être utilisées dans le cadre d'une autre étude.

Ces plages de résistivité font donc office de références pour exploiter toutes les données TEM disponibles dans une région, même celles qui n'ont pas (ou peu) de forages à proximité, afin de déterminer avec justesse l'élévation du toit de la nappe (grâce au contraste de résistivité électrique) et d'identifier les sédiments granulaires pouvant constituer ces aquifères. Cette calibration stratigraphique peut donc être appliquée à d'autres sites. Les résultats TEM obtenus dans une autre région détermineront si cette charte est appropriée ou inadaptée pour un autre site géologique.

En effet, il est préférable d'obtenir une vue d’ensemble et plus juste des gammes de valeurs de résistivité électrique associées à chaque classe sédimentaire, plutôt que d'obtenir un aperçu vague où les gammes de valeurs peuvent parfois atteindre des valeurs excessivement élevées (jusqu'à 150 000 ohms pour les sables et graviers) ou trop basses, ce qui fournit peu d'informations utiles pour l'utilisation et la corrélation des résultats géophysiques obtenus.

En outre, établir l'élévation du toit de la nappe phréatique à partir des contrastes de résistivité électrique obtenus dans les levés TEM et ERT introduit une certaine incertitude quant à sa localisation précise. Cette incertitude peut atteindre des ordres de grandeur de l'ordre du décimètre et, dans certains cas, probablement même du mètre. Ces variations sont inhérentes à la nature des méthodes géophysiques employées, qui, bien que puissantes pour l'estimation des niveaux piézométriques, présentent des limites de résolution qui doivent être soigneusement considérées dans l'interprétation des données.

LISTE DES REFERENCES

Abu-Hassanein, Z.S., Benson, C.H., and Blotz, L.R. 1996. Electrical resistivity of compacted clays. Journal of geotechnical engineering, 122: 397–406. American Society of Civil Engineers. doi:10.1061/(ASCE)0733-9410(1996)122:5(397).

Benn, D., and Evans, D.J.A. 2010. Glaciers and glaciation. In 1ST edition. Routledge, London and New York. doi:10.4324/9780203785010.

Burt, A. 2018. Three-dimensional hydrostratigraphy of the Orangeville Moraine area, southwestern Ontario, Canada. Canadian Journal of Earth Sciences, 55: 802–828. GeoScienceWorld. doi:10.1139/cjes-2017-0077.

Chesnaux, R., Lambert, M., Walter, J., Fillastre, U., Hay, M., Rouleau, A., Daigneault, R., Moisan, A., and Germaneau, D. 2011. Building a geodatabase for mapping hydrogeological features and 3D modeling of groundwater systems: Application to the Saguenay–Lac-St.-Jean region, Canada. Computers & Geosciences, 37: 1870–1882. Elsevier. doi:10.1016/j.cageo.2011.04.013.

Constable, S.C., and Parker, R.L. 1987. Occam's inversion: A practical algorithm for generating smooth models from electromagnetic sounding data. Geophysics, 52: 289–300. Society of Exploration Geophysicists. doi:10.1190/1.1442303.

Daigneault, R.-A., and Occhietti, S. 2006. Les moraines du massif Algonquin, Ontario, au début du Dryas récent, et corrélation avec la Moraine de Saint-Narcisse. Géographie physique et Quaternaire, 60: 103–118. Les Presses de l'Université de Montréal. doi:10.7202/016823ar.

Danielsen, J.E., Auken, E., Jørgensen, F., Søndergaard, V., and Sørensen, K.I. 2003. The application of the transient electromagnetic method in hydrogeophysical surveys. Journal of applied geophysics, 53: 181–198. Elsevier. doi:10.1016/j.jappgeo.2003.08.004.

Dewar, N., and Knight, R. 2020. Estimation of the top of the saturated zone from airborne electromagnetic data. Geophysics, 85: EN63–EN76. Society of Exploration Geophysicists and American Association of Petroleum …. doi:10.1190/geo2019-0539.1.

Dietrich, J.C., Bunya, S., Westerink, J.J., Ebersole, B.A., Smith, J.M., Atkinson, J.H., Jensen, R., Resio, D.T., Luettich, R.A., and Dawson, C. 2010. A high-resolution coupled riverine flow, tide, wind, wind wave, and storm surge model for southern Louisiana and Mississippi. Part II: Synoptic description and analysis of Hurricanes Katrina and Rita. Monthly Weather Review, 138: 378–404. doi:10.1175/2009MWR2907.1.

Douglas, R.J.W., Poole, W.H., Sanford, B. V, Williams, H., and Kelly, D.G. 1970. Geology and Economic minerals of Canada. In Geology and economic minerals of canada. Geological Survey of Canada Ottawa, Ontario. pp. 649–662.

Dyke, A., and Prest, V. 1987. Late Wisconsinan and Holocene history of the Laurentide ice sheet. Géographie physique et Quaternaire, 41: 237–263. doi:10.7202/032681ar.

Evans, D. 2005. Glacial landsystems. In 1ST edition. Edited ByRoutledge. Routledge, London (UK) and New York (USA). doi:10.4324/9780203784976.

Ferland, P., and Occhietti, S. 1990. Révision du stratotype des Sédiments de Saint-Pierre et implications stratigraphiques, vallée du Saint-Laurent, Québec. Géographie physique et Quaternaire, 44: 147–158. Les Presses de l'Université de Montréal. doi:10.7202/032814ar.

Fitterman, D. V, and Labson, V.F. 2005. Electromagnetic induction methods for environmental problems. In Near-surface geophysics. Edited by S. of E. Geophysicists. Society of Exploration Geophysicists, Houston, TX. pp. 301–356. doi:10.1190/1.9781560801719.ch10.

Fitterman, D. V, and Stewart, M.T. 1986. Transient electromagnetic sounding for groundwater. Geophysics, 51: 995–1005. Society of Exploration Geophysicists. doi:10.1190/1.1442158.

Girard, F. 2001. Architecture et hydrostratigraphie d'un complexe morainique et deltaïque dans la région de Saint-Raymond de Portneuf, Québec. PhD Thesis, Université du Québec, Institut national de la recherche scientifique, Quebec (Qc).

Globensky, Y. 1987. Géologie des Basses-Terres du Saint-Laurent. Ministère de l'énergie et des ressources, direction générale de l'exploration géologique et minérale, Québec (Qc).

Goldman, M., and Kafri, U. 2020. Geoelectric, Geoelectromagnetic and Combined Geophysical Methods in Groundwater Exploration in Israel. In The Many Facets of Israel's Hydrogeology, First. Springer, Cham, Switzerland. doi:10.1007/978-3-030-51148-7.

Grenier, C., and Denis, R. 1974. Etude hydrogeomorphologique dans la region du Lac Maskinongé, Québec. Canadian Journal of Earth Sciences, 11: 733–754. NRC Research Press Ottawa, Canada.

Jones, N.L., Davis, R.J., and Sabbah, W. 2003. A comparison of three-dimensional interpolation techniques for plume characterization. Groundwater, 41: 411–419. Wiley Online Library. doi:10.1111/j.1745-6584.2003.tb02375.x.

Kafri, U., Goldman, M., and Lang, B. 1997. Detection of subsurface brines, freshwater bodies and the interface configuration in-between by the time domain electromagnetic method in the Dead Sea Rift, Israel. Environmental Geology, 31: 42–49. Springer. doi:10.1007/s002540050162.

Kalisperi, D., Kouli, M., Vallianatos, F., Soupios, P., Kershaw, S., and Lydakis-Simantiris, N. 2018. A transient ElectroMagnetic (TEM) method survey in north-central coast of Crete, Greece: evidence of seawater intrusion. Geosciences, 8: 107. Multidisciplinary Digital Publishing Institute. doi:10.3390/geosciences8040107.

Kemna, A., Binley, A., and Slater, L. 2004. Crosshole IP imaging for engineering and environmental applications. Geophysics, 69: 97–107. Society of Exploration Geophysicists. doi:10.1190/1.1649379.

Landry, B., Beaulieu, J., Gauthier, M., Lucotte, M., Moingt, S., Occhietti, S., Pinti, D.L., and Quirion, M. 2012. Notions de géologie. In Modulo, Montréal, 4nd ed. Modulo, Montréal (Qc).

Larocque, M., Meyzonnat, G., Ouellet, M.-A., Graveline, M.-H., Gagné, S., Barnetche, D., and Dorner, S. 2015. Projet de connaissance des eaux souterraines de la zone Vaudreuil-Soulanges: rapport final déposé au ministère du Développement durable, de l'Environnement et de la Lutte contre les changements climatiques. Université du Québec à Montréal, Montréal, Québec.

Légaré-Couture, G., Leblanc, Y., Parent, M., Lacasse, K., and Campeau, S. 2018. Three-dimensional hydrostratigraphical modelling of the regional aquifer system of the St. Maurice Delta Complex (St. Lawrence Lowlands, Canada). Canadian Water Resources Journal/Revue canadienne des ressources hydriques, 43: 92–112. Taylor & Francis. doi:10.1080/07011784.2017.1316215.

Lévesque, Y., St-Onge, G., Lajeunesse, P., Desiage, P., and Brouard, E. 2019. Defining the maximum extent of the Laurentide Ice Sheet in Home Bay (eastern Arctic Canada) during the Last Glacial episode. Boreas, 49: 52–70. Wiley Online Library. doi:10.1111/bor.12415.

MacInnes, S., and Raymond, M. 2001. ZONGE Data Processing Two-Dimensional, Smooth-Model CSAMT Inversion version 3.00. Zonge Engineering and Research Organization, Inc. p. 41.

MacInnes, S., and Raymond, M. 2005. STEMINV: Smooth model TEM Inversion. Tucson, AZ.

Margold, M., Stokes, C.R., and Clark, C.D. 2015. Ice streams in the Laurentide Ice Sheet: Identification, characteristics and comparison to modern ice sheets. Earth-Science Reviews, 143: 117–146. doi:10.1016/j.earscirev.2015.01.011.

McCarter, W.J. 1984. The electrical resistivity characteristics of compacted clays. Geotechnique, 34: 263–267. Thomas Telford Ltd. doi:10.1680/geot.1984.34.2.263.

McClymont, A.F., Hayashi, M., Bentley, L.R., Muir, D., and Ernst, E. 2010. Groundwater flow and storage within an alpine meadow-talus complex. Hydrology & Earth System Sciences, 14. doi:10.5194/hess-14-859-2010.

McCormack, R. 1983. Etude hydrogéologique de la rive nord du Saint-Laurent. Énergie et ressource naturelle (Service des eaux souterraines), Québec (Qc). p. 188.

Nabighian, M.N., and Macnae, J.C. 1991. Time domain electromagnetic prospecting methods. Electromagnetic methods in applied geophysics, Tulsa, USA, 2: 427–509. doi:10.1190/1.9781560802686.

Nadeau, L., and Brouillette, P. (n.d.). Carte structurale de la région de Shawinigan (SNRC 31I), Province de Grenville, Québec. Commission Géologique du Canada, dossier public, 3012. doi:10.4095/205047.

Occhietti. 1977. Stratigraphie du Wisconsinien de la région de Trois-Rivières-Shawinigan, Québec. Géographie physique et Quaternaire, 31: 307–322. Les Presses de l'Université de Montréal. doi:10.7202/1000280ar.

Occhietti. 2007. The Saint-Narcisse morainic complex and early Younger Dryas events on the southeastern margin of the Laurentide Ice Sheet. Géographie physique et Quaternaire, 61: 89–117. Les Presses de l'Université de Montréal. doi:10.7202/038987ar.

Occhietti, ChartierH, M., Hillaire-Marcel, C., Cournoyer, M., Cumbaa, S., and Harington, R. 2001. Paléoenvironnements de la Mer de Champlain dans la région de Québec, entre 11 300 et 9750 BP: le site de Saint-Nicolas. Géographie physique et Quaternaire, 55: 23–46. Les Presses de l'Université de Montréal. doi:10.7202/005660ar.

Palacky, G. 1987. Resistivity characteristics of geological targets, in electromagnetic methods in applied geophysics, edited by Misac Nabighian, Society of Exploration Geophysicists. Society of Exploration Geophysicists, 1: 55–129.

Palacky, G.J. 1993. Use of airborne electromagnetic methods for resource mapping. Advances in space research, 13: 5–14. Elsevier. doi:10.1016/0273-1177(93)90196-I.

Pandey, L.M.S., Shukla, S.K., and Habibi, D. 2015. Electrical resistivity of sandy soil. Géotechnique Letters, 5: 178–185. Thomas Telford Ltd. doi:10.1680/jgele.15.00066.

Parent, M., and Occhietti, S. 1988. Late Wisconsinan deglaciation and Champlain sea invasion in the St. Lawrence valley, Québec. Géographie physique et Quaternaire, 42: 215–246. Les Presses de l'Université de Montréal. doi:10.7202/032734ar.

Parent, M., and Occhietti, S. 1999. Late Wisconsinan deglaciation and glacial lake development in the Appalachians of southeastern Québec. Géographie physique et Quaternaire, 53: 117–135. Les Presses de l'Université de Montréal. doi:10.7202/004859ar.

Parriaux, A., and Nicoud, G. 1993. De la montagne à la mer, les formations glaciaires et l'eau souterraine. Exemple du contexte Nord-alpin occidental. Quaternaire, 4: 61–67. Association française pour l'étude du quaternaire. doi:10.3406/quate.1993.1993.

Parsekian, A.D., Singha, K., Minsley, B.J., Holbrook, W.S., and Slater, L. 2015. Multiscale geophysical imaging of the critical zone. Reviews of Geophysics, 53: 1–26. Wiley Online Library. doi:10.1002/2014RG000465.

Reynolds, J.M. 2011. An introduction to applied and environmental geophysics. In 2nd edition. John Wiley & Sons, West Sussex, UK.

Rivers, T., Gool, J.A.M. van, and Connelly, J.N. 1993. Contrasting tectonic styles in the northern Grenville province: Implications for the dynamics of orogenic fronts. Geology, 21: 1127–1130. Geological Society of America. doi:10.1130/0091-7613(1993)021<1127:CTSITN>2.3.CO;2.

Sass, O. 2006. Determination of the internal structure of alpine talus deposits using different geophysical methods (Lechtaler Alps, Austria). Geomorphology, 80: 45–58. Elsevier. doi:10.1016/j.geomorph.2005.09.006.

Schrott, L., Hufschmidt, G., Hankammer, M., Hoffmann, T., and Dikau, R. 2003. Spatial distribution of sediment storage types and quantification of valley fill deposits in an alpine basin, Reintal, Bavarian Alps, Germany. Geomorphology, 55: 45–63. Elsevier. doi:10.1016/S0169-555X(03)00131-4.

Shukla, S.K., and Yin, J.-H. 2006. Fundamentals of geosynthetic engineering. In 1ST edition. Edited ByCRC Press. Taylor and Francis, Balkema, London (UK). doi:10.1201/9781482288445.

Sorensen, K.I., Auken, E., and Thomsen, P. 2000. TDEM in groundwater mapping—a continuous approach. Symposium on the Application of Geophysics to Engineering and Environmental Problems 2000,: 485–491. Society of Exploration Geophysicists. doi:10.4133/1.2922780.

Stokes, C.R. 2017. Deglaciation of the Laurentide Ice Sheet from the Last Glacial Maximum. Cuadernos de investigación geográfica., 43: 377–428. Universidad de La Rioja. doi:10.18172/cig.3237.

Tricart, J. 1983. S. Occhietti, Le Quaternaire de la région de Trois-Rivières-Shawinigan, Québec. Contribution à la paléogéographie de la vallée moyenne du St-Laurent et corrélations stratigraphiques. In Annales de géographie. Edited by Armand Colin. Persée-Portail des revues scientifiques en SHS, Paris, France. pp. 242–245.

Walter, J., Rouleau, A., Chesnaux, R., Lambert, M., and Daigneault, R. 2018. Characterization of general and singular features of major aquifer systems in the Saguenay-Lac-Saint-Jean region. Canadian Water Resources Journal/Revue canadienne des ressources hydriques, 43: 75–91. Taylor & Francis. doi:10.1080/07011784.2018.1433069.

Wise, S. 2000. Assessing the quality for hydrological applications of digital elevation models derived from contours. Hydrological processes, 14: 1909–1929. Wiley Online Library. doi:10.1002/1099-1085(20000815/30)14:11/12<1909::AID-HYP45>3.0.CO;2-6.

Zimmerman, D., Pavlik, C., Ruggles, A., and Armstrong, M.P. 1999. An experimental comparison of ordinary and universal kriging and inverse distance weighting. Mathematical Geology, 31: 375–390. Springer. doi:10.1023/A:1007586507433.

CHAPITRE 3

ELECTRICAL RESISTIVITY OF SATURATED AND UNSATURATED SEDIMENTS IN NORTHEASTERN CANADA

Le chapitre 3 de cette thèse est présenté sous la forme d'un article scientifique. Il s'agit du deuxième outil d'investigation développé dans notre approche méthodologique pour mieux évaluer le potentiel aquifère d'un milieu de dépôt quaternaire hétérogène et anisotrope.

Ce chapitre suggère des valeurs de résistivité électrique pour des sédiments saturés et non saturés au Québec sous forme d'une charte de résistivité. La base de données de cette étude est constituée de levés géophysiques de surface (TEM) ainsi que de données stratigraphiques et hydrogéologiques provenant de forages réalisés dans cinq régions de la province de Québec, au Canada : la Mauricie, l'Abitibi-Témiscamingue, le Saguenay-Lac-Saint-Jean, la Charlevoix et la Haute-Côte-Nord. Les stations TEM ont été sélectionnées près des sites où l'on retrouve les forages, les coupes stratigraphiques et les levés piézométriques, afin d'obtenir une relation pétrophysique empirique et locale et d'établir ainsi une charte de résistivité électrique des sédiments. Cette charte propose donc des gammes de résistivité applicables à quatorze classes de sédiments saturés et non saturés, dont sept n'ont jamais été incluses dans des études précédentes : les argiles limoneuses, les argiles avec du sable/gravier/cailloux, les silts argileux non saturés avec du sable, les sables limoneux saturés et non saturés, et les sables argileux saturés et non saturés avec du gravier.

Les résultats de cette étude peuvent fournir aux scientifiques et aux praticiens des caractéristiques précises de la résistivité électrique d'une large gamme de sédiments saturés et non saturés des régions nordiques, permettant ainsi une évaluation plus précise des ressources en eau souterraine.

Le présent article a été soumis à la revue Environmental Earth Sciences (IF : 3,15) le 17 novembre 2022 et a été publié le 2 juin 2023. https://doi.org/10.1007/s12665-023-10998-w

Yan Lévesque [1, 2]*, Julien Walter [1, 2], Romain Chesnaux[1, 2], Sebastien Dugas[3] and David Noel[1]

[1] Université du Québec à Chicoutimi, Department of Applied Sciences, Saguenay, QC, G7H 2B1 Canada;

[2] Centre d'études sur les ressources minérales (CERM), Groupe de recherche risque ressource eau (R2EAU), Université du Québec à Chicoutimi, Saguenay, QC, Canada G7H 2B1, Canada

[3] Université du Québec à Rimouski, Bas Saint-Laurent, QC, Canada G5L 3A1

Email: julien_walter@uqac.ca; romain_chesnaux@uqac.ca; sebastien_dugas@uqar.ca; david_noel@uqac.ca

*corresponding author: yan.levesque1@uqac.ca

Orcid ID: YL: 0000-0002-6198-6315; RC: 0000-0002-1722-9499; JW: 0000-0003-2514-6180

3.1 ABSTRACT

This study presents typical values of electrical resistivity for common saturated and unsaturated sediments in Québec in the form of a resistivity chart. The database for this study consists of surface geophysical investigations (i.e., Transient Electromagnetic (TEM) Surveys) together with stratigraphic and hydrogeological data from boreholes drilled among five regions of the Province of Québec in Canada: Mauricie, Abitibi-Témiscamingue, Saguenay-Lac-Saint-Jean, Charlevoix and Haute-Côte-Nord. TEM stations were selected near the sites where boreholes,

stratigraphic cross-sections and piezometric surveys were acquired to derive an empirical and local petrophysical relationship and establish a resistivity chart of the sediments. This chart proposes ranges of resistivity applying to fourteen classes of common sediments, seven of which have never been included in previous studies: silty clay, clay with sand/gravel/pebbles, unsaturated clayey silt with sand, saturated and unsaturated silty sand and saturated and unsaturated clayey sand and gravel. A standardization method was developed and used in this study to produce an accurate and representative chart, and to eliminate outliers that might distort the results and reduce their relevance. This method was designed with the aim of mitigating the impact of outliers and ensuring a reliable and consistent dataset. The findings from this study may provide scientists and practitioners with precise electrical resistivity characteristics of typical saturated and unsaturated sediments, enabling a more accurate assessment of groundwater resources.

Keywords: Resistivity chart, transient electromagnetic surveys (TEM), stratigraphy, statistical analysis, sediments, hydrogeophysics

3.2 INTRODUCTION

The electrical resistivity of sediments is related to soil characteristics such as water content, grain size, relative density, and geochemical properties. Different subsurface geological materials can share similar resistivity values (Palacky 1987, 1993, Danielsen et al. 2003, Reynolds 2011, Goldman and Kafri 2020). Therefore, assigning specific resistivity values to some geomaterials can be challenging. As a result, several resistivity values for the same geomaterial can be found in the literature. For example, the widely used resistivity ranges for common sediments such as clay, silt, sand, sand-gravel, and gravel (Reynolds 1987a, 2011, Telford et al. 1990, Palacky 1993, Van Heteren et al. 1998, Neal and Roberts 2000, Neal 2004, Goutaland 2008) are compiled from several ground penetrating radar (GPR) studies. This geophysical method utilizes electromagnetic waves (more specifically microwaves from MHz to GHz) to probe subsurface materials (Beres Jr. and Haeni 1991, Van Heteren et al. 1998, Neal and Roberts 2000, Neal 2004, Goutaland 2008). However, these compilations often provide resistivity ranges that contradict one another and contain outliers

that are often too high or too low to be representative. For example, Palacky (1993), Neal et al. (2000, 2004) and Heteren et al. (1998) proposed resistivity values up to 10,000 Ωm, 143,000 Ωm and 150,000 Ωm for unsaturated sand and gravel, respectively, whereas Knight (2018), Reynolds (2011) and Goutaland (2008) proposed maximum values of 150,225 and 1,400 Ωm, respectively. This is one example among many and shows just how contradictory some of the charts can be. When the maximum and minimum values for the same class of sediments vary by several orders of magnitude, it is difficult to determine which type of sediment is responsible for the acquired electrical resistivity. The outliers and the uncertainties found in some of these proposed charts can be explained in several ways: 1) Nearby boreholes do not systematically validate the geophysical results. 2) The water level (i.e., water table) is not systematically measured in the boreholes or wells near the geophysical results. Therefore, it is difficult to differentiate between water-saturated and unsaturated sediments, and the resistivity values associated with these types of sediments become random and imprecise. 3) They do not consider sediments intermixed with other sediments (e.g., sand with clay, sand and gravel with clay, sand with silt, among others). If the targeted sediments are mixed with other types of sediments characterized by a substantial difference in resistivity, the resistivity results are skewed for that class of sediment. Indeed, unlike clay and silt, sand, gravel and pebbles provide higher resistance to the passage of electric current; therefore, resistivity tends to increase as the sand and gravel contents increase and the clay and silt contents decrease. 4) If the results come from regions where the pore fluid conductivity is high (e.g., coastal environments), the presence of a large amount of seawater nearby may introduce a bias in the acquired resistivity. Due to a high quantity of electrically charged particles (i.e., ions), seawater is very conductive, and its presence inside the sediments, even in small amounts, will significantly reduce the resistivity. 5) Excessively low and/or high resistivity values (i.e., outliers) are found in these charts for several sediment classes. For example, the charts by Palacky (1993) and Neal et al. (2000, 2004) show that saturated and unsaturated sands can reach resistivity values up to 10,000 Ωm and sometimes even higher; Heteren et al. 1998 records values up to 100,000 Ωm. In comparison, the resistivity of unsaturated sand in this study, Goutaland (2008) and Reynolds (2011) report values of up to 900, 1,000 and 1,050 Ωm.

Because outliers distort resistivity ranges, they should be removed to create a more representative resistivity chart for common saturated and unsaturated sediments.

Previous charts lack precision regarding the correlation between common saturated and unsaturated sediments and electrical resistivity. The question that arises here is how to determine the ranges of resistivity associated with each type of sediment with the greatest accuracy. To answer this question, a chart should incorporate geophysical results that 1) were compared and verified with data from nearby boreholes or stratigraphic cross-sections; 2) were compared to boreholes that have information on the groundwater level and therefore can establish a clear differentiation between saturated and unsaturated sediment; 3) implement a method to remove outliers and create a chart with a more representative range of values; and 4) ensure that the sediment classes studied were not mixed with seawater and/or other sediments, which could significantly affect the resistivity values. If the sediments are intermixed, one should consider proposing resistivity ranges for specific mixes of sediments (e.g., sand and gravel with clay, sand and clay, sand and silt).

In this study, we provide a singular and comprehensive resistivity database and present an accurate chart of resistivity for common Quaternary deposits. This database consists of the results of surface geophysical investigations (i.e., transient electromagnetic, TEM, method) and stratigraphic and hydrogeological data from boreholes drilled in five regions in the Province of Québec, Canada (Fig. 37): Mauricie, Abitibi-Témiscamingue (AT), Saguenay-Lac-Saint-Jean (SLSJ), Charlevoix (C) and Haute-Côte-Nord (HCN). The varied origin and wide variety of data allow us to correlate 4,042 resistivity values (i.e., observed values (Ncount) in Table 5) with as many as fourteen classes of sediments in Eastern Canada. The varied origins and wide variety of data suggest that the obtained results are representative of the Quaternary sediments typically found in northern regions as a whole.

TABLE 5: Raw results of TEM soundings with their associated sedimentary facies for 14 classes of sediments, their number of results (Ncount), the minimums and maximums values obtained for each class (Min and Max), their numerical threshold of 5% (R05 and R95) and the number of rejected data (ie., <R05 or >R95) for each class of sediments. DNA means not applicable.

Lithology	Water saturation	Ncount	Min	R05	R95	Max	Rejected
Clay sgp	DNA	1034	14.3	20.34	174.82	226.6	104
Clay	DNA	1070	0.8	1.4	63.4	110.5	105
Clayey sand and gravel	No	30	127.6	133.8	401.7	413	2
Clayey sand and gravel	Yes	33	94.7	101.54	285.18	311.6	4
Clayey sand	No	85	30.6	31.78	261.5	318.8	8
Clayey sand	Yes	35	45.3	47.68	196.1	218.1	4
Clayey silt	DNA	102	22	23.7	289.96	373.3	10
Sand and gravel	No	303	164.8	303.17	1430	2045.2	29
Sand and gravel	Yes	337	116.3	179.84	914.1	1198.2	34
Sand	No	325	103.1	231.9	786.7	1058.9	31
Sand	Yes	186	73.2	119.16	566.9	652	18
Silty clay	DNA	136	11.4	19.35	166.46	183.6	14
Silty sand	No	109	106.9	140.8	536.19	578.9	10
Silty sand	Yes	257	80.2	94.08	439.49	664.7	26

Quaternary sediments found in these five regions are related to three distinct geological provinces: the Grenville Province, Superior Province and St. Lawrence Platform. A variety of glacial deposits (e.g., subglacial or melt-out till, juxtaglacial and fluvioglacial deposits) and glaciomarine sediments (e.g., deep-sea marine deposits, proximal and distal glaciomarine deposits, coastal and deltaic sandy deposits) were considered (Occhietti 1977, Veillette and Thibaudeau 2004, Légaré-Couture et al. 2018). As part of the Groundwater Knowledge Acquisition Program (PACES; (Walter et al. 2018, Boumaiza et al. 2021a, 2021b, 2021c, 2022, Lévesque et al. 2023b), sponsored by the Québec Ministry of the Environment (MDDELCC), geophysical data were gathered (i.e., spatial references database; Chesnaux et al. 2011). In total, 111 TEM stations, 75 boreholes, 10 stratigraphic cross-sections and 51 piezometric surveys were acquired from the geodatabase. TEM stations (1D

resistivity models) were selected near the sites where boreholes, stratigraphic cross-sections and piezometric surveys were available. These direct measurements were used to calibrate the geophysical results and obtain an equivalent resistivity for each saturated and unsaturated sediment class. In this paper, we present a chart with fourteen classes of sediments: clay, silty clay, clay with sand/gravel/pebbles, unsaturated clayey silt with sand, saturated and unsaturated sand, saturated and unsaturated silty sand, saturated and unsaturated clayey sand, saturated and unsaturated sand and gravel with pebbles, saturated and unsaturated clayey sand and gravel. Seven of these classes have not, to the best of our knowledge, been previously included in studies: silty clay, clay with sand/gravel/pebbles, unsaturated silt with clay and sand, saturated and unsaturated silty sand, saturated and unsaturated clayey sand and gravel. As the relationship between resistivity and lithology is fundamental to any characterized geophysical resistivity, or to any electromagnetic survey aiming to determine subsurface variations, the findings from this study will aid researchers and private-sector practitioners (e.g., hydrogeologists, engineers and geophysicists) in achieving greater precision when identifying the electrical resistivity properties of different saturated and unsaturated sediments, thus enabling more accurate assessment of groundwater resources.

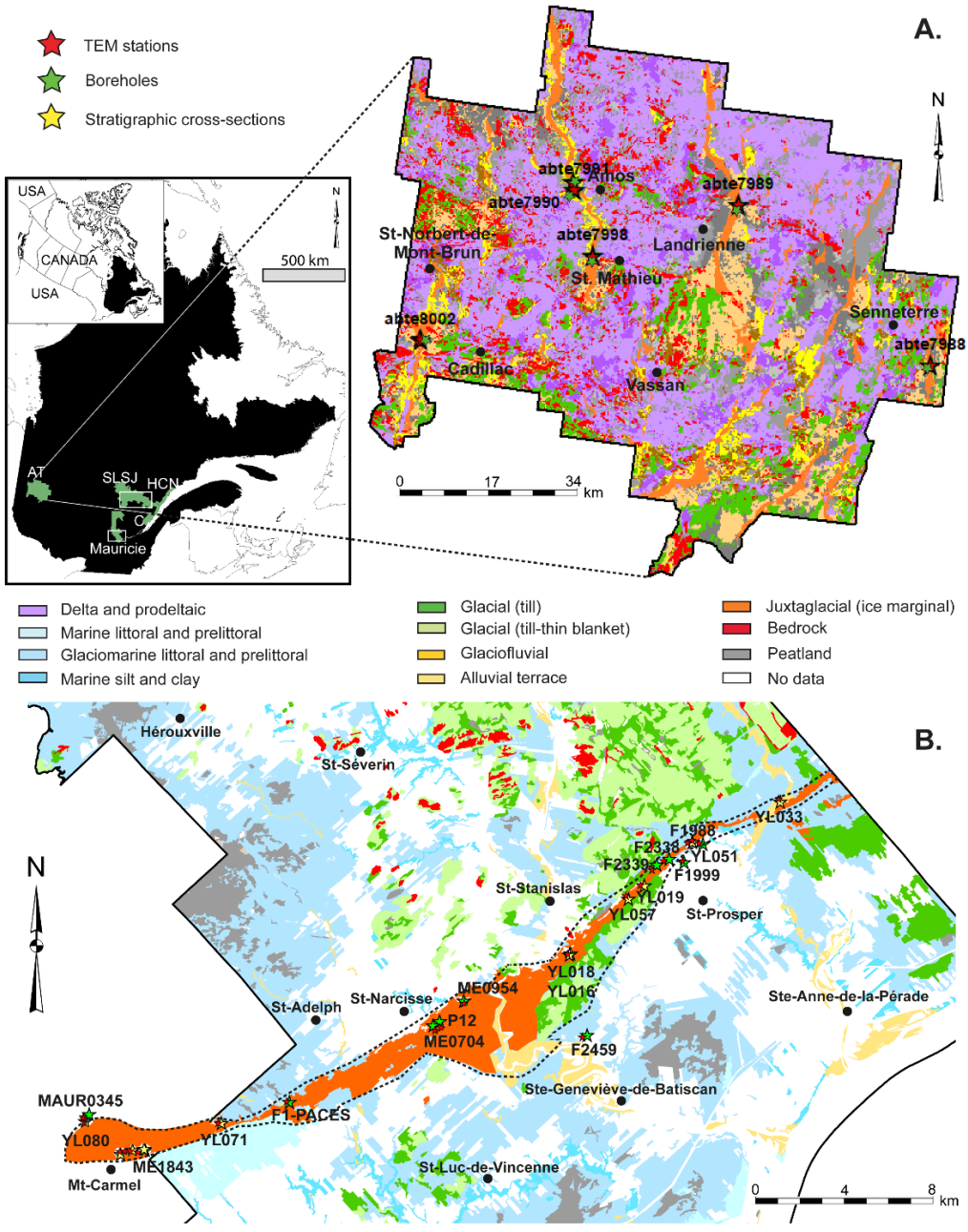

Figure 37: **(Left)** General map of the study area spanning over five regions of the Province of Québec in Canada: Mauricie, Abitibi-Temiscamingue (AT), Charlevoix (C), and Haute-Côte-Nord (HCN), Saguenay-Lac-Saint-Jean (SLSJ). **(Right and bottom)** Surface deposit map of Quaternary sediments and location of TEM stations, boreholes, and stratigraphic cross-sections acquired in **A.** Abitibi-Temiscamingue (AT); **B.** Mauricie. The black dashed lines in figure 37B represent the boundary of the Saint-Narcisse Moraine and the white rectangles represent the extension of Mauricie and SLSJ studies area. The surface deposit maps of Quaternary sediments are adapted from CERM-PACES (2011-2022) and from PACES-Abitibi (2022).

3.3 GEOLOGICAL BACKGROUND

North of the St. Lawrence River, the Province of Québec mainly consists of Precambrian rocks of the Canadian Shield. Within the Province of Québec, the administrative regions of Mauricie, AT, SLSJ, C and HCN covers an area of approximately 432,517 km^2 (Figs. 37-38). The geology of these regions is characterized by bedrock units covered by Quaternary sediments of highly variable thickness and particle size distribution. The bedrock encountered in the Mauricie, AT, C, HCN and SLSJ belong to three distinct geological provinces: the Grenville Province, the Superior Province and St. Lawrence Platform (Brisebois and Brun 1994, Rivers 2017).

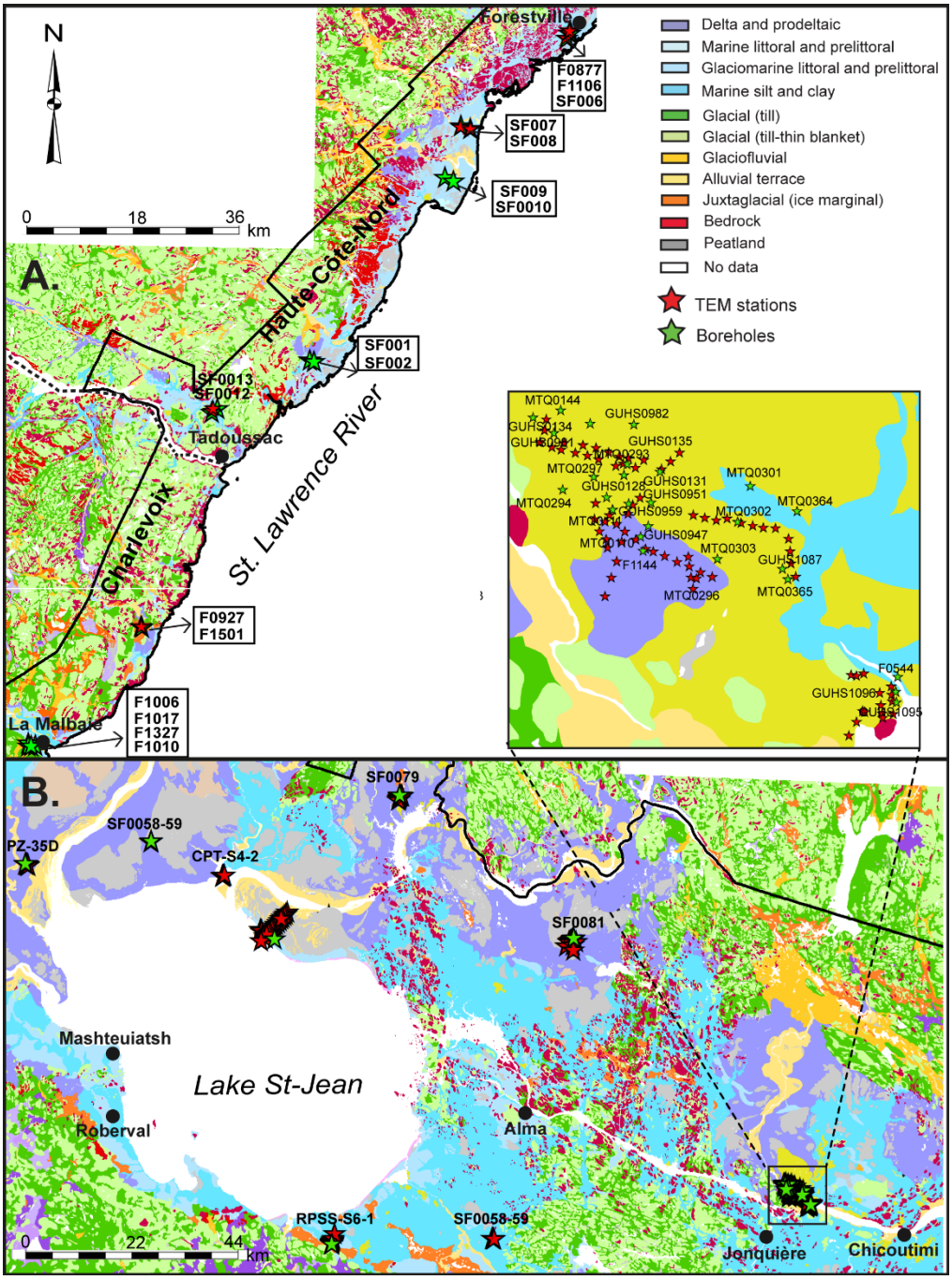

Figure 38: Surface deposit map of Quaternary sediments and location of TEM stations and boreholes acquired in **A.** Charlevoix (C) and Haute-Côte-Nord (HCN); **B.** Saguenay-Lac-Saint-Jean (SLSJ). The black dashed line in figure 38A represents the boundary between the Charlevoix and Haute-Côte-Nord regions. The surface deposit maps of Quaternary sediments are adapted from CERM-PACES (2011-2022).

3.3.1 BASEMENT GEOLOGY

The Grenville Province

The Grenville Province is the Precambrian shield's youngest geological province, mainly consisting of intrusive igneous and high-grade metamorphic rocks (Rivers 2017). The Grenville Province covers nearly 600,000 km^2 in Québec and makes up most of Mauricie, C, HCN and SLSJ. It forms the southeastern limit of the Superior Province and is subdivided into two parts, parautochthonous and allochthonous. The lithological composition of the Grenville Province is variable depending on the regions and is mainly characterized by the presence of anorthosite, mangerite, charnockite, orthogneiss, paragneiss, migmatite, and marble (Rivers 2017).

The St. Lawrence Platform

The St. Lawrence Platform stretches along the southern margin of the Canadian Shield, covers an area of ~30,000 km^2 and is bounded to the southeast by the Appalachian Province. The St. Lawrence Platform is composed of basal Paleozoic sedimentary rocks covered by a thick layer of Quaternary sediments. The sedimentary rocks mainly consist of Ordovician sandstone (Black River Group), carbonate (Trenton Group) and shales (Lorraine Group, and Utica Shale of the Trenton Group) that were deposited in a marine environment (Occhietti 1977). The St. Lawrence Platform is divided into two sectors: the St. Lawrence Lowlands, which broadly consist of the Montréal-Québec area and includes part of the Mauricie and Charlevoix regions, and the Anticosti Platform, which extends over the HCN region.

The Superior Province

The Superior Province is the center of the Canadian Shield and one of the planet's largest Archean cratons. It occupies a large portion of the North American continent, making up nearly half of the Province of Québec (~750,000 km^2). It is subdivided into a dozen sub-provinces, and it stretches from the Great Lakes to the west coast of Ungava Bay and includes the AT region, more precisely into the geological sub-province of Abitibi (Bostock 1970). The Superior Province is only related to AT and absent from the other considered territories. This province is bordered to the north

by the Churchill Province and to the southeast by the Grenville Province (Bostock 1970). The lithological composition of Superior Province consists of high-grade metamorphic gneiss (granulite amphibolite), belts of volcanic and granitic rocks, metasedimentary rocks and plutonic rocks (Card 1990). The land under study is located in the central part of the Abitibi sub-province, the most extensive Archean volcano-sedimentary belt worldwide (Bostock 1970, Card 1990). This zone comprises sequences of predominantly volcanic rocks (basalt and rhyolite) framed or intersected by granitoid batholiths. These intrusions include synvolcanic plutons, tonalitic gneiss, and younger plutons that vary in composition, ranging from quartz diorite to granite and syenite (Card 1990).

3.3.2 QUATERNARY SEDIMENT DEPOSITS

The Laurentide Ice Sheet (LIS) covered most of Canada during the Last Glacial Period (LGP) and reached thicknesses of nearly five kilometers (Dyke 2004, Benn and Evans 2010, Lévesque et al. 2019). This ice sheet was a mass of moving ice that transported sediments to create glacial deposits, mainly made up of diamictons (i.e., tills). The LIS retreated from the southern region of Canada approximately 18,000 years ago, leaving several glacial outwashes (Dyke 2004, Margold et al. 2015). Ice retreat was swiftly followed by a marine transgression and the formation of major seas in the actual Province of Québec, known as the Laflamme Sea, Champlain Sea, Iberville Sea, Tyrrell Sea and Goldthwait Sea. These seas covered the SLSJ, Mauricie and C, HCN regions with deep-sea marine deposits, mainly massive or stratified clay, which are covered by regressive littoral and prelittoral deposits (i.e., coastal and deltaic sandy deposits) in topographically low areas (Occhietti 1977, Veillette and Thibaudeau 2004, Légaré-Couture et al. 2018). Farther north, Lake Ojibway covered the region of AT with a large clay plain that occurs as mainly varve deposits with a total thickness varying from 1 to 60 m (Veillette and Thibaudeau 2004). The glacial history of these five regions (i.e., Mauricie, AT, C, HCN and SLSJ) produced most of the sediments, and these glacial sediments are covered mainly by a thick layer of Quaternary deposits that overlie the bedrock and were formed entirely during the Late Wisconsinian. The resulting stratigraphy is made up of glacial deposits, fluvioglacial deposits and glaciolacustrine deposits (Veillette and Thibaudeau 2004,

Occhietti 2007, 2018, Légaré-Couture et al. 2018) interspersed with sequences of shallow deltaic marine sediments and deep marine sediments from inland seas. Glacial deposits corresponding to till mainly result from the erosion of crystalline rocks. The thickness of the till varies from 1–20 m, and the cover is discontinuous on the surface, mainly bordering and covering areas of high topography emerging from the clay plain. Glacial features include glacial deposits and fluted landforms (e.g., eskers, kames, kettles, drumlins, moraines). In the Mauricie region, most of the data collected are related to the Saint-Narcisse Moraine. Its thickness can reach up to 100 m, although it generally varies between 1 and 20 m locally (Occhietti 1977, Légaré-Couture et al. 2018, Lévesque et al. 2021, 2023a). According to Occhietti (2007), a variety of sedimentary facies make up the stratigraphy of the moraine, including proximal and distal glaciomarine deposits, juxtaglacial and fluvioglacial deposits (i.e., ice-marginal outwash; Occhietti 1977; Occhietti 2007), as well as till wedges and melt-out till that were deposited during the last glaciation.

3.4 METHODOLOGY

3.4.1 FIELD DATA COLLECTION

This study collected TEM data over five regions, covering 111 TEM surveys acquired in 45 locations spread over the Province of Québec in Canada. Transient electromagnetic induction (TEM) is an active method for measuring electrical resistivity and it consists of a primary electromagnetic field (EMF) generated into a transmitter loop (Tx) of electrical wire deployed on the ground. As the primary field interacts with the subsurface geological materials, the decay of the EMF generates a secondary magnetic field containing information about underground electrical properties. Its amplitude is detected and measured by a receiving electrical loop (Rx) deployed on the surface. This loop (Rx) is connected to a receptor that measures the rate of decay of the electromagnetic current, which is then inversed in electrical resistivity (Nabighian 1988, Fitterman and Labson 2005). The process of inversion (with raw data) enables the determination of parameters for a geophysical model using measurements of the model's response. This involves the measurement of observable quantities to infer the physical properties of the subsurface for geological interpretation. The TEM method does not involve direct electrical contact with the ground through electrodes and thus is

effective in various environments (i.e., swamps, coastal areas, moraines, forests, and mountains Kalisperi et al., 2018; Parsekian et al., 2015). The TEM method can be used for depths ranging from a few meters to several hundred meters, where the depth of investigation is determined by the size of the loop, the strength of the initial current, and the response of the subsurface to the electric current. Results of this study were collected using an NT-32 transmitter and a 32II multifunction GDP-Receiver (MacInnes and Raymond 2001). The NT-32 unit consists of a portable battery and a transmitter-receiver (TX-RX) console that operate using a square-sized loop configuration of 20 m by 20 m transmitter loop (Tx) and a 5 m by 5 m receiver loop (Rx; in-loop configuration) for the measured induced voltage. The pulse current in the generating loop was set to 3A and the frequency of the filter was set to 32 Hz at 50 % duty cycle. The turn-off time is 1.5 μs with the damping resistor set to 250 Ωm. The NanoTEM equipment consists of a high-speed sampling card with a fixed gain stage of Å~10. Therefore, to optimize the results and make an effective receiver coil area (250 m^2), the receiver moment is multiplied by a factor of 10. Data are stacked in 8 blocks of 4,096 cycles each, giving 32,768 stacks. This results in a noise level of approximately 10 μV/A. Due to the combination of various TEM surveys collected among different areas, the device was always calibrated with the same standards (i.e., according to the manufacturer's standards) at the beginning of each station, so the "absolute" electrical resistivities from each site can be compared (Foged et al. 2013).

3.4.2 Study database

The database for this study consists of 111 TEM surveys, 10 stratigraphic cross-sections, 51 piezometric surveys, and 75 boreholes collected from five regions in the Province of Québec, Canada: Mauricie, AT, C, HCN and SLSJ. In the Mauricie region, 11 boreholes, 10 stratigraphic cross-sections, and 24 TEM stations were sampled (Table 6). The water table elevation is indicated for each borehole and stratigraphic cross-sections (Table 6). In cases where elevation data for the water table was not available for a specific location, we constructed the resistivity chart using only the resistivity values of impermeable sediments (i.e., clay), while disregarding the resistivity values of permeable sediments such as sand and sand-gravel. The data are mainly derived from the Saint-Narcisse Moraine area (Fig. 37A), located in the Mauricie region in the Province of Québec. These Quaternary deposits are mainly composed of juxtaglacial and fluvioglacial sand (i.e., ice-marginal

outwash) and sand and gravel (i.e., until wedges, subglacial or melt-out until ice-marginal outwash). In topographically low areas adjacent to the moraine, horizons of deep marine clay (i.e., distal glaciomarine) deposited by the Champlain Sea are usually covered by regressive sand (i.e., proximal glaciomarine).

TABLE 6: TEM stations with nearby boreholes and stratigraphic cross-sections, as well as their associated electrical resistivity values for the regions of Mauricie. Depths are identified by parentheses. The blue color in the electrical resistivity column represents the depths at which the water table was reached. The X in the water table column means that piezometric data are unavailable at this location. In such cases, only clay was used to create the chart, and the sediment classes written in red in the borehole column were not used.

TEM stations	Boreholes	Stratigraphic cross-sections	Electrical resistivity (Ohm.m)	Topographic elevation (m)	Water table (m)
L1_DN_ST8-9		**YL051** (0-14) fine to medium sand	(0-14) 100-450	ST8-9: 100 YL051: 96	17
L2_DN_ST11	**F1988 (PE-1)** (0-50) sand and silt with pebbles (50-55) medium sand		(0-30) 100-770 (> 30) no data	ST11: 73 F1988: 67	53
L3_DN_ST1	**F1999** (0-24) clay with gravel (24-39) gravel and clay (39-46) fine sand		(0-5) no data (5-24) 50-180 (24-39) 180-240 (39-46) 195-240	ST1: 60 F1999: 65	24
L2_ST3		**YL071** (0-3) sand and gravel (3-5) fine to medium sand (5-11) fine to medium sand with gravel	(0-3) 650-695 (3-5) 625-650 (5-11) 445-625	ST3: 137 YL071: 137	11
L3_ST1	**F1-PACES** (0-6) medium to coarse sand (6-12) fine to medium sand with clay (12-46) clay		(0-6) 320-405 (6-12) 110-320 (12-46) 15-110	ST1: 114 F1-PACES: 114	No water
L5_ST3		**YL033** (0-18) fine sand	(0-18) 260-355	ST3: 72 YL033: 70	No water
L6_ST5		**YL057** (0-3) sand and gravel	(0-3) 620	ST5: 120 YL057: 120	No water
L6_ST7		**YL019** (0-9) sand and gravel with boulders	(0-3) no data (3-9) 430-745	ST7: 120 YL019: 123	No water
L7_ST1		**COMP016-18** (0-11) sand and gravel with pebbles and boulders (11-16) medium to coarse sand (16-18) fine to medium sand	(0-11) 460-720 (11-16) 345-460 (16-18) 300-345	ST1: 139 COMP016-18: 139	18
L9_ST1		**YL076:** (0-11) sand and gravel	(0-11) 450-650	ST1: 175 YL076: 172	No water
L9_ST2-3		**YL079** (0-5) sand and gravel with pebbles (5-20) fine to coarse sand	(0-5) 875 (5-20) 300-730	ST2: 176 ST3: 181 YL079: 181	No water
L9_ST5		**YL074** (0-15) sand and gravel with pebbles (15-20) fine to medium sand	(0-15) 530-910 (15-20) 260-530	ST5: 180 YL074: 180	No water
L9_ST5	**ME1843** (0-13) fine to coarse sand and gravel (13-22) sand		(0-13) 540-910 (13-22) 215-540	ST5: 180 ME1843: 180	No water
L10_ST1-2	**MAUR0345** (0-19) sand and gravel		(0-14) 370-820 (14-19) 250-370	ST1: 140 ST2: 141 MAUR0345: 140	14

TEM stations	Boreholes	Stratigraphic cross-sections	Electrical resistivity (Ohm.m)	Topographic elevation (m)	Water table (m)
L10_ST5		**YL080** (0-12) fine to coarse sand	(0-12) 380-540	ST5: 146 YL080: 146	14
L12_ST4	**F2459** (0-25) fine to medium sand (25-63) clay		(0-3) no data (3-25) 100-690 (25-63) 20-100	ST4: 31 F2459: 34	X
L13_ST1	**ME0704** (0-8) sand and gravel (8-19) sand and gravel with clay (19-27) clay		(0-8) 150-230 (8-19) 60-150 (19-27) 40-60	ST1: 118 ME0704: 118	1
L13_ST3	**P12** (0-9) sand		(0-9) 110-150	ST3: 118 P12: 118	2
L17_ST1	**ME0954** (0-13) sand and gravel with clay (13-27) sand with clay		(0-2) no data (2-8) 320-415 (8-13) 200-320 (13-27) 60-200	ST1: 116 ME0954: 118	8
L18_ST3	**F2338** (0-22) fine sand and gravel with silt		(0-3) 550-660 (3-22) 330-550	ST3: 113 F2338: 110	3
L19_ST4	**F2339** (0-6) fine to coarse sand with gravel and silt (6-14) sand and gravel with silt (14-20) fine to coarse sand with silt and gravel (20-25) sand and gravel with silt		(0-6) 270-275 (6-14) 275-310 (14-20) 310-350 (20-25) 350-460	ST4: 110 F2339: 110	2

For the AT region, 6 boreholes (water level included) and 10 TEM stations were collected (Table 7). Quaternary deposits found in the AT are mainly composed of juxtaglacial sand and gravel with pebbles (i.e., lodgement till, subglacial or melt-out till) and fluvioglacial sand (i.e., ice-marginal outwash).

TABLE 7: TEM stations with nearby boreholes and stratigraphic cross-sections, as well as their associated electrical resistivity values for the regions of Abitibi-Temiscamingue (AT). Depths are identified by parentheses. The blue color in the electrical resistivity column represents the depths at which the water table was reached.

TEM stations	Boreholes (m)	Electrical resistivity (Ohm.m)	Topographic elevation (m)	Water table (m)
S1AL1_ST1 (S1AL1)	**abte7988** (0-15) sand and gravel (15-23) gravel and pebbles (23-33.5) sand and gravel with pebbles	 (0-15) 165-335 (15-23) 335-550 (23-33.5) 550-850	ST1: 342 abte7988: 343	13
S4AL1_ST7-ST8	**abte8002** (0-4.5) sand with clay (4.5-9) fine sand with silt and gravel (9-16.5) gravel with pebbles and coarse sand 16.5-30) medium to coarse sand and gravel with pebbles (30-37) sand with gravel (till ?)	 (0-4.5) 75-125 (4.5-9) 125-200 (9-16.5) 200-685 (16.5-30) 685-1500 (30-37) 660-1250	ST8: 373 ST7: 361 abte 8002: 373	37
S5AL1ST1	**abte7990** (0-11) medium to coarse sand with clay (11-44) coarse sand with gravel and pebbles (44-49) medium sand and gravel with pebbles (49-56) gravel with pebbles and coarse sand (56-65) medium sand with gravel and pebbles	 (0-11) 75-300 (11-44) 275-1400 (44-49) 660-815 (49-56) 300-1030 (56-65) 140-300	ST1: 345 abte7990: 362	44
S5BL1_ST2	**abte7991** (0-11) fine to medium sand (11-32) fine to medium sand with silt (32-37) fine to medium sand with clay, silt and gravel	 (0-8) 680-800 (8-11) 590-680 (11-32) 370-590 (32-37) 370-475	ST2: 328 abte7991: 327	8
S5DL1_ST1-ST4	**abte7998** (0-10.5) fine to medium sand with gravel (10.5-18) fine sand with silt (18-28.5) medium sand with gravel (28.5-39) fine to medium sand with gravel (39-54) sand with gravel and pebbles	 (0-10.5) 215-315 (10.5-18) 275-370 (18-28.5) 335-450 (28.5-39) 440-560 (39-54) 500-605	ST1: 336 ST2: 337 ST3: 337 ST4:337 abte7998: 337	21
S7CL1_ST4-ST5	**abte7989** (0-7.5) medium to coarse sand with gravel and pebbles (7.5-15) gravel with pebbles and sand (15-21) medium to coarse sand with gravel (21-35) gravel with pebbles (35-55) coarse sand and gravel (55-65) coarse sand and gravel (till)	 (0-7.5) 300-330 (7.5-15) 330-380 (15-21) 320-420 (21-35) 395-750 (35-55) 750-1020 (55-65) 1020-1120	ST4: 370 ST5: 375 abte7989: 375	36

C and HCN have 8 and 9 boreholes, respectively, as well as 12 and 9 TEM stations (Tables 8 and 9). For each of the boreholes acquired in these two regions, the water table level was indicated. Quaternary deposits in C, HCN are composed of deep-sea marine clays from the Goldthwait Sea (i.e., distal glaciomarine) overlying coastal and deltaic sandy deposits (i.e., proximal glaciomarine). Further inland, we found periglacial deposits of fluvial and lacustrine origin with sand and gravel/pebbles and boulders (i.e., subglacial or melt-out till), sand, and clay.

TABLE 8: TEM stations with nearby boreholes and stratigraphic cross-sections, as well as their associated electrical resistivity values for the regions of Charlevoix (C). Depths are identified by parentheses. The blue color in the electrical resistivity column represents the depths at which the water table was reached.

TEM stations	Boreholes	Electrical resistivity (Ohm.m)	Topographic elevation (m)	Water table (m)
KANN-TL1_ST4-5	**F1017** (0-15) fine to medium sand and silt and clay (15-40) silt with gravel and clay (40-50) sand and gravel (till)	 (0-15) 30-170 (15-40) 140-440 (40-50) 440-810	ST4: 113 ST5: 113 F1017: 106	15
KANN-TL2_ST1-2	**F1010** (0-15) fine to coarse sand with gravel (15-18) sand and gravel with silt and clay (till)	(0-4) no data (4-8) 350-395 (8-15) 160-350 (15-18) 130-160	ST1-2: 141 F1010: 145	8
KANN-TL3_ST1-2	**F1006** (0-20) fine to coarse sand with gravel and silt	 (0-12) 250-580 (12-20) 170-325	ST1: 146 ST2: 147 F1006: 146	12
KANN-TL3_ST4	**F1327** (**0**-6) medium to coarse sand with gravel (6-18) fine sand	 (**0**-6) 400-550 (6-13) 275-400 (13-24) 205-275	ST4: 139 F1327: 133	13
STSNTL1ST1-2	**F1501** (0-6) fine to coarse sand with gravel, pebbles and boulders (6-14) sand and gravel with silt, gravel, pebbles, boulders (14-43) fine to medium sand with silt (43-53) sand and gravel with pebbles (till)	 (0-3) no data (3-6) 580 (6-14) 350-580 (14-43) 165-405 (43-53) 405-945	ST1-2: 166 F1501: 169	14
STSNTL1ST2-3	**F0927** (0-21) sand and gravel with silt (21-31) fine sand with silt (31-38) sand and gravel with silt (38-55) sand and gravel and pebbles (till)	 (0-7) 600-725 (7-21) 275-600 (21-31) 240-275 (31-38) 275-360 (38-55) 360-1050	ST2-3: 164 F0927: 162	7

TABLE 9: TEM stations with nearby boreholes and stratigraphic cross-sections, as well as their associated electrical resistivity values for the regions of Côte-Nord (CHCN). Depths are identified by parentheses. The blue color in the electrical resistivity column represents the depths at which the water table was reached.

TEM stations	Boreholes	Electrical resistivity (Ohm.m)	Topographic elevation (m)	Water table (m)
COLNTL1_ST1	**F0877**	(0-15) 460-790	ST1: 52	15
	(0-18) sand	(15-18) 340-460	F0877: 52	
	(18-31) fine sand and silt	(18-31) 145-340		
COLNTL1_ST2	**F1106**		ST2: 39	No water
	(0-43) clay and silt	(0-43) 55-180	F1106: 41	
	(43-124) clay	(43-124) 15-55		
COLNTL1_ST3	**SF005**		ST3: 45	No water
	(0-2) fine sand and pebbles	(0-2) 175	SF005: 45	
	(2-22) clay and pebbles	(2-22) 70-175		
	(22-34) clay	(22-34) 60-80		
FORNTL1_ST2	**SF008**	(0-6) 520-615	ST2: 96	6
	(0-13) sand with pebbles	(6-13) 330-520	SF008: 96	
	(13-21) sand and silt	(13-21) 120-330		
	(21-30) clay with sand	(21-30) 70-120		
FORNTL2_ST1	**SF007**	(0-4) 770-905	ST1: 92	4
	(0-8) sand and pebbles	(4-8) 580-770	SF007: 90	
	(8-13) fine sand	(8-130 200-580		
	(13-20) silty clay with sand	(13-20) 130-200		
PORLO_ST12	**SF009**		ST12: 83	No water
	(0-21) medium sand with gravel	(0-21) 295-635	SF009: 83	
	(21-28) fine sand with silt	(21-28) 225-295		
PORLOST3	**SF0010**		ST3: 58	No water
	(0-7) sand with gravel	(0-7) 450-540	SF0010: 58	
	(7-15) sand and silt	(7-15) 300-450		
	(15-25) silt with clay	(15-25) 155-300		
	(25-29) clay and silt	(25-29) 155		
BERNTL1ST1	**SF001**		ST1: 40	No water
	(0-5) sand	(0-5) 390-550	SF001: 35	
	(5-13) fine sand with silt	(5-13) 150-390		
	(13-28) clay and silt	(13-28) 30-150		
BERNTL1_ST2	**SF002**	(0-8) 610-1050	ST2: 88	9
	(0-8) sand	(8-29) 215-610	SF002: 84	
	(8-29) fine sand with silt			
SACNTL1_ST1-2	**SF0013**		ST1: 113	No water
	(0-2) sand with silt	(0-2) 205	ST2: 113	
	(2-20) clay and silt and sand	(2-20) 20-205	SF0013: 113	
	(20-29) clay	(20-29) 20-30		
SACNTL1_ST4	**SF0012**		ST4: 115	No water
	(0-2) sand with silt	(0-2) 180-220	SF0012: 113	
	(2-16) clay with silt and sand	(2-16) 20-180		
	(16-27) clay and silt	(16-27) 20-35		

Finally, Quaternary deposits of Saguenay-Lac-Saint-Jean are observed in 41 boreholes and 58 TEM stations (Table 10). The water level is indicated for several boreholes, but when no data were collected on groundwater, only clay and mixed sediment into the clay horizons were used to create the chart. These deposits are composed of deep-sea marine clays from the Laflamme Sea covered by coastal sandy deposits.

TABLE 10: TEM stations with nearby boreholes and stratigraphic cross-sections, as well as their associated electrical resistivity values for the regions of Saguenay-Lac-Saint-Jean (SLSJ). Depths are identified by parentheses. The blue color in the electrical resistivity column represents the depths at which the water table was reached.

TEM stations	Boreholes	Electrical resistivity (Ohm.m)	Topographic elevation (m)	Water table (m)
NTS03L2W_ST 1	**SF0081** (0-7) sand (7-11) sand and gravel (11-38) sand (38-50) silt and clay (50-63) clay	(0-7) 900-940 (3-7) 750-900 (7-11) 650-750 (11-38) 65-650 (38-50) 15-65 (50-63) 4-15	ST1: 173 SF081: 175	8
NTS03L1_ST1	**SF0081** (0-7) sand (7-11) sand and gravel (11-38) sand (38-50) silt and clay (50-63) clay	(0-3) 455 (3-7) 430--455 (7-11) 375-430 (11-38) 110-375 (38-50) 70-110 (50-63) 60-70	ST1: 175 SF081: 175	4
NTS04L1N_ST6	**CPT-S4-2** (0-8) sand and silt (magnetite) (8-40) silt and sand	(0-3) no data (3-8) 150-445 (8-40) 35-150	ST6: 105 CPT-S4-2: 107	1
NTS04L1N_ST7	**CPT-S4-2** (0-8) sand and silt (magnetite) (8-40) silt and sand	(0-3) no data (3-8) 150-445 (8-40) 35-150	ST7: 107 CPT-S4-2: 107	1
NTS6L1_ST1	**RPSS-S6-1** (0-22) clay with pebbles	(0-22) 25-125	ST1: 138 RPSS-S6-1: 138	X
NTS16L1E_ST1	**SF0079** (0-29) fine sand and silt (29-55) clay and silt	(0-29) 20-230 (29-55) 35-200	ST1: 171 SF0079: 163	4
NTS18L1_ST9	**SF0055** (0-9) fine to coarse sand with gravel (9-18) fine sand and silt (18-24) sand and gravel (till)	(0-9) 500-900 (9-13) 435-500 (13-18) 200-435 (18-24) 140-300	ST9: 185 SF0055: 185	13
NTS18L1_ST10	**SF0055** (0-9) fine to coarse sand with gravel (9-18) fine sand and silt (18-24) sand and gravel (till)	(0-9) 500-900 (9-13) 435-500 (13-18) 200-435 (18-24) 140-300	ST10: 185 SF0055: 185	13
NTS35L2_ST1	**PZ-35D** (0-20) sand and gravel (20-25) sand with silt (25-31) clay and silt (31-55) clay	(0-4) 800-1430 (4-20) 260-800 (20-25) 150-400 (25-31) 1-150 (31-55)	ST1:110 PZ-35D: 110	4
NTS35L2_ST2	**PZ-35D** (0-20) sand and gravel (20-25) sand with silt (25-31) clay and silt (31-55) clay	(0-4) 800-1430 (4-20) 260-800 (20-25) 150-400 (25-31) 1-150 (31-55)	ST2:110 PZ-35D: 110	4
NTS104L1_ST1	**SF0058 (ou PZ-S104R)** (0-8) fine to medium sand (8-42) fine sand and silt (42-58) sand and gravel (till)	(0-4) 745 (4-8) 565-745 (8-42) 90-190 (42-58) 190-350	ST1:123 SF0058:121	4
NTS104L1_ST2	**SF0059** (0-8) fine to medium sand with gravel (8-18) fine to medium sand (18-25) silt and fine sand (25-35) clay with silt (35-46) clay	(0-4) 755 (4-8) 555-755 (8-18) 170-555 (18-25) 45-170 (25-35) (35-46) 30-45	ST2:123 SF0059:123	4
L1_SJV_ST1	**F0544** (0-23) clay (23-39) clay with sand and pebbles (39-48) sand and gravel with clay	(0-13) 25-110 (13-23) 25-110 (23-39) 110-265 (39-48) 265-270	ST1: 26 F0544:20	39
L1_SJV_ST2	**F0544** (0-23) clay (23-39) clay with sand and pebbles (39-48) sand and gravel with clay	(0-13) 25-110 (13-23) 25-110 (23-39) 110-265 (39-48) 265-270	ST2: 27 F0544:20	39
L2_SJV_ST2	**GUHS1096** (0-30) clay with gravel (30-35) sand	(0-4) 30-110 (4-30) 30-110 (30-33) 110-160	ST2:16 GUHS1096: 11	30
L3_SJV_ST2	**GUHS1095**	(0-5) no data	ST2: 7	X

TEM stations	Boreholes	Electrical resistivity (Ohm.m)	Topographic elevation (m)	Water table (m)
L3_SJV_ST2	**GUHS1095** (0-24) clay with gravel	(0-5) no data (5-24) 20-65	ST2: 7 GUHS1095: 11	X
L4_SJV_ST1	**GUHS1095** (0-24) clay with gravel (24-28) sand with gravel and clay (till)	(0-5) no data (5-24) 30-105 (24-28) 100-105	ST1: 7 GUHS1095: 11	24
L6_SJV_ST1	**MTQ0296** (0-39) clay with sand and gravel (39-45) fine sand with gravel and clay (till)	 (0-39) 45-180 (39-45) 180-245	ST1: 100 MTQ0296: 99	no water
L6_SJV_ST2	**MTQ0296** (0-39) clay with sand and gravel (39-45) fine sand with gravel and clay (till)	 (0-39) 45-180 (39-45) 180-245	ST2: 100 MTQ0296: 99	no water
L6_SJV_ST3	**MTQ0296** (0-39) clay with sand and gravel (39-45) fine sand with gravel and clay (till)	 (0-39) 45-180 (39-45) 180-245	ST3: 100 MTQ0296: 99	no water
L7_SJV_ST1	**MTQ0111** (0-35) clay with sand (35-43) fine sand	 (0-28) 40-130 (28-35) 40-130 (35-43) 130-185	ST1: 74 MTQ0111: 74	35
L7_SJV_ST2	**MTQ0110** (0-22) clay	 (0-22) 45-105	ST2: 90 GUHS0959: 83	X
L7_SJV_ST3	**F1144** (0-39) clay with sand and gravel (39-44) sand and clay	 (0-39) 35-180 (39-44) 140-165	ST3: 101 F1144: 100	no water
L7_SJV_ST4	**F1144** (0-39) clay with sand and gravel (39-44) sand and clay	 (0-39) 35-180 (39-44) 140-165	ST4: 101 F1144: 100	no water
L7_SJV_ST5	**F1144** (0-39) clay with sand and gravel (39-44) sand and clay	 (0-39) 35-180 (39-44) 140-165	ST5: 99 F1144: 100	no water
L8_SJV_ST1	**GUHS0963** (0-6) clay	 (0-6) 30-35	ST1: 84 GUHS0963: 82	X
L8_SJV_ST2	**MTQ0296** (0-39) clay with sand and gravel (39-45) fine sand with gravel and clay	(0-4) no data (4-39) 35-205 (39-45) 120-155	ST2: 95 MTQ0296: 99	no water
L10_SJV_ST2	**F1144** (0-39) clay with sand and gravel (39-44) sand and clay	 (0-39) 30-50 (39-44) 45-60	ST2: 97 F1144: 100	no water
L10_SJV_ST3	**F1144** (0-39) clay with sand and gravel (39-44) sand and clay	 (0-39) 30-50 (39-44) 45-60	ST3: 96 F1144: 100	no water
L11_SJV_ST1	**MTQ0303** (0-28) clay with sand	 (0-28) 25-150	ST1: 79 MTQ0303: 79	X
L11_SJV_ST2	**MTQ0303** (0-28) clay with sand	 (0-28) 25-150	ST2: 78 MTQ0303: 79	X
L11_SJV_ST5	**MTQ0302** (0-46) clay with sand (46-61) clay	 (0-46) 15-60 (46-61) 5-15	ST5: 69 MTQ0302: 68	X
L11_SJV_ST6	**MTQ0302** (0-46) clay with sand (46-61) clay	 (0-46) 15-60 (46-61) 5-15	ST6: 66 MTQ0302: 68	X
L11_SJV_ST7	**MTQ0301** (0-61) clay	 (0-61) 1-30	ST7: 62 MTQ0301: 60	X
L11_SJV_ST8	**MTQ0301** (0-61) clay	 (0-61) 1-30	ST8: 58 MTQ0301: 60	X
L12_SJV_ST1	**MTQ0364** (0-61) clay	(0-11) no data (11-61) 1-20	ST1: 57 MTQ0364: 68	X
L12_SJV_ST2	**MTQ0365** (0-55) clay	 (0-55) 1-20	ST2: 59 MTQ0365: 51	X
L12_SJV_ST3	**MTQ0365** (0-55) clay	 (0-55) 1-20	ST3: 57 MTQ0365: 51	X
L12_SJV_ST4	**GUHS1087** (0-55) clay	 (0-55) 1-40	ST4: 53 GUHS1087: 51	X

TEM stations	Boreholes	Electrical resistivity (Ohm.m)	Topographic elevation (m)	Water table (m)
L13_SJV_ST1	**GUHS0947** (0-35) clay with sand (35-42) sand with clay	 (0-35) 40-80 (35-42) 80-125	ST1: 102 GUHS0947: 97	no water
L13_SJV_ST2	**GUHS0959** (0-27) clay	 (0-27) 1-2	ST2: 81 GUHS0959: 82	X
L13_SJV_ST3	**GUHS0951** (0-35) clay	(0-2) no data (2-35) 5-40	ST3: 79 GUHS0951: 81	X
L14_SJV_ST1	**MTQ0302** (0-36): clay with sand (36-41) sand and gravel with clay (till)	 (0-36) 15-165 (36-41) 165-300	ST1: 51 MTQ0300: 51	36
L14_SJV_ST2	**GUHS0135** (0-21) clay (21-44) clay with sand and gravel	(0-6) no data (6-21) 15-30 (21-44) 30-140	ST2: 50 GUHS0135: 50	X
L15_SJV_ST1	**GUHS0981** (0-41) clay	 (0-41) 2-35	ST1: 80 GUHS0981: 81	X
L15_SJV_ST2	**GUHS0981** (0-41) clay	 (0-41) 2-35	ST2: 80 GUHS0981: 81	X
L15_SJV_ST4	**MTQ0111** (0-390) clay	 (0-39) 10-45	ST4: 78 MTQ0111: 74	X
L15_SJV_ST5	**MTQ0111** (0-390) clay	 (0-39) 10-45	ST5: 77 MTQ0111: 74	X
L15_SJV_ST6	**MTQ0111** (0-390) clay	 (0-39) 10-45	ST6: 75 MTQ0111: 74	X
L15_SJV_ST7	**MTQ0293** (0-52) clay and sand	 (0-52) 25-100	ST7: 72 MTQ0293: 70	X
L16_SJV_ST1	**GUHS0134** (0-42) clay with sand and gravel	 (0-42) 20-70	ST1: 79 GUHS0134: 79	X
L16_SJV_ST2	**GUHS0982** (0-11) clay with sand (11-52) clay	 (0-11) 40-55 (11-52) 5-25	ST2: 75 GUHS0982: 73	X
L16_SJV_ST3	**GUHS0128** (0-15) clay with sand (15-20) clay	 (0-15) 45-70 (15-20) 20-45	ST3: 73 GUHS0128: 70	X
L16_SJV_ST4	**GUHS0128** (0-15) clay with sand (15-20) clay	 (0-15) 45-70 (15-20) 20-45	ST4: 73 GUHS0128: 70	X
L16_SJV_ST5	**GUHS0128** (0-15) clay with sand (15-20) clay	 (0-15) 45-70 (15-20) 20-45	ST5: 73 GUHS0128: 70	X
L16_SJV_ST6	**GUHS0131** (0-39) clay	 (0-39) 15-40	ST6: 57 GUHS0131: 52	X
L17_SJV_ST2	**MTQ0144** (0-41) clay	(0-1) no data (1-41) 10-30	ST2: 80 MTQ0144: 81	X
L17_SJV_ST3	**GUHS0134** (0-39) clay with sand and gravel	 (0-42) 20-150	ST3: 80 GUHS0134: 79	X

3.4.3 TEM DATA INVERSION

The process of inversion (with raw data) enables the determination of parameters for a geophysical model using measurements of the model's response. Once the data are acquired, the goal is to solve for the subsurface resistivity distribution between the stations through data inversion. The amplitude of the secondary magnetic field is inverted in terms of electrical resistivity, usually as a function of depth. Three processing steps were performed to convert TEM signals into an electrical resistivity model of the ground (Lévesque et al. 2021, 2023c, Richer et al. 2023): 1) Raw data are first

averaged using TEMAVG Zonge software (MacInnes 2001, MacInnes and Raymond 2001). TEMAVG is also used to filter out inconsistent data points and remove them before the inversion. Considering the magnetic field intensity decrease with depth, the amplitude of the field decreases over time, with time as a function of depth. This step represented the results by variation of the apparent resistivity. When the noise level (distortion) increases and the decay rate of the signal becomes discontinuous, the variations of the induced voltage (i.e., dB/dt) significantly increase, and the results obtained are no longer reliable. It is, therefore, necessary to remove these results when processing data with TEMAVG; 2) The 1D inversion model of the transient EM sounding curves is performed using the STEMINV software (MacInnes and Raymond 2001). After importing the data file containing a measured sounding curve from TEMAVG, the software generates a consistent 1D smooth inversion model of electrical resistivity vs. depth based on the iterative Occam inversion scheme (Constable and Parker 1987). Calculations of maximum depth are given in the Zonge manual (MacInnes 2001). Two types of unidimensional (1D) inversion models are most commonly used, namely “by stage” models, which consider the subsoil as a succession of homogeneous layers, as well as “smooth” models, which evaluate a value of electrical resistivity per acquisition time window. An overview of the acquired data, including the measured raw data (shown as crosses), the residual number, the inversion best fit (shown as a black line), and the corresponding resistivity model, is presented in figures 15, 19, 21, 23, 25, 31 and 32. To accommodate the complexity of the stratigraphy, we choose to use a smooth model to identify, with relative ease, possible subtle variations in the electrical resistivity results.

Conversely, smoothing the inverted TEM data may sometimes produce a more gradual change in resistivity than the reality, and can mask abrupt changes in resistivity. Therefore, the thickness of some facies can be shown as greater or smaller than their true thickness (Knight et al. 2018). To solve this problem and to mitigate the influence of non-representative data and minimize their impact on the accuracy of the correlation between TEM results and stratigraphic logs from boreholes, we employed a standardization method in the form of a statistical analysis. Although the instrument can perform accurate measurements, several uncertainties are associated with the data; when uncertain and incomplete data are inverted, a suite of models can fit the data and produce very similar model

responses (Christiansen et al. 2006). The obtained results (i.e., the solution) are also non-unique and depend on the constraints applied in the inversion process. Therefore, the resulting electrical resistivity is associated with a relative uncertainty. In this case, we made the reasonable assumption that by using a statistical method (i.e., the numerical threshold of 5%) to filter away the problematic data, we greatly diminish this relative uncertainty. In addition, the collocated boreholes and TEM data allow us to know the transition layers between facies and thus determine the potential (and sometimes abrupt) resistivity transition with relative precision. After inversion, when the resistivity values and the sedimentary facies do not match, it is often because there are thin layers of sediment in the borehole. In such a case, the borehole and the TEM station are removed from the database. Thus, we kept only the boreholes that have layers thick enough to be significant (>2 meters) to reduce the uncertainty of the results and increase the confidence interval.

In order to establish the relationship between resistivity and lithology (using collocated boreholes and TEM data) and to simplify the correlation, after inversion, a linear interpolation of the TEM results with MATLAB software was performed to obtain results at every meter for each 1D TEM surveys.

3.4.4 RESISTIVITY CHART

3.4.4.1 SITE SELECTION

The database for this study consists of the results of surface geophysical investigations and stratigraphic and hydrogeological data from boreholes. After filtering the data, a total of 111 TEM stations, 75 boreholes, 10 stratigraphic cross-sections and 51 piezometric surveys were compiled from five regions in the Province of Québec in Canada: Mauricie, AT, C, HCN and SLSJ. Boreholes and stratigraphic cross-sections were first compared with the electrical resistivity values of nearby TEM stations (Figs. 37 and 38). The selected boreholes are primarily located within 200 m of the corresponding TEM station (Figs. 37 and 38), and the stratigraphic layers from both hard data (i.e., boreholes) and soft data (i.e., geophysics) were matched. Commonly, according to the depth, each station can be tied to a corresponding change in facies observed in cores and stratigraphic cross-

sections. Therefore, electrical resistivity can be directly associated with each class of sediment derived from boreholes and stratigraphic cross-sections (Tables 6 to 10). Stratigraphic cross-sections were taken mainly in sand pits, and their associated TEM stations were taken near the same position but at a higher elevation. TEM surveys were carried out at the top of several exploited faces in gravel quarries (i.e., sand/gravel pits), which allowed a direct correspondence between the apparent stratigraphy and geophysical response. For each of the selected boreholes, the water levels (i.e., piezometric surveys) are available (Tables 6 to 10). Therefore, recognizing the water level allows us to associate resistivity with saturated or unsaturated sediment using static groundwater levels. Above the groundwater table, resistivity is high and associated with unsaturated sediments. Saturated sediments occur below the water table, and the resistivity associated with these facies is much lower (Tables 6 to 10). To correlate the measured resistivity with each class of sediment, the elevation of the boreholes, stratigraphic cross-sections, and TEM stations had to be determined with precision (Tables 6 to 10). Without reliable elevations, biases would be inserted, and the resistivity values would no longer represent the sediment class according to depth. We used lidar (i.e., 1 m) to accurately determine the elevation (i.e., laser imaging detection and ranging) data. Then, a digital elevation model (DEM) was realized using ArcGIS software, and precise elevations were acquired for each TEM station, borehole, and stratigraphic cross-section (Tables 6 to 10). Without precise elevations, the geophysical responses can be shifted according to the depth of the boreholes (or vice versa). To obtain consistent results, we used the lidar data and inserted a topographic elevation column in Table 6 to 10. Previous studies in the Mauricie and Charlevoix regions have already proposed similar methodologies to correlate stratigraphic and piezometric information with the TEM result to derive an empirical and local petrophysical relationship and establish a resistivity chart (Simard et al. 2015, Lévesque et al. 2021).

3.4.4.2 STATISTICAL PROBABILITY AND STANDARDIZATION

This study was based on five classes of saturated sediments in order to create a resistivity chart (Tables 11 and 12): 1) saturated sand; 2) saturated silty sand (i.e., sand with some silt); 3) saturated clayey sand (i.e., sand with some clay); 4) saturated sand and gravel with pebbles, and 5) saturated clayey sand and gravel. Five classes of saturated sediments have also been used to

create the final resistivity chart (Tables 11 and 12): 1) unsaturated sand; 2) unsaturated silty sand; 3) unsaturated clayey sand; 4) unsaturated sand and gravel with pebbles, and 5) unsaturated clayey sand and gravel. Clay, silty clay (i.e., clay with some silt), clay with sand, gravel/pebbles, and clayey silt with sand were considered impermeable sediments that are neither saturated nor unsaturated. Due to their fine grain size, these sedimentary classes are considered impermeable. However, their total porosity and capillary effect are high, making them similar to saturated sediments because they necessarily contain a significant amount of capillary water (i.e., water bound by cohesion) held in their micropores and maintained against the force of gravity. The lithological classification was selected based on the sediment core classifications obtained from the boreholes. Table 11 provides the ranges of resistivity values obtained solely in this study. It does not include values from other studies.

TABLE 11: Electrical resistivity properties for common saturated, unsaturated, and impermeable sediments in northeastern Canada obtained in this study.

Sediment characteristics		Class name	Electrical resistivity (ohm.m)
Impermeable		Clay	1-65
		Silty clay	20-165
		Clay with sand/gravel/pebbles	20-175
		Clayey silt with sand	25-290
Permeable	Unsaturated	Sand	230-790
		Silty sand	140-535
		Clayey sand	35-260
		Sand and gravel with pebbles	305-1430
		Clayey sand and gravel	135-400
	Saturated	Sand	120-565
		Silty sand	95-440
		Clayey sand	45-195
		Sand and gravel with pebbles	180-915
		Clayey sand and gravel	100-285

For each sediment class, extreme electrical resistivity values sometimes crept into the results after the inversion (Table 5, Fig. 39). These outliers generally represent minor and/or significant facies changes and must be considered in the data compilation, even if they are less frequently reproduced (Table 5, Fig. 39). In fact, infrequent extreme values (outliers) will have an exaggerated influence on the result and the main objective of standardization is to mitigate the influence of these outliers to prevent them from distorting the accuracy of the results. Figure 39 shows the extensive range in value distribution for each sediment class, as well as the presence of extreme data (i.e., extreme minimum and maximum). However, for each of the sediment classes analyzed in this study, the large amount of resistivity is roughly similar and is mainly concentrated around the same range of values (Fig. 39). For example, Table 5 and Fig. 39 show that for all boreholes (or stratigraphic cross-sections) acquired, the maximum resistivity value associated with unsaturated sand is 1,059 Ωm and recurs 1 time. In comparison, resistivity values ranging between 200-450 Ωm and 500-550 Ωm occurred 40 and 46 times, respectively, for unsaturated sand. Consequently, values of > 1,000 Ωm should be included in the data compilation, but by standardizing these values, a less significant influence will be granted to these extreme values than those ranging between 400-450 Ωm and 500-550 Ωm. These high data will end up being outliers of the dataset and will be removed to calculate the range of the final resistivity chart.

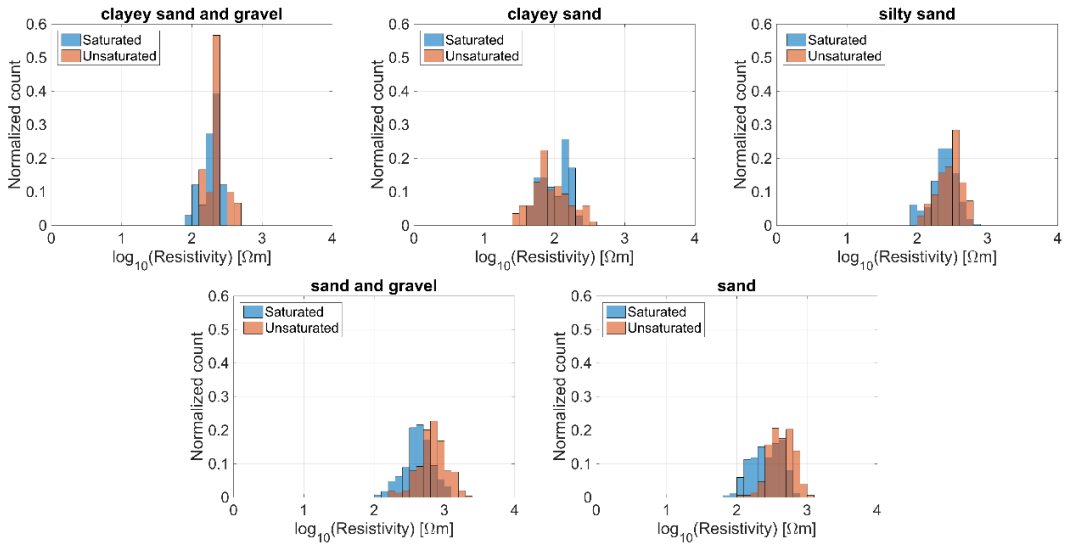

Figure 39: Histogram's plot represents the comparisons of distributions of estimated resistivity values for each saturated sediments and unsaturated sediments class. Tables 6 to 10 display the summary resistivity-lithology relation pertaining to the histograms.

Figure 39 shows five histograms of lithologically attributed resistivity distributions with data distributions that have a general tendency for a log-normal distribution. Here a logarithmic (base 10) transform is applied to all the data sets, and the data has been normalized to be more easily comparable with other sedimentary classes. The normalization performed to build the histograms is the number of values in the sediment classes divided by the total amount of data. Their distributions appear to be mostly unimodal and close to log-normal. Highly peaked and skewed multimodal behavior are observed in some cases (i.e., clayey sand and clayey sand and gravel).

The numerical threshold of 5% is a statistical method frequently used to help scientists in various fields (e.g., mathematics, health care, psychology, geology, applied science) decide whether to reject the less significant results (Davis and Sampson 1986, Aho 2013, Mendenhall and Sincich 2016). It is often used in statistics to give a greater significance to values that occur more frequently. The significance level for a study is chosen before data collection and is typically set to 5% (Craparo 2007, McKillup 2011). The numerical threshold of 5% is a method of standardization and statistical significance often expressed in multiples of the standard deviation or sigma (σ) of a normal distribution

to allow data with different scales of values to be compared with each other. The standard deviation is a statistical analysis method that measures the spread of data around the mean to give a better idea of the dispersion of the data. Sometimes, like the results of this study, data spread widely from the mean. Thus, the mean and standard deviation of the observed data are used to identified the outliers and then judge the frequency or rarity of a resistivity value. By pointing to the resistivity values that repeat less frequently for each class of sediment, it is easier to produce a chart with less extensive ranges of values and, consequently, to be more accurate and significant. In this study, four classes of sediments were abandoned because they lacked data: saturated and unsaturated gravel with pebbles, saturated and unsaturated silt with sand and gravel. These sediment classes were excluded mainly because only a few data could be collected in the boreholes for each class, and their distribution was thus random. The goal of the statistical analysis was to optimize the range of resistivity by filtering outliers for each class of sediment to obtain the best statistical distribution to interpret the results better and propose a more accurate chart. This normalization of the results allows us to assign greater importance to the resistivity values reiterated more frequently and easily target which resistivity ranges are more or less representative for each sediment class. Consequently, the scarcity of certain performances can allow them to be considered unrepresentative, and these outliers were removed from the compilation to establish our resistivity chart.

Several factors influenced the choice of a numerical threshold of 5%, which generally defines the passage from normality to abnormality (Aguert and Capel, 2018). However, in this study, the main determining factor was the measurement objective, which was to generate a chart of representative resistivities for each sediment class. Beyond and below the threshold of 5%, only few resistivity values were removed and filtered from the whole dataset to create the chart. The chart was therefore created by considering all the other categories for each sediment class. For example, the data ranging between 230 and 790 Ωm for unsaturated sand were retained, and the data that were less statistically significant in the range of 230 Ωm to 790 Ωm were removed (Tables 5 and 11).

3.5 RESULTS

3.5.1 TEM STATIONS, BOREHOLES, STRATIGRAPHIC CROSS-SECTIONS AND PIEZOMETRIC SURVEYS

Histograms for all resistivity values of saturated and unsaturated sediments are presented in Figures 39 and 40. Figure 41 presents the resistivity distribution of impermeable sediments. In both saturated and unsaturated sediments, lithological categories are defined based on the grain size, and higher resistivity is associated with coarser sediments. The quantitative values for each grain size were not available in the database. In contrast, fine-grained sediments, such as clayey sand and sand-gravel, exhibit significantly lower resistivities (Fig. 40). To visualize the relationship between resistivity and lithology (using collocated boreholes and TEM data), figures 42, 43, and 44 provide examples of TEM soundings, the resulting electrical resistivity model, and the associated lithological log. As demonstrated in tables 6 to 10 and figures 42, 43, and 44, the TEM data from 1D models show good agreement with sedimentary facies from boreholes.

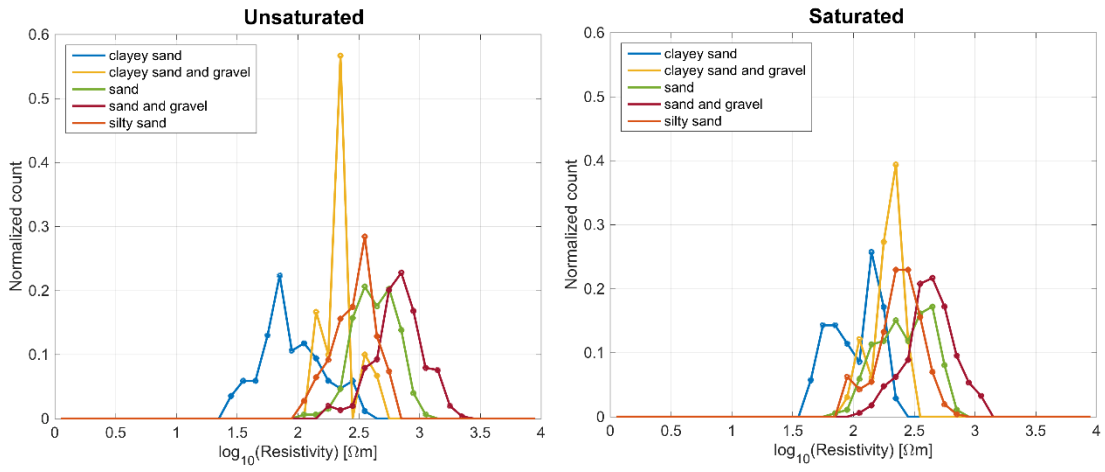

Figure 40: Comparisons of histograms (bin counts) displaying the distribution of estimated resistivity values for both saturated and unsaturated sediment classes.

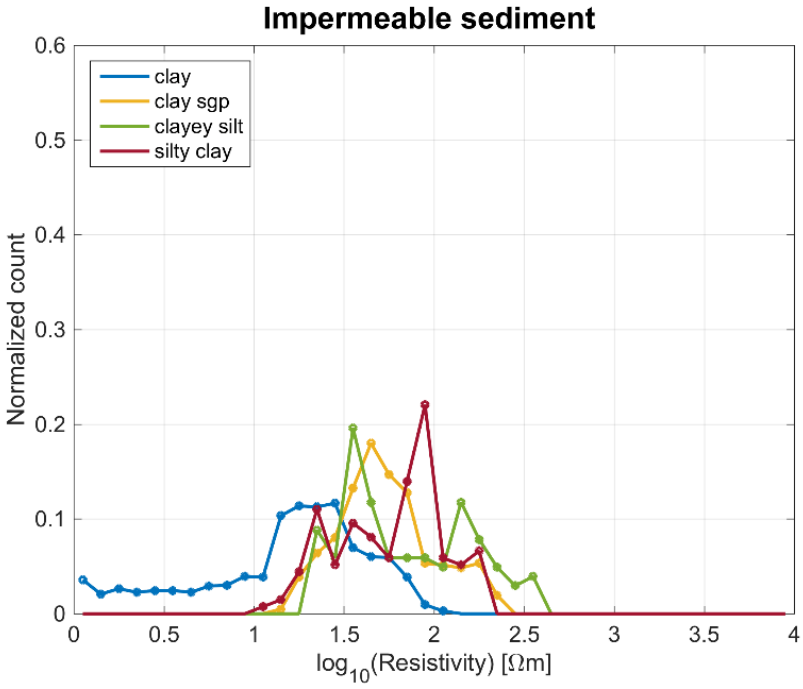

Figure 41: Histogram's plot (bin counts) represents the comparisons of distributions of estimated resistivity values for each impermeable sediments class. Tables 6 to 10 display the summary resistivity-lithology relation pertaining to the histograms.

Table 5 shows that the amount of data collected for each sediment class (Ncount) differs significantly. Consequently, it is essential to mention that when more data are obtained for a class of sediments, the confidence interval is more significant and reliable.

Based on a numerical threshold of 5% and the resulting resistivity range, this chart presents resistivity ranges for fourteen common sediment classes. Table 11 displays the categories assigned to each sediment class to generate the electrical resistivity chart.

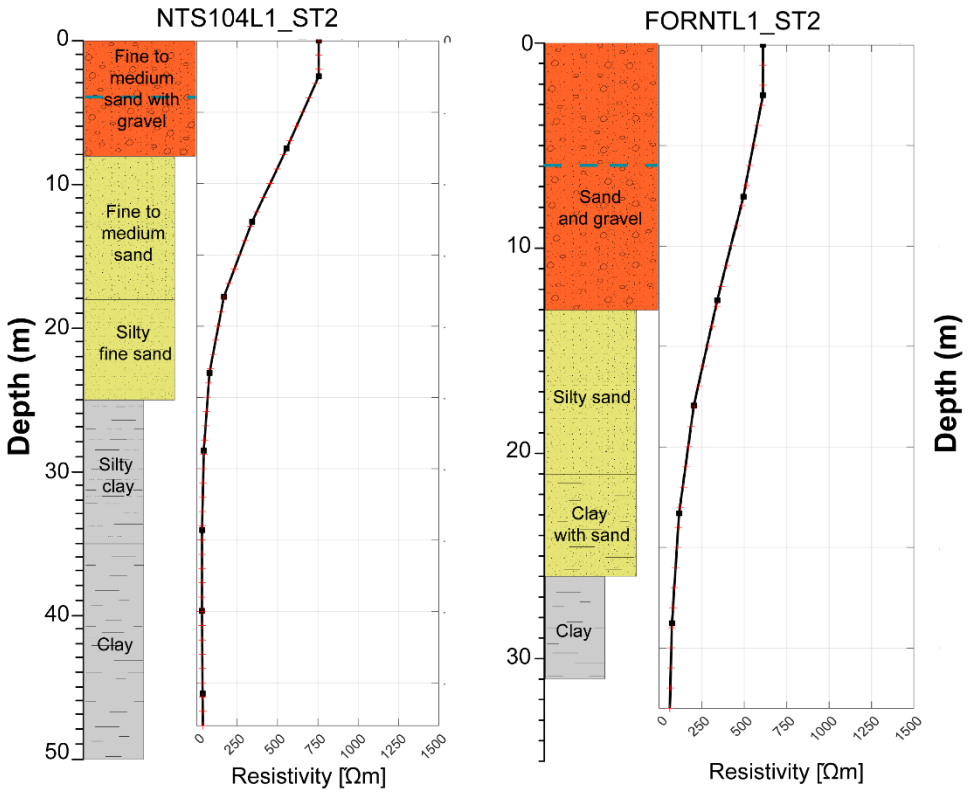

Figure 42: Sediment cores SF0059 **(left)** and SF008 **(right)** were sampled respectively in the Haute-Côte-Nord and Saguenay-Lac-Saint-Jean region and their associated smooth-model TEM inversion from NTS104L1, station 2, and FORNTL1, station 2. The blue dashed line is the water level (related to table 6 to 10). The black dots represent the observed data, and the red lines the interpolated data.

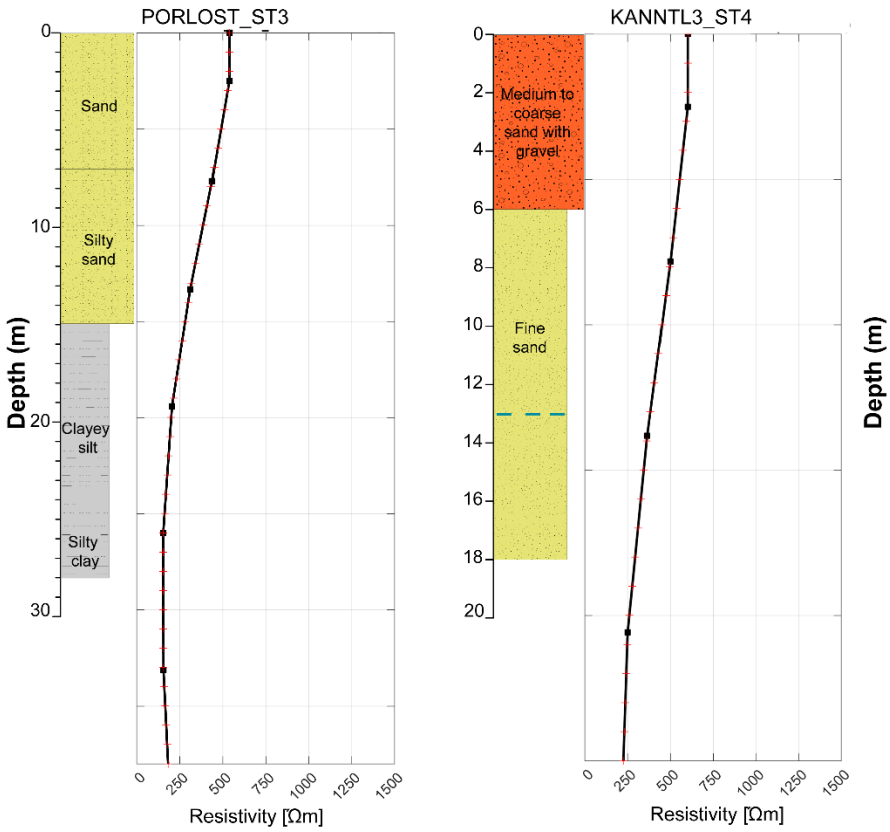

Figure 43: Sediment cores SF0010 **(left)** and F1327 **(right)** were sampled respectively in the Haute-Côte-Nord and Charlevoix region and their associated smooth-model TEM inversion from PORLOST, station 3 and KANNTL3, station 4. The blue dashed line is the water level (related to tables 6 to 10). The black dots represent the observed data, and the red lines the interpolated data.

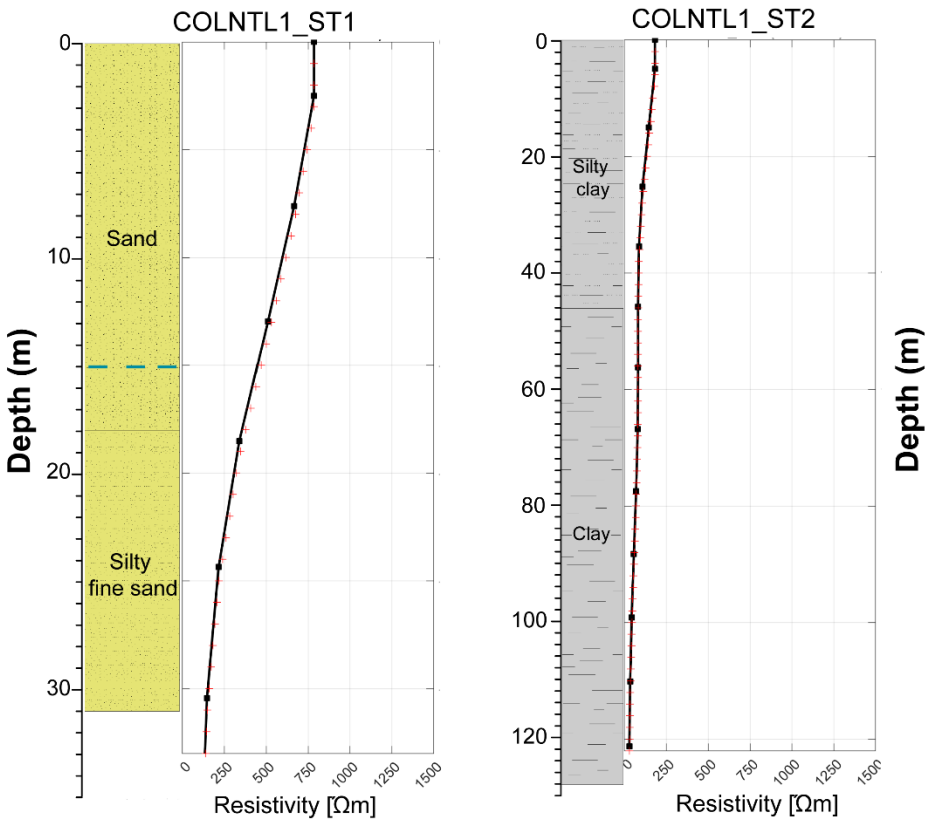

Figure 44: Sediment cores F0877 **(left)** and F1106 **(right)** were sampled in the Haute- ôte-Nord region and his associated smooth-model TEM inversion from COLNTL1, station 1 and COLNTL1, station 2. The blue dashed line is the water level (related to tables 6 to 10).

3.6 DISCUSSION

3.6.1 CAUSE OF VARIATIONS IN ELECTRICAL RESISTIVITY

3.6.1.1 Water content and pore water resistivity

Electrical resistivity is the physical property of geomaterials that has the greatest effect on the TEM measurement (Palacky 1987, 1993). Knight and Endres (2005) have briefly summarized the literature studying the resistivity lithology relationship (Knight and Endres 2005). According to their study and the publication of Reynolds (2011), we expect that the dominant factors linking resistivity and lithology in our study areas are based on two main parameters that cause the electrical resistivity to vary: 1) the water content and the pore water resistivity, 2) the grain size and the clay content (Archie 1942, Reynolds 1987a, 2011, Shukla and Yin 2006, Pandey et al. 2015). Previous studies

have shown that the electrical resistivity method is mainly based on the resistivity of water, which is much lower than the resistivity of soils (Shukla and Yin 2006, Pandey et al. 2015), and at high water contents, the resistivity rapidly decreases (Shukla and Yin 2006, Pandey et al. 2015). In sediments with water in the pore space, the circulation of electric current in the subsurface occurs mainly by volume conduction (or electrolysis) through the water contents of these formations. The primary mechanism for electrical conduction is ionic conduction through the pore water since most of the electrical current is conducted in the pore water (Glover 2015). Previous studies have shown that the resistivity sharply decreases even if there is only a slight increase in water content (Archie 1942, Munoz-Castelblanco et al. 2012, Pandey et al. 2015): as the volume of water-filled porosity increases, the electrical resistivity tends to decrease. In electrical circuits, Ohm's law establishes the correlation between resistance (R), voltage (V), and current (I) to states that R = V/I. V and I represent the potential difference across a resistor and the current passing through it, respectively. This can also be expressed in terms of electric field strength (E; volts/m) and current density J; amps/m²) as:

$$\rho = {}^{\mathrm{E}}/_{\mathrm{J}}\,(\Omega|\mathrm{m}) \qquad (2)$$

The true resistivity can also be expressed as:

$$\rho = {}^{\mathrm{VA}}/_{IL}\,(\Omega|\mathrm{m}) \qquad (3)$$

Where V is the potential difference across a resistor; A and L are the area of the material; and I is the current passing through. The spectrum of resistivity in geological materials is one of the widest among all physical properties, ranging from 16 x 10^{-8} Ωm for native silver to 17^{16} Ωm for pure sulfide. Igneous rocks typically exhibit higher resistivity values, whereas sedimentary rocks tend to be more conductive, primarily due to their porous water content. Metamorphic rocks fall within an intermediate range but display considerable overlap in resistivity values (Telford et al. 1990, Reynolds 2011, Goldman and Kafri 2020). The resistivity of interstitial fluids within sedimentary rocks significantly

exceeds that of the bedrock. Archie (1942) developed an empirical equation to determine the effective resistivity of rock formations (equation 4), considering variables like porosity (ϕ), the ratio of water-filled pores, and the resistivity of water (ρw). Archie's law remains a prevalent model in boreholes, where ρ and ρw represent the effective rock resistivity and the resistivity of pore water, respectively; ϕ denotes porosity; S represents the volumetric fraction of water-filled pores; and a, m, and n are constants, where $0.5 < a < 2.5$; $1.3 < m < 2.5$, and $n = 2$:

$$\rho = a\phi^{-m} s^{-n} \rho_w \qquad (4)$$

For this reason, the conduction of an electric current is mainly influenced by the water contained in the pores or at the interface between the minerals and water in pores (surface electrical conductivity; Reynolds, 2011, 1987a). Consequently, the resistivity of sandy soil (e.g., sand, sand and gravel, sand with silt and/or clay) primarily depends upon the porosity, pore continuity, and permeating fluid. Therefore, the distribution of resistivity in the subsoil can allow us to distinguish geological formations, and the type of sediments present through the water they contain.

3.6.1.2 Saturated and unsaturated sediments in the study area

For the 5 regions targeted in this study (i.e., Mauricie, AT, C, HCN, and SLSJ), we observed, as expected, higher resistivity values above the water table where the sediments are unsaturated. This study identified five types of saturated sediment to be represented in the chart. These saturated sediments can be compared with their unsaturated equivalents: sand, silty sand, clayey sand, sand and gravel with pebbles, and clayey sand and gravel (Table 11, Figs. 39 and 40). For these five classes of sediments, a decrease in resistivity of 20 to 40% is observed when the sediments are saturated (Table 11). According to a previous study, this significant drop shows that at higher water contents, the resistivity rapidly decreases in sediment, which is thought to be primarily a result of electrolytic conduction (Reynolds 1987a, 2011). In this study, we do not consider the transition

between the unsaturated and saturated zones via the capillary fringe, which usually has a thickness ranging from one to two meters. The thickness of the vadose zone is also greater for thinner materials (e.g., clay, silt) than for coarser materials, with stronger capillary rises creating a thicker capillary fringe. Here, we assumed that this transition between facies (i.e., unsaturated to saturated via the capillary fringe) was included in the resistivity ranges for the saturated sediments.

3.6.1.3 Grain size and clay content

Grain size

The grain size and the clay content are the second parameter that causes the electrical resistivity to vary. As Reynolds et al. (2011) noted, grain size and even grain shape can affect bulk electrical and dielectric behavior, which also impact resistivity values (Kemna et al. 2004, Reynolds 2011). Surface conduction is another mechanism that contributes to electrical conduction and is significantly influenced by various grain sizes and grain shapes in sediments. These variations in grain size cause electrical resistivity to decrease as the surface-area-to-volume ratio increases. For example, resistivity will decrease as clay content increases and the grain size decreases (for clay-free sediment: Archie's law; Archie, 1942). If surface conduction contributes to the measured electrical resistivity, we observed, as expected, that higher resistivity is often observed as the sediment grain size increases from clay to silt, sand, gravel, and pebbles. Consequently, fine-grained sediments (i.e., clay and silt) have low resistivity and exert a low resistance to the passage of electric current. For saturated sediments, we would also expect to see resistivity decrease as the grain's size and the porosity of the material increases.

The resistivity chart provided here reflects these particle size changes associated with variations in electrical resistivity. Indeed, clay resistivity values range between 1 and 65 Ωm and increase from 20 to 165 Ωm if silt is found within the clay and from 20 to 175 Ωm if sand and gravel are mixed with clay. These results are consistent with previous work, showing that an increase in electrical resistivity might be caused by the presence of coarser material (Reynolds 1987a, 2011, Van Heteren et al. 1998, Neal and Roberts 2000, Kemna et al. 2004, Neal 2004). The same pattern is

observed for saturated and unsaturated (1) sand, (2) silty sand, and (3) sand and gravel with pebbles. Figures 39 and 40 shows that there does not seem to be any major resistivity difference between saturated and unsaturated sediments for clayey sand and clayey sand-gravel. This is probably due to the presence of smaller-diameter clay particles; these have a greater impact on resistivity values compared to water saturation. The limited amount of data available (Ncount in Table 5) for the clayey sand and clayey sand-gravel sediment classes is also a crucial factor to consider, and slight biases may have crept into the results. As sands have a much larger particle size than clays (0,64-2 mm versus < 4 µm), the resistivity shows a significant increase between materials of the two sizes, from 65 to 790 Ωm, which can represent twelve times the maximum resistivity value of clay (65 Ωm). Similarly, unsaturated sand and gravel with pebble horizons can be highly resistive (up to 1,430 Ωm), more than twenty-two times the maximum value of clay. When sand and gravel are less homogenous (e.g., the presence of silt or clay), they exhibit lower resistivities, such as observed in saturated and unsaturated clayey sand and gravel, which range between 135-400 Ωm and 100-285 Ωm (Table 11).

Clay content

The clay content of soil particles is an important parameter that significantly impacts resistivity variation (Reynolds 2011). In fine materials such as clay and silt, electrical current can flow by surface conduction due to the electrical double layer and interactions at the interface between the solid particles and the liquid phase (Ulrich and Slater 2004, Scott 2006). The electrical resistivity depends mainly on electrolytic conduction through the pore fluid , therefore, its porosity and how this water is distributed through the geological formation (McNeill 1994), but also on its mineralization and the conductive minerals contained in finer sediment. The electrical resistivity of geomaterials is closely related to their electrical double layer, and for clays, the resistivity can decrease to 1 Ωm. All other sediments are more resistive. The bulk resistivity value significantly depends on the clay mineral composition and the clay content. Bulk resistivity refers to the measurement of the volume resistivity of a semiconductive material, and it is determined by the electrical resistivity of the material through which a current pass. As a bulk measurement technique, TEM provides an integrated response over

a large volume of the subsurface and, therefore, inversion of the raw data allows a global resistivity value to be resolved.

If the sediment matrix contains clay minerals (e.g., clayey sand, clayey sand, and gravel), water chemistry has a lesser influence, and the current flow occurs along the clay mineral surface (Waxman and Smits 1968, Barfod et al. 2016). The resistivity of clay-rich sediments decreases with increasing clay content in pore channels. For sandy material, the resistivity can decrease significantly and reach values as low as 35 Ωm (Table 11). Here, four types of impermeable sediment are represented in the chart (i.e., clay, silty clay, clayed silt, clay with sand/gravel/pebbles), and four types of clay content sediment (i.e., saturated and unsaturated clayey sand, saturated and unsaturated clayey sand and gravel). The resistivity observed for clay is the lowest in the chart and usually varies between 1 and 65 Ωm. As the proportion of silt or sand to clay increases, so does resistivity. Clayey sand (i.e., sand with some clay) or clayey silt (i.e., silt with some clay) has a higher resistivity than sandy clay (i.e., clay with some sand) and silty clay (i.e., clay with some silt). For example, when silt horizons are found within the clay, the resistivity increases slightly, up to values that can reach 165 Ωm because the silt is less conductive than the clay; this change represents a potential increase of 250%, compared to the maximum value of clay alone (165 versus 65 Ωm). Clay and silt both give low resistance to the passage of an electric current, and their resistivity values are moderate to very low. If horizons of sand, gravel, or pebbles are found within the clay, the resistivity can increase up to 175 Ωm, for a potential rise of nearly 270% compared to clay alone (175 versus 65 Ωm). In contrast to clay, sand, gravel, and pebbles are much less conductive and give a higher resistance to the passage of an electric current. For saturated and unsaturated sand with clay, the resistivity varies within a correspondingly low range: 45-195 and 35-260 Ωm, respectively. Compared to the resistivity of saturated and unsaturated sand without clay (120-565 and 230-790 Ωm), the potential increase in resistivity can reach up to 300%. It is thought that the low resistivity in saturated and unsaturated sand with clay is a function of the surface conduction generated from the higher clay mineral concentration (Reynolds 2011).

3.6.1.4 Impact of the geological basement on resistivity values

The Superior Province, which includes a major Archean volcano-sedimentary belt, is exclusive to the AT region, while the Grenville Province (the youngest Precambrian shield province, primarily consisting of intrusive igneous and high-grade metamorphic rocks) is found in the Mauricie, SLSJ, CH, and HCN regions. The St. Lawrence Platform, which stretches along the southern margin of the Canadian Shield, is present in the Mauricie and Charlevoix regions. Despite significant variations in the geological basement across regions, no trends were observed in the estimated resistivity values for each class of saturated and unsaturated sediments. As mentioned above, electrical resistivity values primarily vary due to water content and pore water resistivity, grain size, and clay content. Therefore, the sediment composition related to the geological basement has a negligible impact on electrical resistivity values in this study.

3.6.1.6 Accuracy and precision of the results

The accuracy and precision of the results in this study are supported by three criteria that allow us to have confidence in the defined electrical resistivity ranges for lithological categories obtained in this study: 1) Consistency in acquisition, 2) Data normalization, and 3) Variety of sediment classes (see methodology). First, to remain within a range of values considered representative for each measurement and to filter inconsistent data points, the raw data that did not respect magnetic decay were removed and deleted before the inversion was performed, using TEMAVG software. In addition, all data used in this study were collected by the same team and processed using the same methods. Secondly, the electrical resistivity values obtained for each sedimentary class were normalized according to the numerical threshold of 5% to eliminate outliers that could distort the resistivity ranges inserted in the chart (Tables 5 and 11). Finally, the results integrated fourteen classes of glacial sediments (i.e., distal and proximal glaciomarine, fluvioglacial, juxtaglacial) sampled from five regions of the Province of Québec, Canada. This variety of results from various sedimentary environments allows us to hypothesize that a large number of possible resistivity values are represented in the results.

3.6.2 COMPARISON WITH PREVIOUS STUDIES

3.6.2.1 Electrical resistivity chart in this study

This study proposes various ranges of electrical resistivity values related to saturated and unsaturated sediments in eastern Canada. Only a few authors propose ranges of resistivity for sediments (Table 12), and the vast majority focus mainly on common geological materials such as sedimentary rocks (e.g., sandstone, conglomerate, shale), carbonates, sulfides, oxides, granite, and basalt (Telford et al. 1990; Palacky 1993; Reynolds 2011). Furthermore, the resistivity ranges suggested in previous work for classes of sediments mainly focus on clay, sand, sand and gravel, and gravel. Mixed sediments (e.g., silty clay, sandy clay, clayed sand, silty sand, clayey sand, and gravel) are rarely represented due to possible overlap in their values and only a few sedimentary classes (often local) are offered (Reynolds 1987a, 2011, Palacky 1993, Van Heteren et al. 1998, Neal and Roberts 2000, Neal 2004, Goutaland 2008). This study proposes various ranges of resistivity applied to fourteen sedimentary classes (Table 11), seven of which have not been suggested in previous studies: silty clay, clay with sand/gravel/pebbles, unsaturated silt with clay and sand, saturated and unsaturated silty sand and saturated and unsaturated clayey sand and gravel (Table 12). The comparison of our results against those of previous studies (Table 12) assumes that (1) the mineralogy of sediments, regardless of the sedimentary environment, does not exert a significant impact on resistivity; and (2) the quality of instrumentation used in the past was similar, which means that past results were as accurate as those obtained with the new technology used in this study.

TABLE 12: Comparison of electrical properties for seventeen saturated and unsaturated sediment classes.

Material	This study	Palacky 1993	Van Heteren al. 1998	aNeal et al. 2000, 2004	bGoutaland 2008	cReynolds et al. 2011	Knight et al. 2018
Clay	1-65	5-110	1-500	1-500	10-50	4-150	6-10
Silty clay	20-165	---	---	---	---	---	10-13
Clay with sand/gravel/pebbles	20-175	---	---	---	---	---	---
Unsaturated silt	---	---	10-1000	10-1000	10-1000	---	---
Saturated silt	---	---	< 10	10	10-1000	---	---
Clayey silt with sand	25-290	---	---	---	---	---	16-19
Unsaturated sand	230-790	800-10^4	1000-10^5	10^4	80-1000	80-1050	19-150
Saturated sand	120-565	800-10^4	100-1000	1000-10^4	20-200	20-200	19-150
Unsaturated silty sand	140-535	---	---	---	---	---	---
Saturated silty sand	95-440	---	---	---	---	---	---
Unsaturated clayey sand	35-260	---	---	---	---	30-215	---
Saturated clayey sand	45-195	---	---	---	---	30-215	---
Unsaturated sand and gravel	305-1430	800-10^4	16667-142800	17000-150000	30-1400	30-225	19-150
Saturated sand and gravel	180-915	800-10^4	111-1430	100-1450	30-1400	30-225	19-150
Unsaturated clayey sand and gravel	135-400	---	---	---	---	---	---
Saturated clayey sand and gravel	100-285	---	---	---	---	---	---
Unsaturated gravel	---	800-10^4	---	---	---	1400	---
Saturated gravel	---	800-10^4	---	---	---	100	---

[a] Based primarily on Van Heteren et al., 1998, 1996, with additional data from Davis and Annan, 1989; Theimer et al., 1994; Van Overmeeren, 1994). [b] Based on Asprion et Aigner (1997), Beres et Haeni (1991), Gascoyne et Eriksen (2005), Mari et al. (1998), Milsom (2003) et Neal (2000, 2004), Van Heteren et al., 1998. [c] Based on Telford et al. (1990) with additional data from McGinnis and Jensen (1971), Reynolds (1987a), Reynolds and Paren (1980, 1984), and many commercial projects

3.6.2.2 Electrical resistivity charts in previous studies

In previous studies, resistivity charts have often exhibited limited differentiation between saturated and unsaturated sediments, suggesting similar values for these two distinct sediment classes (Table 12). Also, geophysical interpretation often provides information about groundwater level without the validation provided by borehole data (i.e., piezometric surveys). Consequently, proposed resistivity values for saturated sediments often appear lower or higher compared to the results of this study. For example, Neal (2000, 2004) proposes resistivity values for saturated sand and saturated sand-gravel ranging from 1,000 to 10,000 Ωm and from 100 to 1,450 Ωm, respectively, while this study gives values ranging from 120 to 600 Ωm for saturated sand and from 180 to 915 Ωm for saturated sand-gravel. Reynolds et al. (2011) and Goutaland (2008) obtained results ranging from 20 to 200 Ωm for sand and from 30 to 225 Ωm for sand and gravel, which do not reflect the high resistivity typically associated with large particle sizes (Galazoulas et al. 2015; Pandey et al. 2015; Parsekian et al. 2015; Simard et al. 2015; Costabel et al. 2017; García-Menéndez et al. 2018, Greggio et al. 2018; Kalisperi et al. 2018; Pondthai et al. 2020; Elbshbeshi et al. 2022, Othman et al. 2022; Lévesque et al. 2021, 2023a). Knight (2018) obtains results varying between 25 and 150 (above the water table) and 17 and 43 (below the water table) for sand and gravel. These values do not reflect the true resistivity of the sediments and are in contradiction with the values obtained by Neal et al. (2000, 2004) and Van Heteren et al. (1998; Table 12). The results presented in Table 12 are primarily derived from localized studies, which may explain the differences in interpretation observed between various studies, including the present one. It should also be noted that the low values reported by Reynolds et al. (2011) for saturated sand and saturated/unsaturated sand-gravel, are likely due to the bands of discrete clay commonly found within the sand and gravel horizons at the study site in the southern Kano state in Nigeria (Reynolds 1987a), as resistivity tends to decrease in the presence of increased clay content.

Palacky (1993) provided an overview of the typical resistivity ranges of common earth materials using airborne electromagnetic methods (AEMs). AEM also produce slightly different results than ground surveys (e.g., TEM). Like TEM, AEM is also a bulk measurement technique, but it collects data over a much larger volume of subsurface, which can result in reduced resolution of small-scale

features compared to TEM. Palacky (1993) proposed resistivity values for clay, sand, sand-gravel, and gravel ranging from 5 to 110 Ωm and 800 to 10,000 Ωm, respectively (Table 12). While the resistivity values for clay are consistent with the results of this study, ranging from 1 to 65 Ωm, it is challenging to obtain precise information for sand, sand-gravel, and gravel in Palacky's study. AEM is a bulk measurement that covers a much larger volume than TEM; this may obscure small-scale features and cause these three types of sediments to be represented by a similar range of resistivity values.

Furthermore, in comparison to the results of this study, the values suggested by several previous studies (Reynolds 1987b, 2011, Palacky 1993, Van Heteren et al. 1998, Goutaland 2008, Pandey et al. 2015) appear to be high for both saturated and unsaturated sand and sand-gravel (as shown in Table 12). The most recent compilations carried out by Goutaland (2008), and Reynolds et al. (2011) generally seem to obtain similar results to those of the present study. For example, Table 12 shows that for clay, the results obtained in this study ranged between 1 and 65 Ωm, and Goutaland (2008) and Reynolds et al. (2011) obtained values ranging from 10 to 50 Ωm and from 4 to 150 Ωm, respectively. For unsaturated sand, the values are also similar to the results of this study: 230-790 Ωm (this study) versus 80-1000 Ωm (Goutaland) and 80-1050 Ωm (Reynolds). Reynolds (1987, 2011) also had similar results for clayey sand, which had resistivities varying from 30 to 215 Ωm (saturated and unsaturated) versus 35 to 260 Ωm (unsaturated; this study) and from 45 to 195 Ωm (saturated; this study). The compilation by Goutaland (2008) for sand and gravel seems the most consistent with the results obtained in this study. Goutaland obtains resistivity values ranging from 30 to 1,400 Ωm for saturated and unsaturated sand and gravel, and for this study, the resistivity values range from 305 to 1430 Ωm (unsaturated sands and gravels) and from 180 to 915 Ωm (saturated sand and gravel). If the saturated and unsaturated sand and gravel proposed in this study are considered to be the same class of sediment, the results are very similar to those obtained by Goutaland (2008): 30-1400 Ωm vs. 180-1430 Ωm (this study). The similarities observed between this study and the work of Reynolds and Goutaland likely reflect a comparable methodology. Specifically, the geophysical results were validated by proximal boreholes, and data regarding groundwater levels below the surface (i.e., piezometric surveys) were also available, which enabled a clear differentiation between

saturated and unsaturated sediments. Another notable similarity with Reynolds' study and this study is the extensive collection of accessible data and the high number of study sites (i.e., 200) used to establish a local and empirical petrophysical relationship.

3.6.2.3 Obtaining accurate and reliable results

This study's results demonstrate that several resistivity ranges measured are consistent with those reported in recent previous studies for specific sediment classes, including clay, unsaturated sand, and saturated and unsaturated clayey sand, and unsaturated sand and gravel (Table 12). However, for other sediment classes, some resistivity values reported by previous authors in Table 12 appear to be notably lower or higher compared to those observed in this study. To acquire representative results, several methodological issues need to be considered when attributing resistivity values, which can explain the presence of outliers:

- 1) Geophysical results must be systematically verified by boreholes sampled nearby. In order to “ground-truth” the geophysical result, it is necessary to project the boreholes (and/or stratigraphic cross-sections) and compare them to the nearest TEM station (i.e., co-located data). This process enables the electrical resistivity values to be directly associated with the various sediment facies found in these boreholes or stratigraphic cross-sections. Indirect measurements such as those provided by geophysical methods are subject to uncertainty, which poses a major problem. Since geophysical methods provide indirect observations of the subsurface, their results must be validated to confirm the subsurface information. Without proper validation, the predictions based on uncertain results can also be uncertain. Verify geophysical results is essential to provide adequate information, regardless of the stratigraphic complexity. Only after proper validation using direct measurements from boreholes, stratigraphic sections and piezometric data can indirect measurements such as those provided by geophysical methods provide reliable information about the subsurface. However, a significant difficulty encountered by geophysicists is the limited availability and scarcity of direct measurements, given the time-consuming and expensive nature of borehole and drilling campaigns. This scarcity of direct measurements often renders geophysical results and predictions inaccurate, making it challenging to establish their reliability in representing actual subsurface conditions. The

large amount of field data in this study (i.e., boreholes, stratigraphic cross-sections, and piezometric surveys) also significantly decreases the uncertainty associated with geophysics and greatly strengthens the stratigraphic interpretation. The results of this study are based on a rather large dataset, which generally increases the credibility of the conclusions drawn from the electrical resistivity values associated with different sediment classes. The extensive information collected from five regions in the Province of Quebec, Canada (i.e., Mauricie, AT, SLSJ, C, and HCN, covering an area of approximately 432,517 km^2), also offers a broad range of possibilities for understanding the variations in electrical resistivity across different sediment classes. A comprehensive (i.e., large and diverse) dataset enables us to obtain more robust results compared to datasets from highly localized (i.e., local and specific) past studies (Table 12), which were based on relatively small datasets ranging from 0 to 12 stratigraphic logs or up to 200 logs, all collected from a single region (e.g., Central Valley of California, Northern Nigeria, Coast of New England). This constraint in past studies may introduce biases and compromise confidence in their finding as intermixed sediments (e.g., silty clay, clayey sand) in the subsurface can have a substantial impact on the final outcome. It should be noted that a study that is too localized may not provide a comprehensive representation of the full range of resistivity values that can be found for a particular sediment class;

- 2) Observation of the water level, and consequently the water-saturated sediments, must be conducted systematically to obtain a range of values for saturated or unsaturated sediments. Without this information, it can be difficult to differentiate between water-saturated and unsaturated sediments, resulting in imprecise resistivity values. In this study, a much larger number of boreholes located near the TEM stations were initially available. However, out of these boreholes, 77 were excluded due to insufficient piezometric information (i.e., water level elevation). Nonetheless, the study still retains a significant dataset consisting of 75 boreholes, 10 stratigraphic cross-sections, and 51 piezometric surveys, which together provide valuable insights into the resistivity distribution of different saturated and unsaturated sediment classes;

- 3) Extreme minimum and maximum resistivity values are often not representative and can distort the interpretation of geophysical data and the correlation with stratigraphic logs from boreholes.

Therefore, data filtering is necessary to extract a range of representative resistivities for various sediment classes, and to place higher importance on values that occur more frequently. In this study, outlier removal was performed using statistical probability methods;

- 4) Combining multiple geophysical techniques to reduce uncertainty is well-known among geophysicists, as each method has its particular strengths and weaknesses. However, compiling results from various authors using mixed geophysical methods (e.g., TEM, AEM, GPR, ERT) may introduce several biases when producing a resistivity chart. Instead, using a single geophysical method with a common methodology can provide more consistent results. Moreover, the interpretation techniques used to associate resistivity with sediment classes vary widely. In this study, a uniform methodology was employed across all five study regions, which included the use of the same NanoTEM equipment and geophysical method (i.e., TEM) to obtain and process the geophysical results.

Establishing a reliable relationship between resistivity and lithology is a challenging task, and significant overlaps are frequently observed between some classes of saturated and unsaturated sediments. The conversion of resistivity models to lithologic models is not a straightforward process. Previous studies have generally presented results with values that are much higher or much lower compared to the results obtained in this study.

3.7 CONCLUSION

The motivation for this study was to propose typical electrical resistivity values for a wide range of common saturated and unsaturated sediments, to fill a knowledge gap in the current literature. In this chart, the ranges of resistivity are applied to fourteen classes of sediments, seven of which have not been included in previous studies: silty clay, clay with sand/gravel/pebbles, unsaturated silt with clay and sand, saturated and unsaturated silty sand and saturated and unsaturated clayey sand and

gravel. To develop a representative resistivity chart and to avoid distorting the ranges of values proposed for each class of sediments, the following results are incorporated:

- Geophysical results are systematically compared and validated by nearby boreholes or stratigraphic cross-sections, including information about the water table elevation, which allows us to establish a clear differentiation between saturated and unsaturated sediment.
- The sediment classes represented in this chart are not mixed with seawater and/or other sediments that could significantly increase or decrease their resistivity. If the sediments are intermixed with other sediments (e.g., silty clay, clayey sand), we consider it and propose new sediment classes.
- The geophysical data were filtered to remove their extreme minimum and maximum values, and outliers were removed to propose a classification. The data were filtered by using statistical probabilities (i.e., the numerical threshold of 5%) to highlight the more frequently reproduced resistivity values and to give these values a more significant influence in the chart, which includes less extensive ranges of values. The chart will be consequently more accurate and significant.
- The results are not based on a compilation but on raw data collected from five regions of the Province of Québec in Canada using only one geophysical method (i.e., TEM). Moreover, the same correlation technique was used between boreholes and stratigraphic cross-sections and their complementary nearby TEM stations.

This contribution will therefore be beneficial to the scientific community. It could also be used by hydrogeologists, engineers, and geophysicists from the private sector to identify with greater precision the typical electrical resistivity properties for common saturated and unsaturated sediments in similar contexts elsewhere in Québec, Canada, or around the world,. In particular, these results will allow us to better assess groundwater resources using geophysical methods involving electric and electromagnetic radiation (e.g., TEM, ERT, GPR, AEM). This chart can also serve as a valuable tool to facilitate various aspects of subsurface characterization. It can aid in detecting the vadose zone and water table elevation, improving understanding of the distribution and geometry of aquifers and potential groundwater resources, identifying layers of semi-impermeable and semi-permeable

sediments, accurately mapping transitions between different sediment classes, and enhancing numerical hydrogeological models in terms of both validation and calibration.

3.8 CONCLUSION DU CHAPITRE 3

Comme évoqué précédemment, cette charte remplit la fonction essentielle de fournir un cadre de référence pour l'exploitation de toutes les données TEM (ou ERT) acquises sur le terrain, même celles pour lesquelles il n'y a pas de forages à proximité. Malgré les inévitables chevauchements constatés dans toutes les chartes existantes, l'objectif est d'offrir des repères, à la fois à l'échelle régionale et locale, avec une précision améliorée par rapport aux chartes de résistivité préexistantes. L'objectif principal étant d'obtenir une vision exhaustive des couches souterraines et de la stratigraphie régionale et déterminer avec plus de justesse l'élévation du toit de la nappe (grâce aux contrastes de résistivité électrique) et d'identifier les sédiments granulaires susceptibles de constituer ces aquifères.

De surcroît, il est important de souligner que cette charte de résistivité n'a pas été principalement élaborée à des fins de modélisation (pour conduire des modélisations en tant que telles). Dans cette recherche, le lien avec la modélisation (par rapport à la charte de résistivité) est strictement axé sur l'identification des niveaux d'eau souterraine à partir des levés géophysiques (TEM, ERT, etc.). Étant donné que ces niveaux d'eau sont des éléments fondamentaux pour la validation et la calibration des modèles numériques, la charte de résistivité apporte des éléments complémentaires pour l'interprétation des relevés géophysiques obtenus. En effet, elle nous permet de localiser de manière plus précise la nappe phréatique (les sédiments granulaires saturés) grâce aux contrastes de résistivité électrique.

Selon notre analyse, cette charte pourrait également être extrapolée à d'autres sites pour aider à la détection d'aquifères granulaires à nappe libre. En effet, les résultats de cette étude reposent sur un ensemble de données relativement vaste, ce qui accroît généralement la crédibilité des conclusions tirées des valeurs de résistivité électrique associées à différentes classes de sédiments. Les données exhaustives collectées dans cinq régions de la province de Québec, Canada (Mauricie,

AT, SLSJ, C et HCN, couvrant une superficie d'environ 432 517 km2), offrent également une variété de possibilités pour comprendre les variations de la résistivité électrique à travers différentes classes de sédiments. Par conséquent, cette charte pourrait être étendue à d'autres régions contenant des sédiments quaternaires. Un ensemble de données complet (c'est-à-dire large et diversifié) nous permet d'obtenir des résultats plus robustes par rapport à des ensembles de données provenant de zones fortement localisées. Il convient de noter qu'une étude trop localisée peut ne pas offrir une représentation juste de l'ensemble des valeurs de résistivité que l'on peut trouver pour une classe de sédiments particulière.

En fin de compte, les résultats obtenus par la méthode TEM dans une autre région détermineront si cette charte est adaptée ou non à un autre site géologique. Si les résultats corroborent la charte, elle est jugée appropriée ; en revanche, des résultats discordants peuvent être le signe de variables inconnues générant des résultats divergents, telles que la présence abondante d'argile dans les sédiments granulaires ou la forte teneur en minéraux ferromagnétiques (et semi-conducteurs).

Dans les études à venir, l'application d'une loi des mélanges pourrait être envisagée pour expliquer les variations de résistivité et quantifier les pourcentages des différents types de sédiments, offrant ainsi une précision accrue sur les plages de résistivité électrique en fonction des classes de sédiments énoncées dans cette recherche. Cependant, d’un point de vue pratique, bien que cette approche soit scientifiquement intéressante, elle ne constitue pas un apport essentiel. En effet, même si une loi des mélanges était élaborée avec des pourcentages précis (engendrant ainsi la création de plusieurs autres classes de sédiments), les plages de valeurs de résistivité se superposeraient largement, offrant finalement peu d'informations utiles pour la localisation des nappes phréatiques et des sédiments granulaires.

Par exemple, les plages de valeurs associées à des pourcentages spécifiques et ajustés pour les sables fins, moyens et grossiers présenteraient des similitudes considérables et n'auraient guère d'incidence pratique. De plus, obtenir une connaissance précise du pourcentage d'argile contenu dans les sables fins pourrait être d'un intérêt scientifique, mais pour évaluer le potentiel en eau souterraine de la région, ce niveau de détails ne seraient pas essentiels. Ce dont nous avons surtout

besoin, ce sont des outils nous permettant de distinguer avec une précision accrue les sédiments saturés des non saturés (et donc de déterminer l'élévation du toit de la nappe), d'identifier les types de sédiments présents sur le site et surtout de repérer les sédiments granulaires susceptibles de contenir de l'eau souterraine. Dans cette optique, cette charte de résistivité générale prend tout son sens.

Les données indirectes obtenues à partir de méthodes géophysiques rendent souvent difficile la distinction des sédiments saturés des autres types de sédiments présentant des valeurs de résistivité similaires. Toutefois, quelques stratégies permettent d'y parvenir. Voici quelques exemples :

1- La combinaison de différentes méthodes géophysiques peut jouer un rôle crucial dans la distinction des sédiments saturés des autres types de sédiments présentant des valeurs de résistivité similaires. Par exemple, le géoradar s'avère être une méthode excellente pour localiser la nappe phréatique. Cependant, en présence d'argile ou d'une frange capillaire importante dans un environnement sédimentaire, ses résultats peuvent être altérés, voire nuls, en raison de la dispersion des ondes électromagnétiques et de la perte de signal. L'argile perturbe la propagation normale des ondes émises par le géoradar, entraînant une diminution de la qualité du signal renvoyé vers la surface. La perte de signal indique fréquemment la présence de sédiments fins dans l'environnement, ce qui peut être confirmé par d'autres méthodes telles que le TEM et le ERT, qui détectent facilement la présence d'argile. Par contre, les méthodes du TEM et du ERT repose sur l'identification des contrastes élevé de résistivité électrique entre les sédiments saturés et non saturés pour localiser la nappe phréatique, ce qui n'est pas le cas avec la méthode du géoradar. En raison de la permittivité diélectrique élevée de l'eau, la nappe phréatique crée un fort contraste entre les vitesses de propagation dans les sédiments saturés et non saturés, entraînant une réflexion significative de l'énergie émise par le géoradar. Ainsi, la nappe phréatique apparaît comme un réflecteur horizontal continu de large amplitude sur les radargrammes, permettant ainsi l'identification des sédiments granulaires saturés en eau.

2- La présence de levés piézométriques à proximité revêt également une importance significative. Bien qu'ils soient peu nombreux dans une zone d'étude, ces levés offrent un aperçu de l'élévation du toit de la nappe et de la présence de sédiments saturés à une certaine profondeur. Ainsi, si les valeurs de résistivité diminuent considérablement à une profondeur correspondant aux levés piézométriques voisins, il est probable que cela indique la présence de sédiments saturés en eau plutôt que d'un milieu argileux ou limoneux.

3- Le contexte environnemental, paléoenvironnemental et géologique, ainsi que les processus de dépôt, fournissent également des indices sur la nature des sédiments présents dans une région donnée. Par exemple, la présence d'argile aux abords de la moraine de Saint-Narcisse est largement attribuable à l'ancienne Mer de Champlain. Dans les zones topographiquement élevées de la moraine, la présence d'argile est rare voire inexistante, suggérant que des valeurs de résistivité basses dans ces régions indiquent probablement une saturation des sédiments en eau. Bien que cet exemple soit général, il offre néanmoins une indication du type de sédiments présents sur le site. Ainsi, le contexte environnemental, paléoenvironnemental et géologique constitue un outil précieux pour évaluer la nature des sédiments en place, même à une échelle locale.

Finalement, il convient également de souligner qu'une autre méthode géophysique pourrait tout aussi bien fournir des résultats de qualité équivalente, voire supérieure à ceux obtenus par la méthode TEM, pour les plages de résistivité associées aux mêmes classes de sédiments énoncées dans cette charte. Bien que la méthode TEM ait été celle disponible à l'Université du Québec à Chicoutimi pour mener cette étude, une autre méthode géophysique pourrait également se révéler robuste pour établir une charte de résistivité électrique.

LISTE DES REFERENCES

Aguert, M., and Capel, A. 2018. Mieux comprendre les scores z pour bien les utiliser. Rééducation orthophonique, 274: 61–85.

Aho, K.A. 2013. Foundational and applied statistics for biologists using R. CRC Press.

Archie, G.E. 1942. The electrical resistivity log as an aid in determining some reservoir characteristics. Transactions Am. Inst. Min. Metall. Eng., 146: 54–62. Society of Petroleum Engineers. doi:10.2118/942054-G.

Asprion U, Aigner T (1997) Aquifer architecture analysis using ground-penetrating radar: Triassic and Quaternary examples (S. Germany). Environ Geol 31:66–75

Barfod, A.A.S., Møller, I., and Christiansen, A. V. 2016. Compiling a national resistivity atlas of Denmark based on airborne and ground-based transient electromagnetic data. Journal of Applied Geophysics, 134: 199–209. Elsevier.

Benn, D., and Evans, D.J.A. 2010. Glaciers and glaciation. In 1ST edition. Routledge, London and New York. doi:10.4324/9780203785010.

Beres Jr., M., and Haeni, F.P. 1991. Application of ground-penetrating-radar Methods in Hydrogeologie Studies. Groundwater, 29: 375–386. Wiley Online Library. doi:10.1111/j.1745-6584.1991.tb00528.x.

Bostock, H.S. 1970. Physiographic regions of Canada. Geology and economic minerals of Canada,. Geological Survey of Canada.

Boumaiza, L., Chesnaux, R., Walter, J., and Meghnefi, F. 2021a. Assessing response times of an alluvial aquifer experiencing seasonally variable meteorological inputs. Groundwater for Sustainable Development, 14: 100647. Elsevier.

Boumaiza, L., Chesnaux, R., Walter, J., and Stumpp, C. 2021b. Constraining a flow model with field measurements to assess water transit time through a vadose zone. Groundwater, 59: 417–427. Wiley Online Library. doi:10.1111/gwat.13056.

Boumaiza, L., Walter, J., Chesnaux, R., Brindha, K., Elango, L., Rouleau, A., Wachniew, P., and Stumpp, C. 2021c. An operational methodology for determining relevant DRASTIC factors and their relative weights in the assessment of aquifer vulnerability to contamination. Environmental Earth Sciences, 80: 1–19. Springer.

Boumaiza, L., Walter, J., Chesnaux, R., Stotler, R.L., Wen, T., Johannesson, K.H., Brindha, K., and Huneau, F. 2022. Chloride-salinity as indicator of the chemical composition of groundwater: empirical predictive model based on aquifers in Southern Quebec, Canada. Environmental Science and Pollution Research,: 1–19. Springer. doi:10. 1007/ s11356- 022- 19854-z.

Brisebois, D., and Brun, J. 1994. La plate-forme du Saint-Laurent et les Appalaches. Géologie du Québec,: 1–94. Ministère des ressources naturelles Quebec City, QC, Canada.

Card, K.D. 1990. A review of the Superior Province of the Canadian Shield, a product of Archean accretion. Precambrian Research, 48: 99–156. Elsevier.

Chesnaux, R., Lambert, M., Walter, J., Fillastre, U., Hay, M., Rouleau, A., Daigneault, R., Moisan, A., and Germaneau, D. 2011. Building a geodatabase for mapping hydrogeological features and

3D modeling of groundwater systems: Application to the Saguenay–Lac-St.-Jean region, Canada. Computers & Geosciences, 37: 1870–1882. Elsevier. doi:10.1016/j.cageo.2011.04.013.

Christiansen, A.V., Auken, E., and Sørensen, K. 2006. The transient electromagnetic method. In Groundwater geophysics. Springer. pp. 179–225.

Constable, S.C., and Parker, R.L. 1987. Occam's inversion: A practical algorithm for generating smooth models from electromagnetic sounding data. Geophysics, 52: 289–300. Society of Exploration Geophysicists. doi:10.1190/1.1442303.

Costabel S, Siemon B, Houben G, Günther T (2017) Geophysical investigation of a freshwater lens on the island of Langeoog, Germany–Insights from combined HEM, TEM and MRS data. J Appl Geophys 136:231–245.

Craparo, R.M. 2007. Significance level. Encyclopedia of measurement and statistics. SAGE Publications, Thousand Oaks, CA.

Danielsen, J.E., Auken, E., Jørgensen, F., Søndergaard, V., and Sørensen, K.I. 2003. The application of the transient electromagnetic method in hydrogeophysical surveys. Journal of applied geophysics, 53: 181–198. Elsevier. doi:10.1016/j.jappgeo.2003.08.004.

Davis, J.C., and Sampson, R.J. 1986. Statistics and data analysis in geology. Wiley New York.

Davis JL, Annan AP (1989) Ground-penetrating radar for high-resolution mapping of soil and rock stratigraphy 1. Geophys Prospect 37:531–551. https://doi.org/10.1111/j.1365-2478.1989.tb02221.x

Dyke, A.S. 2004. An outline of the deglaciation of North America with emphasis on central and northern Canada. Quaternary Glaciations-Extent and Chronology, Part II: North America, 2b: 373-424. doi:10.1016/S1571-0866(04)80209-4.

Elbshbeshi, A., Gomaa, A., Mohamed, A., Othman, A., and Ghazala, H. 2022. Seismic hazard evaluation by employing microtremor measurements for Abu Simbel area, Aswan, Egypt. Journal of African Earth Sciences, 196: 104734. Elsevier.

Fitterman, D. V, and Labson, V.F. 2005. Electromagnetic induction methods for environmental problems. In Near-surface geophysics. Edited by S. of E. Geophysicists. Society of Exploration Geophysicists, Houston, TX. pp. 301–356. doi:10.1190/1.9781560801719.ch10.

Foged, N., Auken, E., Christiansen, A.V., and Sørensen, K.I. 2013. Test-site calibration and validation of airborne and ground-based TEM systems. Geophysics, 78: E95–E106. Society of Exploration Geophysicists.

Galazoulas, E.C., Mertzanides, Y.C., Petalas, C.P., and Kargiotis, E.K. 2015. Large scale electrical resistivity tomography survey correlated to hydrogeological data for mapping groundwater salinization: a case study from a multilayered coastal aquifer in Rhodope, Northeastern Greece. Environmental processes, 2: 19–35. Springer.

García-Menéndez, O., Ballesteros, B.J., Renau-Pruñonosa, A., Morell, I., Mochales, T., Ibarra, P.I., and Rubio, F.M. 2018. Using electrical resistivity tomography to assess the effectiveness of managed aquifer recharge in a salinized coastal aquifer. Environmental monitoring and assessment, 190: 1–19. Springer.

Glover, P.W.J. 2015. 11.04–Geophysical Properties of the Near Surface Earth: Electrical Properties. Treatise geophys,: 89–137.

Goldman, M., and Kafri, U. 2020. Geoelectric, Geoelectromagnetic and Combined Geophysical Methods in Groundwater Exploration in Israel. In The Many Facets of Israel's Hydrogeology, First. Springer, Cham, Switzerland. doi:10.1007/978-3-030-51148-7.

Goutaland, D. 2008. Caractérisation hydrogéophysique d'un dépôt fluvioglaciaire: évaluation de l'effet de l'hétérogénéité hydrodynamique sur les écoulements en zone non-saturée. Ph.D. dissertation, Lyon University (INSA), France, 246 p.

Greggio N, Giambastiani B, Balugani E, et al (2018) High-resolution electrical resistivity tomography (ERT) to characterize the spatial extension of freshwater lenses in a salinized coastal aquifer. Water 10:1067. https://doi.org/10.3390/w10081067.

Kalisperi, D., Kouli, M., Vallianatos, F., Soupios, P., Kershaw, S., and Lydakis-Simantiris, N. 2018. A transient ElectroMagnetic (TEM) method survey in north-central coast of Crete, Greece: evidence of seawater intrusion. Geosciences, 8: 107. Multidisciplinary Digital Publishing Institute. doi:10.3390/geosciences8040107.

Kemna, A., Binley, A., and Slater, L. 2004. Crosshole IP imaging for engineering and environmental applications. Geophysics, 69: 97–107. Society of Exploration Geophysicists. doi:10.1190/1.1649379.

Knight, R., Smith, R., Asch, T., Abraham, J., Cannia, J., Viezzoli, A., and Fogg, G. 2018. Mapping aquifer systems with airborne electromagnetics in the Central Valley of California. Groundwater, 56: 893–908. Wiley Online Library.

Knight, R.J., and Endres, A.L. 2005. An introduction to rock physics principles for near-surface geophysics. In Near-surface geophysics. Society of Exploration Geophysicists. pp. 31–70.

Légaré-Couture, G., Leblanc, Y., Parent, M., Lacasse, K., and Campeau, S. 2018. Three-dimensional hydrostratigraphical modelling of the regional aquifer system of the St. Maurice Delta Complex (St. Lawrence Lowlands, Canada). Canadian Water Resources Journal/Revue canadienne des ressources hydriques, 43: 92–112. Taylor & Francis. doi:10.1080/07011784.2017.1316215.

Lévesque, Y., Chesnaux, R., and Walter, J. 2023a. Using geophysical data to assess groundwater levels and the accuracy of a regional numerical flow model. Hydrogeology Journal,. doi:10.1007/s10040-023-02591-z.

Lévesque, Y., St-Onge, G., Lajeunesse, P., Desiage, P., and Brouard, E. 2019. Defining the maximum extent of the Laurentide Ice Sheet in Home Bay (eastern Arctic Canada) during the Last Glacial episode. Boreas, 49: 52–70. Wiley Online Library. doi:10.1111/bor.12415.

Lévesque, Y., Walter, J., Boumaiza, L., Lambert, M., Ferroud, A., and Chesnaux, R. 2023b. Multi-technique approach to characterize the hydrogeology of aquifer systems: Application on the Mauricie region of Quebec, Canada (on press). Canadian Water Resources Journal/Revue canadienne des ressources hydriques,.

Lévesque, Y., Walter, J., and Chesnaux, R. 2021. Transient Electromagnetic (TEM) Surveys as a First Approach for Characterizing a Regional Aquifer: The Case of the Saint-Narcisse Moraine, Quebec, Canada. Geosciences, 11: 415–442. Multidisciplinary Digital Publishing Institute. doi:10.3390/ geosciences11100415.

MacInnes, S. 2001. Zonge Engineering and Research Organization, Inc.

MacInnes, S., and Raymond, M. 2001. ZONGE Data Processing Two-Dimensional, Smooth-Model CSAMT Inversion version 3.00. Zonge Engineering and Research Organization, Inc. p. 41.

Margold, M., Stokes, C.R., and Clark, C.D. 2015. Ice streams in the Laurentide Ice Sheet: Identification, characteristics and comparison to modern ice sheets. Earth-Science Reviews, 143: 117–146. doi:10.1016/j.earscirev.2015.01.011.

Mari JL, Arens G, Chapellier D, Gaudiani P (1998) Geophysics for deposits and civil engineering; Geophysique de gisement et de genie civil

McGinnis LD, Jensen TE (1971) Permafrost-hydrogeologic regimen in two ice-free valleys, Antarctica, from electrical depth sounding. Quat Res 1:389–409

McKillup, S. 2011. Statistics explained: An introductory guide for life scientists. Cambridge University Press.

McNeill, J.D. 1994. Principles and application of time domain electromagnetic techniques for resistivity sounding (Technical Note TN-27). Rapport technique, Geonics Limited,.

Mendenhall, W.M., and Sincich, T.L. 2016. Statistics for Engineering and the Sciences. CRC Press.

Milsom J (2003) Field geophysics. John Wiley and sons, Oxford, UK

Munoz-Castelblanco, J.A., Pereira, J.-M., Delage, P., and Cui, Y.-J. 2012. The influence of changes in water content on the electrical resistivity of a natural unsaturated loess. Geotechnical Testing Journal, 35: 11–17. ASTM International.

Nabighian, M.N. 1988. Electromagnetic methods in applied geophysics. Society of Exploration Geophysicists, Tulsa, 2.

Neal, A. 2004. Ground-penetrating radar and its use in sedimentology: principles, problems and progress. Earth-science reviews, 66: 261–330. Elsevier. doi:10.1016/j.earscirev.2004.01.004.

Neal, A., and Roberts, C.L. 2000. Applications of ground-penetrating radar (GPR) to sedimentological, geomorphological and geoarchaeological studies in coastal environments. Geological Society, London, Special Publications, 175: 139–171. Geological Society of London. doi:10.1144/GSL.SP.2000.175.01.12.

Occhietti. 1977. Stratigraphie du Wisconsinien de la région de Trois-Rivières-Shawinigan, Québec. Géographie physique et Quaternaire, 31: 307–322. Les Presses de l'Université de Montréal. doi:10.7202/1000280ar.

Occhietti. 2007. The Saint-Narcisse morainic complex and early Younger Dryas events on the southeastern margin of the Laurentide Ice Sheet. Géographie physique et Quaternaire, 61: 89–117. Les Presses de l'Université de Montréal. doi:10.7202/038987ar.

Occhietti, S. 2018. Lithostratigraphie du quaternaire de la vallée du saint-laurent : méthode , cadre conceptuel et séquences sédimentaires. doi:10.7202/032813ar.

Othman, A.A., Beshr, A.M., Abd El-Gawad, A.M.S., and Ibraheem, I.M. 2022. Hydrogeophysical investigation using remote sensing and geoelectrical data in southeast Hiw, Qena, Egypt. Geocarto International, 37: 14241–14260. Taylor & Francis.

Palacky, G. 1987. Resistivity characteristics of geological targets, in electromagnetic methods in applied geophysics, edited by Misac Nabighian, Society of Exploration Geophysicists. Society of Exploration Geophysicists, 1: 55–129.

Palacky, G.J. 1993. Use of airborne electromagnetic methods for resource mapping. Advances in space research, 13: 5–14. Elsevier. doi:10.1016/0273-1177(93)90196-I.

Pandey, L.M.S., Shukla, S.K., and Habibi, D. 2015. Electrical resistivity of sandy soil. Géotechnique Letters, 5: 178–185. Thomas Telford Ltd. doi:10.1680/jgele.15.00066.

Parsekian, A.D., Singha, K., Minsley, B.J., Holbrook, W.S., and Slater, L. 2015. Multiscale geophysical imaging of the critical zone. Reviews of Geophysics, 53: 1–26. Wiley Online Library. doi:10.1002/2014RG000465.

Pondthai, P., Everett, M.E., Micallef, A., Weymer, B.A., Faghih, Z., Haroon, A., and Jegen, M. 2020. 3D Characterization of a Coastal Freshwater Aquifer in SE Malta (Mediterranean Sea) by Time-Domain Electromagnetics. Water, 12: 1566. Multidisciplinary Digital Publishing Institute. doi:10.3390/w12061566.

Reynolds, J.M. 1987a. The role of surface geophysics in the assessment of regional groundwater potential in northern Nigeria. Geological Society, London, Engineering Geology Special Publications, 4: 185–190. Geological Society of London.

Reynolds, J.M. 1987b. Dielectric analysis of rocks-a forward look. In Geophysical journal of the royal astronomical society. Blackwell science ltd osney mead, oxford, england. p. 457.

Reynolds, J.M. 2011. An introduction to applied and environmental geophysics. In 2nd edition. John Wiley & Sons, West Sussex, UK.

Richer, B., Saeidi, A., Boivin, M., Rouleau, A., and Lévesque, Y. 2023. Development of a methodology for predicting landslide hazards at a regional scale. Geoenvironmental Disasters, 10: 1–19. SpringerOpen. doi:10.1186/s40677-022-00231-4.

Rivers, T. 2017. The Grenville Province as a large hot long-duration collisional orogen - Insights from the spatial and thermal evolution of its orogenic fronts Geological Society , London , Special Publications The Grenville Province as a large hot long-duration collisio. doi:10.1144/SP327.17.

Scott, J.B. 2006. The origin of the observed low-frequency electrical polarization in sandstones. Geophysics, 71: G235–G238. Society of Exploration Geophysicists.

Selley. R, Robin L, Cocks M, Plimer Y, Gascoyne (2005) Encyclopedia of geology, First. Elsevier, Oxford, UK

Shukla, S.K., and Yin, J.-H. 2006. Fundamentals of geosynthetic engineering. In 1ST edition. Edited ByCRC Press. Taylor and Francis, Balkema, London (UK). doi:10.1201/9781482288445.

Simard, P.T., Chesnaux, R., Rouleau, A., Daigneault, R., Cousineau, P.A., Roy, D.W., Lambert, M., Poirier, B., and Poignant-Molina, L. 2015. Imaging Quaternary glacial deposits and basement topography using the transient electromagnetic method for modeling aquifer environments. Journal of Applied Geophysics, 119: 36–50. Elsevier. doi:10.1016/j.jappgeo.2015.05.006.

Telford, W.M., Geldart, L.P., and Sheriff, R.E. 1990. Applied geophysics. In 2nd edition. Edited ByC.U. Press. Cambridge university press, Cambridge.

Theimer BD, Nobes DC, Warner BG (1994) A study of the geoelectrical properties of peatlands and their influence on ground-penetrating radar surveying1. Geophys Prospect 42:179–209

Ulrich, C., and Slater, L. 2004. Induced polarization measurements on unsaturated, unconsolidated sands. Geophysics, 69: 762–771. Society of Exploration Geophysicists.

Van Heteren S, Fitzgerald DM, Mckinlay PA, Buynevich I V (1998) Radar facies of paraglacial barrier systems: coastal New England, USA. Sedimentology 45:181–200

Van Overmeeren RA (1994) Georadar for hydrogeology. First Break 12:401–408

Veillette, J.J., and Thibaudeau, P. 2004. Géologie des formations en surface et histoire glaciaire. Cadillac, Québec: Geological Survey of Canada,“A” Series Map A, 2019.

Walter, J., Rouleau, A., Chesnaux, R., Lambert, M., and Daigneault, R. 2018. Characterization of general and singular features of major aquifer systems in the Saguenay-Lac-Saint-Jean region. Canadian Water Resources Journal/Revue canadienne des ressources hydriques, 43: 75–91. Taylor & Francis. doi:10.1080/07011784.2018.1433069.

Waxman, M.H., and Smits, L.J.M. 1968. Electrical conductivities in oil-bearing shaly sands. Society of Petroleum Engineers Journal, 8: 107–122. Society of Petroleum Engineers.

CHAPITRE 4

USING GEOPHYSICAL DATA TO ASSESS GROUNDWATER LEVELS AND THE ACCURACY OF A REGIONAL NUMERICAL FLOW MODEL

Le chapitre 4 de cette thèse est présenté sous la forme d'un article scientifique et constitue le troisième outil d'investigation développé dans notre approche méthodologique visant à mieux évaluer le potentiel aquifère d'un milieu de dépôt quaternaire hétérogène et anisotrope. Ce chapitre met de l'avant l'utilisation de données géophysiques pour déterminer avec précision les niveaux d'eau dans un aquifère granulaire à nappe libre. Pour développer cet outil, deux simulations numériques ont été effectuées à l'aide du logiciel FEFLOW, l'une basée sur des données piézométriques régionales et l'autre sur des données géophysiques.

Les deux analyses numériques ont confirmé que les niveaux d'eau simulés, et les RMS obtenus à partir des données piézométriques et des différentes méthodes géophysiques (c.-à-d., TEM, ERT et GPR) étaient similaires, soit 3,81 et 2,76 m, respectivement. Grâce à une approche de modélisation discrète, cette étude montre que les niveaux d'eau souterrains estimés à l'aide des méthodes géophysiques sont comparables à ceux déterminés par observation directe. Les résultats illustrent comment les données géophysiques peuvent compléter les observations directes (telles que les forages et les levés piézométriques) afin de fournir des informations hydrauliques supplémentaires aux modélisateurs hydrologiques.

Cette contribution fournit à la communauté des modélisateurs un ensemble de nouveaux outils pour améliorer les modèles numériques d'écoulement régionaux, qui sont essentiels pour une gestion appropriée des ressources en eau souterraine. Ainsi, les méthodes géophysiques peuvent être une alternative peu coûteuse, non destructive, rapide, robuste et efficace aux méthodes d'observation directe pour caractériser les niveaux d'eau, les dimensions internes et la variabilité stratigraphique des aquifères non confinés dans les régions où les données sont limitées, permettant ainsi une évaluation plus précise des ressources en eau souterraine.

Le présent article a été soumis à la revue Hydrogeology Journal (IF : 3,18) le 17 juin 2022 et a été publié le 5 janvier 2023. https://doi.org/ 10.1007/s10040-023-02591-z.

Yan Lévesque [1, 2]*, Romain Chesnaux [1, 2], Julien Walter [1, 2]

[1]Université du Québec à Chicoutimi, Department of Applied Sciences, Saguenay, QC, G7H 2B1 Canada;

[2]Centre d'études sur les ressources minérales (CERM), Groupe de recherche risque ressource eau (R2EAU), Université du Québec à Chicoutimi, Saguenay, QC, Canada G7H 2B1, Canada

Email: romain_chesnaux@uqac.ca; julien_walter@uqac.ca

*corresponding author: yan.levesque1@uqac.ca

Orcid ID: YL: 0000-0002-6198-6315; RC: 0000-0002-1722-9499; JW: 0000-0003-2514-6180

4.1 ABSTRACT

The use of geophysical data to accurately determine water levels is demonstrated for an aquifer within the Saint-Narcisse moraine in the Mauricie region of southeastern Québec, Canada. Two numerical simulations were conducted using FEFLOW, one based on regional piezometric data and the other using geophysical data; the data were acquired through transient electromagnetic (TEM), electrical resistivity (ERT), and ground-penetrating radar (GPR) surveys. The three-dimensional geological and groundwater flow model was based on data from 94 boreholes, 5 stratigraphic cross-sections, and 20 TEM, 6 ERT (~ 960 m) and 4 GPR (~0.97 km) surveys. Both numerical analyses confirmed the simulated water levels, and the root mean square errors obtained

from the piezometric data and the multiple geophysical techniques were similar at 3.69 m and 2.76 m, respectively. Through a discrete modeling approach, this study shows that groundwater levels estimated using geophysical tools and methods and those determined by direct observation are comparable. The outcome illustrates how geophysical data can complement direct observations to provide additional hydraulic information to hydrologic modellers. Geophysical surveys provide an extensive set of soft data that can be leveraged to improve groundwater flow models and determine groundwater levels, particularly in areas characterized by limited direct piezometric information.

Keywords: Canada, numerical modeling, geophysical methods, aquifer properties, groundwater monitoring

4.2 INTRODUCTION

Using three-dimensional (3D) groundwater flow models is now standard practice for managing water resources and visualizing flow scenarios through Quaternary deposits. Numerical modeling provides a cost-effective tool for several areas (e.g., engineering, environment, mining, water management; Shi and Polycarpou 2005; Dunlap and Tang 2006; Chesnaux et al. 2013; Lévesque et al. 2016; Lévesque et al. 2017) and can be used to improve the protection of aquifers and adequately manage groundwater resources (Calvache et al. 2009, Preisig et al. 2014, Hudon-Gagnon et al. 2015, Cui et al. 2021). The construction of 3D hydrogeological models is usually not a simple task and remains particularly challenging when attempting to accurately characterize the complex architecture of regional aquifers (Ross et al. 2005). Building a reliable 3D model of an aquifer ideally relies on combining multiple avenues of investigation, e.g., borehole data, geophysical data, and sedimentology. Various simplifications of the stratigraphic reconstruction and parameters (e.g., the complex entanglement of the stratigraphic units, grain size variation, anisotropy, and materials properties) are often necessary. However, groundwater flow models must aim to provide the highest level of representativity of the natural system being modeled (Allen et al. 2008), although the targeted accuracy of a numerical model relates directly to its primary purpose and use (Hudon-Gagnon et al.

2011, 2015). Regardless of model complexity, validating model performance is crucial for groundwater models because recharge, hydraulic conductivity, and other model inputs cannot be measured accurately (Hill 2006). Only after a proper validation against observational data can numerical models provide adequate information and be used as a decision-making tool to properly manage groundwater resources (Doherty 2003). A major problem for groundwater management using computer models is that the final model is undermined by uncertainty. If the model parameters (e.g., hydraulic conductivity, recharge) are uncertain, so are model predictions (Gallagher and Doherty 2007). Consequently, a significant difficulty encountered by modelers is the lack of availability of observational data to confirm a model's reliability in representing actual aquifer conditions. Observational data (obtained mainly from boreholes and piezometric data) are used to validate the model's performance; however, the limited availability and scarcity of these data, given the time-consuming and expensive nature of borehole drilling campaigns, often renders modeling inaccurate. Moreover, boreholes are generally limited in number with considerable distance between sites, hindering the establishment of a correlation among sites. Boreholes are also often located along roads and near accessible and urbanized areas. This non-uniform distribution can result in a poor distribution of data sites, further complicating the validation of a numerical model.

Because of the potential to have a relatively dense spatial coverage, geophysical surveys can provide a large set of soft data to help model these aquifers (Slater 2007). Furthermore, geophysical surveys can efficaciously investigate subsurface sediments and provide a non-invasive, inexpensive, and effective means of characterizing the internal dimensions of the aquifers and their stratigraphic variability. Geophysical techniques have proven their ability to improve the geological framework and hydrostratigraphic characterization of aquifers, including hydraulic properties, spatial extension, and flow paths (McClymont et al. 2010; Galazoulas et al. 2015; Pandey et al. 2015; Parsekian et al. 2015; Simard et al. 2015; Costabel et al. 2017; García-Menéndez et al. 2018, Greggio et al. 2018; Kalisperi et al. 2018; Marker et al. 2015; Pondthai et al. 2020; Elbshbeshi et al. 2022, Othman et al. 2022). Over the past decade, many studies have been conducted using geophysical data to improve the accuracy of numerical modeling by incorporating additional data. The extensive literature studying these hydrogeophysical approaches is reviewed by Binley et al. (2010) and briefly summarized here,

highlighting what one might expect to be the dominant factors linking geophysics and hydrological model development. Some of these past studies use calibration to adjust hydrological model parameters to minimize the misfit between measured geophysical data and simulated variables (Gallagher and Doherty 2007, Huisman et al. 2010, Claes et al. 2020). Some authors go further and calibrate a physical-mathematical model of water flow to identify hydraulic properties and parameters of the vadose (unsaturated) zone (Binley and Beven 2003, Huisman et al. 2003, Farmani 2008, Binley et al. 2010, Yu et al. 2021). Several studies also demonstrate the ability of ground-penetrating radar (GPR) methods to enhance the estimation of the parameter distributions in the shallow subsurface (Kowalsky et al. 2004, Busch et al. 2013) or to estimate hydraulic parameters and propose approaches to validate if numerical experiments assume erroneous initial conditions (Tran et al. 2014, Yu et al. 2021). The ERT and GPR methods can also provide accurate hydrogeophysical parametrization for flooding events (Huisman et al. 2010) or capture heterogeneous soil properties and system states to assess and predict subsurface flow and contaminant transport (Kowalsky et al. 2005). Finally, some authors simply convert geophysical properties to observed hydrologic properties (e.g., water content) through a petrophysical relationship (Hinnell et al. 2010, Tran et al. 2014, Lévesque et al. 2021). Only a limited number of studies have employed a combination of various geophysical methods to enhance the precision of numerical modeling. Furthermore, to the best of the authors' knowledge, the utilization of water levels obtained from multiple geophysical techniques for validating the robustness of a numerical hydrogeological model remains largely unexplored. Lévesque et al. (2021, 2022) recently developed methods to locate the water table more accurately by improving the geophysical interpretation of regional stratigraphy and piezometric levels. These new methods represent an effective means of augmenting the amount of data available to validate the numerical model's performance. In fact, when only one or a small number of geophysical methods are used to enhance numerical modeling, the information may be far from complete.

This study's main goals are to (1) accurately assess water levels and provide additional information to flow models by combining multiple geophysical techniques; and (2) demonstrate that groundwater levels obtained through direct observation and from geophysical data are comparable. Indeed, the combination of geophysical methods can provide a valid alternative to geological and

piezometric data obtained from direct methods (drilling). The first validation of the model's performance (with boreholes) confirms the model's reliability for representing actual aquifer conditions and for subsequent simulations to evaluate the accuracy of geophysics-estimated data to confirm simulated water levels. The model's performance using both data sets is also compared through the root mean squared (RMS) error. Geophysical data were collected from the Saint-Narcisse moraine in eastern Mauricie (Québec, Canada) during the summer of 2020 and 2021. This data collection formed part of the Groundwater Knowledge Acquisition Program (PACES; Walter et al. 2018), sponsored by the Québec Ministry of the Environment (MDDELCC). Multiple surficial geophysical investigations, i.e., transient electromagnetic surveys (TEM), electrical resistivity tomography (ERT), and ground-penetrating radar (GPR), were applied to characterize this area of the Saint-Narcisse moraine aquifer. In addition to these collected geophysical data, the study included 94 boreholes, 5 stratigraphic cross-sections, and 26 piezometric surveys from the PACES spatial reference geodatabase for the study region (Chesnaux et al. 2011) to build the 3D geological model and validate reliability of the 3D flow model in representing real aquifer conditions.

4.3 STUDY AREA AND GEOLOGICAL OVERVIEW

4.3.1 BASEMENT GEOLOGY

The study area is located in the southeastern portion of the Mauricie region, situated between Montréal and Québec City (Fig. 45), and is characterized by the Saint-Narcisse moraine cutting across the region. The study area overlies both the St. Lawrence Lowlands and the Grenville Province and is characterized by a relatively flat topography. To the north of the moraine lies the Grenville Province, the youngest province of this Precambrian Canadian Shield, comprising high-grade igneous and intrusive metamorphic rocks (Rivers et al. 1993). The lithologic composition of the Grenville Province varies depending on the area; anorthosite, mangerite, charnockite, orthogneiss, paragneiss, migmatite, and marble are the main rocks found near the study area (Cloutier et al. 2013, Légaré-Couture et al. 2018). St. Lawrence Platform, i.e., St. Lawrence Lowlands, composed of Paleozoic sedimentary rocks, lies in the southern portion of the study area. These Paleozoic rocks

are composed of shales (Utica and Lorraine groups), carbonate (Trenton group), and Ordovician sandstone (Black River group), deposited in a marine environment (Occhietti 1977, Légaré-Couture et al. 2018). The St. Lawrence Platform is bordered to the southeast by the Appalachians and by the Canadian Shield to the northwest.

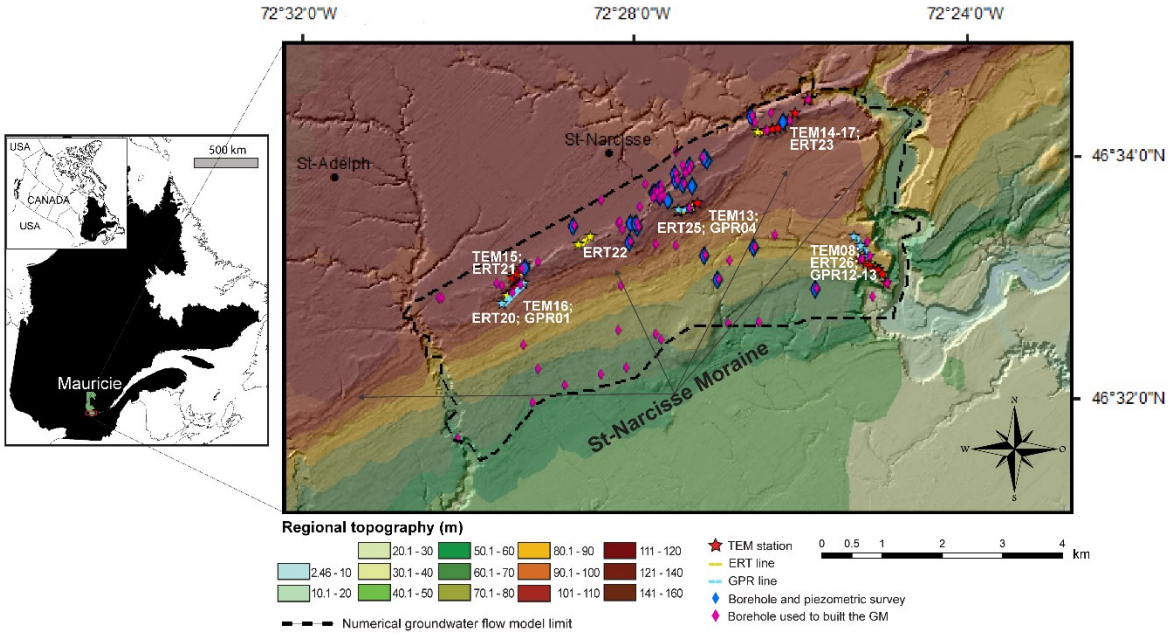

Figure 45: Regional topography of the study area and location of geophysical surveys and boreholes, i.e., piezometric surveys, acquired from the Saint-Narcisse moraine. The dashed black line represents the maximum extent of the numerical model proposed in this study. The blue rectangle in the map of North America **(top left)** represents the approximate location of the study area (not at scale). GM 3D groundwater model, TEM transient electromagnetic survey, ERT electrical resistivity surveys, GPR ground-penetrating radar surveys.

4.3.2 QUATERNARY SEDIMENT DEPOSITS AND THE SAINT-NARCISSE MORAINE

During the last glacial maximum (LGM), the LIS covered most of eastern Canada and produced glacial deposits composed mainly of diamicton, i.e., tills, by crushing, removing, and transporting rocks and sediments (Dyke 2004, Margold et al. 2015, Lévesque et al. 2019). Numerous frontal moraines produced during the deglacial phase record the often climate-related phases of LIS advance and retreat (Evans 2005, Benn and Evans 2010, Landry et al. 2012). The Saint-Narcisse morainic

complex in eastern Canada is a remarkably well-preserved, discontinuous frontal moraine that is one of the longest documented frontal moraines in Canada (Daigneault and Occhietti 2006). This long ridge, composed of glacial sediments, extends nearly 1400 km (Daigneault and Occhietti 2006) with a thickness of up to 120 m, although it varies locally between 1 and 20 m (Occhietti 1977). Quaternary surface deposits associated with the Saint-Narcisse moraine in the Mauricie region are related to the last glaciation, i.e., Wisconsinan glaciation and consists of various sedimentary facies that make up its stratigraphic sections: proximal and distal glaciomarine deposits, juxtaglacial and fluvioglacial deposits, i.e., ice-marginal outwash, subglacial or melt-out tills, and till wedges (Occhietti 2007).

During deglaciation, the isostatic depression caused by the Laurentide ice sheet (LIS) combined with a rapid global rise in sea level led to a marine transgression and the incursion of the Champlain Sea into the southern Mauricie region. The sea flooded the valleys of the St. Lawrence Lowlands and led to deposits reflecting both shallow and deep marine environments, i.e., proximal and distal glaciomarine deposits. This marine transgression reached an elevation of about 200 m asl (i.e., above present-day sea level; Parent and Occhietti 1988; Parent and Occhietti 1999) and lasted over 1800 years (13–11.2 cal. ka BP). During the early Holocene, the isostatic rebound triggered a marine regression, and the Champlain Sea deposited regressive sands during its retreat. During this regression, the Champlain Sea also deposited a thick layer of clay covered by regressive sand in low-lying areas around the moraine. During the Younger Dryas readvance of the LIS, the Champlain Sea reworked the glacial tills set down during the LGM and deposited proximal glaciomarine sediments on the sides and on top of the moraine, i.e., at higher elevations (Dyke and Prest 1987, Parent and Occhietti 1988, Daigneault and Occhietti 2006, Occhietti 2007). The till and fluvioglacial deposits were reworked by waves and currents to form visible terraces on the seaward side of the moraine (Fig. 45). These terraces are essentially composed of coastal and sublittoral sands deposited in the shallowest areas of the Champlain Sea (Occhietti et al. 2001, Occhietti 2007, Légaré-Couture et al. 2018). This imposing glacial-sediment complex is partially confined on its sides by clay, thus retaining water inside the morainic system. This geological entity is a deposit known for its complex stratigraphy and heterogeneity; it is also known that the main depositional sequence resulted in a series of thick interbedded sand and sand-gravel layers overlying a discontinuous till over the bedrock.

Although the moraine extends over 1400 km, this project focuses on 8 km around the municipality of Saint-Narcisse, the moraine's eponym. In this southeastern portion of the Mauricie region, the primary groundwater source is exploited locally to supply the surrounding municipalities, e.g., Saint-Narcisse, Saint-Prosper, and Saint-Maurice, attesting to the local aquifer capacity of the moraine.

4.4 MATERIALS AND METHODS

4.4.1 DATA COLLECTION

Information for producing the 3D stratigraphic and 3D groundwater flow models for this section of the moraine aquifer relied on fieldwork and the compilation of existing regional data from the spatial reference database of the Groundwater Knowledge Acquisition Program (PACES; Chesnaux et al. 2011; Walter et al. 2018). Data from 94 boreholes and 26 piezometric surveys (from boreholes) were acquired from the existing geodatabase. Also, 5 stratigraphic cross-sections, 20 TEM surveys (i.e., 20 stations), 4 ERT surveys (~960 m), and 4 GPR surveys (~0.97 km) were obtained during the summers of 2020 and 2021.

4.4.2 GEOPHYSICAL METHODS

4.4.2.1 GROUND-PENETRATING RADAR (GPR)

GPR is a non-invasive geophysical method that uses electromagnetic waves to detect electrical discontinuities representing changes in subsurface materials (Beres Jr and Haeni 1991; Neal 2004; Reynolds 2011). In many aspects, GPR is analogous to sonar techniques and seismic reflection and works by the transmission, propagation, reflection, and reception of discrete pulses of high frequency (MHz) electromagnetic energy (Reynolds 1987, Davis and Annan 1989). This energy is transmitted into the ground, where it encounters materials of differing electrical properties, e.g., rock type, grain size, grain shape, porosity, pore-fluid electrical conductivity, and saturation. Variations in these properties lead to changes in the velocity of the propagating electromagnetic wave (Davis and Annan 1989, Baker 1991, Neal 2004). As the dielectric properties of unconsolidated

sediments are primarily controlled by water content (Topp et al. 1980, Davis and Annan 1989), variations in porosity or the proportion of fluid occupying pore spaces significantly alter the velocity of the electromagnetic wave, thus producing reflections. GPR can provide accurate estimates (approximately to the meter) of water table height (Neal 2004; Reynolds 2011). A sufficient contrast between the relative dielectric constant of unsaturated and saturated materials will cause a significant proportion of the energy emitted by the device to be reflected; the water table is displayed as a horizontal reflection having a large amplitude on radargrams. GPR data across the study area were collected in 2021 to locate the water table, covering approximately 0.97 km of completed surveys (Fig. 45).

For the GPR surveys, a MALÅ GX (Ground Explorer) GPR system manufactured by MALÅ Geoscience were operated (now ABEM/MALÅ) with a MALÅ Controller application and real-time interpretation support and cloud storage via MALÅ Vision. A 12-V battery powered the GPR, and two shielded antennae were used, i.e., MALÅ GX HDR antennae, at 160 and 500 MHz. A 160 MHz antenna was also used because it provided the depth range required to locate the water table (generally located between 1 and 5 m) in this area of the moraine and also offered the necessary vertical resolution (approximately 0.1 m). The 160 MHz antenna has a maximum depth penetration of 5 to 15 m, depending on the sediment's velocity. The GPR data were collected in a continuous recording mode with a real-time interpretation from MALÅ AI at two-way travel-time settings that varied between 50 and 200 ns. All radargrams were processed using the MALÅ Vision program, and mean velocity was assumed on the basis of the interpretation of the sedimentary facies described by Lévesque et al. (2021) for this area of the Saint-Narcisse moraine, $v = 0.065\ m \cdot ns^{-1}$ for saturated sand, and $v = 0.1\ m \cdot ns^{-1}$ for unsaturated sand. In fact, Lévesque et al. (2021) propose a stratigraphic calibration chart that links the sedimentary facies (i.e., clay, sand, sand-gravel), the associated electrical resistivity, and water content of the Saint-Narcisse moraine in Eastern-Mauricie. This chart, combined with the electrical resistivity values acquired using the TEM and the ERT, gives us an overview of the type of sediment located on the subsurface. Consequently, it allows us to determine fairly accurate velocity data for most GPR sites.

4.4.2.2 ELECTRICAL RESISTIVITY TOMOGRAPHY (ERT)

ERT is a geophysical method used to describe the intrinsic resistance of electric current flow in geological media and estimate the spatial distribution of the bulk electrical resistivity. The bulk electrical resistivity is mainly related to sediment/rock type, porosity, saturation, grain size, and pore-fluid electrical properties. This method detects the water table and the conductivity differences in water saturation below the ground surface (Loke 2000, Reynolds 2011). For this study, vertical electrical soundings (VES) of resistivity were undertook using a Syscal Pro resistivity meter with a Wenner electrode configuration. The investigation depth of this instrument is about 45 m with 48 switchable electrodes, totaling 360 quadrupoles (Wenner arrays). Each resistivity profile consisted of a line of 48 electrodes, with 5 m spacing for a total length of 235 m. The least-squared inversion was processed using RES2DINV software to develop a model of subsurface resistivity, hereafter referred to as the true resistivity–depth profile (Loke and Barker 2006, Reynolds 2011). Outliers were removed from the data set before the final inversion (Loke 2006). The inversion required 3 to 5 iterations after the absolute error no longer changed significantly, and the results were less than 10%. The absolute error option displays the distribution of the percentage difference between the logarithms of the measured and calculated apparent resistivity values (Loke and Barker 1995, 2006, Loke 1999).

4.4.2.3 TRANSIENT ELECTROMAGNETIC INDUCTION (TEM)

TEM consists of a primary electromagnetic field (EMF) generated into a transmitter loop (Tx) of electrical wire deployed on the ground (20 × 20 m). As the primary field interacts with the subsurface geological materials, the decay of the EMF generates a secondary magnetic field that contains information about underground electrical properties. The TEM method does not involve direct electrical contact with the ground through electrodes and thus is effective in various environments, such as a glacial environment deposits (Parsekian et al. 2015, Kalisperi et al. 2018). The receptor loop (Rx; 5 × 5 m) is connected to a receptor that measures the rate of decay of the electromagnetic current, which is then inverted in electrical resistivity (Nabighian 1988, Fitterman and Labson 2005). Depth of investigation is determined by the size of the loop, the strength of the initial

current, and the resistance of the subsoil. TEM surveys were undertaken using an NT-32 transmitter and a 32II multifunction GDP receiver (MacInnes and Raymond 2001). The NT-32 unit consists of a portable battery and a transmitter–receiver (TX-RX) console that operate a square-sized transmitter loop (Tx) and receiver loop (Rx; in-loop configuration) for the measured induced voltage. Once the data were acquired, they were inverted to deduce the subsurface apparent resistivity distribution. First, the raw data were averaged using TEMAVG Zonge software (MacInnes and Raymond 2001, MacInnes et al. 2001). This step also filtered inconsistent data points, i.e., outliers, that must be deleted before the inversion. The second step used STEMINV software (MacInnes and Raymond 2001, MacInnes et al. 2001) to produce a consistent 1D smoothed inversion model of electrical resistivity versus depth on the basis of the iterative Occam inversion scheme (Constable and Parker 1987). Finally, MODSECT software was used to build a 2D model using the 1D resistivity model acquired with STEMINV (MacInnes et al. 2001; MacInnes and Raymond 2001). MODSECT interpolates vertical columns with Catmul–Rom splines to visualize the geometry of the geoelectrical structure of each line.

For TEM and ERT surveys, the resistivity values were associated with unsaturated and saturated sediments, above and below the water table. The electric current circulates in the sediment, mainly by volume conduction (or electrolytic conduction) through the pore water of these sediments (Abu-Hassanein et al. 1996, Shukla and Yin 2006, Pandey et al. 2015). Consequently, above the water table, resistivity values are high and associated with unsaturated sediments, whereas below the water table, the associated resistivity values are much lower and are related to saturated sediments. The high contrast between different values of electrical resistivity (between unsaturated and saturated sediments) determines the location of the water table. When the resistivity values are greater than 1,000 Ωm, the bedrock is reached because the electrical resistivity values of crystalline or sedimentary rocks are significantly higher than those of sediments. These rocks have resistivity values ranging between 1,000 and 100,000 Ωm (Palacky 1993).

For ERT and GPR, the observed point-based locations were selected at the beginning and end of each 2D line. Additional observed points could also have been used at different distances along

the 2D profile, but for a regional scale numerical model, these points being very close to each other, it was not necessary to add more. Indeed, the two extremities of a 2D profile (the greatest distance between the observation points) provided a suitable density of information. Each station serves as a location for the observed points for the TEM.

4.4.3 3D MODELING AND MODEL PARAMETERS

4.4.3.1 3D GROUNDWATER FLOW MODEL

The 3D groundwater flow was modeled using the FEFLOW® 7 modeling and simulating software. FEFLOW employs a finite-element numerical method, simulating groundwater flow by solving the basic balance equations in porous and fractured media for complex geometries (Diersch 2013). The finite-element method can easily incorporate properties such as anisotropy and heterogeneity or irregular and curved aquifer boundaries into the numerical model (Diersch 2013). Such particularities are typically observed in unconsolidated aquifers. This software allows modeling in 1D, 2D, or 3D in a steady or transient state and saturated (or not) conditions. In this case, the system is considered to be saturated. The simulations were undertaken using the free and movable surface mode and a steady-flow regime for an unconfined granular aquifer overlying the bedrock. The model also uses an adaptive grid, which allows the model surface to correspond to the elevation of the free surface, thus representing an unconfined aquifer.

4.4.3.2 STRATIGRAPHIC RECONSTRUCTIONS AND THE 3D GEOLOGICAL MODEL

A discrete modeling approach was selected to build the 3D geological model and obtain an accurate and coherent computer representation of this Quaternary basin, covering an area of about 26 km². This stratigraphic reconstruction using Leapfrog Geo was necessary to provide a more detailed and realistic stratigraphic representation than possible via flow simulation software such as FEFLOW. This 3D geological model is easily exported from Leapfrog in interoperability mode with FEFLOW. The 3D geomodeling system Leapfrog Geo software package (ARANZ Geo Ltd.) was used for this part of the model development. This software is designed to build and analyze geologic objects and their properties. However, delineating confining layers and subsurface aquifers in these complex

heterogeneous settings is challenging, and require an accurate stratigraphic reconstruction to build an accurate 3D flow model.

The modeling process began by determining the top boundary using a digital elevation model (DEM) produced with ArcGIS. Precise elevations (i.e., in meters) for each borehole, stratigraphic cross-section, and geophysical data were acquired, i.e., TEM, ERT, and GPR, to increase the precision in the top layers. To accurately determine the elevation, i.e., ~1 m, LiDAR, i.e., laser imaging detection and ranging data were used. Emphasized precise elevations are important to ensure that the obtained geophysical results and water table elevations (acquired by piezometric surveys in the boreholes) were not erroneous and introduced bias and error into the numerical flow model. Then the upper surfaces of the sand and sand-gravel as the major units in the moraine were modeled (Fig. 46), a deposit known for its complex stratigraphy and heterogeneity. Simulated as a discontinuous layer between sand and bedrock, the till unit has a local maximum thickness of 25 m and an average thickness of 1 to 5 m (Occhietti 2007). A combination of bedrock and till units underlie this aquifer, although they are unevenly distributed. The sand unit directly overlies bedrock where there is no till. Each layer is constrained by an upper surface and a lower surface for a total of 4 layers (homogeneous), three of which are from Quaternary deposits, i.e., sand, tills, sand and gravel (Fig. 45). This stratigraphic reconstruction is simplified, and several critical parameters are not considered, including grain size variations and the complex entanglement of the stratigraphic units. Several authors as demonstrated that simplified models are often the most accurate, and modelers can simplify a model without significant loss of accuracy in the simulation (Benzaazoua et al. 2004, Hill 2006, Hudon-Gagnon et al. 2015, Doherty and Moore 2020). The hydraulic properties of the materials, i.e., hydraulic conductivity, porosity, and the grid, were integrated directly into Leapfrog Geo. Then, the hydrogeological limits were determined according to the boundary conditions necessary to build a numerical flow model, i.e., the Croche and Batiscan rivers to the east and west and two impermeable zones to the north and south (Figs. 45 and 46). These impermeable zones are related to the thick layer of clay deposited by the Champlain Sea during the Holocene. A model layer comprised a grid of tetrahedral elements in both 2D and 3D, and the grid was refined at the model's

edge for a total of 166,348 elements and 83,376 nodes. In Leapfrog, to build a 3D model, the modeler first need to generate the meshing in a 2D model.

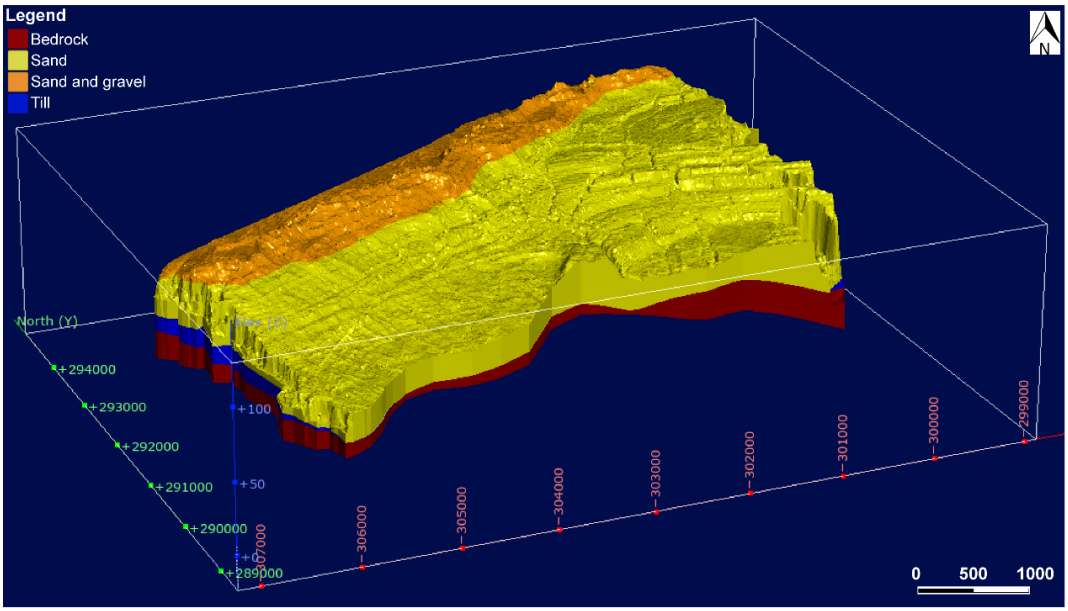

Figure 46: A simplified 3D geological model of the unconfined aquifer of the study area within the Saint-Narcisse moraine, southeastern Québec, depicting four layers of stratigraphic architecture. The model covers approximately 26 km^2. The vertical exaggeration 15x.

4.4.3.3 MODEL PARAMETERS AND MATERIAL PROPERTIES

The parameters to calculate groundwater flow included the rate of groundwater recharge, the bottom and the top elevation of the aquifer, and the hydraulic conductivity, i.e., Kxx, Kyy, Kzz, respectively. Because many towns and villages in the southeastern Mauricie region use groundwater as a source of drinking water supply, there are a number of available hydrogeological consulting reports covering a large part of the region. These reports constitute an essential source of information regarding pumping test data, which have been used to assign hydraulic conductivity to the sediments/layers. The vertical hydraulic conductivity (Kzz) was set using 10% of the horizontal value (Kxx/Kyy; Table 13), according to a well-established rule of thumb (Hudon-Gagnon et al. 2015).

TABLE 13: Properties of materials in the groundwater model of the Saint-Narcisse moraine. ø means that the bedrock was considered an impervious limit at the base of the moraine aquifer.

Hydraulic Parameters (measured)		
Geological layer	Kxx and Kyy (m/j)	Kzz (m/j)
Sand and gravel	18.72	1.87
Sand (littoral and fluvioglacial)	4.72	0.47
Tills	1.52	0.15
Bedrock	ø	ø

The recharge for the entire Saint-Narcisse moraine aquifer in southeastern Mauricie was set at 350 mm·year. The recharge of the Mauricie region is well constrained because of the previous work of the PACES investigations in the Lanaudière and Mauricie regions of Québec (the PACES-LAMEMCN program; Chesnaux et al. 2011; Walter et al. 2018). An element investigated by PACES was the hydraulic connections between bedrock aquifers and the overlying granular aquifers. Boumaiza et al. (2022) calculated the recharge of the Mauricie region using a water budget approach (Steenhuis and Van der Molen 1986), which considers that the difference between the input and output fluxes of water in the aquifer system is equal to the change in water storage (Boumaiza et al. 2020, 2022). For this study area, the parameters used to calculate the recharge were the estimated vertical inflow from rainfall and snowmelt, the surface runoff (RuS), and the actual evapotranspiration (AET).

4.4.3.4 BOUNDARY CONDITIONS

Boundary conditions are a crucial parameter for constraining the simulation. In FEFLOW, boundary conditions can be simulated according to various conditions: fixed-head boundary (Dirichlet conditions), fluid flux (Newman conditions), and fluid transfer (Cauchy conditions). In this study area, the model's northern and southern limits were considered impermeable (no-flow boundary related to clay) because the granular deposits, i.e., sand/sand and gravel, composing the moraine beyond these limits are not present in this area. The low flow of groundwater through the impermeable clay layer

(i.e., in low-lying areas around the moraine, north and south) that overly the bedrock is considered unimportant for flow dynamics in the moraine aquifer system. The eastern and western boundaries of the model are considered fluid-transfer conditions, and the nodes are assigned/located along the Batiscan River to the east between 69 m and 11 m (i.e., elevation) and the Croche River to the west between 96 m and 52 m. The eastern and western limits are set at the Batiscan and Croche rivers, as the aquifer lies between these rivers and has a connection to them. Moreover, given the high contrast between hydraulic conductivity values in crystalline rock and granular deposits, the bedrock was considered as an impervious limit at the base of the moraine aquifer, which stretches across the whole model. A combination of bedrock and till units underlie this aquifer, and given that the till unit is discontinuous and unevenly distributed, the sand unit sometimes directly overlies the bedrock. The flow model did not consider groundwater pumping from municipal wells as these are not present in the study area. The private wells were not considered because of their negligible pumping rate at a regional scale, and their values are not precisely known.

4.5 RESULTS

4.5.1 GEOPHYSICAL RESULTS AND THE WATER TABLE

All three geophysical methods clearly identified the water levels in saturated sediments (Figs. 47, 48, 49 and 50) in the electronic supplementary material (ESM)). The water table elevation was often identifiable, as was the height of the bedrock when the survey was sufficiently deep. The uncertainty of water-level elevation was approximately 1 m when interpreted with the ERT raw data. From the diffusion equation related to electrical currents, the resolution of the resistivity method (ERT) decreases exponentially with depth (Loke and Barker 1995; Loke and Barker 1996; Loke 1999). However, it is nonetheless possible to determine a structure having a size of 1 m at a depth of less than 10 m (Loke and Barker 1995; Loke and Barker 1996; Loke 1999), a sufficient resolution to accurately determine water levels in this study.

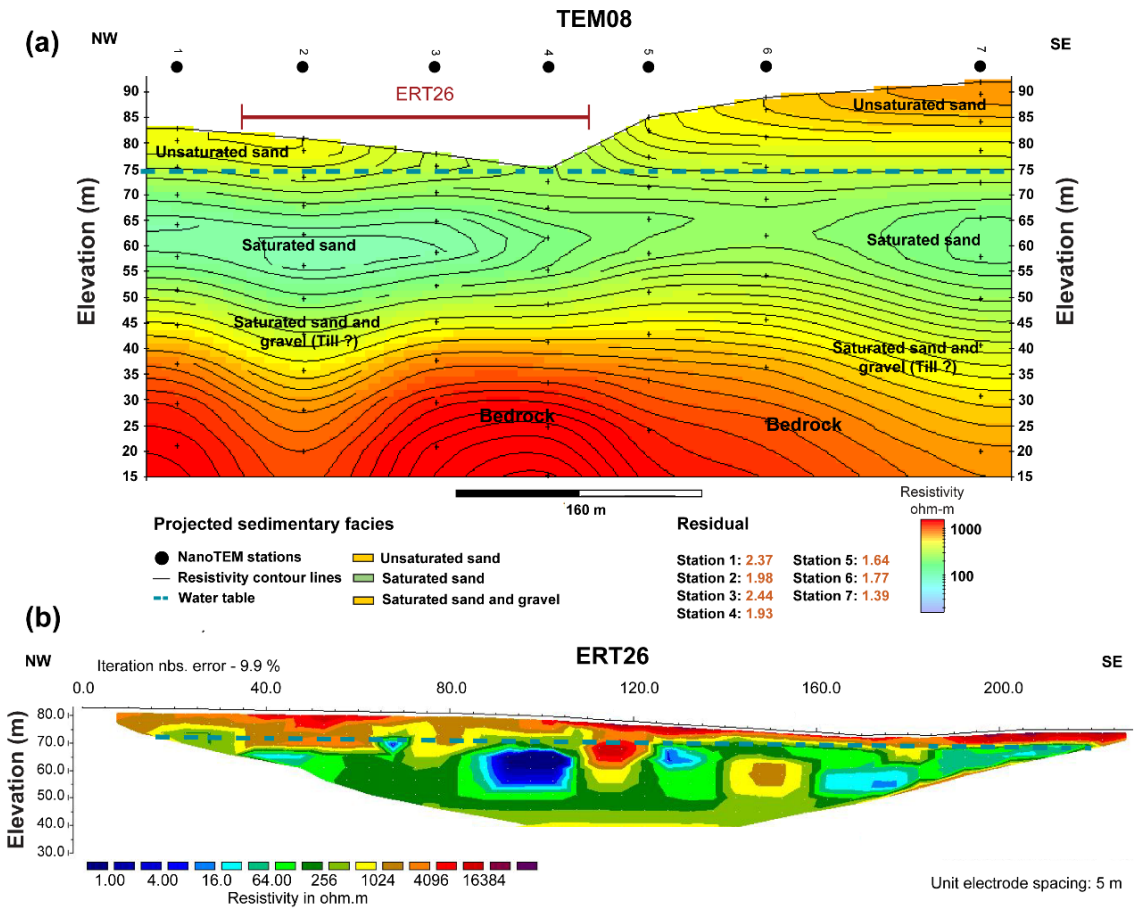

Figure 47: **a.** The interpreted 2D TEM Section TEM08 acquired from the study site along the Saint-Narcisse moraine, southeastern Québec. The surface deposit elevation was obtained from LiDAR data. The blue-dashed line represents the projected water table obtained from direct observations (boreholes, piezometric surveys); **b.** True resistivity– depth profile of ERT26 for the same location and water table (blue-dashed line).

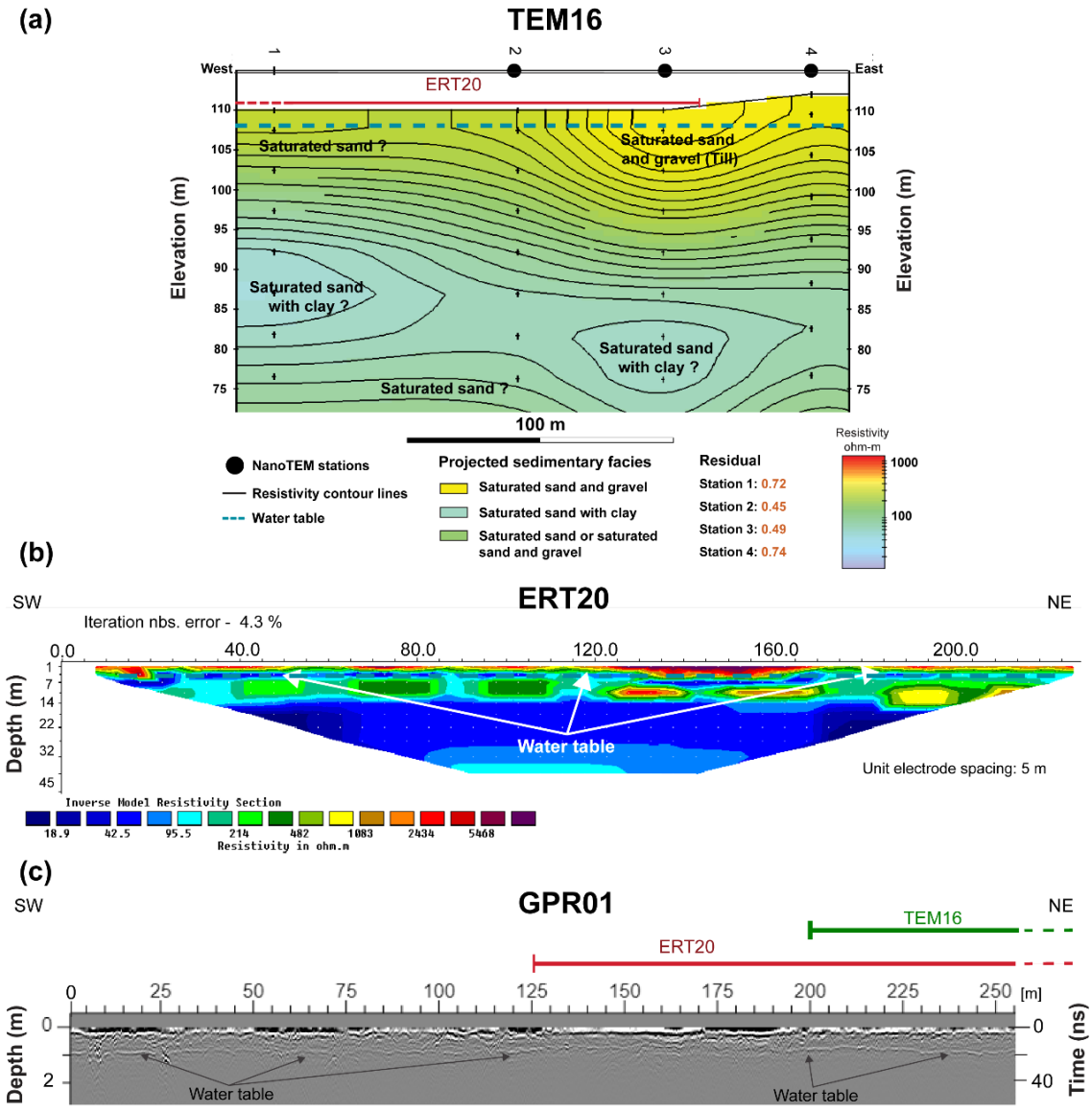

Figure 48: **a.** The interpreted 2D TEM Section TEM16 acquired from the study site along the Saint-Narcisse moraine, southeastern Québec. The surface deposit elevation was obtained from LiDAR data. The blue-dashed line represents the projected water table acquired from direct observations (boreholes, piezometric surveys); **b.** True resistivity–depth profile of ERT20 for the same location and water table (arrowheads); **c.** Radargram GPR01 acquired using 160 MHz antennae with a MALÅ GX (Ground Explorer) system for the same location. The water table reflection is clearly visible at about 1 m depth (arrowheads).

The water table was distinctly evident as a horizontal and continuous reflector on radargrams (Figs. 47, 48, 49 and 50). The reflection arising from the water table may be seen clearly as a coherent reflection with a large amplitude in GPR12 and GPR13 (Fig. 49).

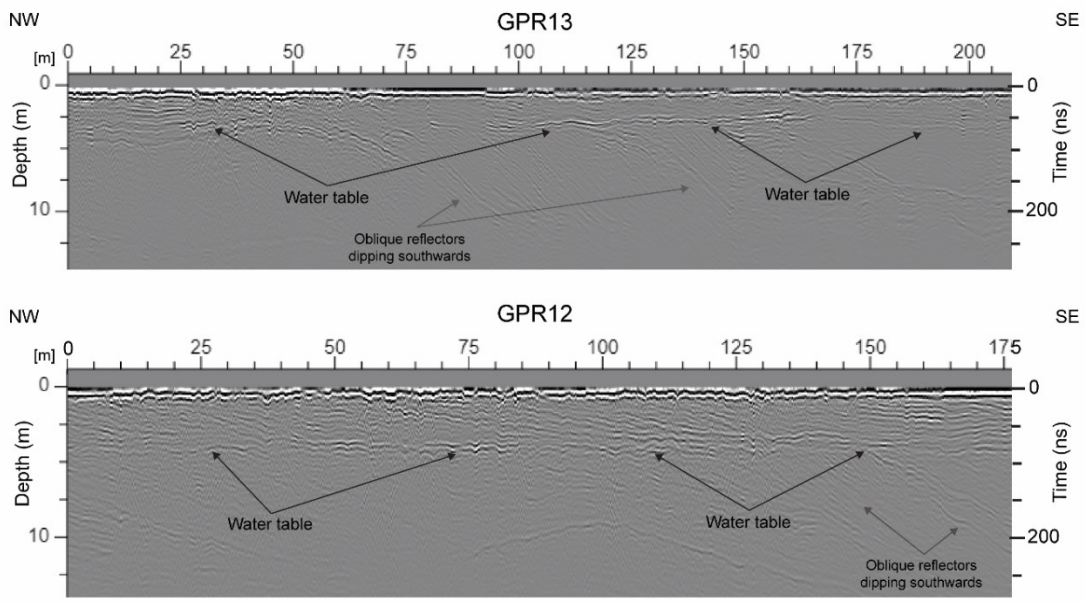

Figure 49: Radargrams were acquired from the study site along the Saint-Narcisse moraine, southeastern Québec, using 160 MHz antennae and a MALÅ GX (Ground Explorer) system. The water table reflection is clearly seen at about 4 m depth (flat-lying reflection, arrowheads) and multiple oblique southward-dipping reflectors.

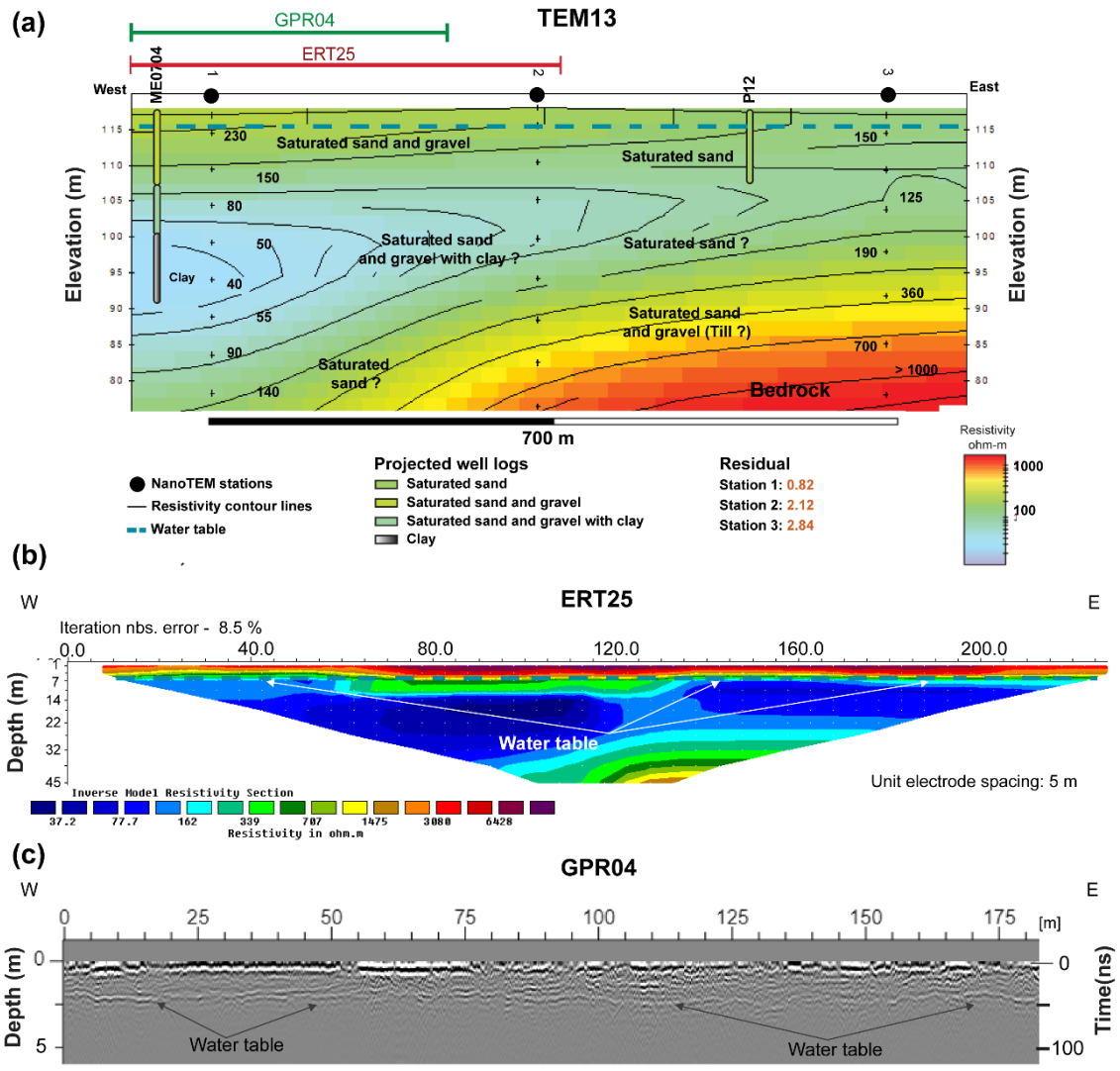

Figure 50: **a.** The interpreted 2D TEM Section TEM13 acquired from the Saint-Narcisse moraine, southeastern Québec (Lévesque et al. 2021). The surface deposit elevation was obtained from LiDAR data. The blue dashed line represents the projected water table determined from direct observations (boreholes, piezometric surveys); **b.** True resistivity-depth profile of ERT25 for the same location, showing the top of the water table (arrowheads); **c.** Radargram GPR04 acquired using 160 MHz antennae with a MALÅ GX (Ground Explorer) system at the same location. The water table reflection is evident at a depth of about 2.5 m (arrowheads).

4.5.2 MODELING

4.5.2.1 SIMULATION RESULTS

A single groundwater model was developed for the unconfined aquifer of this section of the Saint-Narcisse moraine. The evaluation of model performance validates the quality and accuracy of

a simulation performed by two flow models using observed and simulated results. The validation used regional groundwater level data determined through either borehole data or geophysical methods. To validate the performance of each model, a root mean square error (RMS; Equation 1) were calculated. In this study, the term "validate the performance of a model" (or "validation") means confirming the relevance of the results acquired from a numerical analysis using observed geophysical or piezometric data. Here, geophysics-estimated groundwater levels also serve as observed data. The RMS acts as an indicator of modeling quality in terms of model precision and accuracy and indicates the reliability of the model in representing reality (Chesnaux et al. 2017, Dewar and Knight 2020).

The resulting numerical flow model from the simulation (Figs. 51 and 52) showed that the groundwater flows from the northwest topographic summit of the moraine toward the southeast. The hydraulic relationship between groundwater and rivers is strong, and the aquifer replenishes both the Croche and Batiscan rivers. The global water budget for the model produced a total regional flow of 17,684 $m^3 \cdot day^{-1}$ and an imbalance value (i.e., water mass balance) of −0.33 $m^3 \cdot day^{-1}$ for the study area. The imbalance value shows the numerical error of the mass transport for the specified subdomain over the entire simulation period. It is the difference between the change in model storage and net boundary fluxes by summing the mass amount of all boundaries, storage losses and gains, sources and sinks, and internal transfers. The imbalance value should be close to 0 (residual mass − balance error) to confirm that the simulation achieved good convergence and provided consistent results.

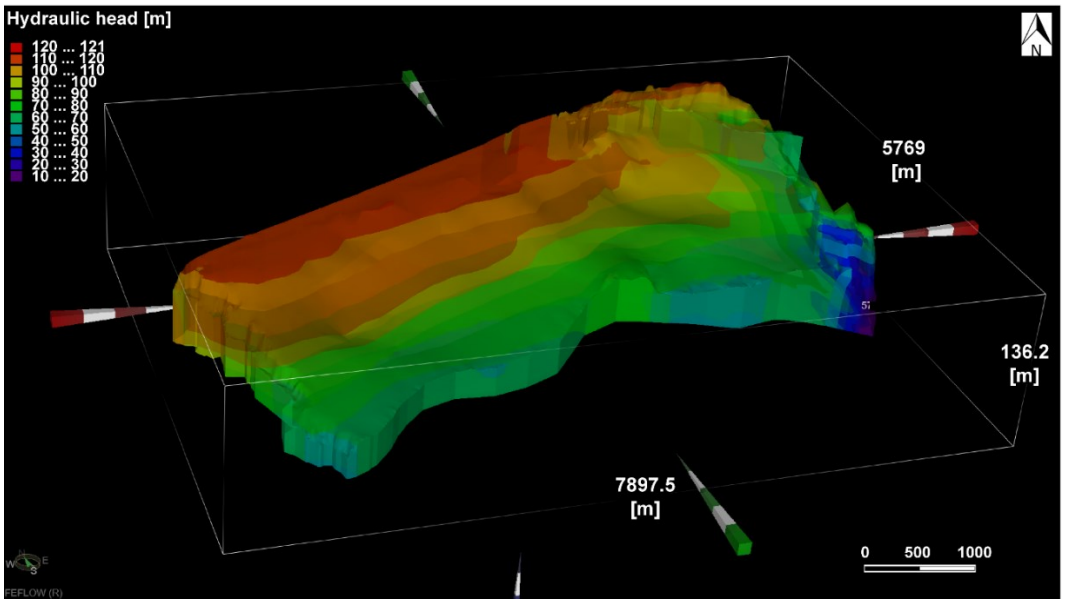

Figure 51: 3D flow model of the Saint-Narcisse moraine unconfined aquifer, southeastern Québec. Equipotential lines represent the simulated hydraulic head. The simulation results show a maximum hydraulic head in the northwest with a general southeastern flow.

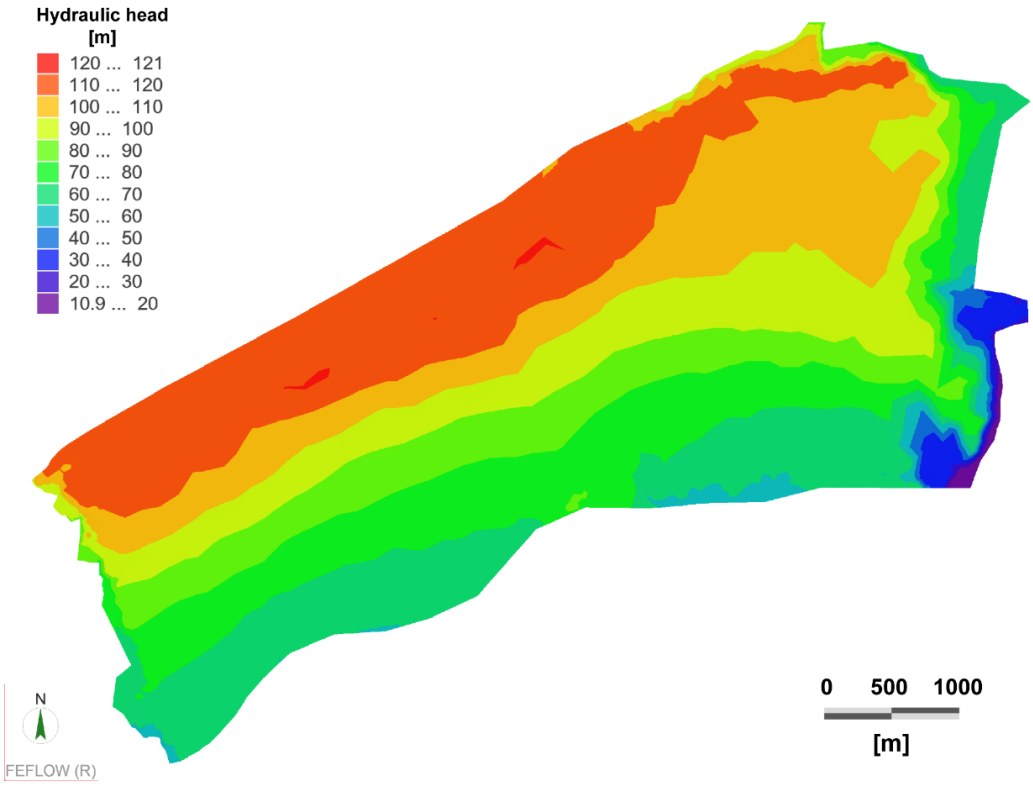

Figure 52: Simulated equipotential lines of the hydraulic head over the study area along the Saint-Narcisse moraine in southeastern Québec. The simulation results show a maximum hydraulic head in the northwest with a general southeastern flow.

4.5.2.2 COMPARISON OF NUMERICAL RESULTS WITH BOREHOLE DATA (PIEZOMETRIC SURVEYS)

The study area contained a relatively high number (26) of piezometric surveys. The high number of boreholes for this relatively small area, i.e., 26 km², ensures a proper interpolation of static groundwater levels. The water table varied between 0 and 10.5 m below the ground surface, depending on the topographic elevation. An interpolated map of groundwater depth, i.e., piezometric map, of the Saint-Narcisse moraine in the Mauricie region was built by Lévesque et al. (2021), confirming the groundwater levels of this study. This map was created to define regional piezometry using a sizable number of evenly distributed piezometric surveys, i.e., 465 surveys, conducted on and around the Saint-Narcisse moraine. Then, the simulated hydraulic head, i.e., water table

elevation, was compared with the observed water levels from the 26 boreholes used to evaluate the model's performance and validate the quality and accuracy of the simulation (Table 14).

Table 14: Hydraulic head in the study area acquired from 26 piezometric surveys of boreholes (observed) and numerical results (simulated).

ID	Boreholes	Date of drilling	Observed (m)	Simulated (m)
1	S769	15-09-1981	112.04	114.49
2	S770	15-09-1981	114.64	115.70
3	S967	15-09-1983	103.81	105.23
4	S969	27-07-1982	77.75	75.13
5	S1012	23-09-1990	108.61	114.15
6	S1527	18-12-1987	84.89	86.14
7	S2067	26-05-2005	84.75	88.23
8	S2123	06-06-2005	61.54	65.28
9	S3050	17-04-2017	105.79	112.45
10	F2240	26-09-1990	112.42	115.21
11	F2241	26-09-1990	112.8	115.62
12	F2425	01-01-2002	117.46	119.54
13	F2426	01-01-2002	111.38	118.70
14	F2427	01-01-1987	116.12	117.13
15	F2430	01-01-1987	106.61	113.40
16	F2433	01-01-1987	105.97	113.22
17	F2424	01-01-1987	111.64	116.98
18	F2435	29-03-2007	115.35	117.34
19	F2438	29-03-2007	110.7	115.07
20	F2439	30-03-2007	114.21	115.94
21	F2440	30-03-2007	113.94	117.72
22	F2429	23-05-1985	116.79	114.56
23	YL017	21-08-2020	114	116.90
24	YL018	22-08-2020	109	109.71
25	YL022	23-08-2020	118	118.68
26	YL020	24-08-2020	115	113.84

After validation, this model produced a RMS of 3.69 m (Fig. 53), a relatively low value indicating an acceptable degree of representativity (acceptable RMS value; Wise 2000; Chesnaux 2013; Chesnaux et al. 2017). The simulation results matched very well with the observational data (see Fig. 53 showing a good correlation between the simulated and observed values; R2 = 0.9994). These results show the model's acceptable representativity to simulate the hydraulic head and underground flow within this portion of the Saint-Narcisse moraine.

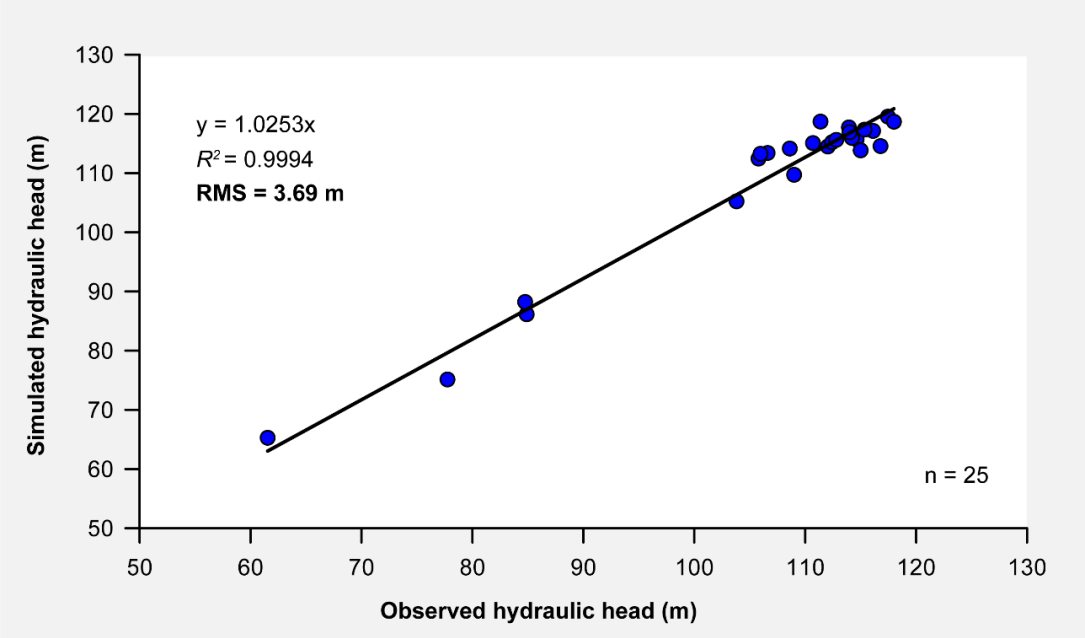

Figure 53: Root mean square error (RMS) of the hydraulic head from the numerical results (simulated values) and the borehole-based observed values (observed values) for the study site along the Saint-Narcisse moraine aquifer, southeastern Québec. The observed values were acquired from 26 boreholes (piezometric surveys). The black line represents the line of perfect fit.

4.5.2.3 COMPARISON OF NUMERICAL RESULTS WITH GEOPHYSICAL RESULTS

Similar to the borehole data, the geophysical results produced a large amount of water depth–related data (Figs. 45, 47, 48, 49 and 50). Thirty-three inferences of groundwater depth were obtained through the three geophysical methods (Table 15). Access to some remote areas of the moraine was challenging to conduct geophysical surveys; therefore, the obtained survey data were not always evenly distributed, and the results contained gaps in the south–central and southwestern areas of the model.

TABLE 15: Hydraulic head in the study area as acquired from 33 observations of the groundwater depth on the basis of TEM, ERT, and GPR geophysical methods (observed) and numerical results (simulated). For each geophysical survey, the water level has been estimated to be at approximately the same elevation.

ID	Stations	Date of surveys	Observed (m)	Simulated (m)
1	ERT20_1	21-08-2020	108	111.15
2	ERT20_48	21-08-2020	108	111.16
3	ERT23_1	22-08-2020	111	112.37
4	ERT23_48	22-08-2020	111	110.03
5	ERT25_48	14-10-2020	116	114.64
6	ERT26_1	14-10-2020	76	78.83
7	ERT26_48	14-10-2020	76	70.74
8	TEML8_1	14-08-2020	76	79.91
9	TEML8_2	14-08-2020	76	77.02
10	TEML8_3	14-08-2020	76	74.11
11	TEML8_4	14-08-2020	76	71.56
12	TEML13_2	22-08-2020	117	114.71
13	TEML13_3	22-08-2020	117	114.04
14	TEML14_1	22-08-2020	109	108.76
15	TEML14_2	22-08-2020	109	109.26
16	TEML14_3	22-08-2020	109	110.15
17	TEML15_1	15-10-2020	109	113.59
18	TEML15_2	15-10-2020	109	114.12
19	TEML16_1	15-10-2020	108	111.04
20	TEML16_2	15-10-2020	108	110.85
21	TEML16_3	15-10-2020	108	110.87
22	TEML16_4	15-10-2020	108	111.28
23	TEML17_1	16-10-2020	110	110.89
24	TEML17_2	16-10-2020	110	109.81
25	TEML17_3	16-10-2020	110	109.23
26	GPR1A	11-10-2021	108	111.95
27	GPR1B	11-10-2021	108	111.76
28	GPR4A	11-10-2021	118	117.09
29	GPR4B	11-10-2021	118	115.50
30	GPR12A	12-10-2021	79	76.64
31	GPR12B	12-10-2021	79	82.02
32	GPR13A	12-10-2021	84	88.60
33	GPR13B	12-10-2021	84	83.82

After the validation of the quality and accuracy of the simulation (the model's performance), the simulated hydraulic head (compared with the water levels obtained using geophysics-estimated groundwater levels) produced a RMS of 2.76 m (Fig. 54), a low value indicating a reliable model, confirmed by the R2 of 0.9989 for the correlation between the simulated and observed values. As observed with the borehole-based validation, the geophysical method–based model performance validation confirmed that the model represented reality and could be used to simulate the hydraulic head and underground flow in this region of the Saint-Narcisse moraine.

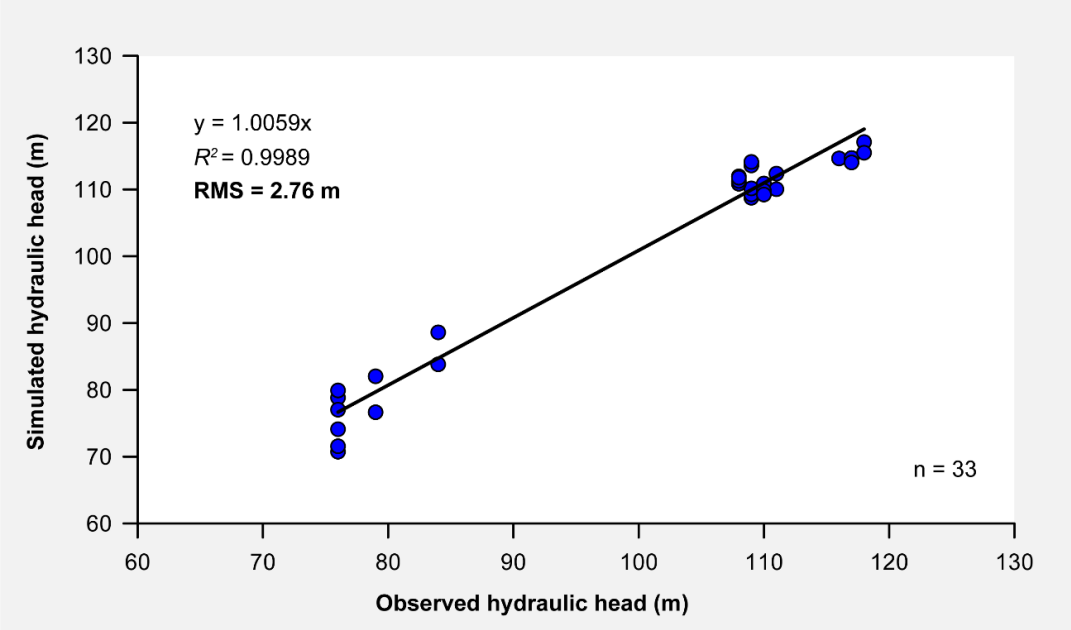

Figure 54: Root mean square error (RMS) of the hydraulic head from the numerical results (simulated values) and the geophysical method-based observed values (observed values) for the study area along the Saint-Narcisse moraine aquifer, southeastern Québec. The observed values were acquired from 33 observations of water levels derived from transient electromagnetic (TEM), electrical resistivity (ERT), and ground-penetrating radar (GPR) surveys. The black line represents the line of perfect fit.

4.6 DISCUSSION

4.6.1 ACCURATELY ASSESSING WATER LEVELS USING MULTIPLE GEOPHYSICAL APPROACHES

In this study, geophysical data provided an excellent complement to direct observations (e.g., borehole logs, stratigraphic cross-sections, and piezometric surveys in wells) and were shown to be

an effective alternative to borehole surveys for characterizing the internal structures of deposits, the water table, and flow directions. The coupling of the ERT and GPR results with the TEM results of Lévesque et al. (2021) allowed us to accurately estimate the groundwater level. Furthermore, these TEM surveys were validated using boreholes and piezometric surveys aimed at locating and delineating the aquifers of this portion of the Saint-Narcisse moraine and the associated water levels (Lévesque et al. 2021). The uncertainty of water-level elevation was approximately 1 m at a depth of less than 10 m for the ERT and TEM raw data (Loke and Barker 1995; Loke and Barker 1996; Loke 1999). All three geophysical methods identified the water levels in saturated sediments (Figs. 47, 48, 49 and 50). By combining these different data sets, the uncertainty associated with the location of groundwater levels is significantly reduce and provide an additional tool to determine hydraulic heads for the numerical flow model. Combining multiple geophysical techniques can significantly reduce the uncertainty inherent to geophysical methods, which are indirect observations of the subsurface. In the last decades, several contributions have used multiple geophysical techniques to complement direct observations. For example, Bowling et al. (2005, 2007) applied this approach to define conceptual geological models, and Bersezio et al. (2007) and Goutaland (2008) used multiple techniques to obtain a more complete analysis of sedimentary deposits and stratigraphic units. Combining multiple approaches allowed Costabel et al. (2017) and McClymont et al. (2011) to investigate the extent and depth of three freshwater lenses on North Sea islands and groundwater flow paths within proglacial moraine, respectively (McClymont et al. 2011, Costabel et al. 2017). Li et al. (2021) coupled TEM, nuclear magnetic resonance (NMR), and audio-frequency magnetotellurics (AMT) with stochastic groundwater modeling to predict the hydrological impact of a copper in situ recovery operation in the Kapunda region of South Australia (Li et al. 2021).

Combining multiple geophysical techniques to reduce uncertainty is critical because each method has its particular strengths and weaknesses. For example, TEM and ERT are often used; however, their resolution is sometimes not sufficiently fine to locate the water table precisely or characterize the sedimentary architecture. Thus, combining TEM and ERT with GPR allows us to reduce the amount of missing information between geophysical measurements, the water table, and sedimentary units. On the other hand, TEM and the ERT often provide information about the water

table at greater depths, as well as the lithology of a sedimentary deposit, which the GPR cannot provide.

Unlike GPR, which is more suited to characterizing poorly conductive sediments, e.g., sands and/or gravels Bristow and Jol 2003), TEM and ERT produce a good resolution in conductive grounds but have the disadvantage of characterizing resistant soils with difficulty (Spies and Frischknecht 1991). Indeed, there is a loss of signal when electromagnetic waves generated by the GPR encounter conductive deposits such as clay, volcanic ash, and saline environments (Reynolds 2011, Pondthai et al. 2020). ERT works very well on resistive and conductive, e.g., silts and clays, sedimentary deposits (Baines et al. 2002), but contact with the electrodes can be problematic if the environment is highly resistant, e.g., dry sand, boulders, gravel, frozen ground, ice, or laterite. As observed by Reynolds (2011), “ERT relies on being able to apply current into the ground, and if the resistance of the current electrodes becomes anomalously high, the applied current may fall to zero, and the measurement will fail.” TEM and GPR may be more effective in this situation, as they operate without contact with the medium (Kalisperi et al. 2018). TEM and ERT can obtain results, i.e., water table summit depth, at greater depths because GPR surveys depend on the conductive property of the materials, and the maximum depths of investigation rarely go beyond 20 m (Beres Jr. and Haeni 1991, Asprion and Aigner 1997, Mari et al. 1998, Milsom 2003, Neal 2004, Gascoyne and Eriksen 2005). In contrast, TEM and ERT can be applied from a few to hundreds of meters in depth (Galazoulas et al. 2015, Kalisperi et al. 2018). The GPR and ERT methods provide vertical sections (2D) of the subsoil, but TEM profiles are produced through interpolations between 1D soundings, and the limitations of this approach bear uncertainty related to the interpolation and the smoothing. Moreover, TEM does not permit characterizing the top subsurface layers under the transmission/reception device, and a “blind” thickness of 1 to 3 m is present depending on the configuration of the sounding, i.e., the type of device used, the size of the coil, the intensity of the current injected (Goutaland 2008, Reynolds 2011). Geometric errors in transmitter–receiver positions and topographic effects can also skew TEM results (Reynolds 2011). For ERT, the closer the electrodes, the better the resolution (Reynolds 2011). To obtain a satisfactory resolution and desired

depth, installing many electrodes over several hundred meters is necessary, but this approach requires greater resources and time.

Among these three geophysical approaches, the GPR was the most accurate for estimating the groundwater levels, given that the water table position was clear as a continuous, horizontal reflector having a large amplitude on radargrams (Figs. 47, 48, 49 and 50). The reflection produced by the water table in GPR12 and GPR13 can be seen clearly as a coherent reflection with a large amplitude (Fig. 49). Thus, the water table and the sedimentary characteristics (e.g., sedimentary structures, lithologic limits, horizon with high organic matter content) generate radar reflections, and fine vertical decametric-scale resolutions are also visible on radargrams (Neal 2004). Because of the high dielectric permittivity of the water, the water table reflects a strong contrast between the propagation speeds of radar in saturated and unsaturated sediments. Reynold (2011), however, commented that the water table can be sometimes difficult to detect with GPR because a contrast in the relative dielectric constant is necessary to reflect a significant proportion of the energy. A thick capillary zone makes it more difficult to obtain a clear contrast between the unsaturated and saturated sediments, and the total reflected energy is diminished greatly; the resulting reflection amplitude is too low to identify the water table clearly.

The geophysical methods of TEM and ERT are utilized to locate the water table in granular sediments by identifying contrasts in electrical resistivity. When a high contrast in electrical resistivity values is observed in TEM and ERT profiles (Figs. 16, 20, 22, 26, 27, 28, 30, 47), it often indicates the presence of the water table. Ideally, this observation should be corroborated by the GPR method and/or nearby piezometric surveys to strengthen this assertion. However, certain geophysical profiles exhibit no observable contrast in resistivity values (Figs. 24, 34A, B), which remain similar at the surface and in depth until the bedrock is reached. In this case, unless there is presence of clay, clayey sediments, or nearby interference, the GPR method typically confirms the presence of the water table at the surface (with a absence of vadose zone), and manual surface piezometric surveys may also confirm this observation. This, at least, is the method adopted in this study to detect and validate the presence of the water table. The advantage of combining several geophysical methods is that the

weaknesses of one method can be compensated by the other applied methods, especially if the complementary approaches are specifically chosen for this purpose. Multiple geophysical approaches (relying on various methods to collect data) and the amount of available geophysical data provided an opportunity to determine groundwater levels, and their combination significantly diminished the uncertainty of the results.

4.6.2 RMS AND THE VALIDATION OF A NUMERICAL FLOW MODEL WITH GEOPHYSICAL DATA

This study demonstrated that simulated water levels using multiple and combined geophysical approaches matched observed levels. The RMS obtained for the borehole-based validation of the model performance using piezometric data closely matched that of the geophysical method–based results at 3.69 m and 2.76 m, respectively. An ideal RMS value would theoretically be 0 m, signifying the model predicts exactly the observed water-level data with no difference between the observed and simulated water levels. The lower the RMS, the higher the accuracy of the model output to represent actual aquifer conditions. However, it is rare to obtain an RMS of 0 m because several parameters are to be considered, such as the uncertainties related to the seasonal variations in water levels at a regional scale, measurement errors, simplification of the stratigraphy, and the spatial heterogeneity of borehole distribution. For example, it is necessary to consider that the piezometric surveys were not all collected in the same season or during the same year, and there will necessarily be seasonal variations in water levels between spring and autumn or between different years. Indeed, northern regions (e.g., Québec and Canada) are characterized by high seasonal contrasts, and it is usual to observe water levels that vary by several meters depending on the season or the year.

In hydrogeology, an RMS better than a few meters cannot be expected and the results obtained for geophysical and borehole datas are acceptable and represent well the natural variations of the water levels. For this reason, this steady-state model is considered to be of good quality. Nevertheless, even when a numerical model is accurate, modelers cannot expect to produce a true picture of the subsurface and hydrogeological processes because of the limitations and efficacy of the investigation tools. In reality, most models are too simple because they cannot represent the

heterogeneity and the complexity of subsurface processes with perfect fidelity (Doherty and Moore 2020). Model success depends on the use and scale of the model in question, with the scale critical to the model's required complexity and detail, "Learning how to define the optimal compromise between simplicity and complexity is one of the biggest challenges facing current modeling practice" (Doherty and Christensen 2011). A hydrogeological flow model at the local scale may require very precise data, whereas a regional-scale model can successfully determine water levels, confirm flow directions, or assess transit flows even with average deviations of a few meters. Theoretically, the larger the scale, the higher the RMS, given that the database must contain more data to fulfill the needs of the study (a larger surface to cover) and consequently, the numerical simulation will necessarily lose accuracy and precision. Therefore, larger-scale models naturally present greater possibilities of errors, inconsistencies, and uncertainty. For a steady-state numerical model at the regional scale such as this study model (~26 km^2), a deviation of 3 to 4 m is satisfactory and indicates the model's reliability in representing reality. The same RMS, however, may not be valid for more local applications.

To evaluate the reliability of the geophysical data to represent actual aquifer conditions, the same step as for boreholes were used: a numerical simulation was conducted using FEFLOW® software and validate whether this model is suitable using multiple geophysical data sets (i.e., TEM, ERT, and GPR). The low RMS, i.e., 2.76 m, obtained after simulation with geophysically estimated data, suggests that the model is reliable in terms of accuracy and precision and is also consistent with the first validation of the model's performance carried out using borehole data, i.e., a RMS of 3.69 m. Consequently, geophysical data are an excellent addition for validating a flow model to provide additional hydraulic information and complement direct observations (i.e., boreholes and piezometric surveys).

4.6.3 AVAILABLE APPROACHES TO CONSTRAIN A NUMERICAL FLOW MODEL WITH GEOPHYSICAL DATA

Geophysical methods offer indirect observations of the subsurface. Consequently, they must be validated to confirm the subsurface information (in this case, groundwater depth). Several

approaches are available to develop representative groundwater flows model and correctly locate the water levels using geophysical data. The first approach, as mentioned in section ‘Accurately assessing water levels using multiple geophysical approaches’, is detecting water levels using various geophysical techniques. In such a case, the acquired results related to groundwater depth from one geophysical method are compared with those obtained from another (or multiple) method for the same location. The second approach involves acquiring existing data from piezometric surveys (mainly from boreholes and private and municipal wells). As suggested by Lévesque et al. (2021), only a few boreholes and/or piezometric surveys are required to validate geophysical results and the true location of the water table. This validation approach involves comparing the stratigraphic and piezometric information with the geophysical results to derive an empirical and local petrophysical relationship. This correlation between direct and indirect observations allows extrapolating the results, i.e., water levels, over a larger area, even for zones lacking observational information. For example, borehole data—stratigraphy—can be correlated with electrical resistivity values acquired with TEM or ERT surveys for unsaturated and saturated Quaternary deposits. Then, the resistivity values associated with each class of sediment can be transposed to the geophysical data acquired in areas having no or limited drilling or piezometric surveys and thus extend the coverage of groundwater level estimates (Lévesque et al. 2021). If there are sufficient piezometric data from boreholes to validate the model directly, geophysical approaches can also provide an additional tool to acquire water levels, especially in remote areas. Geophysical data can therefore improve the accuracy of a numerical model by increasing the total data set, i.e., boreholes and geophysical data, to validate the simulated water levels. As mentioned by Hill (2000) in her "Guidelines for effective model calibration," the most important steps to develop a high-quality model are to apply the principle of parsimony (i.e., start very simple and build complexity slowly) and use a broad range of information (soft data) to constrain the problem (Hill 2000, Boumaiza et al. 2021). Indeed, using more data to validate the quality and accuracy of the simulation and eventually perform a calibration makes it easier to identify a model's shortcomings and improve and even correct these weaknesses. Correcting these shortcomings and improving the model's accuracy will necessarily affect the results, such as the flow direction, the hydraulic head, the global water budget, and the water balance. The results will be more accurate;

the water mass balance will be closer to 0 to confirm that the simulation achieves good convergence and provides consistent results. The hydraulic head, the flow directions, and the global water budget will also be more accurate and more representative of reality.

Finally, for TEM, ERT, and GPR methods, a chart of electrical resistivity values (or relative dielectric permittivity for GPR) for saturated and unsaturated sediments can be helpful to detect the water levels in Quaternary deposits. Abrupt variations in electrical properties are generally associated with the boundary between saturated and unsaturated sediments, thereby identifying the water table. These charts link the sedimentary facies, i.e., clay, tills, sand, sand and gravel, and gravels, the associated electrical resistivity, and the water content (Reynolds 1987, 2011, Neal and Roberts 2000, Neal 2004, Lévesque et al. 2023). Lévesque et al. (2022) also demonstrated that although overlap of the electrical resistivity exists in the distributions between sediment classes, saturated and unsaturated sediment overlaps minimally for a given sediment class. Consequently, TEM and ERT can accurately identify the presence of water in Quaternary deposits and provide valuable information regarding water levels.

Moreover, the water table observed in radargrams, i.e., via GPR, is often clearly detectable as a coherent horizontal reflection with a large amplitude (Fig. 49; Reynolds 2011). If the capillary zone is thin, there is a sharp contrast in the relative dielectric constant between saturated and unsaturated sediments to reflect a significant proportion of the energy. Consequently, the reflection arising from the water table is clearly visible (Fig. 49; Reynolds 2011). Occasionally, the radargram reveals oblique reflections, i.e., stratification, associated with interfaces between sandy and clayey sediments or sandy layers of different grain sizes. Such southward-dipping reflectors were frequently observed in the Saint-Narcisse moraine (Fig. 49). These oblique reflections often indicate the flow directions at the origin of these structures (Cojan and Renard 2013) and can also be used to validate flow directions obtained from the numerical simulation. The dipping reflectors recorded in these surveys (Fig. 49) suggest that the current trend is from northwest to southeast, confirming the results from numerical modeling.

4.7 CONCLUSION

This study illustrated the relevance of using geophysical data to accurately assess water levels and provide additional information to flow models. Geophysical data can provide hydraulic information and a larger set of soft data to validate simulated water levels, especially in areas having limited direct piezometric observations. The need to ensure that model outputs match field measurements is often limited by cost, as acquiring field data in hydrogeology is expensive and time-consuming, particularly hard data such as boreholes and piezometers. Geophysical methods, including TEM, ERT, and GPR, provide an inexpensive, non-destructive, fast, robust, and effective means of characterizing the water levels, the internal dimensions, and stratigraphic variability of unconfined aquifers in data-sparse regions. This contribution provides the groundwater modeling community with a set of new tools to improve regional numerical flow models, which are essential for properly managing groundwater resources worldwide.

4.8 CONCLUSION DU CHAPITRE 4

Cette étude propose un modèle géologique tridimensionnel (élaboré avec Leapfrog) simplifié principalement en raison du manque de données granulométriques détaillées provenant des forages, ainsi que de la localisation des lentilles de sédiments, ainsi que leur délimitation spatiale. Bien que ces lentilles de sédiments (sable, gravier, sable-gravier, etc.) soient observables sur le terrain, les forages sont trop éloignés pour les identifier et les délimiter avec précision dans un modèle numérique. Il est cependant important de souligner que plusieurs auteurs ont démontré que les modèles simplifiés sont souvent les plus précis. Les modélisateurs peuvent simplifier un modèle sans perte significative de précision dans la simulation (Benzaazoua et al., 2004 ; Hill, 2006 ; Hudon-Gagnon et al., 2015 ; Doherty et Moore, 2020 ; Fortier et al., 2020). En réalité, la plupart des modèles sont très simples car ils ne peuvent pas représenter l'hétérogénéité et la complexité des processus souterrains avec une fidélité parfaite (Doherty et Moore, 2020). Le succès du modèle dépend de l'utilisation et de l'échelle du modèle en question, l'échelle étant cruciale pour la complexité et le

niveau de détail requis par le modèle. "Apprendre à définir le compromis optimal entre la simplicité et la complexité est l'un des plus grands défis auxquels est confrontée la pratique actuelle de la modélisation" (Doherty et Christensen, 2011). Un modèle d'écoulement à l'échelle locale peut nécessiter des données très précises, tandis qu'un modèle à l'échelle régionale (tel que celui de cette étude) peut déterminer avec succès les niveaux d'eau, confirmer les directions d'écoulement ou évaluer les flux de transit même avec des écarts moyens de quelques mètres. Théoriquement, plus l'échelle est grande, plus les incertitudes sont élevées, étant donné que la base de données doit contenir plus de données pour répondre aux besoins de l'étude (une plus grande surface à couvrir) et, par conséquent, la simulation numérique perdra nécessairement en précision et en justesse.

Concernant les connexions hydrauliques entre l'aquifère granulaire en nappe libre et le substratum rocheux sous-jacent, elles sont présentes malgré la considération de la conductivité du substratum rocheux comme nulle. Évaluer ces connexions et le potentiel d'un réseau de fractures représente toutefois un défi au sein de cette étude en raison de la pénurie de données et du manque de méthodes d'évaluation spécifiques propres au domaine de l'hydrogéologie. Dans cette perspective, le substratum rocheux a été simplement envisagé comme imperméable. Cette hypothèse découle du fait que, même en présence d'un réseau de fractures dans cette zone de la moraine de Saint-Narcisse, les conductivités hydrauliques associées sont probablement grandement inférieures à celles des sédiments granulaires sus-jacents. Ainsi, le substratum rocheux a été traité comme imperméable dans cette étude, tout en notant que cette assertion demeure hypothétique.

Finalement, en raison de contraintes techniques, aucune analyse de vitesse n'a été effectuée pour déterminer les vitesses du géoradar dans le sable saturé (v = 0.065 m/ns) et non saturé (v = 0.1 m/ns). Ces valeurs ont été obtenues à partir du logiciel MALÅ Vision, utilisé pour générer les radargrammes, étant le seul outil disponible pour le traitement des données de géoradar dans cette étude. Ce logiciel offre un choix restreint de vitesses GPR pour divers types de sédiments. Par exemple, les vitesses pour les sables et les graviers, voire même uniquement pour les graviers, ne sont pas proposées dans les options. Cette lacune pourrait potentiellement influencer les résultats et la localisation de la nappe phréatique, introduisant ainsi un certain degré d'incertitude quant à sa

position précise. Cette incertitude peut varier de l'ordre du décimètre à, dans certains cas, du mètre. Ces variations sont inhérentes à la nature du traitement des données par le logiciel MALÅ Vision et au choix restreint de vitesses GPR, qui, bien qu'efficaces pour l'estimation des niveaux piézométriques, présentent des limites de résolution devant être soigneusement prises en compte dans l'interprétation des données. Toutefois, comme mentionné précédemment, les autres méthodes géophysiques telles que le TEM et l'ERT confirment l'élévation du toit de la nappe, validant ainsi la justesse des résultats obtenus avec le géoradar, indépendamment de la vitesse GPR choisie ou disponible. Le cas échéant, tout biais introduit serait minime. Par conséquent, les vitesses de v = 0.065 m/ns pour le sable saturé et v = 0.1 m/ns pour le sable non saturé ont été utilisées pour la plupart des radargrammes.

LISTE DES REFERENCES

Abu-Hassanein, Z.S., Benson, C.H., and Blotz, L.R. 1996. Electrical resistivity of compacted clays. Journal of geotechnical engineering, 122: 397–406. American Society of Civil Engineers. doi:10.1061/(ASCE)0733-9410(1996)122:5(397).

Allen, D.M., Schuurman, N., Deshpande, A., and Scibek, J. 2008. Data integration and standardization in cross-border hydrogeological studies: a novel approach to hydrostratigraphic model development. Environmental geology, 53: 1441–1453. Springer. doi:10.1007/s00254-007-0753-3.

Asprion, U., and Aigner, T. 1997. Aquifer architecture analysis using ground-penetrating radar: Triassic and Quaternary examples (S. Germany). Environmental Geology, 31: 66–75. Springer.

Baines, D., Smith, D.G., Froese, D.G., Bauman, P., and Nimeck, G. 2002. Electrical resistivity ground imaging (ERGI): a new tool for mapping the lithology and geometry of channel-belts and valley-fills. Sedimentology, 49: 441–449. Wiley Online Library.

Baker, P.L. 1991. Response of ground-penetrating radar to bounding surfaces and lithofacies variations in sand barrier sequences. Exploration Geophysics, 22: 19–22. CSIRO Publishing. doi:10.1071/EG991019.

Benn, D., and Evans, D.J.A. 2010. Glaciers and glaciation. In 1ST edition. Routledge, London and New York. doi:10.4324/9780203785010.

Benzaazoua, M., Fall, M., and Belem, T. 2004. A contribution to understanding the hardening process of cemented pastefill. Minerals Engineering, 17: 141–152. doi:10.1016/j.mineng.2003.10.022.

Beres Jr., M., and Haeni, F.P. 1991. Application of ground-penetrating-radar Methods in Hydrogeologie Studies. Groundwater, 29: 375–386. Wiley Online Library. doi:10.1111/j.1745-6584.1991.tb00528.x.

Bersezio R, Giudici M, Mele M (2007) Combining sedimentological and geophysical data for high-resolution 3-D mapping of fluvial architectural elements in the Quaternary Po plain (Italy). Sediment Geol 202:230–248

Binley, A., and Beven, K. 2003. Vadose zone flow model uncertainty as conditioned on geophysical data. Groundwater, 41: 119–127. Wiley Online Library.

Binley, A., Cassiani, G., and Deiana, R. 2010. Hydrogeophysics: opportunities and challenges. Bollettino di Geofisica Teorica ed Applicata, 51.

Boumaiza, L., Chesnaux, R., Walter, J., and Stumpp, C. 2020. Assessing groundwater recharge and transpiration in a humid northern region dominated by snowmelt using vadose-zone depth profiles. Hydrogeology Journal, 28: 2315–2329. Springer. doi:10.1111/gwat.13056.

Boumaiza, L., Chesnaux, R., Walter, J., and Stumpp, C. 2021. Constraining a flow model with field measurements to assess water transit time through a vadose zone. Groundwater, 59: 417–427. Wiley Online Library. doi:10.1111/gwat.13056.

Boumaiza, L., Walter, J., Chesnaux, R., Lambert, M., Jha, M.K., Wanke, H., Brookfield, A., Batelaan, O., Galvão, P., and Laftouhi, N. 2022. Groundwater recharge over the past 100 years:

regional spatiotemporal assessment and climate change impact over the Saguenay-Lac-Saint-Jean region, Canada. Hydrological Processes,: e14526. Wiley Online Library. doi:10.1002/hyp.14526.

Bowling JC, Harry DL, Rodriguez AB, Zheng C (2007) Integrated geophysical and geological investigation of a heterogeneous fluvial aquifer in Columbus Mississippi. J Appl Geophys 62:58–73

Bowling JC, Rodriguez AB, Harry DL, Zheng C (2005) Delineating alluvial aquifer heterogeneity using resistivity and GPR data. Groundwater 43:890–903

Bristow, C.S., and Jol, H.M. 2003. An introduction to ground penetrating radar (GPR) in sediments. Geological Society, London, Special Publications, 211: 1–7. Geological Society of London.

Busch, S., Weihermüller, L., Huisman, J.A., Steelman, C.M., Endres, A.L., Vereecken, H., and Van Der Kruk, J. 2013. Coupled hydrogeophysical inversion of time-lapse surface GPR data to estimate hydraulic properties of a layered subsurface. Water Resources Research, 49: 8480–8494. Wiley Online Library.

Calvache, M.L., Ibáñez, S., Duque, C., Martín-Rosales, W., López-Chicano, M., Rubio, J.C., González, A., and Viseras, C. 2009. Numerical modelling of the potential effects of a dam on a coastal aquifer in S. Spain. Hydrological Processes: An International Journal, 23: 1268–1281. Wiley Online Library. doi:10.1002/hyp.7234.

Chesnaux, R. 2013. Regional recharge assessment in the crystalline bedrock aquifer of the Kenogami Uplands, Canada. Hydrological sciences journal, 58: 421–436. Taylor & Francis. doi:10.1080/02626667.2012.754100.

Chesnaux, R., Dal Soglio, L., and Wendling, G. 2013. Modelling the impacts of shale gas extraction on groundwater and surface water resources. In Proceedings of GeoMontreal 2013, 11e conférence conjointe SCG/AIH-SNC sur les eaux souterraines.

Chesnaux, R., Lambert, M., Walter, J., Dugrain, V., Rouleau, A., and Daigneault, R. 2017. A simplified geographical information systems (GIS)-based methodology for modeling the topography of bedrock: illustration using the Canadian Shield. Applied Geomatics, 9: 61–78. Springer. doi:10.1007/s12518-017-0183-1.

Chesnaux, R., Lambert, M., Walter, J., Fillastre, U., Hay, M., Rouleau, A., Daigneault, R., Moisan, A., and Germaneau, D. 2011. Building a geodatabase for mapping hydrogeological features and 3D modeling of groundwater systems: Application to the Saguenay–Lac-St.-Jean region, Canada. Computers & Geosciences, 37: 1870–1882. Elsevier. doi:10.1016/j.cageo.2011.04.013.

Claes, N., Paige, G.B., Grana, D., and Parsekian, A.D. 2020. Parameterization of a hydrologic model with geophysical data to simulate observed subsurface return flow paths. Vadose Zone Journal, 19: e20024. Wiley Online Library. doi:10.1002/vzj2.20024.

Cloutier, V., Blanchette, D., Dallaire, P.-L., Nadeau, S., Roy, M., and Rosa, E. 2013. Projet d'acquisition de connaissances sur les eaux souterraines de la Baie-James (phase 1).

Cojan, I., and Renard, M. 2013. Sédimentologie-3e édition. Dunod, Paris, France.

Constable, S.C., and Parker, R.L. 1987. Occam's inversion: A practical algorithm for generating smooth models from electromagnetic sounding data. Geophysics, 52: 289–300. Society of Exploration Geophysicists. doi:10.1190/1.1442303.

Costabel, S., Siemon, B., Houben, G., and Günther, T. 2017. Geophysical investigation of a freshwater lens on the island of Langeoog, Germany–Insights from combined HEM, TEM and MRS data. Journal of Applied Geophysics, 136: 231–245. Elsevier.

Cui, T., Sreekanth, J., Pickett, T., Rassam, D., Gilfedder, M., and Barrett, D. 2021. Impact of model parameterization on predictive uncertainty of regional groundwater models in the context of environmental impact assessment. Environmental Impact Assessment Review, 90: 106620. Elsevier. doi:10.1016/j.eiar.2021.106620.

Daigneault, R.-A., and Occhietti, S. 2006. Les moraines du massif Algonquin, Ontario, au début du Dryas récent, et corrélation avec la Moraine de Saint-Narcisse. Géographie physique et Quaternaire, 60: 103–118. Les Presses de l'Université de Montréal. doi:10.7202/016823ar.

Davis, J.L., and Annan, A.P. 1989. Ground-penetrating radar for high-resolution mapping of soil and rock stratigraphy 1. Geophysical prospecting, 37: 531–551. Wiley Online Library. doi:10.1111/j.1365-2478.1989.tb02221.x.

Dewar, N., and Knight, R. 2020. Estimation of the top of the saturated zone from airborne electromagnetic data. Geophysics, 85: EN63–EN76. Society of Exploration Geophysicists and American Association of Petroleum. doi:10.1190/geo2019-0539.1.

Diersch, H.-J.G. 2013. FEFLOW: finite element modeling of flow, mass and heat transport in porous and fractured media. Edited BySpringer Science & Business Media. Springer Science & Business Media. doi:10.1007/978-3-642-38739-5_1.

Doherty, J. 2003. Ground water model calibration using pilot points and regularization. Groundwater, 41: 170–177. Wiley Online Library. doi:10.1111/j.1745-6584.2003.tb02580.x.

Doherty, J., and Christensen, S. 2011. Use of paired simple and complex models to reduce predictive bias and quantify uncertainty. Water Resources Research, 47. Wiley Online Library. doi:10.1029/2011WR010763.

Doherty, J., and Moore, C. 2020. Decision support modeling: data assimilation, uncertainty quantification, and strategic abstraction. Groundwater, 58: 327–337. Wiley Online Library. doi:10.1111/gwat.12969.

Dunlap, E., and Tang, C.C.L. 2006. Modelling the mean circulation of Baffin Bay. Atmosphere-Ocean, 44: 99–109. Taylor & Francis. doi:10.3137/ao.440107.

Dyke, A., and Prest, V. 1987. Late Wisconsinan and Holocene history of the Laurentide ice sheet. Géographie physique et Quaternaire, 41: 237–263. doi:10.7202/032681ar.

Dyke, A.S. 2004. An outline of the deglaciation of North America with emphasis on central and northern Canada. Quaternary Glaciations-Extent and Chronology, Part II: North America, 2b: 373-424. doi:10.1016/S1571-0866(04)80209-4.

Evans, D. 2005. Glacial landsystems. In 1ST edition. Edited ByRoutledge. Routledge, London (UK) and New York (USA). doi:10.4324/9780203784976.

Farmani, M.B. 2008. Estimation of Unsaturated Flow Parameters by Inverse Modeling and GPR Tomography.

Fitterman, D. V, and Labson, V.F. 2005. Electromagnetic induction methods for environmental problems. In Near-surface geophysics. Edited by S. of E. Geophysicists. Society of Exploration Geophysicists, Houston, TX. pp. 301–356. doi:10.1190/1.9781560801719.ch10.

Galazoulas, E.C., Mertzanides, Y.C., Petalas, C.P., and Kargiotis, E.K. 2015. Large scale electrical resistivity tomography survey correlated to hydrogeological data for mapping groundwater salinization: a case study from a multilayered coastal aquifer in Rhodope, Northeastern Greece. Environmental processes, 2: 19–35. Springer.

Gallagher, M., and Doherty, J. 2007. Parameter estimation and uncertainty analysis for a watershed model. Environmental Modelling & Software, 22: 1000–1020. Elsevier. doi:10.1016/j.envsoft.2006.06.007.

Gascoyne, J.K., and Eriksen, A.S. 2005. Engineering geology| Geophysics. Elsevier.

Goutaland, D. 2008. Caractérisation hydrogéophysique d'un dépôt fluvioglaciaire: évaluation de l'effet de l'hétérogénéité hydrodynamique sur les écoulements en zone non-saturée. Ph.D. dissertation, Lyon University (INSA), France, 246 p.

Greggio, N., Giambastiani, B., Balugani, E., Amaini, C., and Antonellini, M. 2018. High-resolution electrical resistivity tomography (ERT) to characterize the spatial extension of freshwater lenses in a salinized coastal aquifer. Water, 10: 1067. Multidisciplinary Digital Publishing Institute. doi:10.3390/w10081067.

Hill, M.C. 2000. Methods and guidelines for effective model calibration. In Building partnerships, U.S. Geolo. Denver, Colorado. pp. 1–10.

Hill, M.C. 2006. The practical use of simplicity in developing ground water models. Groundwater, 44: 775–781. Wiley Online Library. doi:10.1111/j.1745-6584.2006.00227.x.

Hinnell, A.C., Ferré, T.P.A., Vrugt, J.A., Huisman, J.A., Moysey, S., Rings, J., and Kowalsky, M.B. 2010. Improved extraction of hydrologic information from geophysical data through coupled hydrogeophysical inversion. Water resources research, 46. Wiley Online Library.

Hudon-Gagnon, E., Chesnaux, R., Cousineau, P.A., and Rouleau, A. 2011. A methodology to adequately simplify aquifer models of quaternary deposits: preliminary results. In Proceedings of GeoHydro 2011, joint meeting of the Canadian Quaternary Association and the Canadian Chapter of the International Association of Hydrogeologists.

Hudon-Gagnon, E., Chesnaux, R., Cousineau, P.A., and Rouleau, A. 2015. A hydrostratigraphic simplification approach to build 3D groundwater flow numerical models: example of a Quaternary deltaic deposit aquifer. Environmental earth sciences, 74: 4671–4683. Springer. doi:10.1007/s12665-015-4439-y.

Huisman, J.A., Hubbard, S.S., Redman, J.D., and Annan, A.P. 2003. Measuring soil water content with ground penetrating radar: A review. Vadose zone journal, 2: 476–491. Wiley Online Library.

Huisman, J.A., Rings, J., Vrugt, J.A., Sorg, J., and Vereecken, H. 2010. Hydraulic properties of a model dike from coupled Bayesian and multi-criteria hydrogeophysical inversion. Journal of Hydrology, 380: 62–73. Elsevier.

Kalisperi, D., Kouli, M., Vallianatos, F., Soupios, P., Kershaw, S., and Lydakis-Simantiris, N. 2018. A transient ElectroMagnetic (TEM) method survey in north-central coast of Crete, Greece: evidence of seawater intrusion. Geosciences, 8: 107. Multidisciplinary Digital Publishing Institute. doi:10.3390/geosciences8040107.

Kowalsky, M.B., Finsterle, S., Peterson, J., Hubbard, S., Rubin, Y., Majer, E., Ward, A., and Gee, G. 2005. Estimation of field-scale soil hydraulic and dielectric parameters through joint inversion of GPR and hydrological data. Water Resources Research, 41. Wiley Online Library.

Kowalsky, M.B., Finsterle, S., and Rubin, Y. 2004. Estimating flow parameter distributions using ground-penetrating radar and hydrological measurements during transient flow in the vadose zone. Advances in Water Resources, 27: 583–599. Elsevier. doi:10.1016/j.advwatres.2004.03.003.

Landry, B., Beaulieu, J., Gauthier, M., Lucotte, M., Moingt, S., Occhietti, S., Pinti, D.L., and Quirion, M. 2012. Notions de géologie. In Modulo, Montréal, 4nd ed. Modulo, Montréal (Qc).

Légaré-Couture, G., Leblanc, Y., Parent, M., Lacasse, K., and Campeau, S. 2018. Three-dimensional hydrostratigraphical modelling of the regional aquifer system of the St. Maurice Delta Complex (St. Lawrence Lowlands, Canada). Canadian Water Resources Journal/Revue canadienne des ressources hydriques, 43: 92–112. Taylor & Francis. doi:10.1080/07011784.2017.1316215.

Lévesque, Y., Saeidi, A., and Rouleau, A. 2016. Estimating earth pressure exerted by the backfill on the vertical pillars in underground mine stopes. Edited by Proceedings of the 69th Canadian Geotechnical Conference and the 11th Joint CGS/IAH-CNC Groundwater Conference (GeoVancouver-2016). Vancouver, BC, Canada. pp. 1-7. https://doi.org/10.6084/m9.figshare.20407218. doi:10.6084/m9.figshare.20407218.v1.

Lévesque, Y., Saeidi, A., and Rouleau, A. 2017. An earth pressure coefficient based on the geomechanical and geometric parameters of backfill in a mine stope. International Journal of Geo-Engineering, 8: 1–15. Springer. doi:10.1186/s40703-017-0065-8.

Lévesque, Y., St-Onge, G., Lajeunesse, P., Desiage, P., and Brouard, E. 2019. Defining the maximum extent of the Laurentide Ice Sheet in Home Bay (eastern Arctic Canada) during the Last Glacial episode. Boreas, 49: 52–70. Wiley Online Library. doi:10.1111/bor.12415.

Lévesque, Y., Walter, J., and Chesnaux, R. 2021. Transient Electromagnetic (TEM) Surveys as a First Approach for Characterizing a Regional Aquifer: The Case of the Saint-Narcisse Moraine, Quebec, Canada. Geosciences, 11: 415–442. Multidisciplinary Digital Publishing Institute. doi:10.3390/ geosciences11100415.

Lévesque, Y., Walter, J., Chesnaux, R., Dugas, S., and David, N. 2023. Electrical resistivity of saturated and unsaturated sediments in northeastern Canada (on press). Environmental earth sciences,.

Li, C., Doble, R., Hatch, M., Heinson, G., and Kay, B. 2021. Constraining regional-scale groundwater transport predictions with multiple geophysical techniques. Journal of Hydrology: Regional Studies, 36: 100841. Elsevier.

Loke, M.H. 1999. Time-lapse resistivity imaging inversion. Proceedings of the 5th Meeting of the Environmental and Engineering. Geophysical Society European Section, Em1,: 1–12. doi:10.4133/1.2922877.

Loke, M.H. 2000. Electrical imaging surveys for environmental and engineering studies: A practical guide to 2-D and 3-D surveys. In Electronic version available from http://www. terra plus. com. Penang, Malaysia.

Loke, M.H. 2006. RES2DINV ver. 3.55, Rapid 2-D resistivity & IP inversion using the least-squares method. Software Manual, 139: 131–152. doi:10.1111/j.1365-2478.1996.tb00142.x.

Loke, M.H., and Barker, R.D. 1995. Least-squares deconvolution of apparent resistivity pseudosections. Geophysics, 60: 1682–1690. Society of Exploration Geophysicists. doi:10.1190/1.1443900.

Loke, M.H., and Barker, R.D. 2006. Practical techniques for 3D resistivity surveys and data inversion1. Geophysical prospecting, 44: 499–523. European Association of Geoscientists & Engineers. doi:10.1111/j.1365-2478.1996.tb00162.x.

MacInnes, S., Durham, J., Dickerson, J., Snyder, S., and Zonge, K. 2001. Fast TEM for UXO mapping at Gambell, Saint Lawrence Island, Alaska. In UXO/Countermine Forum.

MacInnes, S., and Raymond, M. 2001. ZONGE Data Processing Two-Dimensional, Smooth-Model CSAMT Inversion version 3.00. Zonge Engineering and Research Organization, Inc. p. 41.

Margold, M., Stokes, C.R., and Clark, C.D. 2015. Ice streams in the Laurentide Ice Sheet: Identification, characteristics and comparison to modern ice sheets. Earth-Science Reviews, 143: 117–146. doi:10.1016/j.earscirev.2015.01.011.

Mari, J.L., Arens, G., Chapellier, D., and Gaudiani, P. 1998. Geophysics for deposits and civil engineering; Geophysique de gisement et de genie civil.

Marker, P.A., Foged, N., He, X., Christiansen, A. V, Refsgaard, J.C., Auken, E., and Bauer-Gottwein, P. 2015. Performance evaluation of groundwater model hydrostratigraphy from airborne electromagnetic data and lithological borehole logs. Hydrology and Earth System Sciences, 19: 3875–3890. Copernicus GmbH. doi:10.5194/hess-19-3875-2015.

McClymont, A.F., Hayashi, M., Bentley, L.R., Muir, D., and Ernst, E. 2010. Groundwater flow and storage within an alpine meadow-talus complex. Hydrology & Earth System Sciences, 14. doi:10.5194/hess-14-859-2010.

McClymont, A.F., Roy, J.W., Hayashi, M., Bentley, L.R., Maurer, H., and Langston, G. 2011. Investigating groundwater flow paths within proglacial moraine using multiple geophysical methods. Journal of Hydrology, 399: 57–69. Elsevier.

Milsom, J. 2003. Field geophysics. John Wiley and sons, Oxford, UK.

Nabighian, M.N. 1988. Electromagnetic methods in applied geophysics. Society of Exploration Geophysicists, Tulsa, 2.

Nadeau L, Brouillette P Carte structurale de la région de Shawinigan (SNRC 31I), Province de Grenville, Québec 'Structural map of the Shawinigan region (NTS 31I), Province of Grenville, Québec'. Commission Géologique du Canada 'Geological Survey of Canada', Doss public 3012:. https://doi.org/10.4095/205047

Neal, A. 2004. Ground-penetrating radar and its use in sedimentology: principles, problems and progress. Earth-science reviews, 66: 261–330. Elsevier. doi:10.1016/j.earscirev.2004.01.004.

Neal, A., and Roberts, C.L. 2000. Applications of ground-penetrating radar (GPR) to sedimentological, geomorphological and geoarchaeological studies in coastal environments. Geological Society, London, Special Publications, 175: 139–171. Geological Society of London. doi:10.1144/GSL.SP.2000.175.01.12.

Occhietti. 1977. Stratigraphie du Wisconsinien de la région de Trois-Rivières-Shawinigan, Québec. Géographie physique et Quaternaire, 31: 307–322. Les Presses de l'Université de Montréal. doi:10.7202/1000280ar.

Occhietti. 2007. The Saint-Narcisse morainic complex and early Younger Dryas events on the southeastern margin of the Laurentide Ice Sheet. Géographie physique et Quaternaire, 61: 89–117. Les Presses de l'Université de Montréal. doi:10.7202/038987ar.

Occhietti, ChartierH, M., Hillaire-Marcel, C., Cournoyer, M., Cumbaa, S., and Harington, R. 2001. Paléoenvironnements de la Mer de Champlain dans la région de Québec, entre 11 300 et 9750 BP: le site de Saint-Nicolas. Géographie physique et Quaternaire, 55: 23–46. Les Presses de l'Université de Montréal. doi:10.7202/005660ar.

Palacky, G.J. 1993. Use of airborne electromagnetic methods for resource mapping. Advances in space research, 13: 5–14. Elsevier. doi:10.1016/0273-1177(93)90196-I.

Pandey, L.M.S., Shukla, S.K., and Habibi, D. 2015. Electrical resistivity of sandy soil. Géotechnique Letters, 5: 178–185. Thomas Telford Ltd. doi:10.1680/jgele.15.00066.

Parent, M., and Occhietti, S. 1988. Late Wisconsinan deglaciation and Champlain sea invasion in the St. Lawrence valley, Québec. Géographie physique et Quaternaire, 42: 215–246. Les Presses de l'Université de Montréal. doi:10.7202/032734ar.

Parent, M., and Occhietti, S. 1999. Late Wisconsinan deglaciation and glacial lake development in the Appalachians of southeastern Québec. Géographie physique et Quaternaire, 53: 117–135. Les Presses de l'Université de Montréal. doi:10.7202/004859ar.

Parsekian, A.D., Singha, K., Minsley, B.J., Holbrook, W.S., and Slater, L. 2015. Multiscale geophysical imaging of the critical zone. Reviews of Geophysics, 53: 1–26. Wiley Online Library. doi:10.1002/2014RG000465.

Pondthai, P., Everett, M.E., Micallef, A., Weymer, B.A., Faghih, Z., Haroon, A., and Jegen, M. 2020. 3D Characterization of a Coastal Freshwater Aquifer in SE Malta (Mediterranean Sea) by Time-Domain Electromagnetics. Water, 12: 1566. Multidisciplinary Digital Publishing Institute. doi:10.3390/w12061566.

Preisig, G., Cornaton, F.J., and Perrochet, P. 2014. Regional flow and deformation analysis of basin-fill aquifer systems using stress-dependent parameters. Groundwater, 52: 125–135. Wiley Online Library. doi:10.1111/gwat.12034.

Reynolds, J.M. 1987. Dielectric analysis of rocks-a forward look. In Geophysical journal of the royal astronomical society. Blackwell science ltd osney mead, oxford, england. p. 457.

Reynolds, J.M. 2011. An introduction to applied and environmental geophysics. In 2nd edition. John Wiley & Sons, West Sussex, UK.

Rivers, T., Gool, J.A.M. van, and Connelly, J.N. 1993. Contrasting tectonic styles in the northern Grenville province: Implications for the dynamics of orogenic fronts. Geology, 21: 1127–1130. Geological Society of America. doi:10.1130/0091-7613(1993)021<1127:CTSITN>2.3.CO;2.

Ross, M., Parent, M., and Lefebvre, R. 2005. 3D geologic framework models for regional hydrogeology and land-use management: a case study from a Quaternary basin of southwestern Quebec, Canada. Hydrogeology Journal, 13: 690–707. Springer. doi:10.1007/s10040-004-0365-x.

Shi, X., and Polycarpou, A. a. 2005. Measurement and Modeling of Normal Contact Stiffness and Contact Damping at the Meso Scale. Journal of Vibration and Acoustics, 127: 52. doi:10.1115/1.1857920.

Shukla, S.K., and Yin, J.-H. 2006. Fundamentals of geosynthetic engineering. In 1ST edition. Edited ByCRC Press. Taylor and Francis, Balkema, London (UK). doi:10.1201/9781482288445.

Slater, L. 2007. Near surface electrical characterization of hydraulic conductivity: From petrophysical properties to aquifer geometries—A review. Surveys in Geophysics, 28: 169–197. Springer. doi:10.1007/s10712-007-9022-y.

Spies, B.R., and Frischknecht, F.C. 1991. Electromagnetic sounding. Electromagnetic methods in applied geophysics, 2: 285–426. SEG Tulsa.

Steenhuis, T.S., and Van der Molen, W.H. 1986. The Thornthwaite-Mather procedure as a simple engineering method to predict recharge. Journal of Hydrology, 84: 221–229. Elsevier. doi:10.1016/0022-1694(86)90124-1.

Topp, G.C., Davis, J.L., and Annan, A.P. 1980. Electromagnetic determination of soil water content: Measurements in coaxial transmission lines. Water resources research, 16: 574–582. Wiley Online Library. doi:10.1029/WR016i003p00574.

Tran, A.P., Vanclooster, M., Zupanski, M., and Lambot, S. 2014. Joint estimation of soil moisture profile and hydraulic parameters by ground-penetrating radar data assimilation with maximum likelihood ensemble filter. Water Resources Research, 50: 3131–3146. Wiley Online Library. doi:10.1002/2013WR014583.

Walter, J., Rouleau, A., Chesnaux, R., Lambert, M., and Daigneault, R. 2018. Characterization of general and singular features of major aquifer systems in the Saguenay-Lac-Saint-Jean region. Canadian Water Resources Journal/Revue canadienne des ressources hydriques, 43: 75–91. Taylor & Francis. doi:10.1080/07011784.2018.1433069.

Wise, S. 2000. Assessing the quality for hydrological applications of digital elevation models derived from contours. Hydrological processes, 14: 1909–1929. Wiley Online Library. doi:10.1002/1099-1085(20000815/30)14:11/12<1909::AID-HYP45>3.0.CO;2-6.

Yu, Y., Weihermüller, L., Klotzsche, A., Lärm, L., Vereecken, H., and Huisman, J.A. 2021. Sequential and coupled inversion of horizontal borehole ground penetrating radar data to estimate soil hydraulic properties at the field scale. Journal of Hydrology, 596: 126010. Elsevier. doi:10.1016/j.jhydrol.2021.126010.

CHAPITRE 5

UTILITY OF GEOPHYSICS-DERIVED WATER LEVELS TO CALIBRATE A REGIONAL GROUNDWATER FLOW NUMERICAL MODEL

Le cinquième chapitre de cette thèse prend la forme d'un article scientifique. Il représente le quatrième outil développé dans notre approche méthodologique pour améliorer l'évaluation du potentiel aquifère d'un environnement hétérogène et anisotrope de dépôts quaternaires.

Les modèles numériques d'écoulement des eaux souterraines sont sujets à l'incertitude et, indépendamment de la complexité du modèle, l'optimisation des paramètres hydrauliques (c'est-à-dire la calibration) peut être cruciale, en particulier si les propriétés hydrauliques ne peuvent pas être mesurées avec justesse. Les logiciels modernes de calibration tel que FEPEST permettent de modifier les paramètres hydrauliques initiaux pour obtenir la meilleure correspondance possible entre les données observationnelles mesurées et simulées et de les représenter dans un modèle à un niveau de la complexité plus fidèle au système réel. L'objectif de la calibration est d'assurer qu'un modèle d'écoulement reproduise le plus fidèlement possible le comportement d'un système réel en utilisant un algorithme d'optimisation approprié. Pour ce faire, des observations de niveau d'eau in situ sont nécessaires pour caractériser le système réel et faire en sorte que les paramètres du modèle calibré (c'est-à-dire la conductivité hydraulique, la recharge, etc.) correspondent aux observations sur le terrain. Dans cette étude, les observations de niveau d'eau ont été obtenues via des données géophysiques et démontrent ainsi l'utilité des données géophysiques pour calibrer un modèle numérique d'écoulement régional et compléter les observations directes afin de produire des informations hydrauliques sur une plus grande étendue spatiale.

Afin de développer cet outil (c.-à-d., la calibration) pour évaluer le potentiel aquifère d'un milieu de dépôt quaternaire, une simulation numérique a été effectuée avec le logiciel Feflow® avec des paramètres hydrauliques préalablement définis. Ensuite, ces paramètres initiaux ont été affinés via le logiciel de calibration FEPEST en utilisant des niveaux d'eau dérivés de la géophysique. Enfin, 25 levés piézométriques dans toute la zone d'étude offrent l'occasion de valider les paramètres

récupérés après la calibration du modèle et de comparer les niveaux d'eau souterraine observés et les résultats post-calibration à l'aide du RMS. La valeur relativement faible de RMS (c.-à-d. 3,69 m) indique que les niveaux d'eau dérivés de la géophysique peuvent donner efficacement un ensemble de données de haute qualité pour la calibration de la modélisation hydrologique.

Cette approche innovante pour la calibration des modèles numériques d'écoulement avec des données géophysiques permet d'optimiser des paramètres hydrauliques à moindre coût (grâce à la géophysique) et avec une acquisition de données plus rapide et plus complète. Après la calibration, le modélisateur peut également identifier aisément de nouveaux paramètres hydrauliques dans les zones du modèle où il n'y en avait pas de disponibles.

Le présent article a été soumis dans la revue Environmental Earth Sciences (IF : 3,15) le 13 décembre 2023 et est à ce jour en cours d'évaluation.

Yan Lévesque [1, 2]*, Romain Chesnaux[1, 2], Julien Walter [1, 2], Lamine Boumaiza[3]

[1] Université du Québec à Chicoutimi, Department of Applied Sciences, Saguenay, QC, G7H 2B1 Canada;

[2] Centre d'études sur les ressources minérales (CERM), Groupe de recherche risque ressource eau (R2EAU), Université du Québec à Chicoutimi, Saguenay, QC, Canada G7H 2B1, Canada

[3] University of Waterloo, Department of Earth and Environmental Sciences, Waterloo, ON, N2T 0A4, Canada

Email: romain_chesnaux@uqac.ca; julien_walter@uqac.ca; lamine.boumaiza@uwaterloo.ca;

*corresponding author: yan.levesque1@uqac.ca

Orcid ID: YL: 0000-0002-6198-6315; RC: 0000-0002-1722-9499; JW: 0000-0003-2514-6180; LB: 0000-0001-9953-451X

5.1 ABSTRACT

This study demonstrates the utility of geophysical data to calibrate a numerical model of regional flow and complement direct observations to generate hydraulic information. The study area includes the Saint-Narcisse Moraine's glacial deposits in the eastern Mauricie region of Québec (Canada). To accurately represent the highly complex, heterogeneous, and anisotropic hydrological environment of Saint-Narcisse Moraine's glacial deposits, a 3D geological model and a 3D numerical flow model were developed, both of which were used for calibration purposes. The creation of these models relied on combining the data from 94 boreholes, 5 stratigraphic cross-sections, 20 transient electromagnetic surveys, 6 electrical resistivity tomography surveys, and 6 ground-penetrating radar surveys. Numerical simulation using FeFLOW® software was performed on the 3D geological model, and predefined hydraulic parameters (i.e., hydraulic conductivity and soil porosity) were determined. Subsequently, the initial model parameters were refined via FeFLOW parameter estimation (FePEST) using the geophysics-derived water levels. Finally, the results from 26 piezometric surveys conducted throughout the study area provided an opportunity to 'ground truth' the recovered parameters after model calibration, and compared the observed groundwater levels and post-calibrated results through root mean square error (RMSE). A relatively low RMSE value (i.e., 3.69 m) suggested that geophysics-derived water levels could be used to effectively establish a high-quality dataset for hydrological modeling calibration. This innovative approach to calibrating numerical flow models with geophysical data allows the optimization of hydraulic parameters at both a lower cost and at a faster rate of data acquisition. After calibration, a modeler can easily identify new hydraulic parameters in areas of the model where they have not been previously determined by other means.

Keywords: Numerical modeling, FePest, calibration, geophysical methods, aquifer properties, groundwater monitoring, Eastern Canada

5.2 INTRODUCTION

The modeling of hydrological processes and the visualization of flow scenarios through sedimentation characteristics are now standard practice and essential to properly managing groundwater resources worldwide. In recent decades, several studies have reported the potential of using geophysical techniques (e.g., TEM, ERT, GPR, MMT) to complement direct observations (i.e., borehole and piezometric surveys). These studies provide additional hydraulic information, such as soil hydraulic properties and field-scale estimates of the soil moisture content (Hubbard and Rubin 2000, Huisman et al. 2010, Mboh et al. 2011, Rossi et al. 2015, Moghadas et al. 2017, Yu et al. 2021). The natural heterogeneity of aquifer soils and the commonly heterogeneous fluid flow parameters can cause significant errors in soil parameterization schemes (Boumaiza et al. 2023). Furthermore, the uncertainty of the spatial distributions of boreholes and piezometric surveys often complicates the modeling of groundwater distribution as well as the transport of contaminants. To overcome the disadvantages of point-scale observations (e.g., logs from boreholes) and to avoid creating additional subsurface disturbance, geophysical techniques (inclusive of multiple and combined methods if possible) could considerably improve the model's accuracy (Robinson et al. 2008, Doherty and Moore 2020, Fortier et al. 2020). These methods, including multiple and combined methods if possible, provide additional data to the groundwater modeling community, especially in areas with limited direct observations. Moreover, groundwater models are undermined by uncertainty, and regardless of the model's complexity, the optimization of hydraulic parameters (i.e., calibration) can be critical, especially if the hydraulic properties cannot be accurately measured (Hill 2006). Modern calibration software allows the modification of the initial parameters to give the best possible fit between the measured data and the simulated observational data (Kowalsky et al. 2004), ensuring a representation of the model that matches the inherent complexity of the realistic system (Doherty 2007, Doherty and Moore 2020, Fortier et al. 2020). The objective of calibration is to ensure that a flow model mirrors the same behavior as a real system by using an appropriate optimization algorithm. To accomplish this, in-situ water level observations are necessary in order to characterize the real system and ensure that the parameters of the calibrated model (i.e., the hydraulic conductivity and soil porosity) match the field observations. In this study, the in-situ water level observations were

obtained via geophysical data acquired during the summer's seasons of 2020 and 2021 (Lambert et al. 2022b, Walter et al. 2022).

According to Claes et al. (2020), three methods exist to integrate the geophysical data in order to calibrate a groundwater model. The first method, known as the sequential approach, comprises of three steps: (1) performing an interpretation of the geophysical data to then estimate the subsurface geological material properties (e.g., electrical resistivity, dielectric permittivity); (2) the conversion of the estimated geophysical properties of the subsurface environment into hydrological properties through a petrophysical relationship (e.g., the hydraulic conductivity, soil water content); and (3) the use of the hydraulic properties to constrain a hydrological inversion to build a flow model (Binley and Beven 2003, Chen et al. 2004, Cassiani and Binley 2005, Li et al. 2021). The second method, known as joint inversion, simultaneously inverts different geophysical datasets to minimize the objective function that includes data misfit (for each dataset). Hydrological properties are then deducted from temporal changes in geophysical data (related to the travel times of the electromagnetic signal in the subsurface materials), which can be correlated to hydrological state variables. Geophysical data are used as indirect observations of the subsurface parameters in the model to ensure physical consistency, especially in data-sparse regions (Linde and Doetsch 2016). Several contributions to the hydrological literature have demonstrated the usefulness and applicability of the joint inversion method (Gallardo and Meju 2004, Linde and Doetsch 2016). The third method is a coupled hydrogeophysical inversion that consists of linking the geophysical and hydrological measurements directly during the hydrological inversion process (Kowalsky et al. 2004, 2005, Rucker and Ferré 2004, Lambot et al. 2006, Jadoon et al. 2008, Hinnell et al. 2010). Coupled inversion integrates multiple measurements within the context of hydrological process models. Joint hydrogeophysical inversion, on the other hand, combines multiple types of measurements by first establishing empirical, physical, or statistical relationships between the hydraulic properties of interest and the properties inferred from the gathered geophysical measurements (Ferré et al. 2009). During the coupled hydrogeophysical inversion approach, the groundwater model serves as a robust framework to constrain the inversion of the geophysical data, thereby reducing the associated potential uncertainties. The hydrological model parameters are then iteratively optimized, until the closest

match between the observed and simulated data sets is achieved. This method is particularly well suited for analyzing the geophysical data that are required to monitor changes occurring in the hydrological state variables, making it more effective than the two previously discussed approaches (i.e., joint inversion and sequential approach methods; Huisman et al. 2010).

The use of geophysical data in groundwater modeling has gained popularity in recent years, as it offers valuable insights into various applications, such as (1) groundwater resource management (e.g., Blanco-Canqui and Lal 2007; Hartmann et al. 2014; Galazoulas et al. 2015; Hudon-Gagnon et al. 2015; Pandey et al. 2015; Parsekian et al. 2015; Simard et al. 2015; Costabel et al. 2017; García-Menéndez et al. 2018, Greggio et al. 2018; Kalisperi et al. 2018; Goldman and Kafri 2020; Pondthai et al. 2020; Lévesque et al. 2021; Elbshbeshi et al. 2022; Othman et al. 2022), (2) assessing the impacts of climate change on forests (e.g., Martınez-Vilalta et al. 2002; McDowell and Allen 2015), and (3) modeling contaminants and water flow transport (e.g., Wagner 1992; Vereecken et al. 2007; Hudon-Gagnon et al. 2015; Boumaiza et al. 2021a). Although hydraulic parameters are commonly determined through robust laboratory methods (e.g., Hsieh et al. 1981) and in-situ tests (e.g., pumping tests, slug tests; Abi et al. 2022; Lévesque et al. 2023b) to provide input data for numerical flow models, hydraulic property estimation often fails to represent realistic field conditions. To overcome this limitation, various studies, such as those conducted by Rucker and Ferrée (2004), Kowalsky et al. (2005), and Looms et al. (2008), have utilized the coupled hydrogeophysical inversion approach to integrate time-lapse borehole ground-penetrating radar (GPR) data in hydrological model calibration. In these studies, the time-lapse soil moisture images obtained from GPR measurements were inverted to calibrate the hydraulic parameters.

Several previous studies have employed GPR measurements (including surface, off-ground, and vertical borehole measurements) with a coupled inversion method to estimate the soil hydraulic properties based on the time-lapse soil water content data (e.g., Rucker and Ferré 2004; Kowalsky et al. 2005; Looms et al. 2008; Jadoon et al. 2012; Jonard et al. 2015). However, similar to the present study, the majority of previous research that utilized geophysical measurements to derive additional hydrological information predominantly relied on the sequential inversion approach. This method has

been proven to be useful over the last few decades in constraining critical components of groundwater models such as the hydraulic properties. These properties are used to constrain the hydrological inversion and develop conceptual flow models or geological frameworks (Tran et al. 2014).

Previous studies have used various geophysical methods to provide additional hydrological information. For example, Wagner (2007) employed audio-frequency magnetotellurics (AMT) to model the transport of subsurface radioactive materials under Amchitka Island located in Alaska, while Binley et al. (2002) used cross-hole GPR and ERT measurements to estimate the effective saturated hydraulic conductivity. Marker et al. (2015) used TEM, and Lévesque et al. (2021, 2023a) combined TEM, ERT, and GPR to improve the hydrostratigraphic characterization and determine water table levels for a groundwater model in Norsminde (Denmark) and eastern Mauricie (Canada), respectively. Boucher et al. (2012) used nuclear magnetic resonance (NMR) to estimate the specific yield and transmissivity in sandstone aquifers in Niger (Boucher et al. 2012). Claes et al. (2020) assessed the impact of subsurface structural complexity on the vadose zone by varying the heterogeneity and structural complexity that were derived from background geophysical data using a two-dimensional transport model. Tran et al. (2014) developed a sequential GPR data assimilation technique to simultaneously update the hydraulic parameters and model state by combining GPR measurements, petrophysical relationships (the correlation between geophysical data and stratigraphic data obtained from borehole logging), hydrodynamic models, the maximum likelihood ensemble filter (MLEF) technique, and the state augmentation method. Finally, Li et al. (2021) went further by coupling multiple geophysical methods (i.e., EMT, TEM, and NMR) with stochastic groundwater modeling to predict the hydrological impact of a copper in situ recovery operation in the Kapunda region, South Australia. However, in many studies, the quantification of inherent uncertainties associated with geophysical soft data has been infrequent, potentially introducing bias into outcomes and results. They often assumed significant simplifications of the stratigraphic reconstruction and the input hydraulic parameters, including the oversimplification of the heterogeneity and structural complexity of stratigraphic units, variation in grain size, anisotropy, and material properties. Additionally, these contributions mainly use synthetically calibrated datasets of relatively simple hydrological systems. They typically couple geophysical data with groundwater

models to provide hydraulic information in a deterministic manner, where a single, best-calibrated model is developed and used to make predictions. Furthermore, several studies lacked data obtained from direct observations, such as borehole logging and piezometric surveys, as well as actual field experiments to support the geophysical data. As a result, geophysical data are utilized without validation provided from direct observations, which considerably increases the level of uncertainty in the outcomes. Moreover, the majority of these studies are often based on only one geophysical method to calibrate their models. The process of combining multiple geophysical techniques is known to considerably decrease the inherent uncertainty of geophysical methods, which are indirect observations of the subsurface, and appropriately account for structural inadequacies (Reynolds 1987, 2011, Goutaland 2008, Li et al. 2021, Lévesque et al. 2023a). While some studies have shown the potential benefits of using geophysical data for groundwater modeling, there is still a need for more research on soft data reliability for model calibration. To address this gap, this paper's main objective is to test the reliability of geophysical data for calibrating a regional groundwater flow model. Additionally, this study aims to showcase the effectiveness of combining multiple geophysical techniques (TEM, ERT, and GPR) to illustrate the relevance of geophysical data and groundwater levels in calibrating a regional groundwater flow model.

In the present study, to construct the 3D flow model and perform calibration, 81 boreholes were utilized for determining subsurface stratigraphy. Additionally, 26 piezometric surveys (from the borehole logging) and hydraulic parameters from available hydrogeological consulting reports of the Saint-Narcisse Moraine's glacial deposits in eastern Mauricie, Quebec, were incorporated. The ample availability of borehole logs and piezometric surveys across the region also provides an excellent opportunity to validate the estimated parameters post-calibration by using geophysics-derived water levels as soft data. Such validation ensures that the calibrated model is strongly correlated with water level data obtained directly from boreholes.

Before the 3D numerical flow model was developed, a 3D geological model was constructed to comprehensively depict the actual geological aquifer conditions. Stratigraphic reconstruction, performed using a 3D geomodeling system, was necessary to provide a more detailed and realistic

representation of this highly complex, heterogeneous, and anisotropic hydrological environment. This complex aquifer system provided an ideal environment to test the relevance of geophysics-derived water levels in calibrating a flow model, as it is closer to reality than a simplified model. Groundwater flow parameters included the rate of recharge, porosity, bottom and top elevations of the aquifer, and hydraulic conductivities (i.e., Kxx, Kyy, Kzz). To assess the suitability of geophysical data for calibrating a regional groundwater flow numerical model, this study was undertaken in three stages: (1) calibration of the numerical model parameters using geophysics-derived water levels with FePEST software, (2) estimation of groundwater levels at the borehole locations (observed via piezometric data) using the optimized parameters and the calibrated model with FeFLOW software, and (3) comparison of simulated and observed groundwater levels using the RMSE to evaluate their correlation.

This methodology involves the calibration of a regional-scale numerical groundwater flow model using geophysical data and software such as PEST. It is innovative because geophysical data are not typically used for this purpose. Instead, geophysical data are often used to identify subsurface layer stratigraphy (Lévesque et al. 2021, 2023c) or validate the reliability of such models (Lévesque et al. 2023a). As demonstrated by the calibration in this study, the acquisition of geophysical data are a valuable contribution to aquifer flow modeling, as it highlights its ability (1) to optimize the initial hydraulic parameters; (2) to recover new hydraulic parameters through calibration in areas of the model where they have not been previously determined; and (3) to be consistent with the findings of Lévesque et al. (2023), who showed that geophysical data could accurately estimate groundwater levels at a local and/or regional scale.

In contrast to the original study by Lévesque et al. (2023a), this research introduces notable differences in methodology and outcomes: Lévesque et al.'s original study involved the development of initial geological and groundwater numerical models. They proposed a combination of various geophysical techniques to significantly reduce uncertainties inherent to geophysical methods. The study compared simulated hydraulic heads with geophysics-estimated groundwater levels using the RMSE method. The low RMSE value (2.76 m) demonstrated how geophysical data enhances

hydraulic information, accurately determining water table elevation and validating the numerical model performance.

In this research, initial model parameters underwent refinement through FeFLOW parameter estimation (FePEST) using geophysics-derived water levels. Piezometric surveys from boreholes provided an opportunity to 'ground truth' the recovered parameters post-model calibration. A comparison between observed groundwater levels and post-calibrated results will be conducted and will show the effectiveness of geophysical data in establishing a high-quality dataset for calibrating hydrological models with software like PEST.

5.3 STUDY AREA AND BASEMENT GEOLOGY

The study area is located in the Saint-Narcisse Moraine in the Mauricie region of Québec (Canada; Fig. 55). The moraine overlies both the Grenville Province to the north, which constitutes the youngest province of the Precambrian Canadian Shield (Rivers et al. 1993), and the St. Lawrence Lowlands to the south, which are composed of Paleozoic sedimentary rocks (Occhietti 1977; Globensky 1987). The Saint-Narcisse Moraine is a small section of the Saint-Narcisse morainic complex, a remarkably well-preserved geological feature, which is one of the longest documented discontinuous frontal moraines in Canada (Daigneault and Occhietti 2006). This long ridge, composed of glacial sediments extending over 1400 km (Daigneault and Occhietti 2006), was produced during the last glacial maximum (LGM). The Laurentide Ice Sheet (LIS) covered most of Eastern Canada during the LGM (Dyke 2004; Margold et al. 2015; Lévesque et al. 2019; Brouard et al. 2021, McMartin et al. 2021, Godbout et al. 2023) and produced thick layers of glacial deposits such as what are now moraines. Most of the Quaternary surface deposits in the Mauricie region are related to the last glaciation (i.e., the Wisconsinan glaciation). The Saint-Narcisse Moraine consists of various sedimentary facies, such as juxtaglacial and fluvioglacial deposits, subglacial or melt-out tills, and proximal and distal glaciomarine deposits (Occhietti 2007). The main depositional sequences of the moraine are known for their complex stratigraphy and heterogeneity, resulting in a

series of thick interbedded sand and sand-gravel layers overlying a discontinuous till overlaying the bedrock. This geologically imposing moraine is partially confined on its sides by clay deposits, thus resulting in the retention of water inside the aquifer system. In fact, this moraine is exploited locally for water supply by the surrounding municipalities, attesting to her aquifer capacity.

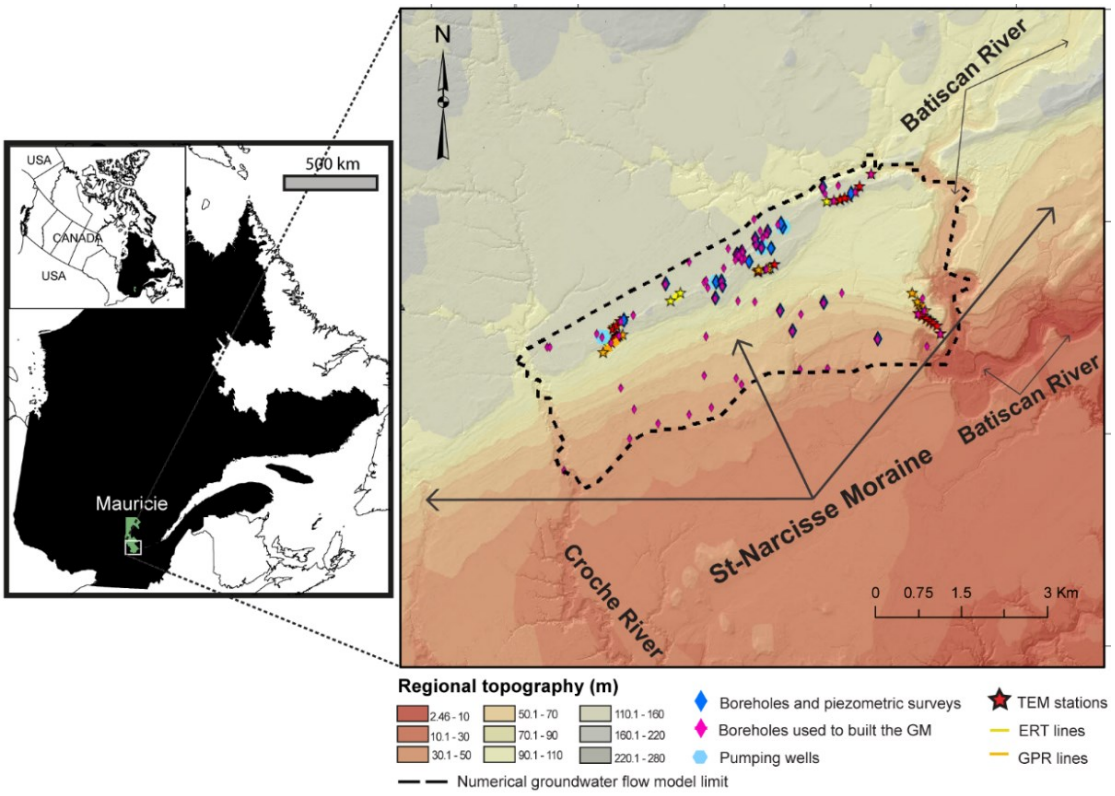

Figure 55: Regional topography of the study area and location of geophysical surveys, pumping wells, and boreholes (i.e., piezometric surveys). The orange stars represent the GPR surveys, and the yellow stars the ERT surveys. The dashed black line represents the maximum extent of the numerical model proposed in this study.

5.4 MATERIALS AND METHODS

To investigate the potential use of geophysical data as a calibration tool for regional numerical groundwater flow models, the methodology involved calibrating the numerical model parameters using FePEST and geophysics-derived water levels. The resulting calibrated model, with optimized parameters, was then imported into FeFLOW, and the groundwater level was compared with the observed piezometric data obtained at the borehole locations. If a close correlation is observed, this

indicates the usefulness of geophysics-derived data for hydrological modeling calibration. Otherwise, poor correlation illustrates that geophysical data are not a valid tool for calibrating a numerical groundwater flow model.

5.4.1 DATA COLLECTION

Five stratigraphic cross-sections, 18 TEM (i.e., 18 stations), 4 ERT (~ 960 m), and 4 GPR surveys (~0.97 km), were completed in the study area during the summers of 2020 and 2021. Stratigraphic cross-sections were acquired from sand pits during the summer of 2020. Afterward, 94 borehole and 25 piezometric surveys (from borehole logs) were extracted from the existing spatial reference database (i.e., geodatabase) of the *Groundwater Knowledge Acquisition Program* (Programme d'acquisition de connaissances sur les eaux souterraines, PACES; Walter et al. 2018; Lévesque et al. 2023b). These data sources relied on fieldwork and compilations and were utilized to produce 3D stratigraphic and 3D groundwater flow models for the Saint-Narcisse Moraine aquifer.

Following the methods used by Lévesque et al. (2023a), 3 geophysical techniques (i.e., TEM, ERT, and GPR) have been combined to provide the hydraulic information and obtain accurate estimates of water table height in order to conduct a numerical simulation using FeFLOW® software. The GPR surveys were acquired with a MALÅ GX (Ground Explorer) GPR system manufactured by MALÅ Geoscience (now ABEM/MALÅ) with a MALÅ controller application, real-time interpretation support, and cloud storage provided via MALÅ Vision. A 12-V battery powered the GPR, and 160 MHz shielded antennae (i.e., MALÅ GX HDR antennae) were used. This antenna has a vertical resolution of approximately 0.1 m, and provides a 5 to 15 m maximum depth penetration, allowing to locate the water table (generally located 1 to 5 m below the ground surface) in this area of the moraine. The two-way travel-time settings varied between 50 and 200 nanoseconds (ns), and all radargrams were processed using the MALÅ Vision program. Lévesque et al. (2021, 2023c) proposed a stratigraphic calibration chart that links the sedimentary facies (i.e., clay, sand, sand-gravel), the associated electrical resistivity, and soil moisture content for this area of the Saint-Narcisse Moraine. Fairly accurate mean velocity for most GPR sites was assumed based on these interpretations: v = 0.1 m/ns for unsaturated sand material and v = 0.065 m/ns for saturated sand material (Lévesque

et al. 2023c). These values were obtained using the MALÅ Vision software, the sole tool available for processing GPR data in this study. The software offers a limited selection of GPR velocities for various sediment types. For instance, velocities for sands and gravels, or even specifically for gravels, are not included among the options provided by MALÅ Vision. This limitation could potentially influence the results and the localization of the water table, introducing a degree of uncertainty regarding its precise position. This uncertainty can range from decimeters to, in some cases, possibly meters. These variations are inherent to the nature of data processing by MALÅ Vision and the restricted choice of GPR velocities, which, although effective for estimating piezometric levels, exhibit resolution limits that must be carefully considered in data interpretation. However, other geophysical methods such as TEM and ERT confirm the elevation of the water table, thereby validating the accuracy of the results obtained with GPR, regardless of the chosen or available GPR velocity. Any potential bias introduced would thus be minimal.

For ERT surveys, vertical electrical soundings (VES) of resistivity were undertaken using a Syscal Pro resistivity meter with a Wenner electrode configuration, totaling 360 quadrupoles (Wenner arrays). Each survey consisted of a line of 48 switchable electrodes, with 5 m spacing for a total length of 235 m. The RES2DINV software allows for the processing of a least-squared inversion in order to develop a true resistivity–depth profile (Loke 2006; Reynolds 2011). After the outliers were removed from the dataset, the final inversion required 3 to 5 iterations after the absolute error reached a value of less than 10%, and no longer had significant variations (Loke 2006; Reynolds 2011). For the RES2DINV software, the absolute error displays the distribution of the percentage difference between the measured and calculated apparent resistivity values (Loke and Barker 1995, 2006; Loke 1999). Following the methods used by Lévesque et al. (2023a), the observed point-based locations of the ERT and GPR surveys were selected at the beginning and end of each 2D line, which provided a suitable density of information. These observed points were very close to each other at a regional scale, and it was not necessary to add more additional points along the 2D ERT and GPR profiles.

TEM surveys were undertaken using an NT-32 transmitter and a 32II multifunction GDP-receiver (MacInnes and Raymond 2001). The NT-32 unit consists of a portable battery and a

transmitter–receiver (TX-RX) console that operates a square-sized transmitter loop (Tx) and receiver loop (Rx; in-loop configuration) for obtaining the measured induced voltage. These loops are connected to a receptor that measured the rate of decay of the electromagnetic current, which is then inverted in electrical resistivity (Nabighian 1988; Fitterman and Labson 2005). Afterward, the acquired data were inverted to deduce the subsurface apparent resistivity distribution as follows: 1) The raw data were averaged using TEMAVG Zonge software (MacInnes and Raymond 2001; MacInnes et al. 2001). Inconsistent data points (i.e., outliers) must be filtered and deleted in TEMAVG before inversion. 2) STEMINV software (MacInnes and Raymond 2001; MacInnes et al. 2001) produces a consistent 1D smoothed inversion model of electrical resistivity versus depth based on the iterative Occam inversion scheme (Constable and Parker 1987). 3) MODSECT software uses the 1D resistivity model acquired from STEMINV to interpolate vertical columns with Catmul–Rom splines (MacInnes and Raymond 2001; MacInnes et al. 2001), build a 2D model, and visualize the geometry of the geoelectrical structure of each line (Lévesque et al. 2021; Richer et al. 2023). For TEM, each station serves as a location for the observed points.

5.4.2 MODEL INPUT PARAMETERS AND 3D PROCESSING

5.4.2.1 GROUNDWATER FLOW MODEL

The 3D groundwater flow model was built using the finite-element numerical code FeFLOW® 7 modeling and simulating software. The finite-element method incorporates geological properties into the numerical model, such as irregular and curved aquifer boundaries, heterogeneity, and anisotropy (Diersch 2013). The FeFLOW software simulates the groundwater flow in 1D, 2D, or 3D, in a steady or transient state, and saturated/unsaturated conditions, by solving the basic balance equations in porous and fractured media for complex geometries (Diersch 2013). This study considers the system as a saturated, unconfined, granular aquifer that is overlying the bedrock. The flow regime is steady, and the simulations utilize an adaptive grid, which is more adaptable for representing unconfined aquifers. This approach allows the model surface to correspond to the elevation of the ground surface.

5.4.2.2 GEOLOGICAL MODEL

Eighty-one boreholes and fourteen stratigraphic cross-sections (from outcrops) were utilized for constructing the geological model. The stratigraphic cross-sections were obtained through field campaigns during the summers 2020 and 2021, and the borehole data were collected from various sources, including public and private organizations such as consulting firms, municipalities, and government agencies. These organizations had archived hydrogeological data over time and these data had been previously explored, even if they were largely underutilized. The stratigraphic reconstruction and the 3D geological model were built with a discrete modeling approach using the Leapfrog Geo software package (ARANZ Geo Ltd.). This software is designed to build and analyze geological objects and their properties, and provide a more realistic, accurate, and detailed stratigraphic reconstruction of the studied Quaternary basin than the FeFLOW software, which is more adapted to simulate flow conditions. This 3D geological model covers an area of approximately 26 km² and is easily exported to FeFLOW with an interoperability mode. Details of the model construction with Leapfrog Geo software are presented in Lévesque et al. (2023a). The model has a total of four layers (homogeneous), three of which are from Quaternary deposits: sand and gravel, tills and sand. The fourth layer is the bedrock. Each layer is constrained by a lower and an upper surface interface, and although they are unevenly distributed, a combination of bedrock and till units underlie this aquifer. The till unit has an average thickness of 1 to 5 m (Occhietti 2007), and is simulated as a discontinuous layer between the sand and bedrock layers. The sand unit directly overlies the bedrock where there is no till deposits present. The hydraulic conductivity for all layers and the grid were integrated directly into Leapfrog Geo. The 3D grid of tetrahedral elements was refined at the model's edge, for a total of 166,348 elements and 83,376 nodes.

5.4.2.3 HYDRAULIC PROPERTIES

The hydraulic conductivity (i.e., Kxx, Kyy, Kzz), effective porosity, groundwater recharge rate, and the bottom/top elevations of the aquifer geological interfaces are the parameters used to calculate the groundwater flow behavior in FeFLOW. The hydraulic properties of the aquifer were estimated from observations made during the pumping well tests, and other research works related to a number

of available hydrogeological consulting reports that encompassed a large portion of the Mauricie region (Table 16). These relevant sources of information primarily related to the groundwater hydraulic conditions and the characteristics of the Quaternary deposits (e.g., consultant reports, eastern Mauricie municipality's geotechnical analysis, private well analysis) and the region's aquifer systems are gathered in a spatially referenced digital database, implemented for the PACES Program in eastern Mauricie (Lévesque et al. 2023b). This geodatabase is an essential source of information for assigning topography, hydraulic conductivity, and effective porosity to the various kind of sediments. According to the well-established principle in hydrogeology, the vertical hydraulic conductivity (Kzz) was set using 10% of the horizontal value (Kxx/Kyy; Table 16). As noted by Freeze and Cherry (1979), the primary cause of anisotropy is the superimposed sedimentary formations and the orientation of clay minerals in unconsolidated sediments. These layered formations often exhibit both horizontal and vertical anisotropy at a ratio of approximately 10:1. In fact, the superimposed sedimentary layers facilitate groundwater flow more easily horizontally than verticaly (Freeze and Cherry 1979). The recharge of the study area (set at 350 mm·year^{-1}) is also a well constrained parameter due to the previous work that has been done for the PACES program investigations in the Mauricie region (Boumaiza et al. 2020, 2021b, 2022; Lévesque et al. 2023b).

TABLE 16: Hydraulic measured parameters for the sand and gravel, the sand and the tills.

Hydraulic Parameters (measured)			
Geological layer	Kxx and Kyy (m/j)	Kzz (m/j)	Effective porosity (n)
Sand and gravel	18.72	1.87	0.2
Sand (littoral and fluvioglacial)	4.72	0.47	0.15
Tills	1.52	0.15	0.08
Bedrock	ø	ø	ø

5.4.2.4 BOUNDARY CONDITIONS

To constrain the model, the eastern and western boundaries are considered fluid-transfer conditions (Cauchy conditions). To the west, the nodes are assigned between 96 m and 52 m (i.e., elevation) along the 2.9 km course of the Croche River, and to the east, between 69 m and 11 m along the 4.1 km course of the Batiscan River (Fig. 55) through the modelled region. We consider that the aquifer is connected to these rivers and lies in between. The model's northern and southern limits were impermeable (no-flow boundary interface) due to the thick layer of clay deposited by the Champlain Sea in low-lying areas around the moraine during the Holocene (Parent and Occhietti 1988, 1999; Occhietti 2007). To the north and south, the low flow rate of groundwater through the impermeable clay layer overlying the bedrock with till units is considered void for flow dynamics in the moraine aquifer system. Given the high contrast between hydraulic conductivity values in crystalline rock and granular deposits, we considered the bedrock at the base of the moraine aquifer and the till to the north and south border to also be impervious limits. Discontinuous and unevenly distributed tills and sand units are overlying the bedrock.

5.4.2.5 CALIBRATION OF THE GROUNDWATER MODEL

The 3D numerical solution solved with FeFLOW® (i.e., hydraulic head, pressure, groundwater-budget balance) is subsequently loaded into the FeFLOW parameter estimation (FePEST®), the Mike DHI graphical user interface for PEST® software developed by Doherty and Christensen in 2011 (Doherty 2007; Doherty and Christensen 2011; Siergieiev et al. 2015). FePEST is an automatic calibration algorithm that adjusts the parameters of groundwater models (i.e., a calibration) to accurately provide an approximation of the system's values.

The Gauss-Levenberg–Marquardt algorithm (GLMA; Hanke 1997) is the fundamental feature of optimizing the model parameters and conducting uncertainty analysis for groundwater model inversion programs such as FePEST®. The GLMA requires a Jacobian matrix (i.e., a sensitivity matrix), which is generated using a finite difference approach (Doherty 2007, Doherty and Moore 2020, Fortier et al. 2020). FePEST iteratively adjusts the parameters (e.g., hydraulic conductivity

(Kxx, Kyy, Kzz), effective soil porosity, specific storage of the aquifer) in such a way that the objective function is minimized (Equation 5).

$$\phi = \left(\sum_{i=1}^{n} w_i \, (h_i{}^{obs} - h_i{}^{sim})^2 \right) \quad (5)$$

The objective function (ϕ) is the sum of the weighted residuals squared, where w is the weight, i is the number of observations and hi ^{obs} – hi ^{sim} is the difference between the observed and the simulated values. The FePEST objective (the calibration) is to find a combination of parameters (e.g., Kxx, Kyy, Kzz, porosity) that produce the minimum ϕ value. Parameter estimation of a nonlinear problem is an iterative process, and when FePEST performs a calibration, the model is run multiple times, and ϕ is minimized through each successive process of iteration. A significant residual result gives a high value of the objective function, and FePEST tracks the progress of lessening the ϕ value by following whether the ϕ is increasing or decreasing. In this study, the groundwater model inversion was performed using the optimization control package PEST++. The subspace regularization and operation mode used singular value decomposition and ensemble smoothing, respectively. On FePEST, the ensemble-smoother method is a Bayesian-based technique that reformulates the GLMA by empirically deriving the Jacobian matrix from an ensemble of random parameter values (Chen and Oliver 2013). This method substantially reduces the calculation time needed to optimize the model by dividing the number of parameters estimated from the number of model iteration runs required (White 2018). Ensemble smoothing aims to produce several model versions that will be considered a representative sample of possible forecasts and parameter sets. In this study, 25 versions (realizations) were produced. Each of these versions satisfies the calibration criterion with different parameter values. The ensemble smoothing model versions are then calibrated using a modified GLMA to reduce the ϕ value until the calibration target (RMSE) is met and is under the condition that the parameter values deviate as little as possible from the initial parameter values. The advantage of creating a multitude of models is that this method covers a wide range of spatial parameters during the initial run and after each parameter upgrade step. In addition, ensemble smoothing requires

significantly fewer model runs and computation time than traditional/classic GLMA optimizations and can make the calibration process much more robust against model instabilities than via the method of numerical differentiation. The noise created by an unstable model is smoothed by the ensemble of the model versions, and thus affects the calibration process to a much lesser degree (Table 17).

TABLE 17: The averages of the 250 pilot points were computed for each sediment class and each hydraulic parameter across the 24 model versions. Subsequently, the means of the 24 versions were averaged to calculate the final calibrated hydraulic conductivity (i.e., Kxx, Kyy, and Kzz) and porosity (n).

Mean of the 250 pilot points for the 24 model versions												
	1	2	3	4	5	6	7	8	9	10	11	12
	Kxx and Kyy (m/j)											
Sand and gravel	18.58	19.33	19.79	20.01	18.54	19.44	19.74	19.76	21.15	19.8	20.82	19.86
Sand	8.22	8.02	8.33	8.65	8.36	8.62	8.39	8.78	7.27	8.75	7.68	8.37
Tills	5.18	5.35	5.15	5.2	5.01	5.17	5.26	5.94	4.77	5.06	4.28	4.86
	Kzz (m/j)											
Sand and gravel	2.0	2.07	2.18	2.18	2.07	2.15	2.15	2.18	2.31	2.1	2.23	2.16
Sand	0.85	0.81	0.83	0.88	0.86	0.89	0.89	0.89	0.76	0.89	0.83	0.90
Tills	0.68	0.70	0.67	0.68	0.65	0.68	0.69	0.77	0.62	0.66	0.56	0.63
	Porosity (n)											
Sand and gravel	0.25	0.18	0.21	0.19	0.23	0.15	0.24	0.26	0.27	0.19	0.2	0.24
Sand	0.17	0.19	0.17	0.23	0.19	0.2	0.26	0.19	0.14	0.16	0.2	0.23
Tills	0.10	0.16	0.09	0.07	0.10	0.25	0.13	0.22	0.10	0.29	0.25	0.36

Mean of the 250 pilot points for the 24 model versions													
	13	14	15	16	17	18	19	20	21	22	23	24	**Mean of the 24 iterations**
	Kxx and Kyy (m/j)												
Sand and gravel	19.0	19.76	19.53	18.71	19.85	19.77	20.52	19.12	21.17	21.54	19.71	20.07	**19.82**
Sand	9.10	8.59	8.37	8.29	8.11	7.59	8.5	8.78	7.14	8.77	6.97	8.41	**8.25**
Tills	5.84	4.43	4.61	4.76	4.88	4.01	5.1	4.8	4.53	4.83	4.55	5.26	**4.95**
	Kzz (m/j)												
Sand and gravel	2.08	2.18	2.16	2.02	2.19	2.18	2.23	2.07	2.31	2.31	2.18	2.21	**2.16**
Sand	0.89	0.90	0.89	0.86	0.85	0.76	0.90	0.91	0.78	0.87	0.73	0.90	**0.86**
Tills	0.76	0.58	0.60	0.62	0.63	0.52	0.67	0.62	0.59	0.62	0.59	0.68	**0.65**
	Porosity (n)												
Sand and gravel	0.19	0.22	0.13	0.17	0.18	0.24	0.19	0.18	0.17	0.24	0.24	0.20	**0.21**
Sand	0.18	0.17	0.19	0.17	0.19	0.15	0.20	0.18	0.18	0.17	0.17	0.19	**0.19**
Tills	0.20	0.13	0.11	0.20	0.17	0.27	0.09	0.14	0.24	0.15	0.16	0.13	**0.17**

Thirty-three observation points using geophysics-estimated groundwater levels that were directly imported with the groundwater model from FeFLOW® provide the reference values for head distributions. In addition, a spatially correlated parameter field was generated in the form of 250 pilot points distributed randomly throughout the territory for Kxx, Kyy, Kzz values, and the effective soil porosity to capture the local heterogeneity of this Quaternary surface deposit environment. The pilot

point method is a spatial parameterization method used for all parameters to commonly improve the match between the measured and simulated observational data (e.g., geophysics-estimated groundwater level measurements). The calibration process involves a subsequent field perturbation at selected locations (the pilot points). This method allows maintaining the knowing patterns of spatial correlation and parameter point measurements to get the best possible fit between the measured and simulated data. The calibration goal is to identify the optimal perturbation at each pilot point location through the inversion of the observational data (Kowalsky et al. 2004). Because there are more pilot points (n = 250) than observation points (n = 33), the calibration allows the modelers to identify new hydraulic parameters in areas of the model where hydraulic parameters have not yet been determined. This study calibrated Kxx, Kyy, and Kzz and the soil porosity. The steps to follow in FePEST to perform a calibration are: 1) build a functional and uncalibrated groundwater numerical model in FeFLOW. This model provides solutions under various input parameter conditions; 2) transfer the model to the plug-in FePEST, and identify the parameters to modify (i.e., hydraulic conductivity (Kxx, Kyy, Kzz) and effective porosity); and 3) give FePEST a series of observation points. In this work, 33 observation points using geophysics-estimated groundwater levels were entered into FePEST. 4) Run the FePEST plug-in. The FePEST plug-in uses the parameter information provided to modify the numerical groundwater flow model and iteratively run FeFLOW models, adjusting the parameters until the model output matches the field observations (in our case, geophysics-derived water levels); 5) the calibrated (optimized) results suggest a series of optimum values for the selected parameters and observation points; 6) Next FePEST generates a FeFLOW file (.fem). This file is our newly calibrated model and can be used in FeFLOW to estimate how the model responds to parameter changes. 7) Let FeFLOW run. Groundwater levels from this new file (the calibrated model) are compared with the observed groundwater level at the borehole locations. If the simulated groundwater levels obtained using geophysics-derived data correlate well with the observed borehole logging data, it indicates the reliability of geophysical data for purposes of hydrological modeling calibration. Conversely, if the correlation is poor, geophysical data may not be a suitable tool for calibrating a numerical groundwater flow model.

5.5 RESULTS

5.5.1 GEOPHYSICS-ESTIMATED GROUNDWATER LEVELS

We utilized 33 groundwater depth inferences (i.e., observed data) obtained through various geophysical methods, which were initially acquired from the results presented in Lévesque et al. 2023a and subsequently applied in this study (Table 15). All three methods clearly identified groundwater levels in the Saint-Narcisse Moraine saturated sediments, with an uncertainty of the groundwater level elevation varying from approximately 1 to 2 m (Lévesque et al. 2021, 2023a). Moreover, the water table is often clearly evident as a continuous and horizontal reflector with a large amplitude on radargrams (Lévesque et al. 2023a, b). The geophysics-estimated groundwater levels are not evenly distributed and contain gaps in the south-central and southwestern areas of the model due to the difficulty of gaining access in several remote areas of the Saint-Narcisse Moraine. On the other hand, the study area is relatively small, i.e., 26 km², and contains a high number (33) of geophysics-estimated groundwater levels, which is enough to ensure a proper interpolation of the static groundwater levels. The 33 inferences of the water table through the geophysical methods varied between 0 and 10 m below the ground surface. These results (the geophysics-estimated groundwater levels) are based on Lévesque et al. (2021), who created an interpolated map of the groundwater depth in order to define the regional piezometry. This piezometric map uses 465 evenly distributed piezometric surveys conducted on areas within and surrounding the Saint-Narcisse Moraine region in eastern Mauricie.

5.5.2 MODELING PROCESS

5.5.2.1 SIMULATION RESULTS USING THE GEOPHYSICS-DERIVED WATER LEVELS

For the simulation in the FeFLOW software, a single groundwater model for the unconfined aquifer of the Saint-Narcisse Moraine was developed. The model suggest that the unconfined aquifer of the moraine replenishes both the Croche and Batiscan rivers, and the groundwater flows from the northwest topographic summit toward the southeast (See Lévesque et al. 2023a for the original model; Fig. 51). The imbalance value (i.e., water mass balance) is −0.33 m³/day, and the global water budget generated a total regional flow of 17,684 m³/day for the area. To achieve good convergence

(i.e., means that the software has generated a solution) and provide consistent results, the imbalance value should be close to 0. In FeFLOW, the imbalance value shows the difference between the change in model storage and the net boundary fluxes.

An RMSE (Equation 1) was calculated to validate the performance of the model simulation and results. Geophysics-estimated groundwater levels serve as the observed data, and the RMSE acts as an indicator of the difference between the simulated and observed groundwater levels. In this stage of the calibration process, the geophysical data act as observation points in the FeFLOW simulation. Subsequently, the numerical simulation is transferred to FePEST for parameter optimization and calibration. The RMSE indicates the reliability of the model in representing the actual groundwater flow behavior (Chesnaux et al. 2017; Dewar and Knight 2020). As previously conducted in Lévesque et al. (2023a), which employs the same methods to assess the model's reliability, the observed water levels from the 33 geophysical inferences of groundwater depth are compared with the simulated hydraulic head. The resulting simulation produced an RMSE of 2.76 m (Fig. 54), a low value that indicated an acceptable degree of representativity (Wise 2000; Chesnaux et al. 2017). The reliability of the correlation between the simulated and observed values is also supported by the value of the regression coefficient (R2) of 0.9989. The simulation results matched the geophysical observational data (Fig. 54) and showed the model's acceptable representativity to simulate the underground flow and hydraulic heads within this portion of the moraine.

5.5.3 CALIBRATION PROCESS

5.5.3.1 CALIBRATING THE INITIAL GROUNDWATER MODEL PARAMETERS USING GEOPHYSICS-DERIVED WATER LEVELS

For each calibration run, sensitivity analysis was performed in FePEST to optimize the numerical model's previous parameters (the original model) and to find the best estimations. Four parameters were iteratively adjusted (calibrated) using FePEST software: the hydraulic conductivities Kxx, Kyy, Kzz, and the effective soil porosity. These parameters were optimized for each sedimentary layer found for the Quaternary surface deposits in this region of the moraine, consisting of surface sand and gravel, sand, and the glacial tills overlying the bedrock. To perform the calibration, FePEST runs ten iterations to find a combination of parameters that produces the minimum value for ϕ

(Equation 5). The initial ϕ started at 18,113 and was minimized at 1,212 after ten iterations (Fig. 56). At the end of the calibration/optimization, the results produce 25 model versions that each satisfy the calibration criterion and present the best estimates (the last iteration) of the parameter values. All the pilot points (250 for each hydraulic parameter) related to each sediment class (i.e., sand, sand-gravel, tills) were averaged to calculate the final calibrated hydraulic parameters.

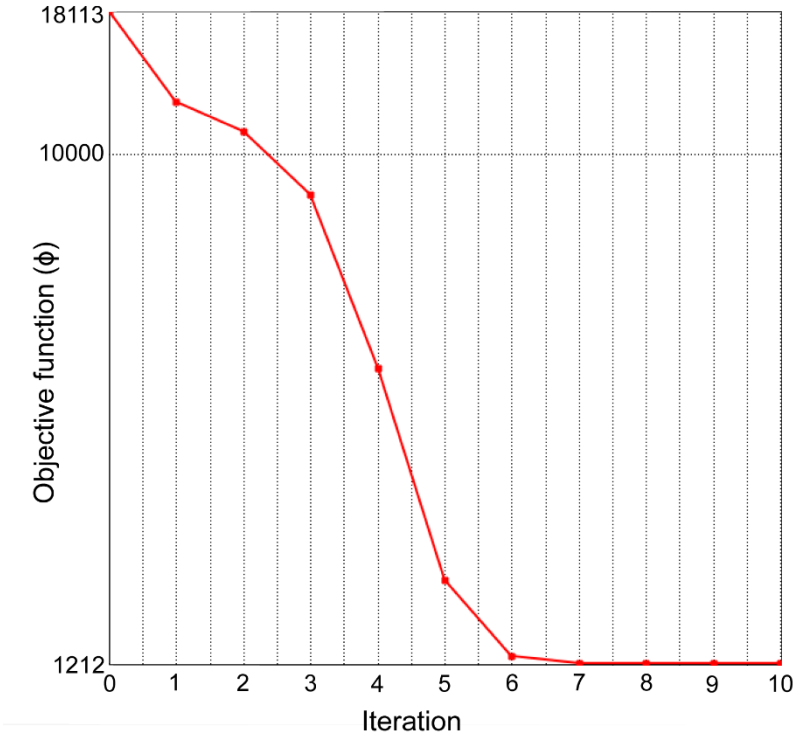

Figure 56: Variation of the objective function for each iteration in FePest.

In this study, to ensure the significance of each version generated by FePEST, we utilized the average of 24 models to determine hydraulic conductivity (i.e., Kxx, Kyy, and Kzz) and porosity (n) after calibration (Table 18). This method is considered representative as it enables the calculation of all acquired results (i.e., possible parameter sets) for each sediment classes in this region of the moraine. The averaged parameter values for each sediment class after calibration is shown in

Tables 17 and 18. The sequential calibration with the FePEST plug-in resulted in minor underestimations of the hydraulic parameters (Tables 16 and 18) and hydraulic head (Fig. 57).

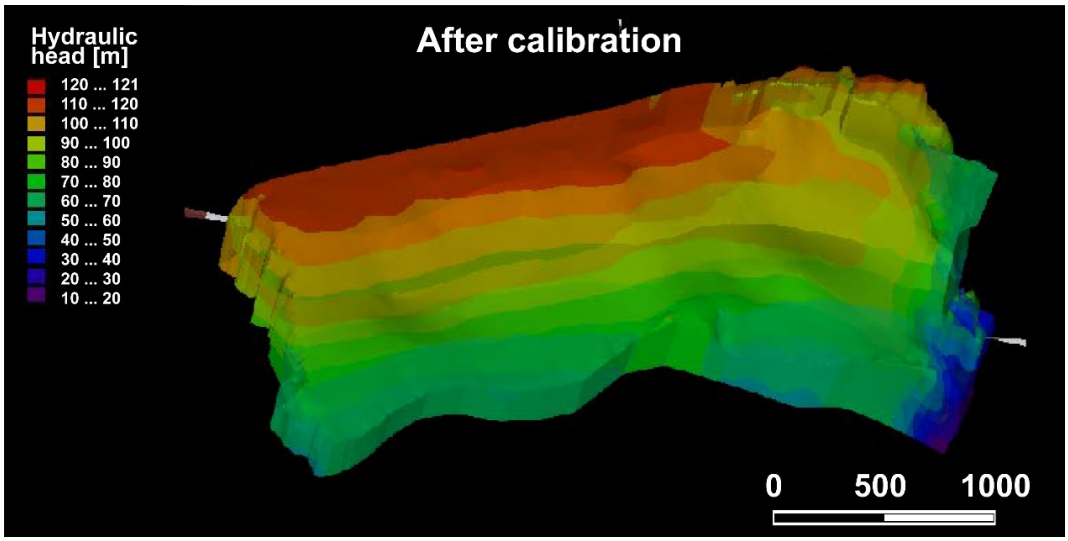

Figure 57: 3D flow models of the Saint-Narcisse Moraine unconfined aquifer (Québec). The model, after the calibration, covers approximately 26 km².

TABLE 18: Hydraulic calibrated parameters for the sand and gravel, the sand and the tills.

Hydraulic Parameters (calibrated)			
Geological layer	Kxx and Kyy (m/j)	Kzz (m/j)	Effective porosity (n)
Sand and gravel	19.82	2.16	0.21
Sand (littoral and fluvioglacial)	8.25	0.86	0.19
Tills	4.95	0.65	0.17
Bedrock	ø	ø	ø

5.5.3.2 USING THE CALIBRATED MODEL PARAMETERS TO ESTIMATE THE GROUNDWATER LEVEL AT THE BOREHOLE LOCATIONS

The optimized parameters obtained from the calibrated model were then employed in FeFLOW to estimate the groundwater levels at 25 borehole locations (observed piezometric data; Table 14). These data were originally reported in Lévesque et al. 2023a. This generated a new simulated model based on the calibrated model parameters obtained through FePEST (Fig. 57). To evaluate success

of the model calibration, statistical parameters, including the RMSE (Equation 1) and regression coefficient (R2), were calculated to assess the difference between the simulated results from the calibrated model and the observed groundwater levels from borehole logs. This provided a measure of the goodness-of-fit between the calibrated model from geophysics-derived water levels (soft data) and the water levels from the borehole logs (hard data).

The observed water levels from borehole inferences of the groundwater depth are compared with the simulated hydraulic head, and the resulting simulation produced a low value for the RMSE of 3.69 m (Fig. 53). The scatter plot shows a reasonable match between the observed and simulated values, with most of the simulated points centered around the line of perfect fit (i.e., 1:1 line). Along with the low RMSE, the regression coefficient (R2) of 0.9994 indicates how strong the linear relationship is between the two datasets. The high R2 confirms that the simulation results strongly matched the observational data from borehole logs (Fig. 53) and shows the model's acceptable representativity and reliability to simulate the subsurface groundwater flow and hydraulic heads within this portion of the moraine.

5.6 DISCUSSIONS

5.6.1 INITIAL NUMERICAL MODEL AND GEOPHYSICS-ESTIMATED GROUNDWATER LEVELS

The initial groundwater model was developed for a glacial aquifer system in the Saint-Narcisse Moraine, located in the Mauricie region of southeastern Québec, Canada. For this model, hydraulic parameters have been predefined. The simulated hydraulic heads were compared against geophysics-estimated groundwater levels through the RMSE method (Fig. 54). After performing the simulation with the geophysical estimated data, the low RMSE value (i.e., 2.76 m) suggests that the initial model is reliable in terms of accuracy and precision (Chesnaux et al. 2017; Dewar and Knight 2020; Lévesque et al. 2023a) and represents the natural variations in the groundwater levels. Lévesque et al. (2023a) illustrated how geophysical data can provide additional hydraulic information to improve groundwater flow models, determine water table heights, and validate the performance of a flow model, particularly in areas characterized by limited direct piezometric information. Validating the initial model is necessary to confirm the relevance of the results that are acquired from the

numerical analysis using geophysical data. Lévesque et al. (2023a) also illustrated that combining multiple geophysical techniques significantly reduces the uncertainty inherent to geophysical methods, which are indirect subsurface observations. This study acquired data through TEM, ERT, and GPR surveys. By combining these methods, we significantly reduced the uncertainty associated with the location of groundwater levels to validate the hydraulic heads acquired from the initial flow model. Each geophysical method has particular strengths and weaknesses, and the advantage of combining them is that the other applied methods can compensate for the weaknesses of one particular method. Consequently, it reduces the amount of missing information (e.g., water table elevations) between geophysical measurements. Their combination significantly diminished the uncertainty of the results and provided an opportunity to accurately determine groundwater levels in order to validate whether the simulated groundwater flow model was suitable (Lévesque et al. 2023a).

5.6.2 CALIBRATION OF THE MODEL PARAMETERS AND COMPARISON WITH GROUNDWATER LEVEL AT THE BOREHOLE LOCATIONS

In hydrological modeling, the calibration procedure is the automatic or manual altering of parameters of a model (e.g., hydraulic conductivity, soil porosity, transmissivity, anisotropy factors) to determine the optimal parameters, and to minimize the misfit between the observed and simulated hydrological responses (i.e., predicted state variables such as groundwater levels). Model calibration aims to ensure that a numerical flow model replicates the behavior of a real-world system as accurately as possible. To achieve this, in-situ water level observational data are crucial to characterize the real-world system, and to ensure that the calibrated model parameters match the field observations. This study used geophysical data as the in-situ water level observations to calibrate the flow model. However, indirect measurements from geophysical methods are subject to uncertainty, which poses a significant challenge. It is difficult to establish the reliability of the geophysical methods in representing actual subsurface conditions and providing reliable information for groundwater modeling due to their indirect observational nature. Nevertheless, this study takes advantage of the abundance of boreholes and piezometric information available throughout the region, which provides an excellent opportunity to 'ground truth' the recovered parameters after performing model calibration. Validation with observed borehole logging data is the most effective

method to reduce potential uncertainties related to geophysical data and to validate the calibration performed by FePEST using the initial numerical model, which incorporates groundwater levels estimated through geophysical approaches.

To calibrate the model, FePEST uses the provided hydraulic parameter information. The model is iteratively run, and the parameters are adjusted until the objective function is minimized and the model output matches the field observations (in this case, geophysics-derived water levels). In this calibration, the initial objective function had a value of 18,113, which was minimized to 1,212 after ten iterations, demonstrating a significant reduction in data misfit and a successful calibration. For a numerical model representing a relatively small region, such as the Saint-Narcisse moraine in the Mauricie section modeled in this study (26 km²), the calibration method provided good results, and the initial parameter values minimally varied (see Tables 16 and 18). However, for larger-scale flow models, differences in hydraulic parameters (related to the spatial variations), such as hydraulic conductivity and soil porosity, are expected to be more significant.

Subsequently, we compared the calibrated model with observational borehole logging data (i.e., directly observed groundwater levels) using the RMSE. The relatively low RMSE value of 3.69 m (Fig. 53) indicated that the post-calibrated simulation results matched the observational data (form the piezometric surveys). Numerous studies have proposed that an RMSE of less than 5 meters is considered acceptable for a regional numerical flow model (Wise 2000; Chesnaux 2013; Chesnaux et al. 2017; Lévesque et al. 2021, 2023a) due to various factors that can influence the variability of the groundwater table over time, including errors associated with measurements, uncertainties related to seasonal fluctuations in water levels at a regional scale, the simplified 3D geological model, and the spatial heterogeneity of the borehole distribution. These potential causes of error may generate differences between the observed and simulated groundwater levels. The calibrated model also shows a good correlation with the observed values from the borehole logs; R2 = 0.9994. These results (RMSE and R2) show the model's acceptable representativity to simulate the hydraulic head and underground flow characteristics with the calibrated parameters from the geophysics-derived water levels. This indicates that the numerical flow model, calibrated with indirect water level data

obtained through geophysical data, is validated by the good correlation with the real groundwater level data obtained from borehole logs. If geophysical data were inadequate for calibrating a flow model, the RMSE from borehole water levels would be significantly higher, indicating inadequate calibration. However, this is not the case. This good match between the calibrated model and the observational borehole logging data means that the geophysics-calibrated hydrological modeling is sufficient, proving the usefulness of geophysical data in hydrological modeling calibration.

A hydrogeologist who wants to incorporate geophysical data into flow modeling, calibrate flow models, and optimize their initial parameters to better reflect reality needs to combine different geophysical methods in order to reduce the uncertainty inherent to geophysical data. Any geophysical method that can accurately locate the water table can be used and combined with other methods. Once groundwater levels are identified with relative accuracy, they can be used to validate the reliability of a numerical flow model (Lévesque et al. 2023a) and/or use it to calibrate the flow model in order to optimize initial hydraulic parameters, or even to recover new hydraulic parameters that are not available.

Key differences between the findings of this study and the original study by Lévesque et al. 2023a are as follows: In Lévesque et al., 2023a, (1) initial geological and groundwater numerical models were developed, and (2) multiple geophysical techniques were combined to reduce uncertainties. (3) Hydraulic heads simulated were compared to geophysics-estimated groundwater levels using the RMSE method, resulting in a low RMSE value of 2.76 m, demonstrating how (4) geophysical data can provide additional hydraulic information for accurately determining water table elevation and validating a flow model's performance.

In this study, the initial model parameters were refined through FeFLOW parameter estimation (FePEST) using geophysics-derived water levels. Piezometric surveys from boreholes provided an opportunity to 'ground truth' the recovered parameters after model calibration. A comparison between observed groundwater levels and post-calibrated results was performed using root mean square error (RMSE), resulting in a relatively low RMSE value of 3.69 m, highlighting the efficacy of geophysical

data in establishing a high-quality dataset for calibrating hydrological models with software such as PEST. This approach complements direct observations, providing reasonable hydraulic information (e.g., hydraulic conductivity (Kxx, Kyy, Kzz) and porosity) at a lower cost and faster data acquisition by optimizing hydraulic parameters. Following calibration using geophysics-derived water levels, a modeler can quickly identify new hydraulic parameters in areas of the model not previously determined by other means.

5.7 CONCLUSION

Uncertainties often undermine groundwater modeling; if the model parameters are uncertain, so is the model prediction. Optimizing the initial parameters to give the best possible fit between the measured and simulated data can be crucial for a groundwater model, especially if the hydraulic properties cannot be measured accurately. This study demonstrates how multiple geophysical techniques and groundwater levels are relevant to calibrating (optimizing) a regional groundwater flow model and could considerably improve its accuracy by recovering reasonable hydraulic parameters. Acquiring field data such as borehole logs and piezometers measurements to ensure that model outputs match field measurements are an expensive and time-consuming process, and combining multiple geophysical techniques overcomes the disadvantage of point-scale observations (i.e., borehole logs). Coupling the geophysical methods appropriately considers the structural inadequacies and significantly reduces the uncertainty inherent to geophysics.

Consequently, high-quality geophysical data can provide an inexpensive, nondestructive, fast, robust, and effective means of characterizing the water levels and give the groundwater modeling community a valuable tool to calibrate a flow model and improve the performance of hydrological modeling, especially in areas with limited borehole logging data. This method using geophysical data represents a novel approach to calibrating models with software such as PEST, allowing the optimization of hydraulic parameters at a lower cost and faster acquisition of data. Incorporating geophysics-derived water levels to calibrate a regional numerical groundwater flow model, or to

validate its reliability is also a promising approach to alleviate uncertainties associated with smaller databases and local interpretation. Geophysical data can provide much more information than borehole logging data, and cover a larger area in the model, ultimately making it more representative and reducing the impact of uncertainties.

This approach leads to significant enhancements in the quality of numerical groundwater flow models, specifically in the 3D representation of aquifers and water tables, as well as in the calibration of the flow model, both of which are critical steps in numerical hydrogeological modeling.

5.8 CONCLUSION DU CHAPITRE 5

Pour cette étude, les méthodes conventionnelles de calibration n'ont pas été préalablement évaluées. Par conséquent, cet outil est considéré comme secondaire, affichant une robustesse moindre par rapport à d'autres approches en termes de travail et de recherche réalisés. Nous disposions d'un modèle numérique 3D de qualité et des données de forage pour valider la calibration effectuée avec les données géophysiques. Il semblait donc naturel de tenter une calibration avec le logiciel FePest afin de vérifier la cohérence des résultats produits par les données géophysiques. Cela s'est avéré concluant. Toutefois, des études plus approfondies pourraient être menées dans cette direction pour mieux valider l'utilisation des données géophysiques pour la calibration et l'estimation de nouveaux paramètres hydrauliques dans une région.

Cet outil d'investigation est donc complémentaire à l'outil précédent, qui utilise les données géophysiques pour valider la fiabilité d'un modèle numérique. Il permet, grâce aux niveaux d'eau dérivés des données géophysiques, de calibrer un modèle numérique et d'obtenir de nouveaux paramètres hydrauliques. Bien qu'il y ait peu de paramètres à calibrer (à savoir Kx, Ky et Kz), l'intérêt principal réside dans l'optimisation des paramètres hydrauliques existants et l'acquisition de nouveaux paramètres dans les zones où ces informations faisaient défaut. Cela enrichit les données disponibles et fournit également un aperçu de l'anisotropie régionale. Cette démarche est réalisable

de manière simple, surtout si un modèle d'écoulement souterrain est déjà en place, en utilisant un logiciel existant comme FePest.

Il est important de souligner que les résultats de cette méthode ne se limitent pas à une douzaine de paramètres hydrauliques, mais génèrent en réalité environ 3000 nouvelles valeurs pour la porosité et les conductivités hydrauliques Kx, Ky et Kz. Ces valeurs sont des moyennes calculées pour simplifier la présentation des résultats. Concrètement, 250 nouvelles valeurs de conductivité hydraulique (en Kx, Ky et Kz) et de porosité effective ont été obtenues pour chacune des classes sédimentaires étudiées (sable, sable et gravier, et tills). Des valeurs de conductivité hydraulique supplémentaires et actualisées dans cette région du modèle numérique auraient été indéniablement précieuses pour confirmer la validité de cette calibration.

Afin d’effectuer cette calibration, un champ de paramètres spatialement corrélés a été généré sous forme de 250 points pilotes répartis de manière aléatoire sur l'ensemble du territoire pour la porosité et les valeurs de conductivité hydraulique Kxx, Kyy, et Kzz. Une répartition différente, plus large ou plus serrée, aurait pu être utilisée afin de moduler l'espacement des points pilotes sur le territoire. La méthode des points pilotes est une technique de paramétrisation spatiale employée pour tous les paramètres afin d'améliorer la correspondance entre les données observationnelles mesurées et simulées, telles que les niveaux piézométriques estimés par la géophysique. Le processus de calibration implique une perturbation de champ subséquente à des emplacements sélectionnés, les points pilotes. Cette méthode, combinée à l'interpolation par krigeage, permet de maintenir les schémas connus de corrélation spatiale et de mesures de points de paramètre, afin d'obtenir le meilleur ajustement possible entre les données mesurées et simulées. Étant donné qu'il y a plus de points pilotes (n = 250) que de points d'observation (n = 33), la calibration permet aux modélisateurs d'identifier de nouveaux paramètres hydrauliques dans des zones du modèle où ceux-ci n'ont pas encore été déterminés. Ainsi, c’est aux emplacements des points pilotes que le logiciel fournit les résultats.

En ce qui concerne l'utilisation des données géophysiques, l'intégralité des stations TEM a été exploitée. Quant aux méthodes ERT et géoradar, il aurait été envisageable d'utiliser toutes les données disponible sur chaque profil (par exemple, tous les 10 m), mais à l'échelle régionale, cela aurait été dépourvu de pertinence. La dimension de l'échelle rend l'utilisation de données trop rapprochées non pertinente pour la validation et la calibration des modèles numériques, étant donné que la nappe phréatique présente des élévations similaires sur une distance de 250 m (longueur des profils ERT). Par conséquent, seules les mesures de niveaux d'eau situées aux extrémités des profils ERT et GPR ont été prises en compte. Par exemple, les électrodes 1 et 48 ont été utilisées pour évaluer les niveaux d'eau sur les profils ERT. Cependant, les profils de géoradar et d'ERT ne fournissaient parfois aucune information exploitable. Par exemple, le toit de la nappe n'était pas clairement discernable dans les profils du géoradar, ou aucun contraste de résistivité net n'apparaissait dans les profils de l'ERT.

En outre, il est important de rappeler ici que l'objectif premier de cette thèse n'est pas de représenter l'hétérogénéité locale dans un modèle hydrogéologique. Cela s'avère irréalisable à l'échelle régionale en raison du manque de données disponibles, notamment des données de forage de qualité en plus grande quantité permettant de bien comprendre la granulométrie et l'étendue des lentilles de sédiments dans la zone étudiée. L'objectif principal est plutot d'évaluer avec une justesse accrue le potentiel en eau souterraine d'un environnement quaternaire hétérogène et anisotrope à une échelle régionale. Pour y parvenir, chaque outil d'investigation, constitue une avancée significative dans l'évaluation du potentiel en eau souterraine à cette échelle. Il est essentiel de considérer l'hétérogénéité à l'échelle régionale, où par exemple, de grandes épaisseurs d'argile jouent le rôle de barrière naturelle imperméable, parfois compartimentant les aquifères granulaires régionaux.

LISTE DES REFERENCES

Abi, A., Walter, J., Saeidi, A., and Chesnaux, R. 2022. A cluster-based multiparametric similarity test for the compartmentalization of crystalline rocks into structural domains. Quarterly Journal of Engineering Geology and Hydrogeology, 55. Geological Society of London.

Binley, A., and Beven, K. 2003. Vadose zone flow model uncertainty as conditioned on geophysical data. Groundwater, 41: 119–127. Wiley Online Library. doi:10.1111/j.1745-6584.2003.tb02576.x.

Blanco-Canqui, H., and Lal, R. 2007. Impacts of long-term wheat straw management on soil hydraulic properties under no-tillage. Soil Science Society of America Journal, 71: 1166–1173. Wiley Online Library.

Boucher, M., Favreau, G., Nazoumou, Y., Cappelaere, B., Massuel, S., and Legchenko, A. 2012. Constraining groundwater modeling with magnetic resonance soundings. Groundwater, 50: 775–784. Wiley Online Library.

Boumaiza, L., Chesnaux, R., Stotler, R.L., Rouleau, A., Levesque, Y., Batelaan, O., Cousineau, P.A., and Missimer, T.M. 2023. A combined laboratory and field-based experimental approach to characterize the heterogeneity of granular aquifers. Hydrogeology journal,: 1–21. Springer. doi:10.1007/s10040-023-02690-x.

Boumaiza, L., Chesnaux, R., Walter, J., and Meghnefi, F. 2021a. Assessing response times of an alluvial aquifer experiencing seasonally variable meteorological inputs. Groundwater for Sustainable Development, 14: 100647. Elsevier.

Boumaiza, L., Chesnaux, R., Walter, J., and Stumpp, C. 2020. Assessing groundwater recharge and transpiration in a humid northern region dominated by snowmelt using vadose-zone depth profiles. Hydrogeology Journal, 28: 2315–2329. Springer. doi:10.1111/gwat.13056.

Boumaiza, L., Chesnaux, R., Walter, J., and Stumpp, C. 2021b. Constraining a flow model with field measurements to assess water transit time through a vadose zone. Groundwater, 59: 417–427. Wiley Online Library. doi:10.1111/gwat.13056.

Boumaiza, L., Walter, J., Chesnaux, R., Brindha, K., Elango, L., Rouleau, A., Wachniew, P., and Stumpp, C. 2021c. An operational methodology for determining relevant DRASTIC factors and their relative weights in the assessment of aquifer vulnerability to contamination. Environmental Earth Sciences, 80: 1–19. Springer.

Boumaiza, L., Walter, J., Chesnaux, R., Lambert, M., Jha, M.K., Wanke, H., Brookfield, A., Batelaan, O., Galvão, P., and Laftouhi, N. 2022. Groundwater recharge over the past 100 years: regional spatiotemporal assessment and climate change impact over the Saguenay-Lac-Saint-Jean region, Canada. Hydrological Processes,: e14526. Wiley Online Library. doi:10.1002/hyp.14526.

Brouard, E., Roy, M., Godbout, P.-M., and Veillette, J.J. 2021. A framework for the timing of the final meltwater outbursts from glacial Lake Agassiz-Ojibway. Quaternary Science Reviews, 274: 107269. Elsevier.

Cassiani, G., and Binley, A. 2005. Modeling unsaturated flow in a layered formation under quasi-steady state conditions using geophysical data constraints. Advances in Water Resources, 28: 467–477. Elsevier.

Chen, J., Hubbard, S., Rubin, Y., Murray, C., Roden, E., and Majer, E. 2004. Geochemical characterization using geophysical data and Markov Chain Monte Carlo methods: A case

study at the South Oyster bacterial transport site in Virginia. Water Resources Research, 40. Wiley Online Library.

Chen, Y., and Oliver, D.S. 2013. Levenberg–Marquardt forms of the iterative ensemble smoother for efficient history matching and uncertainty quantification. Computational Geosciences, 17: 689–703. Springer.

Chesnaux, R. 2013. Regional recharge assessment in the crystalline bedrock aquifer of the Kenogami Uplands, Canada. Hydrological sciences journal, 58: 421–436. Taylor & Francis. doi:10.1080/02626667.2012.754100.

Chesnaux, R., Lambert, M., Walter, J., Dugrain, V., Rouleau, A., and Daigneault, R. 2017. A simplified geographical information systems (GIS)-based methodology for modeling the topography of bedrock: illustration using the Canadian Shield. Applied Geomatics, 9: 61–78. Springer. doi:10.1007/s12518-017-0183-1.

Constable, S.C., and Parker, R.L. 1987. Occam's inversion: A practical algorithm for generating smooth models from electromagnetic sounding data. Geophysics, 52: 289–300. Society of Exploration Geophysicists. doi:10.1190/1.1442303.

Daigneault, R.-A., and Occhietti, S. 2006. Les moraines du massif Algonquin, Ontario, au début du Dryas récent, et corrélation avec la Moraine de Saint-Narcisse. Géographie physique et Quaternaire, 60: 103–118. Les Presses de l'Université de Montréal. doi:10.7202/016823ar.

Dewar, N., and Knight, R. 2020. Estimation of the top of the saturated zone from airborne electromagnetic data. Geophysics, 85: EN63–EN76. Society of Exploration Geophysicists and American Association of Petroleum …. doi:10.1190/geo2019-0539.1.

Diersch, H.-J.G. 2013. FEFLOW: finite element modeling of flow, mass and heat transport in porous and fractured media. Edited BySpringer Science & Business Media. Springer Science & Business Media. doi:10.1007/978-3-642-38739-5_1.

Doherty, J., and Christensen, S. 2011. Use of paired simple and complex models to reduce predictive bias and quantify uncertainty. Water Resources Research, 47. Wiley Online Library. doi:10.1029/2011WR010763.

Doherty, J.E. 2007. Use of PEST and some of its utilities in model calibration and predictive error variance analysis: a roadmap. Brisbane, Australia,.

Doherty, J., and Moore, C. 2020. Decision support modeling: data assimilation, uncertainty quantification, and strategic abstraction. Groundwater, 58: 327–337. Wiley Online Library. doi:10.1111/gwat.12969.

Dyke, A.S. 2004. An outline of the deglaciation of North America with emphasis on central and northern Canada. Quaternary Glaciations-Extent and Chronology, Part II: North America, 2b: 373-424. doi:10.1016/S1571-0866(04)80209-4.

Elbshbeshi, A., Gomaa, A., Mohamed, A., Othman, A., and Ghazala, H. 2022. Seismic hazard evaluation by employing microtremor measurements for Abu Simbel area, Aswan, Egypt. Journal of African Earth Sciences, 196: 104734. Elsevier.

Ferré, T., Bentley, L., Binley, A., Linde, N., Kemna, A., Singha, K., Holliger, K., Huisman, J.A., and Minsley, B. 2009. Critical steps for the continuing advancement of hydrogeophysics. Eos, Transactions American Geophysical Union, 90: 200. Wiley Online Library.

Fitterman, D. V, and Labson, V.F. 2005. Electromagnetic induction methods for environmental problems. In Near-surface geophysics. Edited by S. of E. Geophysicists. Society of Exploration Geophysicists, Houston, TX. pp. 301–356. doi:10.1190/1.9781560801719.ch10.

Fortier, R., Banville, D.-R., Lévesque, R., Lemieux, J.-M., Molson, J., Therrien, R., and Ouellet, M. 2020. Development of a three-dimensional geological model, based on Quaternary chronology, geological mapping, and geophysical investigation, of a watershed in the discontinuous permafrost zone near Umiujaq (Nunavik, Canada). Hydrogeology Journal,. doi:10.1007/s10040-020-02113-1.

Freeze, R.A., and Cherry, J.A. 1979. JA Cherry. 1979. Groundwater. In Prentive-hall, Englewood cliffs, NJ, 604p. rentive-hall, Englewood cliffs, NJ, 604p.

Galazoulas, E.C., Mertzanides, Y.C., Petalas, C.P., and Kargiotis, E.K. 2015. Large scale electrical resistivity tomography survey correlated to hydrogeological data for mapping groundwater salinization: a case study from a multilayered coastal aquifer in Rhodope, Northeastern Greece. Environmental processes, 2: 19–35. Springer.

Gallardo, L.A., and Meju, M.A. 2004. Joint two-dimensional DC resistivity and seismic travel time inversion with cross-gradients constraints. Journal of Geophysical Research: Solid Earth, 109. Wiley Online Library.

García-Menéndez, O., Ballesteros, B.J., Renau-Pruñonosa, A., Morell, I., Mochales, T., Ibarra, P.I., and Rubio, F.M. 2018. Using electrical resistivity tomography to assess the effectiveness of managed aquifer recharge in a salinized coastal aquifer. Environmental monitoring and assessment, 190: 1–19. Springer.

Globensky, Y. 1987. Géologie des Basses-Terres du Saint-Laurent. Ministère de l'énergie et des ressources, direction générale de l'exploration géologique et minérale, Québec (Qc).

Godbout, P.-M., Brouard, E., and Roy, M. 2023. 1-km resolution rebound surfaces and paleotopography of glaciated North America since the Last Glacial Maximum. Scientific Data, 10: 735. Nature Publishing Group UK London.

Goutaland, D. 2008. Caractérisation hydrogéophysique d'un dépôt fluvioglaciaire: évaluation de l'effet de l'hétérogénéité hydrodynamique sur les écoulements en zone non-saturée. Ph.D. dissertation, Lyon University (INSA), France, 246 p.

Hanke, M. 1997. A regularizing Levenberg-Marquardt scheme, with applications to inverse groundwater filtration problems. Inverse problems, 13: 79. IOP Publishing.

Hartmann, A., Goldscheider, N., Wagener, T., Lange, J., and Weiler, M. 2014. Karst water resources in a changing world: Review of hydrological modeling approaches. Reviews of Geophysics, 52: 218–242. Wiley Online Library.

Hill, M.C. 2006. The practical use of simplicity in developing ground water models. Groundwater, 44: 775–781. Wiley Online Library. doi:10.1111/j.1745-6584.2006.00227.x.

Hinnell, A.C., Ferré, T.P.A., Vrugt, J.A., Huisman, J.A., Moysey, S., Rings, J., and Kowalsky, M.B. 2010. Improved extraction of hydrologic information from geophysical data through coupled hydrogeophysical inversion. Water resources research, 46. Wiley Online Library.

Hsieh, P.A., Tracy, J. V, Neuzil, C.E., Bredehoeft, J.D., and Silliman, S.E. 1981. A transient laboratory method for determining the hydraulic properties of 'tight' rocks—I. Theory. International Journal of Rock Mechanics and Mining Sciences & Geomechanics Abstracts, 18: 245–252. doi:https://doi.org/10.1016/0148-9062(81)90979-7.

Hubbard, S.S., and Rubin, Y. 2000. Hydrogeological parameter estimation using geophysical data: a review of selected techniques. Journal of Contaminant Hydrology, 45: 3–34. Elsevier.

Hudon-Gagnon, E., Chesnaux, R., Cousineau, P.A., and Rouleau, A. 2015. A hydrostratigraphic simplification approach to build 3D groundwater flow numerical models: example of a Quaternary deltaic deposit aquifer. Environmental earth sciences, 74: 4671–4683. Springer. doi:10.1007/s12665-015-4439-y.

Huisman, J.A., Rings, J., Vrugt, J.A., Sorg, J., and Vereecken, H. 2010. Hydraulic properties of a model dike from coupled Bayesian and multi-criteria hydrogeophysical inversion. Journal of Hydrology, 380: 62–73. Elsevier. doi:10.1016/j.jhydrol.2009.10.023.

Jadoon, K.Z., Slob, E., Vanclooster, M., Vereecken, H., and Lambot, S. 2008. Uniqueness and stability analysis of hydrogeophysical inversion for time-lapse ground-penetrating radar estimates of shallow soil hydraulic properties. Water resources research, 44. Wiley Online Library.

Jadoon, K.Z., Weihermüller, L., Scharnagl, B., Kowalsky, M.B., Bechtold, M., Hubbard, S.S., Vereecken, H., and Lambot, S. 2012. Estimation of soil hydraulic parameters in the field by integrated hydrogeophysical inversion of time-lapse ground-penetrating radar data. Vadose Zone Journal, 11: vzj2011-0177. Wiley Online Library.

Jonard, F., Weihermüller, L., Schwank, M., Jadoon, K.Z., Vereecken, H., and Lambot, S. 2015. Estimation of hydraulic properties of a sandy soil using ground-based active and passive microwave remote sensing. IEEE transactions on geoscience and remote sensing, 53: 3095–3109. IEEE.

Kalisperi, D., Kouli, M., Vallianatos, F., Soupios, P., Kershaw, S., and Lydakis-Simantiris, N. 2018. A transient ElectroMagnetic (TEM) method survey in north-central coast of Crete, Greece: evidence of seawater intrusion. Geosciences, 8: 107. Multidisciplinary Digital Publishing Institute. doi:10.3390/geosciences8040107.

Kowalsky, M.B., Finsterle, S., Peterson, J., Hubbard, S., Rubin, Y., Majer, E., Ward, A., and Gee, G. 2005. Estimation of field-scale soil hydraulic and dielectric parameters through joint inversion of GPR and hydrological data. Water Resources Research, 41. Wiley Online Library.

Kowalsky, M.B., Finsterle, S., and Rubin, Y. 2004. Estimating flow parameter distributions using ground-penetrating radar and hydrological measurements during transient flow in the vadose zone. Advances in Water Resources, 27: 583–599. Elsevier. doi:10.1016/j.advwatres.2004.03.003.

Lambert, M., Ferroud, A., Desmeules, L.-P., and Walter, J. 2022. CERM-PACES LAMEMCN public report, (Donnees Quebec); https://constellation.uqac.ca/id/eprint/8531/1/ME_Rapport_Scientifique_VF5.pdf.

Lambot, S., Slob, E.C., Vanclooster, M., and Vereecken, H. 2006. Closed loop GPR data inversion for soil hydraulic and electric property determination. Geophysical research letters, 33. Wiley Online Library.

Lévesque, Y., Chesnaux, R., and Walter, J. 2023a. Using geophysical data to assess groundwater levels and the accuracy of a regional numerical flow model. Hydrogeology Journal,. doi:10.1007/s10040-023-02591-z.

Lévesque, Y., St-Onge, G., Lajeunesse, P., Desiage, P., and Brouard, E. 2019. Defining the maximum extent of the Laurentide Ice Sheet in Home Bay (eastern Arctic Canada) during the Last Glacial episode. Boreas, 49: 52–70. Wiley Online Library. doi:10.1111/bor.12415.

Lévesque, Y., Walter, J., Boumaiza, L., Lambert, M., Ferroud, A., and Chesnaux, R. 2023b. Multi-technique approach to characterize the hydrogeology of aquifer systems: Application on the Mauricie region of Quebec, Canada (on press). Canadian Water Resources Journal/Revue canadienne des ressources hydriques,.

Lévesque, Y., Walter, J., and Chesnaux, R. 2021. Transient Electromagnetic (TEM) Surveys as a First Approach for Characterizing a Regional Aquifer: The Case of the Saint-Narcisse Moraine, Quebec, Canada. Geosciences, 11: 415–442. Multidisciplinary Digital Publishing Institute. doi:10.3390/ geosciences11100415.

Lévesque, Y., Walter, J., Chesnaux, R., Dugas, S., and David, N. 2023c. Electrical resistivity of saturated and unsaturated sediments in northeastern Canada. Environmental earth sciences,. doi:10.1007/s12665-023-10998-w.

Li, C., Doble, R., Hatch, M., Heinson, G., and Kay, B. 2021. Constraining regional-scale groundwater transport predictions with multiple geophysical techniques. Journal of Hydrology: Regional Studies, 36: 100841. Elsevier.

Linde, N., and Doetsch, J. 2016. Joint inversion in hydrogeophysics and near-surface geophysics. Integrated imaging of the Earth: Theory and applications,: 117–135. Wiley Online Library.

Loke, M.H. 1999. Time-lapse resistivity imaging inversion. Proceedings of the 5th Meeting of the Environmental and Engineering. Geophysical Society European Section, Em1,: 1–12. doi:10.4133/1.2922877.

Loke, M.H. 2006. RES2DINV ver. 3.55, Rapid 2-D resistivity & IP inversion using the least-squares method. Software Manual, 139: 131–152. doi:10.1111/j.1365-2478.1996.tb00142.x.

Loke, M.H., and Barker, R.D. 1995. Least-squares deconvolution of apparent resistivity pseudosections. Geophysics, 60: 1682–1690. Society of Exploration Geophysicists. doi:10.1190/1.1443900.

Loke, M.H., and Barker, R.D. 2006. Practical techniques for 3D resistivity surveys and data inversion1. Geophysical prospecting, 44: 499–523. European Association of Geoscientists & Engineers. doi:10.1111/j.1365-2478.1996.tb00162.x.

Looms, M.C., Binley, A., Jensen, K.H., Nielsen, L., and Hansen, T.M. 2008. Identifying unsaturated hydraulic parameters using an integrated data fusion approach on cross-borehole geophysical data. Vadose Zone Journal, 7: 238–248. Wiley Online Library.

MacInnes, S., Durham, J., Dickerson, J., Snyder, S., and Zonge, K. 2001. Fast TEM for UXO mapping at Gambell, Saint Lawrence Island, Alaska. In UXO/Countermine Forum.

MacInnes, S., and Raymond, M. 2001. ZONGE Data Processing Two-Dimensional, Smooth-Model CSAMT Inversion version 3.00. Zonge Engineering and Research Organization, Inc. p. 41.

McMartin, I., Godbout, P., Campbell, J.E., Tremblay, T., and Behnia, P. 2021. A new map of glacigenic features and glacial landsystems in central mainland Nunavut, Canada. Boreas, 50: 51–75. Wiley Online Library.

Margold, M., Stokes, C.R., and Clark, C.D. 2015. Ice streams in the Laurentide Ice Sheet: Identification, characteristics and comparison to modern ice sheets. Earth-Science Reviews, 143: 117–146. doi:10.1016/j.earscirev.2015.01.011.

Martınez-Vilalta, J., Piñol, J., and Beven, K. 2002. A hydraulic model to predict drought-induced mortality in woody plants: an application to climate change in the Mediterranean. Ecological Modelling, 155: 127–147. Elsevier.

Mboh, C.M., Huisman, J.A., and Vereecken, H. 2011. Feasibility of sequential and coupled inversion of time domain reflectometry data to infer soil hydraulic parameters under falling head infiltration. Soil Science Society of America Journal, 75: 775–786. Wiley Online Library.

McDowell, N.G., and Allen, C.D. 2015. Darcy's law predicts widespread forest mortality under climate warming. Nature Climate Change, 5: 669–672. Nature Publishing Group.

Moghadas, D., Jadoon, K.Z., and McCabe, M.F. 2017. Spatiotemporal monitoring of soil water content profiles in an irrigated field using probabilistic inversion of time-lapse EMI data. Advances in Water Resources, 110: 238–248. Elsevier.

Nabighian, M.N. 1988. Electromagnetic methods in applied geophysics. In Society of Exploration Geophysicists. Society of Exploration Geophysicists, Tulsa, US.

Occhietti. 1977. Stratigraphie du Wisconsinien de la région de Trois-Rivières-Shawinigan, Québec. Géographie physique et Quaternaire, 31: 307–322. Les Presses de l'Université de Montréal. doi:10.7202/1000280ar.

Occhietti. 2007. The Saint-Narcisse morainic complex and early Younger Dryas events on the southeastern margin of the Laurentide Ice Sheet. Géographie physique et Quaternaire, 61: 89–117. Les Presses de l'Université de Montréal. doi:10.7202/038987ar.

Othman, A.A., Beshr, A.M., Abd El-Gawad, A.M.S., and Ibraheem, I.M. 2022. Hydrogeophysical investigation using remote sensing and geoelectrical data in southeast Hiw, Qena, Egypt. Geocarto International, 37: 14241–14260. Taylor & Francis.

Parent, M., and Occhietti, S. 1988. Late Wisconsinan deglaciation and Champlain sea invasion in the St. Lawrence valley, Québec. Géographie physique et Quaternaire, 42: 215–246. Les Presses de l'Université de Montréal. doi:10.7202/032734ar.

Parent, M., and Occhietti, S. 1999. Late Wisconsinan deglaciation and glacial lake development in the Appalachians of southeastern Québec. Géographie physique et Quaternaire, 53: 117–135. Les Presses de l'Université de Montréal. doi:10.7202/004859ar.

Parsekian, A.D., Singha, K., Minsley, B.J., Holbrook, W.S., and Slater, L. 2015. Multiscale geophysical imaging of the critical zone. Reviews of Geophysics, 53: 1–26. Wiley Online Library. doi:10.1002/2014RG000465.

Pondthai, P., Everett, M.E., Micallef, A., Weymer, B.A., Faghih, Z., Haroon, A., and Jegen, M. 2020. 3D Characterization of a Coastal Freshwater Aquifer in SE Malta (Mediterranean Sea) by Time-Domain Electromagnetics. Water, 12: 1566. Multidisciplinary Digital Publishing Institute. doi:10.3390/w12061566.

Reynolds, J.M. 1987. The role of surface geophysics in the assessment of regional groundwater potential in northern Nigeria. Geological Society, London, Engineering Geology Special Publications, 4: 185–190. Geological Society of London.

Reynolds, J.M. 2011. An introduction to applied and environmental geophysics. In 2nd edition. John Wiley & Sons, West Sussex, UK.

Richer, B., Saeidi, A., Boivin, M., Rouleau, A., and Lévesque, Y. 2023. Development of a methodology for predicting landslide hazards at a regional scale. Geoenvironmental Disasters, 10: 1–19. SpringerOpen. doi:10.1186/s40677-022-00231-4.

Rivers, T., Gool, J.A.M. van, and Connelly, J.N. 1993. Contrasting tectonic styles in the northern Grenville province: Implications for the dynamics of orogenic fronts. Geology, 21: 1127–1130. Geological Society of America. doi:10.1130/0091-7613(1993)021<1127:CTSITN>2.3.CO;2.

Robinson, D.A., Campbell, C.S., Hopmans, J.W., Hornbuckle, B.K., Jones, S.B., Knight, R., Ogden, F., Selker, J., and Wendroth, O. 2008. Soil moisture measurement for ecological and hydrological watershed-scale observatories: A review. Vadose Zone Journal, 7: 358–389. Wiley Online Library.

Rossi, M., Manoli, G., Pasetto, D., Deiana, R., Ferraris, S., Strobbia, C., Putti, M., and Cassiani, G. 2015. Coupled inverse modeling of a controlled irrigation experiment using multiple hydro-geophysical data. Advances in Water Resources, 82: 150–165. Elsevier.

Rucker, D.F., and Ferré, T.P.A. 2004. Parameter estimation for soil hydraulic properties using zero-offset borehole radar: Analytical method. Soil Science Society of America Journal, 68: 1560–1567. Wiley Online Library.

Siergieiev, D., Ehlert, L., Reimann, T., Lundberg, A., and Liedl, R. 2015. Modelling hyporheic processes for regulated rivers under transient hydrological and hydrogeological conditions. Hydrology and Earth System Sciences, 19: 329–340. Copernicus GmbH.

Tran, A.P., Vanclooster, M., Zupanski, M., and Lambot, S. 2014. Joint estimation of soil moisture profile and hydraulic parameters by ground-penetrating radar data assimilation with maximum likelihood ensemble filter. Water Resources Research, 50: 3131–3146. Wiley Online Library. doi:10.1002/2013WR014583.

Vereecken, H., Kasteel, R., Vanderborght, J., and Harter, T. 2007. Upscaling hydraulic properties and soil water flow processes in heterogeneous soils: A review. Vadose Zone Journal, 6: 1–28. Wiley Online Library.

Wagner, B.J. 1992. Simultaneous parameter estimation and contaminant source characterization for coupled groundwater flow and contaminant transport modelling. Journal of Hydrology, 135: 275–303. Elsevier.

Walter, J., Rouleau, A., Chesnaux, R., Lambert, M., and Daigneault, R. 2018. Characterization of general and singular features of major aquifer systems in the Saguenay-Lac-Saint-Jean region. Canadian Water Resources Journal/Revue canadienne des ressources hydriques, 43: 75–91. Taylor & Francis. doi:10.1080/07011784.2018.1433069.

Walter, J., Chesnaux, R., Rouleau, A., Ferroud, A., and Lambert, M. 2022. Résultats du projet d'acquisition de connaissances sur les eaux souterraines du territoire municipalisé de Lanaudière, de l'est de la Mauricie et de la Moyenne-Côte-Nord, PACES-LAMEMCN–section Lanaudière.

White, J.T. 2018. A model-independent iterative ensemble smoother for efficient history-matching and uncertainty quantification in very high dimensions. Environmental Modelling & Software, 109: 191–201. Elsevier.

Wise, S. 2000. Assessing the quality for hydrological applications of digital elevation models derived from contours. Hydrological processes, 14: 1909–1929. Wiley Online Library. doi:10.1002/1099-1085(20000815/30)14:11/12<1909::AID-HYP45>3.0.CO;2-6.

Yu, Y., Weihermüller, L., Klotzsche, A., Lärm, L., Vereecken, H., and Huisman, J.A. 2021. Sequential and coupled inversion of horizontal borehole ground penetrating radar data to estimate soil hydraulic properties at the field scale. Journal of Hydrology, 596: 126010. Elsevier. doi:10.1016/j.jhydrol.2021.126010.

DISCUSSION ET PERSPECTIVES DE RECHERCHE

Lors du projet PACES en Mauricie, l'une des approches les plus prometteuses pour caractériser le potentiel en eau souterraine, les directions d'écoulement et la stratigraphie régionale a été l'utilisation de méthodes géophysiques. Ces méthodes comprenaient des levés électromagnétiques transitoires (TEM), la tomographie de résistivité électrique (TRE) et le géoradar (GPR), qui ont permis de caractériser les aquifères régionaux. Par exemple, les résultats du TEM effectué dans la région de la Mauricie au Québec, notamment dans des secteurs de la moraine de Saint-Narcisse, un milieu de dépôt quaternaire hétérogène et anisotrope, ont révélé la compartimentation d'un système morainique de plusieurs kilomètres, ainsi que la présence de deux grands aquifères granulaires non confinés recouvrant le socle rocheux. L'approche TEM s'est avérée hautement efficace pour étudier la nature stratigraphique de la moraine en Mauricie et produire des cartes hydrogéologiques dans des territoires éloignés où les informations stratigraphiques et piézométriques sont limitées. Ces méthodes géophysiques sont donc particulièrement utiles dans les contextes géologiques où il y a peu de données accessibles. Dans ces régions éloignées, des acquisitions mineures de données directes telles que la réalisation de tests de pompage, de nouveaux forages, des levés piézométriques et une cartographie hydrogéologique plus détaillée des zones ciblées pourraient être envisagées afin de supporter les données indirectes acquises avec les méthodes géophysiques (Knight et al. 2018, Dewar and Knight 2020).

Dans cette étude, l'approche TEM a également été utilisée pour proposer des valeurs typiques de résistivité électrique pour des sédiments saturés et non saturés au Québec, sous la forme d'une charte de résistivité. L'étude s'appuie sur des levés TEM, ainsi que sur des données stratigraphiques et hydrogéologiques provenant de forages réalisés dans cinq régions de la province de Québec au Canada : Mauricie, Abitibi-Témiscamingue, Saguenay-Lac-Saint-Jean, Charlevoix et Haute-Côte-Nord. Cette charte permet d'améliorer l'évaluation des ressources en eau souterraine en fournissant des valeurs de résistivité électrique pour des sédiments quaternaire, qu'ils soient saturés ou non saturés, et compléter ainsi les levées géophysiques (p. ex., TEM et ERT) en fournissant un aperçu des faciès sédimentaires en fonction des variations des valeurs de résistivité électrique

obtenues. Par contre, certaines classes de sédiments n'ont pas été incluses dans cette étude (p. ex., gravier saturé et non saturé, gravier et galets, galets), faute de manque de donnée sur ces types de sédiment. Il est nécessaire de caractériser ces classes de sédiments en termes de résistivité électrique dans les études futures. Par exemple, il serait utile de déterminer les valeurs de résistivité électrique pour les sédiments intermixés avec de l'eau de mer ou d'autres classes de sédiments non représentées dans la charte de résistivité actuelle. Cela permettrait de raffiner les gammes de valeurs proposées dans cette charte et d'améliorer la justesse de l'évaluation des ressources en eau souterraine dans certaines zones.

En outre, certains des chevauchements de valeurs de résistivité entre différentes classes sédimentaires et entre les dépôts saturés et non saturés s’expliquent peut-être par la présence d’eau salée ou saumâtre. De plus, cette charte de résistivité pourrait également être appliquée à la modélisation hydrogéologique numérique, car les contrastes et les fortes variations de résistivité électrique entre les sédiments saturés en surface et les sédiments non saturés en profondeur fournissent un aperçu de l'élévation du niveau de la nappe phréatique, et conséquemment, des directions d’écoulement. En effet, les sédiments saturés présentent des valeurs de résistivité beaucoup plus faibles que les sédiments non saturés (pour une même classe de sédiment). Comme mentionné précédemment, les niveaux d'eau souterraine peuvent servir, entre autres, à valider la qualité d'un modèle numérique d'écoulement et même à effectuer une calibration à l'aide de logiciels tels que FePEST pour optimiser les paramètres hydrauliques et en générer dans les zones où ils n'existaient pas auparavant. Ainsi, en intégrant les informations de la charte de résistivité dans les modèles, il serait envisageable d'améliorer la justesse des prévisions des écoulements d'eau souterraine, de mieux appréhender la distribution et la géométrie des aquifères, ainsi que d'identifier les zones présentant une perméabilité variable comme indiqué par les forts contrastes de résistivité entre les argiles et les sables, par exemple.

Les approches du TEM, du TRE et du GPR peuvent également être appliquées en combinaison avec d'autres méthodologies d'étude, telles que l'utilisation de modèles numériques ou d'analyses géochimiques, afin d'obtenir une vision plus complète des caractéristiques hydrogéologiques des aquifères. Par exemple, en zone continentale, certains aquifères peuvent

renfermer des eaux saumâtres qui interagissent avec l'eau douce présente dans les couches de sous-surface. Ces lentilles d'eau souterraine saumâtre représentent des eaux fossiles laissées en place par d'anciennes mers intérieures telles que la mer de Laflamme et la mer de Champlain (Cloutier et al. 2006, Walter et al. 2017). La détection de ces lentilles d'eau saumâtre est facilitée par les sondages géophysiques, car l'eau salée conduit naturellement l'électricité et permet une circulation aisée des ondes électriques et électromagnétiques. Ainsi, un contraste significatif de résistivité électrique entre les sédiments saturés environnants et les poches d'eau saumâtre se manifestera, permettant d'identifier la distribution actuelle des eaux douces, saumâtres et salées dans le sous-sol, et par conséquent, d'évaluer la qualité des eaux souterraines. De plus, pour accroître la précision, il serait envisageable d'effectuer en laboratoire certains tests de mesure de la résistivité électrique sur différents matériaux géologiques, qu'ils soient saturés ou non saturés.

Conséquemment, des études de modélisation numérique et analytique pourraient être réalisées pour mieux comprendre le comportement des aquifères et prédire les changements potentiels liés aux facteurs climatiques et anthropiques. Cette approche multidisciplinaire (p. ex., géophysique, hydrogéologique, sédimentologique, stratigraphique et géochimique) permettrait ainsi d'obtenir des informations sur la qualité de l'eau, les taux de recharge et les propriétés hydrauliques des aquifères. Comme le suggère cette étude, l'intégration de l'approche géophysique dans les modèles numériques permet d'obtenir une caractérisation plus juste des faciès sédimentaires au sein d'un aquifère, de déterminer la profondeur du socle rocheux, ainsi que d'évaluer le potentiel aquifère global d'une région en termes de géométrie, d'extension et d'épaisseur. Cette approche géophysique permet ainsi d'identifier les zones sensibles quant à l'exploitation des ressources en eau, et de déterminer avec une plus grande justesse les directions d'écoulement et les niveaux d'eau souterraine.

Ce projet de doctorat a démontré l'importance de la géophysique et de l'utilisation des modèles numériques pour une caractérisation plus juste des aquifères. Il a également mis en évidence l'importance et l'utilité des données géophysiques pour identifier les niveaux d'eau souterrain, ainsi que de valider et calibrer des modèles numériques d'écoulement des eaux souterraines, afin de compléter les observations directes (p. ex., forages, levés piézométriques) et

de générer des informations hydrauliques. Cette approche novatrice combine différentes techniques géophysiques telles que le TEM, la TRE et le GPR, ouvrant ainsi la voie à de nouvelles perspectives de recherche et de développement dans le domaine de la modélisation hydrogéologique. Les résultats de cette étude soulignent, entre autres, l'importance de la validation des modèles d'écoulement à l'aide de données de terrain et le développement d'approches de validation croisée qui combinent différentes techniques géophysiques pour évaluer la justesse des résultats d'un modèle. Il est donc maintenant possible de comparer les résultats obtenus à partir des méthodes combinées du TEM, de l'ERT et du GPR afin de valider les niveaux d'eau souterraine prédits par un modèle numérique d'écoulement. Une telle approche de validation combinée renforce la confiance dans les modèles d'écoulement et améliore la justesse des prévisions hydrauliques. De plus, elle permet de tirer pleinement parti des avantages offerts par chaque technique géophysique, en fournissant une vision complète et intégrée des caractéristiques hydrogéologiques des aquifères.

Bien que chaque outil et approche utilisé dans cette thèse ne soit pas inédit individuellement, leur combinaison pour l'étude du potentiel aquifère d'un dépôt quaternaire est novatrice. La principale force de l'interprétation des résultats réside dans la diversité des méthodes utilisées conjointement : l'intégration des données géophysiques, des données de forage, des levés stratigraphiques, et des mesures piézométriques. De plus, la combinaison des outils d'investigation permet une évaluation plus précise de la stratigraphie, de la géométrie, de l'extension spatiale, de l'épaisseur des sédiments saturés, ainsi que des propriétés hydrauliques et des dynamiques souterraines des aquifères régionaux. En combinant ces diverses approches et ces outils d'investigation, la fiabilité et la profondeur des analyses sont significativement améliorées, surmontant les limitations des techniques prises isolément.

Analyse autocritique et lacunes à combler pour les recherches futures

Dans le but de développer de nouveaux outils pour évaluer le potentiel aquifère au sein de dépôts quaternaires hétérogènes, nous avons employé diverses méthodes, telles que des techniques géophysiques, des sondages piézométriques, des forages et des descriptions stratigraphiques. L'objectif était d'obtenir des résultats et de créer des modèles les plus proches possibles de la réalité

(justes) à une échelle régionale, cherchant à caractériser avec la plus grande fidélité possible les aquifères granulaires régionaux en termes de stratigraphie, de géométrie, d'épaisseur et d'étendue. Néanmoins, malgré nos efforts pour nous approcher le plus possible de la réalité des couches de sous-surfaces, des erreurs, inhérentes au domaine de la recherche en sciences de la Terre, pourraient s'être introduites dans les résultats obtenus, engendrant ainsi un certain manque de précision quant aux conclusions de cette étude. Cette section propose donc un survol autocritique des lacunes de cette recherche, identifiant les axes d'amélioration possibles. Cette analyse suggère également des approches devant être développées et perfectionnées pour les travaux futurs.

Premièrement, afin de repérer la présence d'eau souterraine et évaluer l'élévation du niveau d'eau, les méthodes géophysiques telles que la TRE et les sondages TEM et GPR sont principalement performante dans les environnements sédimentaires granulaires. Ces approches ont été exploitées depuis plusieurs années à des fins d'imagerie et de surveillance (Reynolds and Paren 1984; Palacky 1993; Kafri et al. 1997; Brunet et al. 2010; Reynolds 2011; Galazoulas et al. 2015; Pandey et al. 2015; Parsekian et al. 2015; Simard et al. 2015; Costabel et al. 2017; García-Menéndez et al. 2018, Greggio et al. 2018; Kalisperi et al. 2018; Goldman and Kafri 2020; Pondthai et al. 2020; Elbshbeshi et al. 2022; Othman et al. 2022), en raison du contraste significatif de conductivité électrique entre les sédiments saturés et non saturés. Notons cependant que les méthodes TRE, TEM et GPR présentent une moindre sensibilité à la détection des variations de conductivité électrique pour détecter la présence d'eau souterraine dans le substrat rocheux, ce qui résulte en des données de résolution limitée. À notre connaissance, aucune méthode géophysique n'a encore été élaborée pour détecter la présence d'eau dans les formations rocheuses, caractéristique fréquente au Québec. La présence d'un substrat rocheux à faible profondeur complexifie la détection du potentiel en eau souterraine dans des milieux rocheux fracturés. Contrairement aux milieux granulaires où la détection des niveaux d'eau souterraine avec les méthodes géophysiques est plus aisée, ces zones de substrat rocheux présentent des difficultés majeures pour la localisation du toit de la nappe, car même si la nappe phréatique se situe près de la surface, elle devient indétectable en raison de la présence du substrat rocheux, faute de méthode adéquate.

Par conséquent, il devient impératif de développer de nouvelles méthodes géophysiques mieux adaptées à la détection du potentiel aquifère dans des milieux rocheux fracturés. Par exemple, l'application de techniques d'imagerie géophysique avancées tel que la méthode de magnéto-résistivité (MMR), se révèle être plus sensible et mieux adaptée à la détection des variations de résistivité dans les environnements rocheux fracturés (Bouchedda et Giroux 2015, 2017, Bouchedda et al. 2015). En effet, cette méthode présente un fort potentiel et pourrait éventuellement fournir des informations détaillées sur la structure des aquifères en milieu rocheux à différentes échelles spatiales.

Deuxièmement, établir une différenciation claire entre les sédiments saturés et non saturés et localiser précisément la nappe phréatique est un défi. Même si la méthode TEM est capable d'identifier avec précision la présence d'eau souterraine, une quantité significative d'argile granulométrique mélangée aux sédiments granulaires peut fortement faire chuter les valeurs de résistivité électrique . La présence de particules d'argile de plus petit diamètre a un impact important sur les valeurs de résistivité par rapport à la saturation en eau. Par conséquent, la présence d'argile est un facteur crucial à prendre en compte, en particulier pour déterminer avec précision l'élévation des niveaux d'eau souterraine.

Troisièmement, les profils 2D TEM sont des interpolations entre les sondages 1D et présentent une incertitude liée à ces interpolations. Cela signifie qu'entre les emplacements des sondages, les résultats obtenus sont le résultat d'une interpolation effectuée par le logiciel Modsect (MacInnes et Raymond 2001) et qu'il n'y a pas de données réelles qui ont été prélevées en ces endroits. Il est donc primordial de se baser essentiellement sur les résultats obtenus directement sous le sondage 1D effectué et de se fier le moins possible aux résultats suggérés par le logiciel entre les sondages. Par exemple, dans l'article intitulé "Transient Electromagnetic (TEM) Surveys as a First Approach for Characterizing a Regional Aquifer", l'objectif principal consistait à identifier le potentiel en eau souterraine d'une région de la moraine de Saint-Narcisse en Mauricie. Pour atteindre cet objectif, une approche intégrée a été adoptée, impliquant la caractérisation détaillée de la stratigraphie locale et l'établissement de corrélations avec les données provenant des forages réalisés dans ces zones. Les résultats de ces forages ont été minutieusement corrélés avec les

sections stratigraphiques 2D générées par le logiciel. Ces données ont été ensuite exploitées pour mener des étapes cruciales telles que la calibration du modèle et l'établissement de corrélations entre les différentes classes sédimentaires et les valeurs de résistivité observées. L'objectif sous-jacent était de rendre le modèle aussi fidèle que possible à la réalité géologique du site étudié. Malgré tous les efforts déployés, les approximations liées aux interpolations entre les sondages 1D peuvent altérer les résultats finaux, soulignant ainsi l'importance d'une analyse critique continue pour améliorer la précision des modèles hydrogéologiques, particulièrement en ce qui concerne les données géophysiques. Cependant, la résolution des profils est bonne et représentative du milieu lorsque les stations sont rapprochées, comme dans cette étude. En effet, dans ce contexte, il est acceptable et réaliste de représenter les résultats en profils 2D. De plus, cette méthode de représentation est plus visuelle et permet de détecter rapidement à l'œil nu la présence et la profondeur du socle rocheux, l'élévation de la nappe phréatique, ainsi que les sédiments non saturés et saturés du milieu. Bien sûr, les données directes (c'est-à-dire, les relevés piézométriques, les forages, les coupes stratigraphiques) renforcent l'interprétation stratigraphique et réduisent les hypothèses erronées liées au lissage, aux interpolations et aux chevauchements, mais des erreurs inhérentes aux données indirectes sont toujours à considérer.

Quatrièmement, établir une relation fiable entre la résistivité et la lithologie est une tâche ardue, avec des chevauchements significatifs (c'est-à-dire des valeurs de résistivité similaires) fréquemment observés entre certaines classes de sédiments saturés et non saturés. Les articles "Electrical resistivity of saturated and unsaturated sediments in northeastern Canada" et "Transient Electromagnetic (TEM) Surveys as a First Approach for Characterizing a Regional Aquifer", propose des gammes de valeurs de résistivité électrique, mais la conversion des modèles lithologiques en modèles de résistivité n'est pas un processus direct. Par exemple, deux catégories telles que le sable et gravier et le sable présentent un chevauchement substantiel, ce qui rend difficile leur discrimination. Par ailleurs, les variations granulométriques, telles que le sable fin, moyen et grossier au sein d'une même classe de sédiments, n'ont pas été pris en compte. En outre, pour l'ensemble des classes sédimentaires, une certaine hétérogénéité est inévitable, complexifiant davantage la proposition précise de plages de valeurs de résistivité électrique. Par exemple, lorsque le sable et le

gravier présentent un mauvais tri, incluant du limon ou de l'argile (et donc montrant une moindre homogénéité), ils présentent des résistivités sensiblement réduites, ce qui introduit la possibilité de biais au sein des plages de valeurs de résistivité suggérées.

Les résultats de cette étude sur la création d'une charte de résistivité reposent sur des ensembles de données considérables (c.-à-d., 111 levés TEM, 10 coupes stratigraphiques, 51 levés piézométriques et 75 forages collectés dans cinq régions de la province de Québec, Canada pour le chapitre sur la charte de résistivité), augmentant ainsi la crédibilité des conclusions découlant des valeurs de résistivité électrique liées aux différentes classes de sédiments. Toutefois, malgré la quantité de données et la validation systématique des résultats géophysiques par des forages à proximité, des décalages de profondeur peuvent parfois survenir entre les valeurs de résistivité obtenues et les faciès sédimentaires présents dans les forages. Ces décalages de profondeur sont principalement attribuables à deux causes : 1) des erreurs d'échantillonnage liées à des facteurs anthropiques ; 2) l'interpolation des profondeurs et des divers faciès sédimentaires lors du forage, associée aux valeurs de résistivité obtenues par les techniques géophysiques. En effet, lors de la réalisation de forages dans un substrat sédimentaire, des sections de forage (et donc des faciès sédimentaires) peuvent être perdues, rendant difficile l'association de profondeurs précises à différents faciès. Par conséquent, une certaine imprécision peut subsister dans les valeurs de résistivité électrique associées aux divers faciès sédimentaires identifiés dans ces forages.

Ces chevauchements et ces décalages de profondeur mettent en lumière des lacunes inhérente à la charte de résistivité proposée. Des recherches approfondies sont nécessaires pour obtenir des valeurs de résistivité plus précises pour chaque classe sédimentaire, y compris celles qui sont mélangées avec d'autres types de sédiments. Pour atteindre cet objectif, d'autres approches doivent être envisagées. Par exemple, il serait possible de déterminer le pourcentage de chaque type de sédiment présent dans un échantillon, d'établir une classification suggérée pour les différents types de sédiments (mélangés ou non mélangés) associée à chaque pourcentage, et enfin, de proposer des plages de valeurs de résistivité électrique pour chaque classe de sédiments. Bien que cela puisse conduire à une complexité accrue en termes de classes de sédiments, cela améliorerait la précision et la justesse. L'exploration de nouvelles méthodes géophysiques mieux adaptées pour

déterminer les valeurs de résistivité en relation avec les classes de sédiments serait également bénéfique.

Finalement, en ce qui concerne la modélisation numérique et les articles "Using geophysical data to assess groundwater levels" et "Utility of geophysics-derived water levels to calibrate a regional groundwater flow numerical model", le modèle stratigraphique 3D élaboré à l'aide du logiciel Leapfrog est simplifié, ne prenant pas en compte les variations granulométriques avec toute la précision requise. Les faciès sédimentaires moins dominants ont été également omis dans le modèle afin de maintenir cette simplicité et les lentilles de sédiments susceptibles d'accentuer considérablement l'hétérogénéité du milieu n'ont pas été prises en considération. Bien que plusieurs auteurs aient démontré que les modèles simplifiés sont souvent les plus précis, et que les modélisateurs peuvent simplifier un modèle sans perte significative de précision dans la simulation (Benzaazoua et al. 2004, Hill 2006, Hudon-Gagnon et al. 2015, Doherty et Moore 2020, Fortier et al. 2020), le modèle que nous avons élaboré n'est pas entièrement fidèle à l'environnement géologique, entraînant très probablement une perte de précision.

En dernier lieu, le système a été considéré comme saturé jusqu'en surface dans le modèle d'écoulement exécuté à l'aide du logiciel Feflow. Cela signifie que la zone vadose n'a pas été prise en compte, simplifiant ainsi la modélisation mais introduisant inévitablement des possibilités d'erreur dans les résultats. En réalité, dans certaines zones de la moraine, la zone vadose est présente et le niveau d'eau souterraine ne se situe pas nécessairement directement à la surface. Bien que nous ayons opté pour un modèle simplifié, la présence de la zone vadose dans certaines parties du modèle pourrait occasionner des biais dans les résultats. La variation significative de la zone vadose à l'échelle régionale a rendu impossible sa modélisation, car elle présente des différences notables d'une zone à l'autre dans la moraine. Par exemple, au fond d'une carrière, la nappe phréatique est directement en contact avec la surface, éliminant ainsi la présence d'une zone vadose. En revanche, dans d'autres régions, telles que le sud-est du modèle près de la rivière Batiscan, d'épaisses couches de sable peuvent entraîner la présence d’une zone vadose à des profondeurs considérables.

Dans le cadre de ce projet doctoral, nous avons développé plusieurs outils d'investigation, chacun étant orienté dans une direction spécifique. Chacun de ces outils nous fournit des

informations cruciales sur l'hydrogéologie du milieu. Cependant, ces outils sont distincts et complémentaires, abordant divers aspects du problème. Lorsqu'ils sont combinés, ces outils d'investigation offrent une vision plus précise du potentiel aquifère de la région d'étude, en mettant en évidence l'hétérogénéité et l'anisotropie du milieu. Par exemple, l'approche TEM présentée dans l'article "Transient Electromagnetic (TEM) Surveys as a First Approach for Characterizing a Regional Aquifer: The Case of the Saint-Narcisse Moraine, Quebec, Canada" nous permet de déterminer le potentiel global en eau souterraine de cette région, les directions d'écoulement, et d'obtenir un aperçu de l'hétérogénéité régionale, incluant la compartimentalisation des aquifères de cette zone de la moraine.

D'un autre côté, la modélisation numérique réalisée dans les articles "Using Geophysical Data to Assess Groundwater Levels and the Accuracy of a Regional Numerical Flow Model" et "Utility of Geophysics-Derived Water Levels to Calibrate a Regional Groundwater Flow Numerical Model" nous offre un aperçu détaillé, grâce aux méthodes géophysiques, des niveaux d'eau, des directions d'écoulement et des propriétés hydrauliques. Cependant, pour parvenir à ces résultats, nous avons simplifié la stratigraphie pour créer un modèle tridimensionnel. Dans cette approche, la notion d'hétérogénéité n'est pas pleinement prise en compte, étant donné la simplification du modèle stratigraphique. Elle nous fournit néanmoins d'autres informations, offrant une perspective sur le potentiel en eau souterraine, avec un accent particulier sur l'anisotropie. Cela permet d'obtenir un aperçu des propriétés hydrauliques, notamment de la conductivité hydraulique et de l'anisotropie, dans cette région de la moraine. Ceci étant dit, l'objectif de cette thèse de doctorat était de développer des méthodes et de nouveaux outils d'investigation. Une fois ces outils mis au point, il est tout à fait envisageable de rendre la création des modèles 3D plus complexe, d'obtenir un niveau de détail plus élevé, et ainsi d'accéder à des informations plus approfondies sur l'hétérogénéité et l'anisotropie du milieu aquifère. La complexification des modèles stratigraphiques et hydrogéologiques (modèles d'écoulement) 3D n'était pas strictement nécessaire pour atteindre les objectifs spécifiques de cette étude.

Méthodologie suggérée pour les travaux et les recherches futures

Pour reprendre la méthodologie suggérée dans cette étude et utiliser les outils d'investigation mentionnés précédemment pour effectuer des travaux de caractérisation spatiale d'un aquifère régional, voici les étapes à suivre :

1. Effectuer des levés géophysiques de la région d'étude en combinant différentes méthodes, en privilégiant, si possible, des techniques complémentaires telles que le géoradar, le TEM et l'ERT. Les éléments privilégiés dans les résultats géophysiques incluent la profondeur du socle rocheux, l'élévation du toit de la nappe phréatique et l'identification des sédiments granulaires non saturés et saturés, lesquels constituent les réservoirs aquifères. Ces levés géophysiques doivent couvrir un maximum de superficie dans la région d'étude afin de fournir une représentation précise et réaliste des aquifères régionaux.

2. Réaliser une calibration stratigraphique locale et/ou régionale si des forages sont disponibles à proximité des levés géophysiques. Cette calibration permettra de générer une charte de résistivité électrique plus précise, réduisant ainsi le chevauchement des plages de résistivité pour chacune des classes de sédiments. En cas de disponibilité limitée de forages, il est recommandé d'utiliser la charte de résistivité globale suggérée dans cette étude (pour les dépôts quaternaires) comme référence pour déterminer les classes de sédiments en fonction des valeurs de résistivité électrique obtenues.

3. Produire une carte piézométrique si des levés piézométriques sont disponibles dans la région afin de valider la robustesse des résultats géophysiques. Si ce n'est pas le cas, la combinaison des différentes méthodes géophysiques est essentielle pour évaluer la qualité des levés géophysiques obtenus. Les faiblesses d'une méthode seront compensées par les forces d'une autre, permettant ainsi de valider et de fiabiliser les niveaux d'eau dérivés des données géophysiques.

4. Utiliser la majorité des levés géophysiques de qualité disponibles pour produire une cartographie des aquifères granulaires régionaux en nappe libre, en précisant leur géométrie, leur extension régionale et l'épaisseur des sédiments granulaires saturés. Il est également important de bien discerner les compartimentations régionales.

5. Générer un modèle stratigraphique régional tridimensionnel (par exemple avec Leapfrog Geo) et un modèle d'écoulement souterrain (par exemple avec Feflow ou Modflow) dans les zones particulières de l'aquifère régional où plusieurs forages sont disponibles. Cela permet d'obtenir des informations plus précises sur les charges hydrauliques et les écoulements souterrains a l'échelle régionale. Bien qu'il soit probablement impossible de construire ce modèle sur toute la région d'étude, une zone limitée peut néanmoins fournir des informations cruciales sur les conditions hydrauliques souterraines. La fiabilité de ce modèle numérique peut être validée avec les niveaux d'eau souterraine dérivés des différentes méthodes géophysiques combinées.

6. Effectuer une calibration à l'aide d'un logiciel tel que FePest en utilisant les niveaux d'eau dérivés des données géophysiques. Cela permet d'optimiser les paramètres hydrauliques initiaux (par exemple, Kxx, Kyy, Kzz, porosité et recharge) et de potentiellement en générer de nouveaux dans les zones où ces paramètres n'étaient pas disponibles à l'origine. Ainsi, on peut obtenir un aperçu de l'anisotropie à l'échelle régionale et obtenir des paramètres hydrauliques à moindre coût.

Perspectives d'avenir des projets PACES

Les résultats obtenus lors de ce projet de doctorat mettent également en évidence l'importance du projet PACES réalisé dans la région de l'est de la Mauricie pour acquérir des connaissances sur les ressources en eau souterraine. Cependant, cette étude ne représente qu'un aperçu initial des ressources en eau souterraine, et il est nécessaire de poursuivre les recherches afin d'obtenir des informations plus précises, telles que les zones plus vulnérables à la contamination et les potentiels en eaux souterraines disponibles et exploitables. Une approche de recherche complémentaire consisterait à approfondir l'étude de l'est de la Mauricie afin d'estimer de manière plus précise ces zones vulnérables et les potentiels aquifères. Cela pourrait impliquer la réalisation d'études sur les propriétés hydrauliques des aquifères, les caractéristiques hydrogéochimiques de l'eau souterraine, les taux de recharge et les niveaux piézométriques. Comme évoqué dans l'introduction, la cartographie hydrogéologique régionale a généralement recours à des simplifications importantes en identifiant de manière sommaire la présence d'aquifères et d'aquitards de manière très globale. À la suite de l'achèvement des projets PACES au Québec, la prochaine

étape consiste à quantifier de manière plus précise les ressources en eau souterraine. En Effet, les travaux des PACES ont produit une ébauche générale, à l'échelle du sud du Québec, des principaux aquifères formés par les dépôts granulaires du Quaternaire ainsi que des aquifères issus du socle rocheux fracturé (c. -à-d., roches sédimentaires de la Plate-forme du Saint-Laurent et roches cristallines d'âge grenvillien). Actuellement, cette esquisse est de nature quantitative en ce qui concerne le portrait chimique (qualité de l'eau prélevée dans les puits et les forages disponibles), mais elle demeure qualitative en ce qui concerne les limites physiques entre les différentes entités géologiques et les aquifères régionaux potentiels en fonction de leurs propriétés hydrauliques contrastées (perméables ou imperméables). Par conséquent, il est impératif de retourner sur le terrain pour mieux définir les hétérogénéités locales et régionales ainsi que leur influence sur les écoulements souterrains. Ce projet de doctorat s'inscrit dans le prolongement des recherches récentes qui proposent de nouvelles méthodes et outils d'investigation pour une évaluation plus précise du potentiel aquifère des dépôts quaternaires à l'échelle régionale (Sattel et Kgotlhang 2004, Knight et al. 2018, Nadeau et al. 2015, 2018, 2021). Il répond directement à ce besoin émergent en développant des méthodes visant à caractériser de manière plus précise ces hétérogénéités et à évaluer le potentiel aquifère à une échelle intermédiaire entre une grande échelle géographique et l'étude locale spécifique, typiquement menée par les consultants. Il est également crucial de considérer ces outils d'investigation dans une perspective d'évaluation du potentiel en eau souterraine à l'échelle régionale. En outre, c'est leur combinaison, lorsque cela est possible, qui rend cette approche particulièrement intéressante. Pris individuellement, ces outils ne présentent pas une innovation majeure en soi, car chacun a déjà été utilisé par le passé, mais dans des contextes et avec des objectifs différents. Par exemple, les études antérieures n'avaient pas pour objectif l'évaluation du potentiel en eau souterraine d'une région et n'utilisaient pas de modèles numériques.

Le volume significatif d'informations actuelles et futures liées aux eaux souterraines au Québec présente également des défis pour les décideurs et les responsables politiques, tels que l'accès et la gestion des données, ainsi que la compréhension des diverses données sur les eaux souterraines. De plus, les praticiens régionaux de l'eau (p. ex., organisme de bassin versant (OBV), fonctionnaires municipaux) ne possèdent pas toujours l'expertise nécessaire pour comprendre les

concepts avancés associés aux eaux souterraines. Les données actuellement produites dans le cadre des différents Programmes d'acquisition des connaissances sur les eaux souterraines (PACES) ne sont pas suffisamment adaptées aux besoins des praticiens régionaux de l'eau. Elles doivent être interprétées et combinées pour créer des connaissances utilisables dans la planification de l'utilisation du territoire et assurer la préservation durable des ressources en eau, le développement des ressources en eau et la résolution des conflits d'utilisation entre différentes activités économiques et municipales. Les outils techniques seuls ne suffisent pas à exploiter pleinement ces connaissances. Il est nécessaire de compléter ces outils par des conseils personnalisés d'un expert en eaux souterraines. Les bases de données produites par les universités participantes et fournies au MELCC du Québec contiennent d'immenses volumes d'informations. Le défi est d'exploiter ces nouvelles connaissances en les intégrant à la planification territoriale à différentes échelles.

Pour relever ces défis, il est essentiel de continuer à acquérir des connaissances sur les eaux souterraines au Québec, et de mettre à jour les bases de données existantes. Les organismes gouvernementaux, les municipalités et les cabinets de conseil produisent continuellement de nouvelles données pertinentes tels que les forages, les relevés piézométriques, les essais de pompage, les relevés géophysiques et les tests de qualité des eaux souterraines. Ces données doivent être intégrées aux bases de données établies au fur et à mesure de leur production pour garantir leur actualité et leur pertinence pour les projets futurs de gestion et de protection des ressources en eau. Plusieurs organisations, telles que les organismes gouvernementaux, les consultants, les municipalités régionales de comté (MRC), une université ou un consortium d'universités, et les organismes de bassins versants (OBV) peuvent être responsables de la mise à jour de ces données et de la gouvernance de ces bases de données. Cependant, sans une volonté politique claire et forte, la protection des eaux souterraines et une gestion durable ne sont pas assurées. Cela devrait se manifester par des mandats spécifiques, la disponibilité des ressources nécessaires et la création d'outils spécifiques pour assurer la durabilité de cette ressource essentielle.

Divers pays, dont le Canada, proposent des solutions et des méthodes pour améliorer l'accessibilité et l'autonomie d'accès aux bases de données, facilitant ainsi l'échange d'informations

entre les décideurs régionaux et les responsables politiques dans la gestion des ressources en eau. Ces bases de données sont souvent rattachées aux ministères de l'énergie, des mines ou du développement durable, avec peu ou pas de participation du secteur académique. Bien qu'elles aient toutes le même objectif de répondre aux attentes des utilisateurs lorsqu'ils cherchent à acquérir des données géoscientifiques et protéger les ressources en eau, la collaboration public-privé peut rendre ces bases de données inaccessibles au grand public. Cependant, l'accès aux données est essentiel, c'est pourquoi de nombreux pays ont établi des réglementations strictes pour mettre en œuvre des systèmes capables de collecter des informations sur les eaux souterraines et d'établir des bases de données mondiales avec des garanties d'accès facile.

Cela souligne également l'importance cruciale d'incorporer et de maintenir constamment à jour les bases de données hydrogéologiques, qui doivent évoluer au fil du temps grâce à l'intégration systématique des nouvelles données acquises quotidiennement. Cette intégration de données est actuellement réalisable à l'ère du "big data". La densification croissante des données s'accompagne de la capacité d'améliorer en permanence la précision des modèles numériques d'écoulement, assurant ainsi une représentation de plus en plus fidèle du fonctionnement réel des aquifères régionaux. Une telle approche requiert la mise à jour dynamique des modèles numériques existants, abandonnant ainsi l'approche statique traditionnelle prévalente dans les modèles d'écoulement produits par les consultants.

Réflexion sur le potentiel des ressources en eau dans les dépôts glaciaires

L'évaluation du potentiel en eau des dépôts glaciaires, tels que ceux de la moraine de Saint-Narcisse, revêt une importance cruciale pour les communautés locales qui dépendent de ces ressources pour leur approvisionnement en eau potable et leurs activités économiques. Les moraines glaciaires, en raison de leur composition en sédiments granulaires variés, peuvent constituer des aquifères significatifs offrant des réserves d'eau souterraine de qualité.

Les résultats de cette étude soulignent la pertinence de l'intégration des méthodes géophysiques pour cartographier et caractériser les aquifères au sein de ces dépôts quaternaires. En combinant différentes techniques d'investigation, telles que la ERT, le TEM, et le GPR, il est

possible de réaliser une évaluation plus détaillée des caractéristiques hydrostratigraphiques des moraines. Cette approche permet non seulement de déterminer la géométrie et l'extension des aquifères, mais aussi de mieux comprendre l'épaisseur des sédiments saturés et leurs propriétés hydrauliques.

Les dépôts glaciaires, par leur nature hétérogène, présentent souvent des défis en termes de modélisation et de prédiction des ressources en eau. Toutefois, les avancées méthodologiques présentées dans cette thèse démontrent que ces défis peuvent être surmontés grâce à une approche intégrée. La capacité à délimiter précisément les compartiments aquifères, à identifier les zones de recharge et à estimer les dynamiques d'écoulement souterrain offre des perspectives prometteuses pour la gestion durable des ressources en eau.

L'importance de ces études dépasse le cadre académique, car les informations obtenues sont essentielles pour les gestionnaires de l'eau et les décideurs locaux. Elles permettent de planifier l'exploitation des ressources en eau de manière optimale, assurant ainsi la pérennité des approvisionnements pour les communautés locales. De plus, une meilleure compréhension des aquifères glaciaires contribue à la protection des écosystèmes associés et à la prévention des problèmes liés à la surexploitation ou à la contamination des ressources en eau.

Conséquemment, l'étude approfondie des dépôts glaciaires, telle que la moraine de Saint-Narcisse, est non seulement justifiée par la richesse en ressources en eau qu'ils peuvent offrir, mais aussi par leur rôle crucial dans le soutien des communautés locales. La méthodologie développée et appliquée dans cette thèse constitue une avancée significative vers une gestion plus éclairée et durable des aquifères régionaux.

LISTE DE RÉFÉRENCES

Benzaazoua, M., Fall, M., and Belem, T. 2004. A contribution to understanding the hardening process of cemented pastefill. Minerals Engineering, 17: 141–152. doi:10.1016/j.mineng.2003.10.022.

Bouchedda, A., B. Giroux, and M. Allard. 2015. “Down-hole Magnetometric Resistivity inversion for zinc and lead lenses localization at Tobermalug, County Limerick, Irland.” SEG Int. Expo. Annu. Meet., SEG-2015. SEG.

Bouchedda, A., and B. Giroux. 2015. “Synthetic Study of CO2 monitoring using Time-lapse Down-hole Magnetometric Resistivity at Field Reseach Station, Alberta, Canada.” SEG Int. Expo. Annu. Meet., SEG-2015. SEG.

Bouchedda, A., and B. Giroux. 2017. “Joint time-lapse electrical-resistivity tomography and down-hole magnetometric-resistivity inversion for CO2 leakage monitoring.” SEG Tech. Progr. Expand. Abstr. 2017, 1081–1085. Society of Exploration Geophysicists.

Brunet, P., Clément, R., and Bouvier, C. 2010. Monitoring soil water content and deficit using Electrical Resistivity Tomography (ERT)–A case study in the Cevennes area, France. Journal of Hydrology, 380: 146–153. Elsevier.

Cloutier, V., Lefebvre, R., Savard, M.M., Bourque, É., and Therrien, R. 2006. Hydrogeochemistry and groundwater origin of the Basses-Laurentides sedimentary rock aquifer system, St. Lawrence Lowlands, Québec, Canada. Hydrogeology Journal, 14: 573–590. Springer.

Davis, J. L., and A. P. Annan. 1989. “Ground-penetrating radar for high-resolution mapping of soil and rock stratigraphy 1.” Geophys. Prospect., 37 (5): 531–551. Wiley Online Library. https://doi.org/10.1111/j.1365-2478.1989.tb02221.x.

Dewar, N., and Knight, R. 2020. Estimation of the top of the saturated zone from airborne electromagnetic data. Geophysics, 85: EN63–EN76. Society of Exploration Geophysicists and American Association of Petroleum …. doi:10.1190/geo2019-0539.1.

Doherty, J., and Moore, C. 2020. Decision support modeling: data assimilation, uncertainty quantification, and strategic abstraction. Groundwater, 58: 327–337. Wiley Online Library. doi:10.1111/gwat.12969.

Elbshbeshi, A., Gomaa, A., Mohamed, A., Othman, A., and Ghazala, H. 2022. Seismic hazard evaluation by employing microtremor measurements for Abu Simbel area, Aswan, Egypt. Journal of African Earth Sciences, 196: 104734. Elsevier.

Fortier, R., Banville, D.-R., Lévesque, R., Lemieux, J.-M., Molson, J., Therrien, R., and Ouellet, M. 2020. Development of a three-dimensional geological model, based on Quaternary chronology, geological mapping, and geophysical investigation, of a watershed in the discontinuous permafrost zone near Umiujaq (Nunavik, Canada). Hydrogeology Journal,. doi:10.1007/s10040-020-02113-1.

Galazoulas, E.C., Mertzanides, Y.C., Petalas, C.P., and Kargiotis, E.K. 2015. Large scale electrical resistivity tomography survey correlated to hydrogeological data for mapping groundwater salinization: a case study from a multilayered coastal aquifer in Rhodope, Northeastern Greece. Environmental processes, 2: 19–35. Springer.

García-Menéndez, O., Ballesteros, B.J., Renau-Pruñonosa, A., Morell, I., Mochales, T., Ibarra, P.I., and Rubio, F.M. 2018. Using electrical resistivity tomography to assess the effectiveness of

managed aquifer recharge in a salinized coastal aquifer. Environmental monitoring and assessment, 190: 1–19. Springer.

Goldman, M., and Kafri, U. 2020. Geoelectric, Geoelectromagnetic and Combined Geophysical Methods in Groundwater Exploration in Israel. In The Many Facets of Israel's Hydrogeology, First. Springer, Cham, Switzerland. doi:10.1007/978-3-030-51148-7.

Greggio, N., Giambastiani, B., Balugani, E., Amaini, C., and Antonellini, M. 2018. High-resolution electrical resistivity tomography (ERT) to characterize the spatial extension of freshwater lenses in a salinized coastal aquifer. Water, 10: 1067. Multidisciplinary Digital Publishing Institute. doi:10.3390/w10081067.

Hill, M.C. 2006. The practical use of simplicity in developing ground water models. Groundwater, 44: 775–781. Wiley Online Library. doi:10.1111/j.1745-6584.2006.00227.x.

Hudon-Gagnon, E., Chesnaux, R., Cousineau, P.A., and Rouleau, A. 2015. A hydrostratigraphic simplification approach to build 3D groundwater flow numerical models: example of a Quaternary deltaic deposit aquifer. Environmental earth sciences, 74: 4671–4683. Springer.

Kafri, U., Goldman, M., and Lang, B. 1997. Detection of subsurface brines, freshwater bodies and the interface configuration in-between by the time domain electromagnetic method in the Dead Sea Rift, Israel. Environmental Geology, 31: 42–49. Springer. doi:10.1007/s002540050162.

Kalisperi, D., Kouli, M., Vallianatos, F., Soupios, P., Kershaw, S., and Lydakis-Simantiris, N. 2018. A transient ElectroMagnetic (TEM) method survey in north-central coast of Crete, Greece: evidence of seawater intrusion. Geosciences, 8: 107. Multidisciplinary Digital Publishing Institute. doi:10.3390/geosciences8040107.

Knight, R., Smith, R., Asch, T., Abraham, J., Cannia, J., Viezzoli, A., and Fogg, G. 2018. Mapping aquifer systems with airborne electromagnetics in the Central Valley of California. Groundwater, 56: 893–908. Wiley Online Library.

MacInnes, S., and Raymond, M. 2001. ZONGE Data Processing Two-Dimensional, Smooth-Model CSAMT Inversion version 3.00. Zonge Engineering and Research Organization, Inc. p. 41.

Milsom, J. 2003. Field geophysics. Oxford, UK: John Wiley and sons.

Nadeau, S., Rosa, E., Cloutier, V., Daigneault, R.-A., and Veillette, J. 2015. A GIS-based approach for supporting groundwater protection in eskers: Application to sand and gravel extraction activities in Abitibi-Témiscamingue, Quebec, Canada. Journal of Hydrology: Regional Studies, 4: 535–549. Elsevier.

Nadeau, S., Rosa, E., and Cloutier, V. 2018. Stratigraphic sequence map for groundwater assessment and protection of unconsolidated aquifers: A case example in the Abitibi-Témiscamingue region, Québec, Canada. Canadian Water Resources Journal/Revue canadienne des ressources hydriques, 43: 113–135. Taylor & Francis.

Nadeau, S., Rosa, E., Cloutier, V., Mayappo, D., Paran, F., and Graillot, D. 2021. Spatial analysis approaches for the evaluation and protection of groundwater resources in large watersheds of the Canadian Shield. Hydrogeology Journal, 29: 2053–2075. Springer Nature BV.

Neal, A. 2004. "Ground-penetrating radar and its use in sedimentology: principles, problems and progress." Earth-science Rev., 66 (3–4): 261–330. Elsevier. https://doi.org/10.1016/j.earscirev.2004.01.004.

Neal, A., and C. L. Roberts. 2000. “Applications of ground-penetrating radar (GPR) to sedimentological, geomorphological and geoarchaeological studies in coastal environments.” Geol. Soc. London, Spec. Publ., 175 (1): 139–171. Geological Society of London. https://doi.org/10.1144/GSL.SP.2000.175.01.12.

Othman, A.A., Beshr, A.M., Abd El-Gawad, A.M.S., and Ibraheem, I.M. 2022. Hydrogeophysical investigation using remote sensing and geoelectrical data in southeast Hiw, Qena, Egypt. Geocarto International, 37: 14241–14260. Taylor & Francis.

Palacky, G. J. 1988. “Resistivity characteristics of geologic targets.” Electromagn. Methods Appl. Geophys., 53–129.

Palacky, G. J. 1993. “Use of airborne electromagnetic methods for resource mapping.” Adv. Sp. Res., 13 (11): 5–14. Elsevier. https://doi.org/10.1016/0273-1177(93)90196-I.

Pandey, L. M. S., S. K. Shukla, and D. Habibi. 2015. “Electrical resistivity of sandy soil.” Géotechnique Lett., 5 (3): 178–185. Thomas Telford Ltd. https://doi.org/10.1680/jgele.15.00066.

Parsekian, A.D., Singha, K., Minsley, B.J., Holbrook, W.S., and Slater, L. 2015. Multiscale geophysical imaging of the critical zone. Reviews of Geophysics, 53: 1–26. Wiley Online Library. doi:10.1002/2014RG000465.

Pondthai, P., Everett, M.E., Micallef, A., Weymer, B.A., Faghih, Z., Haroon, A., and Jegen, M. 2020. 3D Characterization of a Coastal Freshwater Aquifer in SE Malta (Mediterranean Sea) by Time-Domain Electromagnetics. Water, 12: 1566. Multidisciplinary Digital Publishing Institute. doi:10.3390/w12061566.

Reynolds, J. M. 1982. “Electrical resistivity of George VI ice shelf, Antarctic Peninsula.” Ann. Glaciol., 3: 279–283. Cambridge University Press.

Reynolds, J. M. 1985. “Dielectric behaviour of firn and ice from the Antarctic Peninsula, Antarctica.” J. Glaciol., 31 (109): 253–262. Cambridge University Press.

Reynolds, J. M. 1987a. “The role of surface geophysics in the assessment of regional groundwater potential in northern Nigeria.” Geol. Soc. London, Eng. Geol. Spec. Publ., 4 (1): 185–190. Geological Society of London.

Reynolds, J. M. 1987b. “Dielectric analysis of rocks-a forward look.” Geophys. J. R. Astron. Soc., 457. Blackwell science ltd osney mead, oxford, England.

Reynolds, J. M. 2011. An introduction to applied and environmental geophysics. West Sussex, UK: John Wiley & Sons.

Reynolds, J. M., and J. G. Paren. 1984. “Electrical resistivity of ice from the Antarctic Peninsula, Antarctica.” J. Glaciol., 30 (106): 289–295. Cambridge University Press.

Sattel, D., and Kgotlhang, L. 2004. Groundwater exploration with AEM in the Boteti area, Botswana. Exploration Geophysics, 35: 147–156. Taylor & Francis.

Telford, W. M., L. P. Geldart, and R. E. Sheriff. 1990. Applied geophysics. (C. U. Press, ed.). Cambridge: Cambridge university press.

Van Heteren, S. 1996. “Preserved records of coastal-morphologic and sea-level changes in the stratigraphy of paraglacial barriers.” Unpub. Ph.D. dissertation, Boston University, Massachusetts.

Van Heteren, S., D. M. Fitzgerald, P. A. Mckinlay, and I. V Buynevich. 1998. “Radar facies of paraglacial barrier systems: coastal New England, USA.” Sedimentology, 45 (1): 181–200. Wiley Online Library.

Walter, J., Chesnaux, R., Cloutier, V., and Gaboury, D. 2017. The influence of water/rock− water/clay interactions and mixing in the salinization processes of groundwater. Journal of Hydrology: Regional Studies, 13: 168–188. Elsevier.

CONCLUSION

Les environnements de dépôts quaternaires, notamment les moraines, présentent de grandes réserves d'eau souterraine potentiellement exploitable. Dans le contexte mondial de raréfaction des ressources en eau potable, l'évaluation du potentiel en eau souterraine de ces milieux revêt une importance cruciale pour l'avenir de l'humanité. Afin de répondre à cette nécessité, le développement de nouvelles approches méthodologiques et d'outils d'investigation novateurs est essentiel pour une estimation précise de leur potentiel en eau souterraine.

Cette démarche implique, en premier lieu, une corrélation entre les données stratigraphiques et piézométriques, permettant ainsi la caractérisation des aquifères granulaires régionaux en termes de stratigraphie, de géométrie, d'épaisseur et d'étendue. Une telle approche facilite la caractérisation des aquifères régionaux en utilisant des données géophysiques, offrant une solution pertinente dans des contextes géologiques présentant des lacunes en informations stratigraphiques et piézométriques, rendant la cartographie hydrogéologique complexe. Cette approche permet d'atteindre les objectifs 1, 2 et 3 de la thèse. Ces objectifs sont de (1) Définir la stratigraphie et le contexte géologique du système aquifère de la moraine de Saint-Narcisse; 2) Établir des relations entre les propriétés hydrogéologiques de la moraine et les caractéristiques physiques du sol en ayant recours à des techniques de mesures indirectes; 3) Acquérir une meilleure compréhension des unités hydrogéologiques et du potentiel en eau souterraine approfondie des unités hydrogéologiques et des propriétés hydrauliques des systèmes aquifères dans des environnements de dépôts quaternaires hétérogènes et anisotropes en utilisant de nouveaux outils d'investigation.

Une seconde approche propose une charte des valeurs de résistivité électrique englobant des gammes de résistivité applicables à quatorze catégories de sédiments, tant saturés que non saturés, dont sept n'ont jamais fait l'objet d'études antérieures. Parmi ces nouvelles catégories de sédiments considérées, on retrouve les argiles limoneuses, les argiles avec du sable/gravier/cailloux, les silts argileux non saturés avec présence de sable, les sables limoneux saturés et non saturés, ainsi que les sables argileux saturés et non saturés avec du gravier. Les résultats de cette investigation fournissent aux scientifiques et praticiens des données plus précises sur la résistivité

électrique d'une gamme étendue de sédiments, qu'ils soient saturés ou non saturés, dans les régions nordiques. Ces informations permettent une évaluation plus précise des ressources en eau souterraine, notamment en ce qui concerne la localisation de la nappe phréatique, offrant ainsi des avantages significatifs pour les études hydrogéologiques et la gestion des ressources hydriques. Cette approche permet d'atteindre l'objectif 2 de la thèse.

Une troisième approche préconise l'utilisation de données géophysiques pour une évaluation plus juste des niveaux d'eau dans un aquifère non confiné en milieu granulaire. Grâce à une approche de modélisation discrète, cette étude démontre la comparabilité entre les niveaux d'eau souterrains estimés par les méthodes géophysiques et ceux obtenus par observation directe. Les résultats soulignent la complémentarité des données géophysiques avec les observations directes, telles que les forages et les levés piézométriques, fournissant ainsi des informations hydrauliques supplémentaires pour les modélisateurs hydrologiques. Cette approche permet d'atteindre l'objectif 4 de la thèse. Cet objectif est d'élaborer des approches innovantes de modélisation numérique qui intègrent les données géophysiques afin d'améliorer la caractérisation et l'évaluation du potentiel en eau souterraine d'un aquifère granulaire régional.

Une quatrième approche préconise la calibration des modèles numériques d'écoulement en recourant à des données géophysiques. Cette méthode présente l'avantage d'optimiser les paramètres hydrauliques de manière économique, rapide et exhaustive. Suite à la calibration, le modélisateur est en mesure d'identifier de nouveaux paramètres hydrauliques, même dans les zones du modèle où il n'y en a pas. Cette approche contribue ainsi à améliorer la justesse et la fiabilité des modèles d'écoulement, tout en réduisant les coûts et les délais associés à la collecte de données. Les approches quatre et cinq apportent des contributions significatives à la communauté des modélisateurs en hydrogéologie, car elle propose de nouveaux outils afin d'améliorer les modèles numériques d'écoulement à l'échelle régionale. De cette manière, les méthodes géophysiques permettent une caractérisation plus juste des niveaux d'eau, de la capacité du milieu aquifère à se laisser traverser par des fluides, des dimensions internes, et de la variabilité stratigraphique des aquifères non confinés dans des régions présentant des lacunes en termes de données. Cette approche permet également d'atteindre l'objectif 4 de la thèse.

Dans ces quatre approches, l'intégration de données géophysiques, telles que les relevés TEM, TRE et GPR, s'est avérée cruciale pour compléter les informations directes issues des forages. Cette intégration a ouvert la voie à une modélisation plus juste, ainsi qu'à la caractérisation et à l'évaluation du potentiel en eau souterraine des aquifères granulaires régionaux, facilitant la corrélation entre les données stratigraphiques et piézométriques. Ces méthodes géophysiques, surtout lorsqu'elles sont combinées, ont démontré leur capacité à fournir un ensemble de données plus étendu et mieux réparti pour la modélisation à l'échelle régionale. Chaque méthode possède ses avantages et inconvénients, et leur combinaison contribue indéniablement à réduire les erreurs potentielles liées aux données indirectes. En outre, l'expansion de ces approches à d'autres régions et environnements climatiques permettra une compréhension plus holistique des réserves d'eau souterraine, soutenant ainsi le développement de stratégies de protection adaptées à chaque contexte géographique. Cette étude met en évidence le rôle croissant de la géophysique dans la caractérisation des aquifères et l'évaluation de leur potentiel en eau souterraine, offrant une alternative peu coûteuse, non destructive, rapide, robuste et efficace par rapport aux méthodes d'observation directe.

La contribution principale de cette étude réside dans la proposition d'une approche méthodologique de cartographie hydrogéologique à l'échelle régionale, utilisant de nouveaux outils d'investigation qui, lorsqu'ils sont combinés, permettent de déterminer de manière robuste un modèle conceptuel hydrostratigraphique. Ce modèle pourrait éventuellement faire l'objet d'une estimation quantitative du potentiel en eau souterraine d'un aquifère régional, incluant les paramètres hydrogéologiques tels que les niveaux d'eau, les écoulements souterrains, et les propriétés hydrauliques, par modélisation numérique. Bien que les outils d'investigation et les approches employés dans cette thèse ne soient pas inédits individuellement, leur combinaison spécifique pour l'étude du potentiel aquifère d'un dépôt quaternaire est innovante. La principale force de l'interprétation des résultats réside dans la diversité des méthodes utilisées conjointement : l'intégration des données géophysiques, des données de forage et des levés stratigraphiques, ainsi que des mesures piézométriques. Cette approche intégrée apporte une nouvelle perspective à la caractérisation spatiale des aquifères granulaires en nappe libre à l'échelle régionale. Elle permet

une évaluation plus précise de leur stratigraphie, de leur géométrie, de leur extension spatiale, de l'épaisseur des sédiments saturés, ainsi que de leurs propriétés hydrauliques et de leurs dynamiques souterraines. En surmontant les limitations de chaque approche et de chaque outil d'investigation pris isolément, cette combinaison méthodologique optimise la fiabilité et la profondeur des analyses.

Les projets PACES au Québec ont jusqu'ici enrichi notre compréhension des eaux souterraines à l'échelle suprarégionale. Les outils d'investigation novateurs développés au cours de ce projet doctoral représentent une avancée significative, offrant une compréhension plus approfondie des aquifères à différentes échelles et ouvrant ainsi la porte à la prochaine phase des projets PACES. Ces outils d'investigation permettent d'affiner la compréhension des systèmes aquifères testés lors des projets PACES, en fournissant des informations détaillées sur la stratigraphie, la géométrie, l'étendue et l'épaisseur des aquifères à diverses échelles. En tirant parti des bases de données PACES, une vue plus précise des aquifères à l'échelle régionale et sous-régionale est désormais possible, avec éventuellement la possibilité de calculer des volumes d'eau souterraine et de développer des modèles conceptuels hydrostratigraphiques pour orienter les prévisions futures.